1987

A study of redundancy in two-girder bridges using the finite element method, October 1987

David W. Spear

Celal N. Kostem

A STUDY OF REDUNDANCY IN TWO-GIRDER BRIDGES

USING THE FINITE ELEMENT METHOD

by

David W. Spear
Celal N. Kostem

Fritz Engineering Laboratory
Department of Civil Engineering
Lehigh University
Bethlehem, Pennsylvania

October 1987

Fritz Engineering Laboratory Report No. 432.10

Table of Contents

Abstract

The current practice in the construction of bridges with steel girders is to use a multi-girder approach (3 or more girders). The use of two-girder bridges was discontinued because they were thought to be insufficiently redundant and thus susceptible to collapse resulting from damage to one of the two main girders.

It is currently being thought, however, that the secondary members of 2-girder bridges may provide enough redundancy to prevent collapse in the event of damage to a main girder. With the advent of computer methods, it is now possible to study the bridges in a full three-dimensional form. These methods consider all redundancy and reflect the true behavior of the bridge.

In this report, a two-girder bridge has been studied by the finite element method. Three different sizes of cracks were imposed on one main girder. Additionally, the support and loading conditions were varied.

It was found that a small crack in one main girder produces sizeable deflections, but causes little damage to the bridge. A full-depth crack produces extremely high deflection and causes severe damage to the bridge, yet it is possible that the redundancy is sufficient to prevent total collapse of the structure.

Chapter 1
Introduction

1.1 Description of Problem

The current practice in the construction of bridges with steel girders is to use a multi-girder approach (3 or more girders). Two-girder bridges were often constructed when a when a "longer" length bridge was required until the early 1980s, when their use was discontinued. It was felt that two-girder bridges were susceptible to failure resulting from damage to a main girder, because they were not sufficiently redundant. Damage to one of the main girders was thought to result in catastrophic response and ultimately failure of the structure, since the one remaining off-center girder could not support the entire bridge.

1.2 Objective

Although no bridges of this type were designed and constructed since the early 1980s, there still remain thousands of them throughout the country which were constructed before this time. Many of these bridges have reached an age where it necessary to either replace or repair them, and thus it is prudent to study these bridges in depth to determine their structural behavior.

The current thinking regarding two-girder bridges is that they are non-redundant. That is, the failure of a single primary member (e.g. a main girder) may result in the collapse of the entire structure. Recently, however, it has been realized that the secondary members of two-girder bridges may provide more redundancy than originally thought (see reference 8). If this is truly the case, then these bridges may be safer than currently realized. It is therefore possible that many of the older two-girder bridges may be able to be repaired

rather than replaced, or even that they may be able to withstand more use in their present condition. Additionally, it may mean that a more "practical" two-girder bridge could be substituted for a multi-girder bridge for new construction when a "longer" span is required.

What this report attempts to determine is this: if damage does occur to one of the two girders, what will happen to the bridge? It may experience cracking of the slab, yielding of the girder flanges, or large deflections. Are these critical conditions? Will the bridge collapse, will there be irreparable damage, or will the bridge be able to be repaired after such an event?

This study, then, will explore the effect of imposing different size cracks on the bridge. Additionally, it will explore the effects of various loading conditions, and also of various support conditions. These are further discussed in chapter 3.

1.3 Prototype Bridge

The bridge in this study is based on a basic set of plans from the USDOT/FHA/BPR plans from April 1968. This is shown in figure 1. The bridge considered is a "typical" and generic bridge based on these plans, but is not patterned after any specific actual bridge. It is a 120-foot steel-girder bridge with a 7.5" concrete deck. The overall width is 46', with a 44' clear roadway. There are seven transverse floorbeams spaced evenly at 20' intervals, and 4 longitudinal stringers evenly spaced between the two girders.

For the sake of convenience and consistency, the bridge was defined as "left" and "right," as seen in the top view of figure 2. All loads were applied on the left side. Also, all cracks imposed later in the study were applied on the left side. There are four supports, numbered 9, 10, 11, and 12, which can

also be seen in figure 2.

This finite element model was constructed by Maj. Tom Lenox, a PhD. candidate in Civil Engineering at Lehigh University, who used this model for some work early in his dissertation study.

Chapter 2
Modelling of Bridge

2.1 General

The finite element model used in this study was created using the library of elements in SAP4 - a Structural Analysis Program for Static and Dynamic Response of Linear Systems; it referenced the 1973/1974 edition of the SAP IV manual by Bathe, Wilson, and Peterson, and the SAPIV and SPLT commentaries by Celal N. Kostem. All computing work was performed on the CYBER 850 at Lehigh University.

The bridge is oriented in X-Y-Z space, with the X-axis in the longitudinal direction. The Z-axis is in the transverse direction, and the Y-axis completes the right-hand rule by going up. This is shown in figure 3. Also, for the purposes of this report, using the top view in figure 2, the bridge has been labelled "left" and "right", based on the numbering of the nodes, to facilitate communicating which side of the bridge is being considered.

The midheight of the concrete slab is taken to be the reference plane in the y-direction, so that all other dimensions for the depth of the bridge are negative. The x-axis is along the "left" side of the model, and the z-axis runs from "left" to "right" along the "bottom".

It is fully realized that the model is an idealization of the actual bridge. The nodal points in the model were chosen to most closely fit the location where members joined together, and the joints were idealized to make all the members join at an infinitesimal point. The experience of Celal N. Kostem indicated that this idealization is quite acceptable and gives accurate results.

The units used are kips and inches in all cases.

2.2 Girder/Slab Interaction

The design of the bridge examined assumes full composite action between the slab and the girders. This is modelled by extending the top flange of the girders into the center of the concrete slab, as shown in figure 4. The center of the concrete slab is taken to be the reference plane in the vertical direction, with distances negative downwards. The overall depth of the 7.5" slab and 90" girder is kept accurate by placing the bottom of the girder at y=-97.5". However, since the center of the slab is at y=0, the total depth of the girder is 93.75", not 90" as in the plans. This slight discrepancy is considered negligible in light of the necessity of "practical" modelling of the composite action of the bridge.

2.3 Girders

The girders are major structural components of the bridge and will certainly experience out-of-plane behavior. To account for this, plate-bending elements with membrane stiffness must be used for the web, and beam elements must be used for the bottom flange.

The 90" x 3/8" girder web was divided into three vertical parts. The top part extends from the concrete deck to the top of the floor beams. The center portion extends across the depth of the floor beams, and the bottom portion continues from the bottom of the floor beams to the bottom of the bridge. The numbering of the elements, as shown in figure 5, starts on the "right" side of the bridge, going from the "low" end to the "high" end.

The bottom flange varies in cross-section from 21" x 1" to 24" x 1.5",

24" x 2.25", and finally to 24" x 2.5" at midspan. This is taken into account in the data input. In the cases where the change in flange thickness does not occur at a node, the properties are "smeared" uniformly across the neighboring elements. Shear deformation of the flanges is not considered here. This is reflected by allowing the shear areas of the flanges to be zero. The numbering of the flange elements follows that of the web, starting on the right and going from the low end to the high end.

As stated previously in section 2.2, the top flange is considered to act compositely with the slab and is thus "imbedded" in the concrete. Since this effectively prevents any out-of-plane behavior, truss elements are used. The cross-section of the top flange varies exactly as the bottom flange, and "smearing" is again employed. The numbering is also analagous to that of the bottom flanges.

In addition, vertical stiffeners are included and are modelled with truss elements. Here the stiffeners are not aligned with the nodes, and an equivalent section is calculated to account for this difference.

Material and section properties for the girders are shown in table 1.

2.4 Floor Beams

The floor beams are the major stiffening mechanism for the bridge deck and inherently experience out-of-plane behavior. Thus the web must be modelled with plate bending elements with membrane stiffness, and the flanges must be modelled with beam elements.

The 59" x 3/8" web was broken into 10 transverse divisions but only one vertical division, making an acceptable aspect ratio of 1.31. These divisions were chosen because the vertical stiffeners were located at 45" intervals, and

this provided a logical method of division. The elements were numbered from left to right across the transverse direction and then from bottom to top in the longitudinal direction, for a total of 70 elements. The numbering scheme is shown in figure 6.

The top and bottom flanges of the floor beams are identical and constant at 12" x 1" in cross-section. Both were modelled identically, though they were included as different element groups. The numbering of the flanges follows that of the web, going from left to right and then from bottom to top. Material and section properties for the floor beams are shown in table 2.

2.5 Stringers

Stringers are not designed as major load-carrying members of the bridge, and are included mainly to provide continuity; that is, to connect the deck to the floor beams. They are often indirectly subjected to great wheel loads, but since these are usually in the plane of the web, and since the stringers act compositely with the concrete deck, they do not experience significant amounts out-of-plane behavior. The stringer webs can therefore be modelled with plane stress elements, and the web flanges can be modelled with truss elements.

The stringers were broken into five-foot divisions to easily coincide with the 20-foot divisions of the floor beams. This created 24 sections along the length, for a total of 96 elements, starting from the bottom and going from right to left. This is shown in figure 7.

The web had a constant cross-section of 18 5/8" x 3/8". The top and bottom flanges had constant cross-sections of 8 1/4" x 1/2" and were included as separate elements groups. Material and section properties for the stringers are shown in table 3.

The purpose of the stringers was to connect the bottom of the slab to the top of the floor beams. This can be seen in figure 1. However, assuming composite action between the slab and the stringer, the top flange can again be imbedded in the concrete. This places the top of the stringer at y=0 and the bottom at y=-25, for a total depth of 25", not 21" as specified on the plan. However, this error can be assumed to be small.

2.6 Deck

The deck slab will definitely experience biaxial bending, and it will be modelled with plate-bending elements with membrane stiffness. In-plane torsion, however, will be ignored, and only five degrees of freedom will be considered. It is assumed that the slab is monolithic, and any imbedded reinforcing bars will be ignored, and any drainage slope of the slab will not be considered.

A total of 288 plate-bending elements was used to model this slab. As shown in figure 8, the elements were numbered first in the longitudinal direction from bottom to top, and then from right to left. It should also be noted that the elements were oriented so as to align the local and global axes.

The concrete used has a f_c' of 3400 psi and a Young's Modulus of 3322 ksi. Other material and section properties are shown in table 4.

2.7 Curb and Parapet

Also included in the model was a parapet section, which modelled the sidewalks, railings, curbs, etc., along the outside edge of the bridge. Here plate-bending elements were again used, and the section properties were increased to account for the additional strength provided by these members. The material and section properties for this are shown in table 5.

2.8 Supports

To simulate the support conditions of the bridge, boundary elements were included in the model. One element was included in each global direction at each of the four support locations, for a total of twelve elements. The location of each is shown in figure 2.

The boundary elements are included for two reasons. The first reason is to determine the reactions at each location. With SAP IV, it is impossible to directly find the reactions; thus it is necessary to use boundary elements, which provide us with the opposing force at the node at which it is placed.

The second reason to include boundary elements is to provide a simple method of varying the support conditions. As stated in the introduction, part of the objective of this study is to determine the effect of different support conditions, and boundary elements are the most convenient way to accomplish this. The default stiffness of the springs is $k=10^{8}$; this provides a "fixed" condition in the applied direction. However, by changing the stiffness to $k=10^{-8}$, the effect of the spring can be virtually eliminated without actually removing the element.

Chapter 3
Parametric Study

3.1 Crack Conditions

Various crack conditions were imposed on the bridge to study the effect of damage on the bridge's behavior. The four crack conditions, shown in figures 9 and 10, are as follows:

3.1.1 Intact

In the first case, the bridge was evaluated fully intact as a reference. There was no damage imposed on the bridge.

3.1.2 Crack Level 1

In the first crack condition, a crack was imposed through the bottom flange and lower 13.5" of the web of the "left" girder, as viewed in the top view in figure 2. This crack extends from the bottom of the girder to the bottom of the floor beam and constitutes approximately 14% of the full depth of the girder.

3.1.3 Crack Level 2

The crack extends from the bottom flange to the top of the floor beam, or the lower 72.5" of the web of the "left" girder. This crack measures approximately 74% of the full girder depth. The floor beam which was attached at midspan has been disconnected from the "upper" half of the bridge, yet remains attached to the "lower" half of the bridge, as viewed in figure 2.

3.1.4 Crack Level 3

Here a full-depth crack is imposed, severing the bottom flange, and all 97.5" of the "left" girder web. The midspan floor bean remains attached to the "lower" half of the bridge as for crack level 2.

3.2 Support Conditions

Various support conditions were considered to study the effect of fixed and non-fixed supports on the bridge's behavior. All supports were located at the bottom of the girders at the end of the bridge. The three applied conditions are as follows:

3.2.1 PP/RR

In a pin-pin/roller-roller (pp/rr) situation, two pins and two rollers are used to support the bridge. The pins are idealized, and provide total restraint in the vertical, transverse, and longitudinal directions. The rollers are also idealized, and provide restraint only in the vertical and transverse directions. Here the two pins were applied on the "lower" half of the bridge, as seen in the top view in figure 2. On the "upper" half of the bridge were applied the two rollers. The pins were given reference numbers 9 and 10; the rollers were numbered 11 and 12. This idealizes a "fixed-expansion" condition.

Each pin was idealized by a vertical boundary element, a longitudinal boundary element, and a transverse boundary element, each with a spring constant of $k=10^8$, and connected to nodes with zero degrees of freedom. It was assumed that these would prevent any movement in their specified direction and that they would also show the resisting force at that location.

The rollers were idealized with boundary elements in the vertical and

transverse directions with spring constants of $k=10^8$ to prevent translation in those directions. In the longitudinal direction, boundary elements were applied with a spring constant of $k=10^{-8}$. This value of k is so low that it will provide virtually no resistance to movement in the longitudinal direction, and it is effectively non-existent. This approach was used to ease the change from pin to roller, as it could be quickly accomplished by changing only the spring constant.

3.2.2 PP/PR

The pp/pr condition consisted of three pins and roller. This was accomplished by changing the roller at location 11 to a pin, leaving the single roller in the upper left corner at location 12. This position was chosen because it was on the opposite side of the bridge from the loading and crack conditions (i.e. the loading and cracks were applied on the "left" side of the bridge; the third pin was added to the "right" side). All pins and rollers were modelled in the same manner as stated in section 3.2.1.

3.2.3 PP/PP

Although two-girder bridges are usually designed with two pins and two rollers, this idealization rarely remains an actuality after the bridge is put into service. Dirt and corrosion often lock the joint and eliminate its possible translation. Thus a fully fixed condition must be studied.

For this third condition, the support at location 12 was changed from a roller to a pin. The bridge is now fully locked with pins at all supports, idealizing a "fixed-fixed" support condition. Translation in all directions is prevented by the twelve boundary elements.

3.3 Loading Conditions

The bridge was loaded with a variety of standard vehicles based on the AASHTO and PennDOT specifications. The two trucks used were the AASHTO HS20-44 standard and the PennDOT 204 kip permit vehicle.

The AASHTO HS20-44 vehicle, hereafter referred to simply as the HS20-44, is shown in figure 11. The AASHTO specifications dictate that the distance from the front axle to the drive axles is 14 feet. The distance from the drive axles to the rear axles can vary from 14 to 28 feet. In order to maximize the moment applied to the bridge, the minimum distance of 14 feet is used.

The PennDOT 204 kip permit vehicle, hereafter referred to as the Permit Vehicle, is shown in figure 12.

Seven basic load conditions were considered:

1. 1 HS20-44 at edge. The truck was placed as close to the edge as possible. The 6-foot truck was centered in its 10-foot-wide lane, leaving it two feet from the inside edge of the parapet.

2. 2 HS20-44 side-by-side at edge. The vehicle in load condition 1 was left as is, and to it was added a second HS20-44 truck as close to the edge as possible. The 10-foot wide lane and the two-foot inset left this second truck 12 feet from the inside of the parapet.

3. 1 HS20-44 at centerline. The truck was placed so that its wheels straddled centerline. Each wheel was then three feet from the centerline of the bridge.

4. 2 HS20-44 side-by-side at centerline. Two trucks were placed as close as possible to, and on opposite sides of the centerline. They were place going in opposite directions, and two feet from the centerline.

5. 1 Permit Vehicle at edge. As in load case 1, the truck was placed as close as possible to the edge. This vehicle is also six feet wide in a 10-foot lane, leaving it two feet from the edge.

6. 1 Permit Vehicle at centerline. As in load case 3, the truck was place straddling centerline, leaving each wheel three feet from center.

7. Dead load only. The dead load of each component of the bridge was applied as the only load on the bridge.

Load conditions 1 - 6 are shown in figures 13 through 15.

In addition, dead load was added to each of cases 1 through 6 by superposition of the output. Separate runs were not made for each of the load cases; rather, superposition was assumed to be implicit for all stresses and displacement.

To maintain some level of consistency throughout the study, all loads were applied on the "left" side of the bridge, as shown in the top view in figure 2. All drive axles were placed at midspan, with the trucks traveling from "top" to "bottom."

For each of load cases 1 through 6, wheel loads were broken into vertical nodal point loads by simple statics. The nodal loads were applied at the level of the concrete slab, i.e. the level of the roadway, and the impact factor was ignored in all cases.

3.4 Description of Cases

In this study there are three different support conditions, four crack conditions, and thirteen load conditions, thereby resulting in 156 case studies. The support and crack conditions were broken into twelve cases, as shown in table 6. Cases 1-3 considered the intact bridge: case 1 was for pp/rr supports, case 2 was for pp/pr supports, and case 3 was for pp/pp supports. Similarly, cases 4-6 considered the first crack level, cases 7-9 considered the second crack level, and cases 10-12 considered the full-depth crack.

In each of these twelve cases, the seven original load conditions were

applied. The dead load was also superimposed onto each of the live load cases to produced separate live load only and live plus dead conditions for each case.

It is important to note the differentiation between the terms "conditions" and "cases." "Conditions" is used to refer to the various supports, loadings, and crack levels which are applied to the structure. The "cases" are the 12 different combinations of support and crack "conditions" studied together in a single SAPIV run, and are shown in table 6.

Chapter 4
Discussion of Results

4.1 Intact Bridge

4.1.1 Midspan Deflections

The midspan live load deflection profiles for the intact bridge are shown in figures 16 - 18.

As expected, it can be seen that for the symmetrical support conditions (cases 1 and 3) and symmetrical loading conditions (load conditions 3, 4, and 6) the response is also symmetrical. For the non-symmetrical loading conditions (1, 2, and 5) the response is non-symmetrical, with the largest deflection under the applied load.

Comparing cases 1 and 2, it can be seen that, by adding a third pin on the right side (unloaded side), the deflections on the right decrease by approximately 50%, while there is virtually no change to the left side deflections. Thus with non-symmetrical support conditions, the response is also non-symmetrical.

Considering case 3, it is found that adding a fourth pin to the left side (loaded side) reduced the deflections on the left side by 50%, while the right side deflections remain unchanged. Here there again are symmetrical support conditions, and thus symmetrical response for symmetrical loading.

It should also be noticed in comparing load conditions 2 (two HS20-44 at edge) and 5 (Permit Vehicle at edge) that the Permit Vehicle causes a much more severe response. Its deflection on the left is 65% greater than the HS20-44 vehicles, and the right side deflection is actually positive (deflecting

"up"), whereas the two HS20-44 give a slightly negative response (deflecting "down"). Also comparing load conditions 4 (two HS20-44 at centerline) and 6 (Permit Vehicle at centerline), we see that the Permit Vehicle provided a consistently higher response of approximately 25%.

When adding the dead load in cases 1 - 3, shown in figures 19 - 21, the same patterns develop as in the live load cases. Again, adding a third pin reduces deflections on that side, while others remain constant. Adding a fourth pin decreases the response on that side alone. The dead load is also a symmetrical loading condition, which gives a symmetrical response for symmetrical support conditions.

The main difference the dead load shows is a much more "grouped" response than live load alone. This is because it is a larger load and provides a larger reponse, which tends to "wash out" the effects of the live load. This is especially noticeable in case 2, where the third pin is added.

One thing that should not be overlooked when reading the graphs is that superposition of the deflections is assumed. This implies a linear addition of dead load to live load; and although the percentage difference between load conditions may appear to decrease when the dead load is included, the algebraic difference remains exactly the same, as it should.

4.1.2 Bottom Flange Stresses

Plots of bottom flange stresses of the intact bridge from near support to near midspan are shown in figures 22 - 33. Four load conditions are shown: Load condition 2 (LC-2, two HS20-44 at edge), LC-4 (two HS20-44 at centerline), LC-5 (Permit Vehicle at edge), and LC-6 (Permit Vehicle at centerline). For each load condition, the left and right side stresses are plotted

on the same graph, and the dead load stresses are added by superposition and plotted above.

The first thing that can be noticed from these plots is the symmetrical response from symmetrical load conditions (LC-4 & LC-6) and symmetrical support conditions (cases 1 & 3). This is what was expected to be found, and it agrees well with the symmetrical response found in the midspan deflections.

For the non-symmetrical load conditions (LC-2 & LC-5), the response is also found to be non-symmetrical, with higher stresses on the loaded (left) side than on the unloaded side. This is especially noticeable in LC-5, which is more skewed than LC-2.

Each of the points on these plots is the location of a change in thickness of the bottom flange. It should be noted that the stresses increase at each location, with the exception of the fourth point, which consistently shows a decrease in stress. This is more pronounced under live plus dead load than under live load alone.

For a pp/rr situation, all the flanges are in tension for all load conditions. They also tend to follow, with the exception of the fourth point, a generally smooth trend.

The addition of a third pin on the right side places the right side flanges into compression at the supports, while remaining in tension towards midspan. The dead load, being a greater loading condition, tends to have higher compression at the supports and higher tension near midspan than the live load. The left side stresses remain unchanged, and thus all symmetry is eliminated. In addition, the right side no longer experiences a decrease in stress at any point, but shows a somewhat parabolic increase from compression to tension

throughout.

Introducing a fourth pin to the left side of the structure shows results similar to those from adding the third pin. Now both left and right side flanges are in compression at the supports and in tension near midspan. And again the live plus dead load conditions show more compressive stresses at the supports and more tensile stresses at midspan than the corresponding live load conditions.

Comparing load conditions 2 and 5, shows that the Permit Vehicle produces stresses twice as great as the HS20-44 vehicles on the left side, but smaller stresses on the right side. This is because the Permit Vehicle is heavier and more skewed than the HS20-44 vehicles side-by-side.

4.1.3 Total Longitudinal Slab Stress

The total longitudinal bottom fiber stresses in the concrete slab are plotted in figures 34 - 39. These include both the membrane stresses and the bending stresses across the slab at midspan.

Initially, the pp/rr plots look very random and disjointed. But upon closer inspection, it is seen that the symmetrical loading conditions (4 & 6) do indeed give symmetrical responses. It can also be seen that for the non-symmetrical loading conditions the maximum stress is under the load (left side), and varies to near zero on the unloaded side. One reason for the seemingly random stresses is the low magnitude of the stresses. Here the maximum compressive stress is 200 psi, and the maximum tensile stress is 60 psi; both of these show stresses far below the critical values.

The addition of a third pin into the structure seems to have no effect on the distribution of stresses. Although this result seems odd, it is consistent

with the other parameters studied here.

It can also be seen that a fourth pin does not change the stress behavior in the slab, an observation which is generally not in keeping with other parameters. Again, one explanation for this could be the low magnitude of the stresses.

When the dead load is added to cases 1 - 3, the stresses become somewhat more "grouped" than for live-load-only cases. It can also be observed that the symmetrical loadings produce symmetrical response. For this intact bridge, a shift in the range of stresses can be seen, which is due to the large magnitude and symmetry of the dead load. In the live load cases, the stresses were evenly balanced between tension and compression; here all values are compressive and vary between 150 and 500 psi.

Again the third and fourth pins have virtually no effect on the stresses.

Comparing load conditions 2 and 5, it is found that the Permit Vehicle produces more "extremes" in stresses than the HS20-44 vehicles do; i.e., the tensile stresses are in greater tension (200 vs. 120 psi), and the compressive stresses are in greater compression (5 psi vs. 0 psi). Comparing conditions 4 and 6, it is found that the Permit Vehicle produces far worse conditions than the HS20-44. The Permit Vehicle loading is always in compression, whereas the HS20-44 vehicle vascillates between tension and compression.

4.1.4 Horizontal Reactions

Plots of horizontal longitudinal reactions at the four support points are shown in figures 40 - 45.

In a pp/rr situation, there are only two pins, and thus their forces must be equal and opposite, since they must sum to zero. This is indeed the case for the intact bridge. It should also be noticed that for symmetrical loading conditions (3, 4, and 6) there are no horizontal forces.

In a pp/pr situation the third pin is added on the unloaded side, that is, the "right" side, as viewed in the top view of figure 2. With the addition of the third pin, there is a great increase in reactions, of varying magnitudes, depending on the symmetry of the loading. Symmetrical loadings show an enormous increase from zero to almost 140 kips for load condition 6. Non-symmetrical loading conditions also show very large increases, though they end with substantially smaller reactions. In all cases, however, virtually all the force is taken by the two right side pins, #9 and #11.

Adding a fourth pin shows a return to symmetrical response. For symmetrical loading conditions there is two-way symmetry; for non-symmetrical loadings, there is symmetry only about midspan. For these non-symmetrical cases the left pins take substantially more load than the right pins, with the degree of asymmetry increasing with the asymmetry of the loading. It can also be seen that the fourth pin produces no change in the maximum force for symmetrical conditions.

The addition of dead load causes a great increase in the reactions, but the tendencies remain the same as for live load only. This is because superposition is used for the dead load cases, and dead load is also symmetric. Comparing

load conditions 2 and 5, some interesting results are discovered. For symmetrical support conditions (cases 1 and 3) the Permit Vehicle produces significantly worse effects than the HS20-44 vehicles. For case 2, however, the HS20-44 vehicles produce reactions 2.5 times greater than the Permit Vehicle. For symmetrical load condtions 4 and 6 the Permit Vehicle causes stresses 25% greater than the HS20-44 vehicles.

4.2 Crack Level 1

4.2.1 Midspan Deflections

The midspan live load deflection profiles for cases 4 - 6 are shown in figures 46 - 49.

Comparing case 4 to case 1 it can be seen that for a pin-pin/roller-roller (pp/rr) condition, the introduction of a small crack causes an increase in deflection of 50% on the left side (cracked and loaded side). The deflections on the right side are virtually unchanged by the crack. Case 5 shows the same progression as case 2, that adding another pin on the right side reduced the right side deflections by 50%, while the deflections on the left side remain unchanged. And from case 6 it can be seen that adding the fourth pin reduced the left side deflections by 50%.

Now that damage has been imposed on the structure, it is no longer symmetrical, and it will no longer show symmetrical response to any loading condition. From cases 4 and 6, it can be found that the symmetrical loading cases show a response which is not symmetrical by approximately 30%, and which is greater on the cracked side, as was expected.

Comparing load conditions 2 and 5, it can again be found that the Permit

Vehicle provides a more severe response. It gives a deflection 60% greater on the left side than the HS20-44 vehicles, and again has a positive deflection on the right side. Load conditions 4 and 6 show that for symmetrical loading, the Permit Vehicle gives a response which is consistently 20% greater than the HS20-44 vehicles.

When dead load is added to the first cracked condition (figures 49 - 51), a greater deflection occurs on the cracked side than the uncracked side. Because the dead load is a symmetrical loading, it will show a greater response on the cracked side. And because it is a greater load than the live load, it again tends to "wash out" the effects of the vehicle loadings.

The effect of added pins, however, can still be seen in cases 4 - 6. The effect of the third pin is even greater here, as it decreases the right deflections by 50 - 75%. The left deflections remain constant as before. The effect of the fourth pin is also significant, as it reduces the left side deflections by 60 - 70%. It is noteworthy to observe that the extra pins have a greater effect in reducing deflections after the crack is imposed than in the intact bridge.

4.2.2 Bottom Flange Stresses

Plots of bottom flange stresses for a bridge with a small crack are shown in figures 52 - 63.

Comparing these to the plots for the intact bridge, it can be seen that the small crack causes very little change in any stresses under pp/rr and pp/pr conditions. The stresses at each point are virtually identical to the intact bridge. Adding a third pin has the same effect as before of causing the right side to go into compression near the supports and to remain in tension near midspan.

Adding a fourth pin has a slightly greater effect, since it is on the cracked and loaded side. The right side stresses remain unchanged, but the left side stresses decrease about 1 ksi for live load and 3 ksi for live plus dead load.

Although the stresses changed very little in most instances here, it is important to note the beginnings of an important trait: the lack of symmetrical response under symmetrical loading and support conditions. For example, in case 4 load condition 6 there is a slight difference between the left and right side stresses under live load, and a difference of 0.5 ksi under live plus dead load. This becomes even more evident under pp/pp conditions, as seen in case 6. Here the left and right stresses differ by almost 1 ksi for live load only, and over 2.5 ksi for dead plus live. It appears as if the right side remained constant and the left side changed, with the left side having a numerically lower stress at all times.

4.2.3 Total Longitudinal Slab Stress

Plots of total longitudinal bottom fiber stress in the slab across the transverse direction at midspan are shown in figures 64 - 69.

One obvious change which can be seen here is that the compressive stresses on the left side have decreased over 50%, i.e., they have become more positive, for all load conditions. No longer do the symmetrical cases produce symmetrical results; rather, the stresses on the cracked side have become less compressive. The unsymmetrical cases produce an analagous situation: the loaded side has stresses approximately equal to those on the unloaded side. Thus, the crack seems to want to place the slab in tension.

The addition of the third pin makes a small (10 - 20%) decrease in the compressive stresses on the right side. The left side stresses remain

approximately the same.

Adding a fourth pin to the structure produces no changes in the right side stresses, but the left side stresses increase in compression by 50-75%. In spite of this increase, the right side has a compression stress 30% less than in case 3. However, the maximum compressive stress is still only 160 psi, and is in no danger of cracking.

By adding the dead load, there is a reversal of the trends noted in the uncracked structure. Now the stress under the load is in less compression than the unloaded side, which is opposite to the uncracked bridge. The stresses also tend to be more "grouped" than before, varying from -.3 to -.45 ksi on the right and -.1 to -.15 ksi on the left.

Again it is apparent that the third pin makes little difference.

The fourth pin has the same effect as before, reducing the stresses significantly across the width. All stresses are now in compression, and are contained in a smoother and narrower band.

4.2.4 Horizontal Reactions

Horizontal reactions in the longitudinal direction for crack level 1 are shown in figures 70 - 75.

For a pp/rr situation, the forces are no longer zero for the symmetrical load conditions, but reactions of approximately 1 kip. Reactions for the other loadings have increased 30% to 50%.

Adding the third pin for case 5 shows tendencies and results almost identical to case 2. The only difference is a very small increase in the force taken by pin #10.

Case 6 shows the same tendencies as case 3, but no longer is there

symmetry. The forces remain nearly constant on the right side, but forces on the left increase approximately 15%.

Load conditions 2 and 5 show tendencies similar to the intact structure. For cases 4 and 6, the Permit Vehicle loading is worse; for case 5, the HS20-44 loading is worse. In load conditions 4 and 6, the Permit Vehicle consistently causes greater reactions.

4.3 Crack Level 2

4.3.1 Midspan Deflections

The live load deflection profiles for cases 7 - 9 are shown in figures 76 - 78.

For the pp/rr condition there is a very large increase in the left side deflections. The maximum deflection is now 4.7", or five times that of the intact bridge, and 3.5 times that of the crack level 1 bridge. The shape of the curves has also changed at this point. No longer are the curves smooth, but instead there are extremely large deflections on the left under the point of load, with constant slope to a near-zero deflection on the right. And, of course, there is no symmetry in the response. It should also be noticed that the right side deflections have actually decreased a fraction of an inch due to uplift from the tremendous left side deflections.

Adding the third pin to the structure seems to have a negligible effect on the deflections. This is most likely due to the extreme nature of the left side deflections, which may "wash out" any noticeable reduction on the right side.

The fourth pin has a dramatic effect on the left side deflections, reducing them by a factor of five, and to a level almost equal to case 1. This implies

that the fourth pin will inhibit the crack opening from widening, and thus reduce the effect of the crack. This argument is further supported by noting that the deflected shape in the pp/pp situation has become much smoother and almost approximates a symmetrical response for the symmetrical loading conditions. Additionally, it should be noted that the fourth pin has little effect on the right side deflections.

Comparing load conditions 2 and 5, the Permit Vehicle again has a 50% higher maximum deflection than the HS20-44 vehicles, and it still has a positive (upward) deflection on the right side due to uplift. Comparison of load conditions 4 and 6 shows that the Permit Vehicle produces deflections which exceed those of the HS20-44 vehicles by 20%. These ratios remain nearly constant regardless of the support conditions.

After adding the dead load (shown in figures 79 - 81), the deflected shapes have nearly constant slopes. The maximum deflection is now -12.7" for load condition 5. It can also be seen that the third pin makes virtually no difference, implying that the effect of the crack outweighs the effect of the pin.

The addition of the fourth pin reduces the left side deflections ten-fold, to a level 1.5 times that of case 6. The shape of the deflection curves becomes much smoother, although there is no longer any approximation of symmetry. The dead load has become the predominant factor determining the level of deflection, making all deflection curves somewhat the same. It is therefore pointless to make comparisons between load conditions.

4.3.2 Bottom Flange Stresses

Plots of the bottom flange stresses for a bridge with a mid-depth crack are shown in figures 82 - 93.

With the larger crack, the changes in stresses are no longer small, as they were from crack level 1. There are now significant increases in stress, although there are no stresses which approach a critical level.

One obvious change that can be seen is the increased lack of symmetrical response for symmetrical cases. For load conditions 4 and 6 there is a difference of 0.5 - 1.0 ksi between left and right side stresses for live load, and 2 ksi for dead plus live load. It is interesting to note that for these cases, the right side stresses increase while the left side stresses decrease by the same amount, so that the undamaged side is forced to take more of the load.

For most cases under pp/rr and pp/pr conditions, the increased crack size caused significant increases in stresses. When a fourth pin is added, the stresses show a substantial increase. Between cases 3 and 6, the maximum compressive stresses more than double. For symmetrical load condition 4, the stresses at the supports increase from less than 2 to over 4 ksi in compression. When dead load is included, compressive stresses increase from 8.7 ksi to 19 ksi. Near midspan, tension stresses remain near a constant level of 0 ksi for live and a maximum of 6 ksi for live plus dead. It is also interesting to note that at the supports the most extreme stress is on the left side and in compression, while at midspan the most extreme stress is on the right and in tension. There also remains a nearly constant difference of 2 ksi between left and right for live load, and 7 - 10 ksi for live plus dead. For non-symmetrical load case 5, the same tendencies are observed, yet the maximum compressive stress is now 23

ksi.

4.3.3 Total Longitudinal Slab Stress

Plots of total longitudinal bottom fiber slab stress (membrane plus bending) at midspan are shown in figures 94 - 99.

Applying a mid-depth crack to the left girder produces a very large increase in the stresses on the left side of the slab. In the pp/rr condition, there are stresses up to 1.7 ksi, well above the tensile strength of concrete and most likely cracking the slab across the entire width of the bridge. Stresses on the right side increase slightly, but still remain near zero or slightly in compression. The curves have become very "grouped". They show no symmetry, but show a consistent tendency of tensile stresses under the load and crack.

As found previously, adding the third pin opposite the crack causes no noticeable reduction in stresses.

The presence of the fourth pin, however, causes a very large reduction in stresses throughout the slab. Once again stresses are small ($\pm$100 psi) and appear to be scattered, though they appear to be slightly in compression under the load. The results of this plot show similarities to cases 1 and 3.

It is also very important to notice the similarities between the behavior of the slab stresses and midspan deflections when the fourth pin is added. Here the stresses show an enormous decrease when the fourth support is fixed; similarly the midspan deflections dropped severely under the same condition. This implies that the fourth pin tends to quell the effect of crack by preventing it from "opening."

Adding the dead load to the structure shows the same effects as live load

alone, only the results are more disasterous. There are now tensile stresses up to 4.5 ksi, producing cracking of the slab. Again the third pin causes no change in behavior.

Again the fourth pin causes a reduction in stresses, so that they are still "grouped", yet small ($\pm$300 psi). They also still show tensile stresses under the load and crack.

4.3.4 Horizontal Reactions

Horizontal reactions in the longitudinal direction for crack level 2 are plotted in figures 100 - 105.

As the crack depth increases from 14% to 74% there is a great increase in reactions. For the pp/rr condition in case 7, the reactions are five times the values of case 1, with a maximum of over 20 kips from load condition 5. There is a lack of symmetry from loading conditions 3, 4, and 6, which also show stresses ten times greater than in case 7.

In a pp/pr situation there is again a great increase in stress, with most of the load being taken by the right side pins. For symmetrical cases, this force is opposed by pin #9 on the right. For non-symmetrical loadings, more force is taken on the left, so that the greatest reactions are diagonally across from one another. The asymmetry of the reactions increases with the asymmetry of the loadings. The reactions have not increased from case 5 to case 8, but the distribution has shifted greatly, with less force being taken by pin 9, and more force being taken by pin 10. It should also be noted that the reactions are generally greater for non-symmetrical support conditions (pp/pr) than for symmetrical supports.

In case 9 (pp/pp) there is again more force taken on the left for non-

symmetrical cases. There is also an increase in the asymetric response of the symmetrical cases, such that more force is taken on the left side. In addition, the magnitudes have increased another 40% - 50% over case 6, to levels that are almost double those in case 3.

4.4 Crack Level 3

4.4.1 Midspan Deflections

As seen in figures 106 - 111, increasing the damage to a full-depth crack further increases the deflections. For the pp/rr condition in case 10, it can be seen that the deflections again double over the level of case 7, to a level ten times that of case 1. The deflection curves again have nearly constant slopes, with a maximum deflection under the point of the load, and a near-zero deflection on the right. All load cases tend to "bunch" together and show no symmetry in any case. As before, the third pin makes virtually no change.

When adding the fourth pin (case 12), the deflections decrease by a factor of 10, and return to a level comparable to case 9 (pp/pp) and case 1 (pp/rr). The curves have also become much smoother and within 30% of being symmetrical. This again shows that the effect of the fourth pin is to close the crack.

Comparisons of load conditions are identical to those in crack level 2.

The results of adding dead load are shown in figures 109 - 111. The maximum deflection now approaches 24", and the curves vary linearly to zero from left to right. Again the third pin makes little, if any, improvement.

The fourth pin reduces deflections on the left side to one-tenth their unpinnned level. The deflections are now similar to those in case 9, and twice

those in case 3.

4.4.2 Bottom Flange Stress

Plots showing bottom flange stress for a full-depth crack are shown in figures 112 - 123.

It is found that the larger crack causes a further increase in stresses throughout the bridge. However, the increase is small compared to the increase caused by the mid-depth crack.

Under a pp/rr situation, the stresses again continue to stray from any sort of symmetrical response under symmetrical conditions. The right side stresses continue to increase slightly, and the left side stresses decrease by the same amount. This effect is more pronounced under dead plus live conditions than under live load alone.

Under pp/pr conditions, the same tendencies are seen, but the response curve is slightly more even. For the non-symmetrical load conditions it can be seen that the right side stresses under live load approach zero.

When the fourth pin is added, the compression stresses in the left side continue to become greater, to a maximum of 25 ksi. The difference between right and left side stresses also increases slightly, but much less than the increase caused by crack level 2.

4.4.3 Total Longitudinal Slab Stress

Plots showing the variation of longitudinal bottom fiber slab stress (membrane plus bending) across midspan are shown in figures 124 - 129.

The full-depth crack under pp/rr conditions shows behavior very similar to the mid-depth crack in section 4.3.2. There are very high tensile stresses under the load and crack, yet the values are much higher, with a maximum value of +5.5 ksi. This will certainly cause cracking of the slab. The right side stresses have also increased to a value near zero.

The addition of a third pin causes no real changes, yet the fourth pin helps greatly. The plots are still "grouped" and in tension, showing the presence of the crack, yet there is also a twenty-fold decrease in stresses, to a maximum of +300 psi. This may or may not cause cracking in the slab. The maximum stress is still three times the value found in case 9 (mid-depth crack).

The addition of the dead load shows effects similar to, yet worse than, those found from the mid-depth crack. Stresses up to almost +16 ksi can now be found, instead of +5 ksi in case 7.

Again the third pin helps little, and the fourth pin causes a dramatic reduction in stresses. The right side stresses are still the same as in case 9; the left side shows a fifteen-fold decrease in stress, to a maximum of +0.8 ksi, or 2 - 5 times those in case 9.

4.4.4 Horizontal Reactions

Horizontal reactions in the longitudinal direction for crack level 3 are shown in figures 130 - 135.

In case 10 there is a further doubling of reactions from the larger crack. The maximum forces are now 10 times greater than in case 1, with a maximum of 38 kips.

The addition of the third pin in case 11 produces increases reactions as before, with the resulting stresses only 10% greater than in case 8. In addition, pin #10 (left) takes more load than before, and increases the diagonal reactions. For symmetrical loadings, pins 9 and 11 continue to take the majority of the force, though pin 10 takes slightly more than before. Non-symmetrical loadings produce highly unsymmetrical responses, with pin 10 taking most of the load.

Case 12 shows tendencies as before, with 10% higher stresses than in case 9. The proportions taken by various pins remain the same.

4.5 Bottom Flange Model

4.5.1 Description

In any steel girder bridge, there is the possibility of large stresses caused by transverse (i.e. out-of-plane) differential translation of the girder web. The repetitive nature of the live loading can also lead to fatigue failure, since the stresses applied will vary in a cyclical manner. Extensive study in this area has been performed and presented in a report (see reference 8).

In this bridge, the possibility of such translation occurs in the girder web between the bottom of the floor beam and the lower girder flange. Here the point of the web intersecting the floor beam and the web at the bottom flange

will show individual displacements (delta z). The difference in these two translations, referred to as "delta-delta", is the cause of the large stresses.

To more accurately determine the stresses in this area, a finite element submodel was constructed of a vertical section of the web at midspan. Beam elements were used, where the longitudinal dimension of the beam modelled the vertical dimension of the web. Further, a unit width of the web was taken as the width (b) of the beam, and the thickness of the web was used for the thickness (h) of the the beam. Displacements and rotations were applied at each end of the beam as found from the output of the global bridge model. The submodel then outputted the stresses at each point along the length of the web.

4.5.2 Results

The maximum stresses for each of the 12 cases are shown in tables 7 and 8. The stresses for the intact structure are very low, and generally lie below 1 ksi. As the crack is imposed, the stresses increase gradually. The addition of a fourth pin in the structure causes a distinct decrease in stress from delta-delta, as observed in previous conditions. When a full-depth crack is imposed, the stresses increase greatly. For live load alone, the maximum stress is over 20 ksi; for live plus dead load, the maximum is 40 ksi.

In addition to checking the maximum stresses in the web, it is also necessary to consider the live load stress range as discussed in section 10.3 of the AASHTO specification. From this it is possible to determine whether fatigue cracking could result. From table 7 it can be seen that for load conditions 2, 4, and 6 the maximum stress range is less than 15 ksi. The AASHTO specifications indicate that this range will allow over 2,000,000 cycles

without being in danger of crack propogation. Load condition 5 causes stresses up to 22 ksi, limiting it to only 100,000 cycles. However, since this is a maximum one-time permit loading, it is unlikely that this loading would propogate cracking.

These data show that for a normal intact structure, the stresses causes by the delta-delta effect are not critical. It is, then, a local effect. However, as the depth of the crack increases, the stresses become critical and must be taken into consideration.

It is important to recall, however, that the model used in this study was designed with the intent of showing global behavior of the bridge. Thus it is a relatively crude model, and such fine measurements as these must be studied more carefully before any definite conclusions can be reached.

Chapter 5
Summary

5.1 Behavior of Intact pp/rr Bridge

The initial bridge behaved as would be predicted. Some of its tendencies are as follows.

1. The bridge showed a symmetrical response for symmetrical loading conditions (lc 3, 4, & 6). This was due to a completely symmetrical bridge (girders, floor beams, stringers, deck), symmetrical support conditions, and the symmetrical loadings. This also helped to verify the accuracy of the model.

2. The largest deflection at midspan was under the load, whether for symmetrical or non-symmetrical load condition.

3. Stresses in the bottom girder flanges were in tension at all points along the length. At points of change in cross-section, the stress increased at each location, with the exception of the fourth point, at which it decreased slightly.

4. Longitudinal bottom fiber slab stresses (membrane plus bending) at midspan were very small (60 - 200 psi), and the deck was in no danger of failing.

5. Horizontal reactions at the pins were very small, being less than 4 kips under any non-symmetrical loadings. Under symmetrical loadings, the horizontal reactions were zero.

6. In most conditions, the addition of the dead load "washed out" the effect of the live load, due to the greater size of the load.

5.2 Effect of Cracks

The three crack levels changed the behavior of the bridge, sometimes quite significantly. The major tendencies of the cracks are listed below.

5.2.1 Crack Level 1

Overall, the effect of the smallest crack was minimal, though there are a few exceptions. The most notable effect was a lack of symmetrical response under any conditions. Though this difference was small, it showed a tendency which would later increase.

1. The midspan deflections increased by approximately 50% on the left (loaded & cracked) side. Right side deflections remained constant.
2. Bottom flange stresses remained constant.
3. Slab stresses became less compressive, and approached zero stress.
4. Horizontal longitudinal reactions increased slightly. No longer were there zero stresses for symmetrical loadings.

5.2.2 Crack Level 2

The increase from a 14% crack to a 74% crack showed the most significant changes to the behavior of the bridge. Here the stresses increased greatly, and deflections became very large. In addition, the curves became very "grouped" and had constant slopes, as the effect of the crack concentrated itself under the point of load and location of the crack. More specific tendencies are listed below.

1. Midspan deflections increased five-fold over the intact condition under the point of load. Sometimes this caused an upwared deflection on the right side, due to the uplift from the large left-side deflections.
2. Bottom flange stresses doubled again.
3. Bottom fiber slab stresses increased greatly to 1.7 ksi in tension. This will certainly cause failure of the slab.
4. Horizontal longitudinal reactions increased five-fold. This effect parallels the flange stresses, as an increase in one causes an increase in the other.

5.2.3 Crack Level 3

The full-depth crack causes further increases in the stresses and deflections in the bridge. The increases are generally not as large, however, as those from the second crack level. The curves continue to have constant slopes, especially after the addition of the dead load.

1. Midspan deflections again double, to a maximum of almost two feet (24").
2. Bottom flange stresses increase slightly again, but are not in danger of yielding.
3. Bottom fiber slab stresses continue to increase. Stresses are now well beyond failure level, and it is likely that the slab will completely fail in the transverse direction.
4. Horizontal longitudinal reactions again double.

5.3 Effects of Support Conditions

The addition of the third and fourth pins to the supports produced distinct and unique results.

5.3.1 Effects of PP/PR

The addition of the third pin (see section 3.2) had significant effects on the structure in the intact condition. As the level of the crack increased, however, this pin had increasingly less influence on behavior.

1. Midspan deflections decreased on the right side (pinned side), but not on the left side for the intact structure. This pin had less and less effect as the crack size increased, and had no effect on the fully-cracked bridge.
2. Bottom girder flange stresses on the right side went from being fully in tension to being in compression at the supports and in tension near midspan. The curves showed an approximately parabolic increase in stresses from compression to tension.

3. Longitudinal bottom fiber stresses in the slab changed very little.

4. Horizontal longitudinal reaction forces were taken on the right by pins 9 and 11 for the intact structure. As the crack level increased, more load was taken diagonally across the structure by pins 10 and 11.

5.3.2 Effects of PP/PP

The fourth pin (see section 3.2) had an important effect on the bridge, and produced effects much more noticeable than the third pin.

1. The pin prevented the structure from expanding longitudinally on the left side, and thus inhibited the opening of the crack. This significantly reduced the effect of the crack.

2. Midspan deflections decreased significantly (up to twenty-fold) on the left side, but not on the right side. This effect increased with the size of the crack. The deflections from the fully-cracked pinned bridge (case 12) were approximately equal to those of the intact pp/rr bridge (case 1).

3. The left side bottom girder flange stresses also went to compression at supports and tension near midspan.

4. Bottom fiber slab stresses changed very little for the intact structure. However, as the crack size increased, the lack of crack opening caused the stresses to drop from disasterous values to a non-critical level.

5. Horizontal longitudinal reactions increase greatly as the fourth pin attempts to prevent the crack from propogating. This pin prevents the crack from opening, but as a result, horizontal reactions become very large.

5.4 Comparison of Load Conditions

In this study six live load conditions were studied. To determine the worst loading situation, various conditions were compared, usually comparing two HS20-44 vehicles to one Permit Vehicle. Load condition 2 (LC-2, two HS20-44 at edge) was compared with LC-5 (one Permit at edge); LC-4 (two AASHTO at centerline) was compared with LC-6 (one Permit at centerline). LC-1 (one HS20-44at edge) and LC-3 (one HS20-44 at centerline) were not found to be critical, and thus were not included in the final comparisons.

The comparisons were initially made for an intact bridge; it is found, however, that the same tendencies hold for the damaged bridges. The one exception to this is in the slab stresses: in the last two crack conditions, stresses are so high that all load conditions produce similar results, and cracking has occured, making any comparisons worthless.

The following results were determined:

1. LC-5 produces maximum midspan deflections 50% greater than LC-2. LC-5 is much more skewed, and shows slightly positive deflections opposite the load.

2. LC-6 produces deflections 20% greater than LC-4 across the entire width of the slab.

3. LC-5 causes bottom flange stresses three times those of LC-2 for pp/rr and pp/pr conditions. For pp/pp situations, this difference drops to 20%. LC-5 is more skewed than LC-2, and shows only residual stresses opposite the load.

4. LC-6 shows stresses 25 - 50% higher than LC-4 for unpinned girders. When pins are added to either side, that side shows similar stresses for LC-4 and LC-6.

5. For the intact bridge, LC-5 shows approximately 50% higher stresses than LC-2, and LC-6 shows stresses 20% higher than LC-4.

6. For horizontal reactions, LC-5 produces forces twice as great as LC-2

for symmetrical support conditions (pp/rr & pp/pp). Conversely, LC-2 produces forces 2.5 times as great as LC-5 for non-symmetrical support conditions (pp/pr).

7. LC-6 causes horizontal reactions 20 - 50% greater than LC-4.

5.5 Condition and Repairability of Bridge

This study was concerned with the redundancy of two-girder bridges. Part of its intent was to determine the level of damage sustained by the bridge if a main girder was cracked, and to learn whether the bridge would be damaged yet repairable, damaged irreparably, or would collapse entirely.

The study shows the following results:

1. The intact bridge fully loaded shows no yielding.

2. Crack level 1 produces high deflections, but probably no yielding of steel, and no cracking of the slab. This bridge is probably repairable.

3. Crack level 2 produces large deflections and cracking of the slab, but the girders should not yield. There is a possibility that the bridge would not collapse, yet be irreparable.

4. Crack level 3 would crack the slab across the width of the bridge but would not cause yielding in the girders. It would experience very large deflections. There is a possibility that the bridge would not collapse, yet it is difficult to discern whether or not it could be repaired.

5.6 Further Research

This report has studied the effect of applying various support, loading, and crack conditions to a two-girder bridge. Yet there are many more parameters which could be considered. Some examples of this are:

1. Study results 3 & 4 of section 5.5 further using a non-linear analysis to determine the final condition of the structure.

2. Apply a partial longitudinal restraint to the bridge at the level of the slab.

3. When the slab reaches its yield point, remove it from the model, since it can no longer provide support.

4. Apply the third pin on the loaded and cracked side.

5. Study the effect of the cracked girder on the floor beams.

6. Provide only partial longitudinal restraint for two of the pins in a pp/pp condition.

References

1. Kostem, Celal N., "User's Manual for Program SPLT," Fritz Engineering Laboratory Report No. 400.29, January 1985.

2. Kostem, C. N., Sap IV Commentary

3. Bathe, K.-J., Wilson, E. L.; Peterson, F. E.; "SAP4 - A Structural Analysis Program for Static and Dynamic Response of Linear Systems," EERC Report 73-11, University of California at Berkeley, Berkeley, CA, 1973.

4. Reference Manual, Lotus 1-2-3, Release 2; Lotus Development Corporation Inc., Cambridge, MA, 1985

5. Freestyle User's Guide, Select Information Systems, Inc., Kentfield, CA; 1984.

6. Standard Plans for Highway Bridges, Volume-II, Structural Steel Superstructures, Federal Highway Administration, Washington, D. C., 1968.

7. Chen, S. S., Daniels, J. H., Wilson J. L., "Computer Study of a Single Span Two-Girder Bridge, Interim Report," Fritz Engineering Report 503.1, March 1986.

8. Fisher, Thomas A., Kostem, C. N,; "The interaction of Primary and secondary members in Multi-Girder Composite Bridges using Finite Elements," Fritz Lab Report No. 432.5, June 1979.

ACKNOWLEDGMENTS

The authors would like to thank Major Thomas A. Lenox for the preparation of the finite element model, without which, this project would not have been possible; Mr. Gary C. Ormiston for his invaluable input concerning the bridge behavior and the organization of the report; and the Lehigh University Computing Center for their assistance with the computing facilities.

E = 29000 ksi v = 0.3 in/in

A441 steel

$\alpha_x = \alpha_y = \alpha_z = 0.0$

weight density = 0.00029 kip/in^3

$C_{xx} = E/(1-\nu^2) = 31868$ ksi $C_{xs} = 0.0$

$C_{xy} = \nu E/(1-\nu^2) = 9560$ ksi $C_{ys} = 0.0$

$C_{yy} = C_{xx} = 31868$ ksi $G_{xy} = E/2(1+\nu) = 11154$ ksi

Web size = 97.5" x 0.375"

Top and Bottom Flange Sections

	1	2	3	4
b	21.0	24.0	24.0	24.0
h	1.0	1.5	2.25	2.5
axial area	21.0	36.0	54.0	60.0
shear area 2	0.0	0.0	0.0	0.0
shear area 3	0.0	0.0	0.0	0.0
torsional	7.0	27.0	91.1	125.0
I_2	771.8	1728.0	2592.0	2880.0
I_3	1.75	6.75	22.8	31.3

formulas : axial area = b x h

$I_3 = bh^3/12$ $I_2 = hb^3/12$

torsional = $bh^3/3$

Table 1: Material and Section Properties for Girders

$E = 29000$ ksi $\quad \nu = 0.3$

A36 steel

weight density $= 0.00029$ kip/in^3

$C_{xx} = E/(1-\nu^2) = 31868$ ksi $\quad C_{xs} = 0.0$

$C_{xy} = \nu E/(1-\nu^2) = 3560$ ksi $\quad C_{ys} = 0.0$

$C_{yy} = C_{xx} = 31868$ ksi $\quad G_{xy} = E/2(1+\nu) = 11154$ ksi

$\alpha_x = \alpha_y = \alpha_z = 0.0$

web size $= 58" \times 3/8"$

Flanges:

$b = 12$ in. $\quad h = 1$ in.

axial area $= 12 \times 1 = 12$ in^2

shear area 2 $=$ shear area $3 = 0.0$

torsional $= bh^3/3 = 4$ in^4

$I_2 = b^3h/12 = 144$ in^4

$I_3 = bh^3/12 = 1$ in^4

Table 2: Material and Section Properties for Floor Beams

WEB

weight density = 0.00029 kip/in^3

$E_n = E_s = E_t$ = 29000 ksi

A36 steel

$\nu_{ns} = \nu_{nt} = \nu_{st}$ = 0.3 in/in

G_{ns} = 11150 ksi

$\alpha_n = \alpha_s = \alpha_t$ = 0.0000065 in/in/F°

FLANGES

E = 29000 ksi

α = 0.0

weight density = 0.00029 kip/in^3

b = 8 1/4 in. h = 1/2 in.

area = b x h = 4.125 in^2

Table 3: Material and Section Properties for Stringers

$f_c' = 3400$ psi $\qquad \nu = 0.2$

$E = 3322$ ksi

thickness $= 7.5$ in

$\alpha_x = \alpha_y = \alpha_z = 0.0$

$C_{xx} = E/(1-\nu^2) = 3460$ ksi $\qquad C_{xs} = 0.0$

$C_{xy} = \nu E/(1-\nu^2) = 692$ ksi $\qquad C_{ys} = 0.0$

$C_{yy} = C_{xx} = 3460$ ksi $\qquad G_{xy} = E/2(1+\nu) = 1380$ ksi

Table 4: Material and Section Properties for Concrete Slab

$E = 3322$ ksi $\qquad \nu = 0.2$ in/in

$f_c' = 3400$ psi

Weight Density $= 0.0000868$ kip/in^3

$I_3 = 40945.5$ in^4 $\qquad I_2 = 2592$ in^4

Torsion $= 6096.4$ in^4

Table 5: Material and Section Properties for Parapet

Case	Intact	Crack Level 1	Crack Level 2	Crack Level 3	PP/RR	PP/PR	PP/PP
1	X				X		
2	X					X	
3	X						X
4		X			X		
5		X				X	
6		X					X
7			X		X		
8			X			X	
9			X				X
10				X	X		
11				X		X	
12				X			X

Table 6: Description of Cases

Stress

Live Load Only

Case	L/R	2	4	5	6	DL only
1	L	0.467	1.068	0.553	-0.771	-0.259
	R	1.082	-1.068	0.910	0.771	0.259
2	L	0.427	0.986	0.570	-5.086	-0.551
	R	1.125	1.233	12.156	0.883	0.666
3	L	0.512	-1.117	0.356	-0.735	-0.293
	R	0.948	1.117	0.641	0.735	0.293
4	L	-0.851	-0.254	-2.367	-0.826	-2.394
	R	-1.516	1.143	-2.151	0.872	1.155
5	L	-1.325	-1.221	-2.515	-2.054	-6.857
	R	-1.623	1.327	-2.174	1.106	2.007
6	L	0.871	-0.482	0.896	-0.264	-0.510
	R	1.078	0.948	-1.240	0.635	0.339
7	L	-7.019	3.376	-11.217	-5.679	-18.581
	R	3.733	2.703	4.924	2.732	7.467
8	L	-7.573	-5.248	-11.430	-6.784	-22.579
	R	3.706	2.651	4.907	2.666	7.232
9	L	0.747	-0.313	0.770	-0.360	0.867
	R	1.433	1.163	-1.613	0.893	1.232
10	L	-13.820	-8.930	-20.962	-11.029	-36.062
	R	5.244	3.875	6.869	4.097	11.379
11	L	-14.327	-9.792	-21.286	-12.122	-40.043
	R	5.180	3.766	6.818	3.960	10.889
12	L	0.695	-0.225	0.803	-0.491	1.007
	R	-1.582	-1.326	-1.558	1.175	1.524

Table 7: Lower Web Stresses

Stress

Live Load + Dead Load

Case	L/R	2	4	5	6
1	L	0.467	1.068	0.553	-0.771
	R	1.082	-1.068	0.910	0.771
2	L	0.427	0.986	0.570	-5.086
	R	1.125	1.233	12.156	0.883
3	L	0.512	-1.117	0.356	-0.735
	R	0.948	1.117	0.641	0.735
4	L	-0.851	-0.254	-2.367	-0.826
	R	-1.516	1.143	-2.151	0.872
5	L	-1.325	-1.221	-2.515	-2.054
	R	-1.623	1.327	-2.174	1.106
6	L	0.871	-0.482	0.896	-0.264
	R	1.078	0.948	-1.240	0.635
7	L	-7.019	3.376	-11.217	-5.679
	R	3.733	2.703	4.924	2.732
8	L	-7.573	-5.248	-11.430	-6.784
	R	3.706	2.651	4.907	2.666
9	L	0.747	-0.313	0.770	-0.360
	R	1.433	1.163	-1.613	0.893
10	L	-13.820	-8.930	-20.962	-11.029
	R	5.244	3.875	6.869	4.097
11	L	-14.327	-9.792	-21.286	-12.122
	R	5.180	3.766	6.818	3.960
12	L	0.695	-0.225	0.803	-0.491
	R	-1.582	-1.326	-1.558	1.175

Table 8: Lower Web Stresses

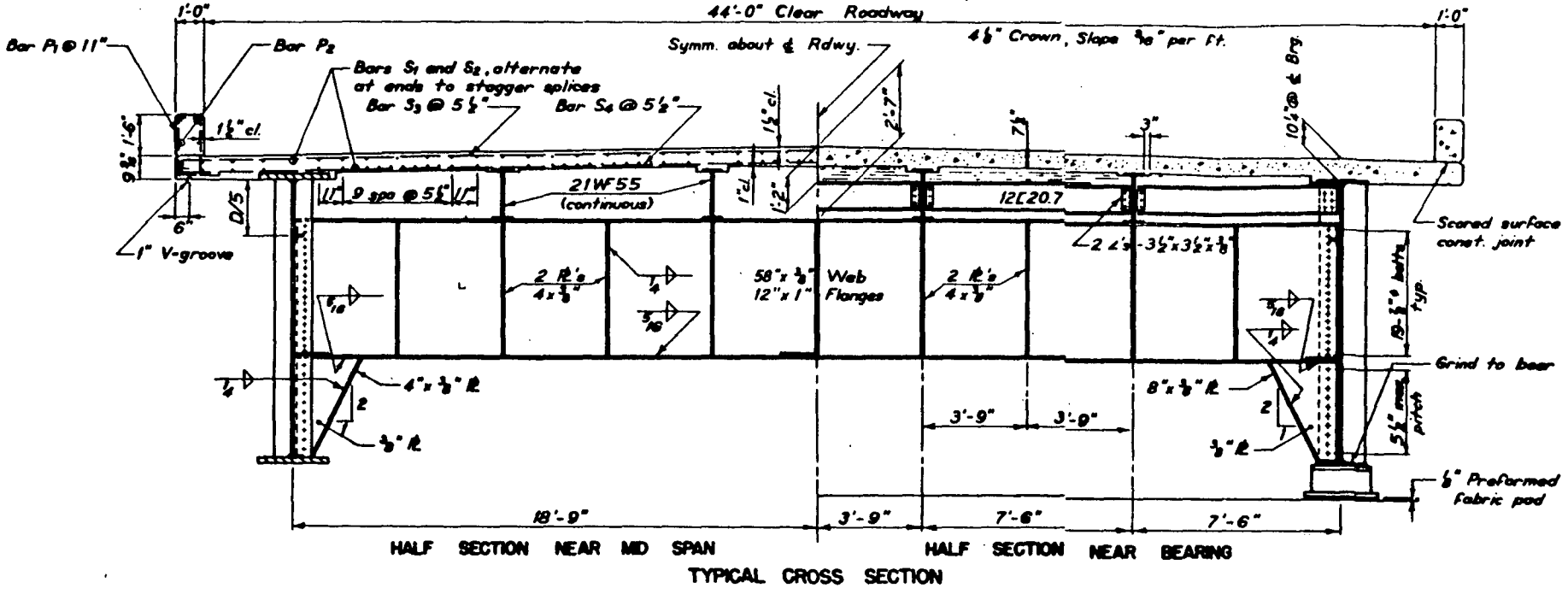

Figure 1: Cross Section of Bridge

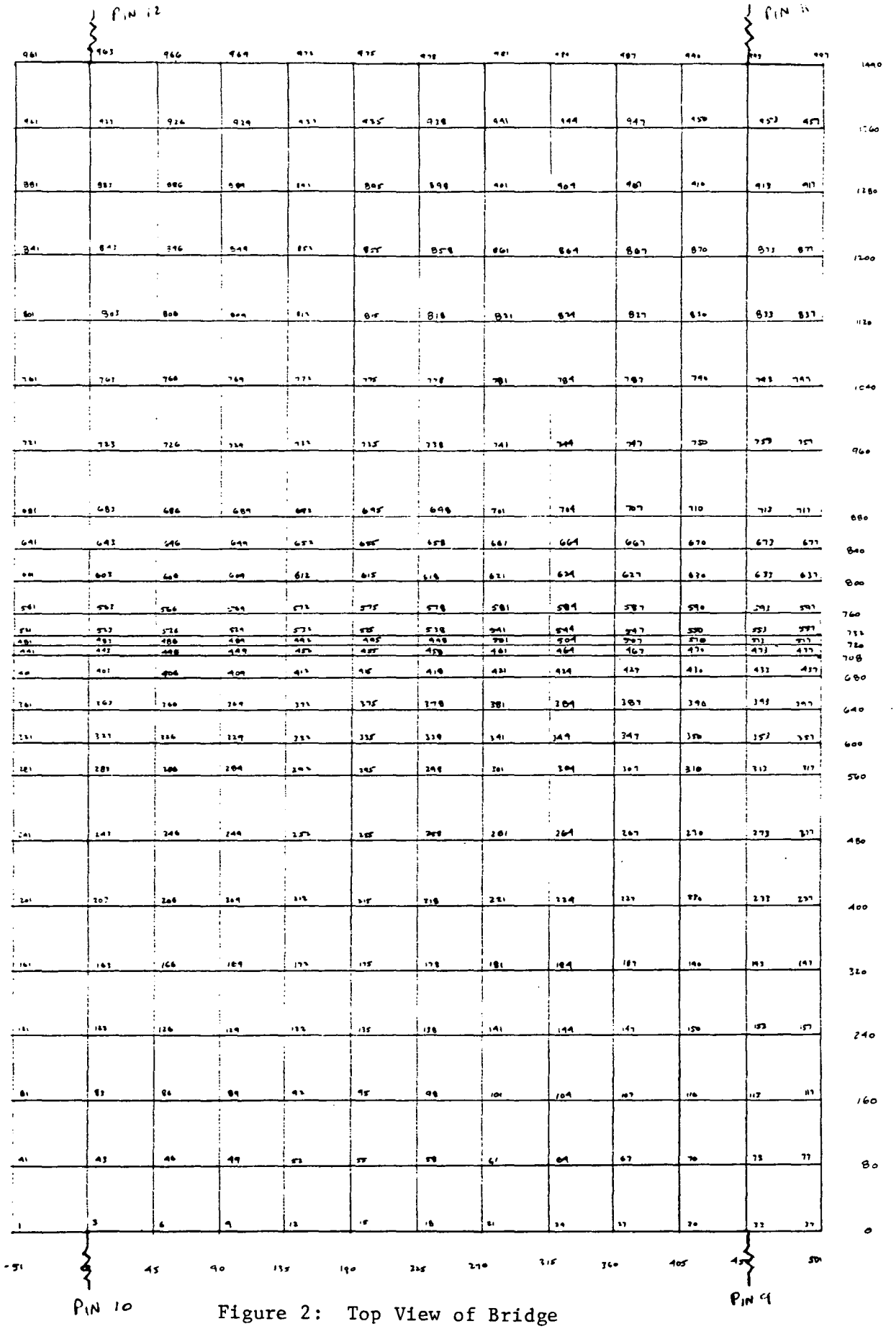

Figure 2: Top View of Bridge

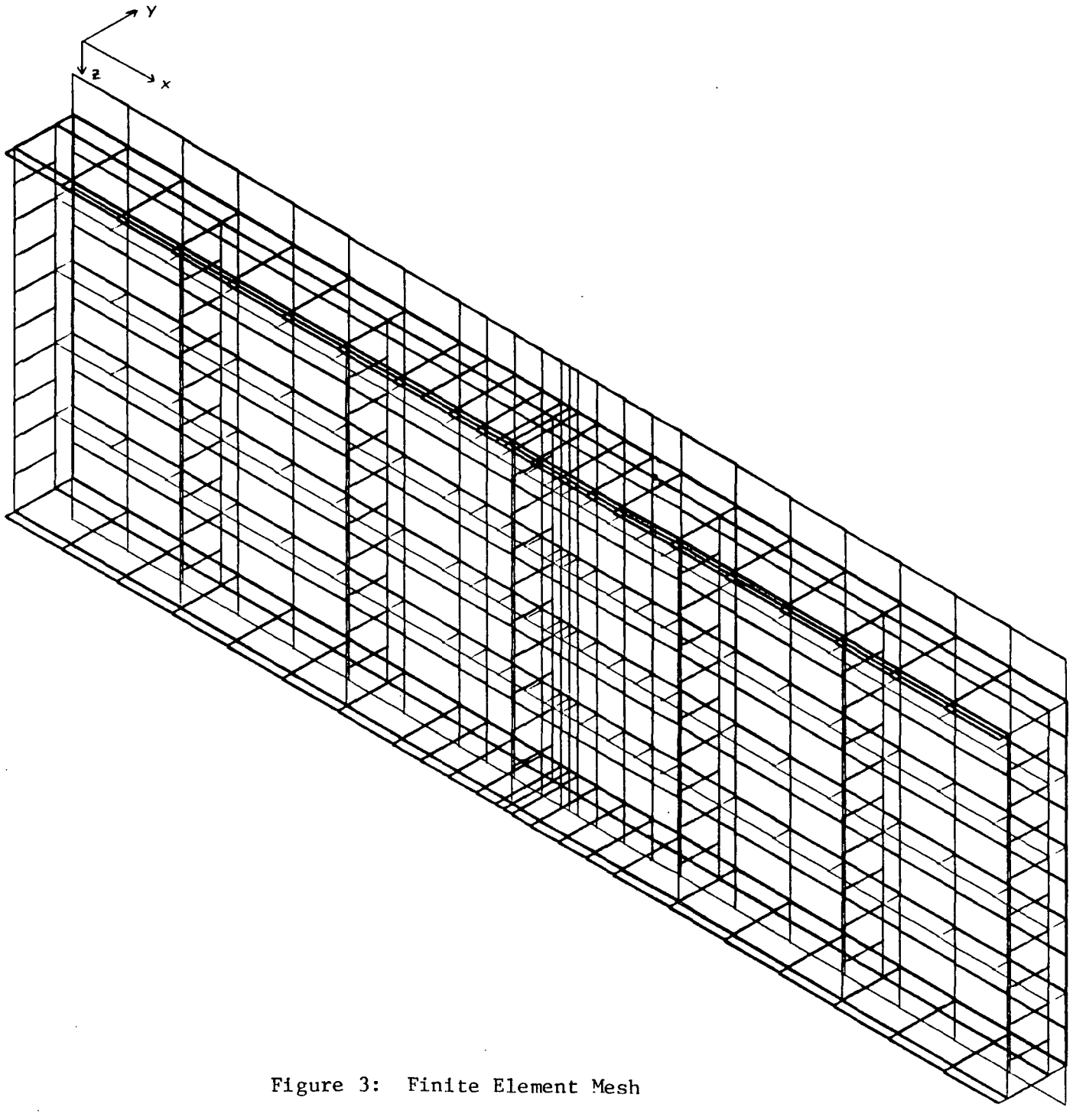

Figure 3: Finite Element Mesh

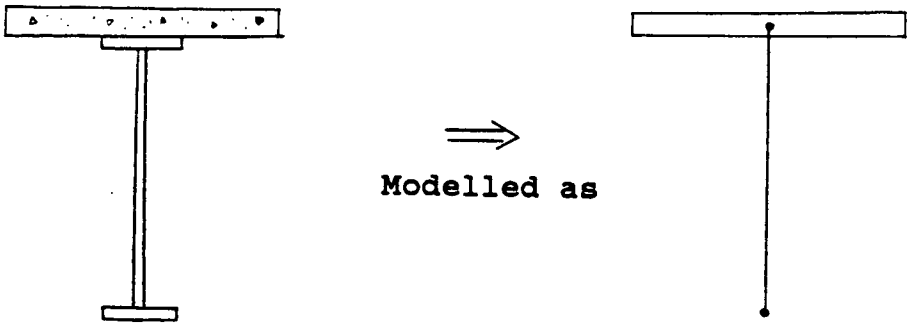

Figure 4: Modelling of Top Girder Flange

1	2	3	4	5	6	7	8	9	10	11	12	13	14	15	16	17	18	19	20	21	22	23	24
1	2	3				7			10				14			17			20			23	24
1	2	3			6			9				13			16			19			22	23	24

Pin # 9 **Right Girder** **Pin # 11**

25	26	27	28	29	30	31	32	33	34	35	36	37	38	39	40	41	42	43	44	45	46	47	48
25	26	27				31				35				39			42			45		47	48
25	26	27			30				34				38			41			44		46	47	48

Pin # 10 **Left Girder** **Pin # 12**

Figure 5: Numbering of Girders

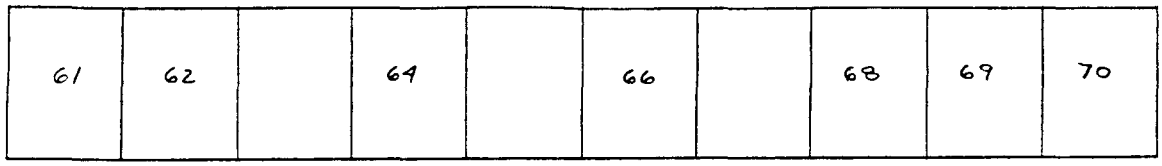

Top Floor Beam

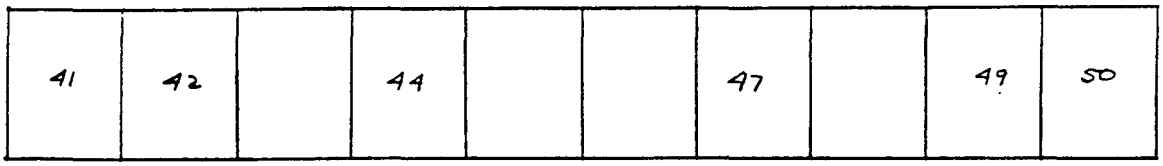

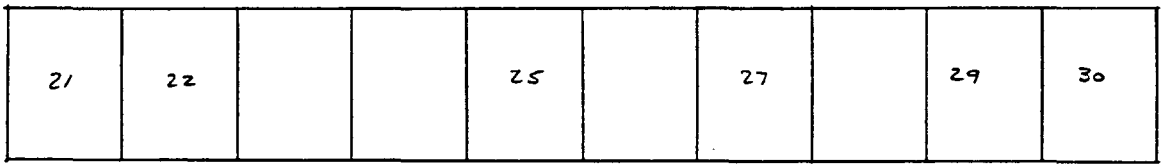

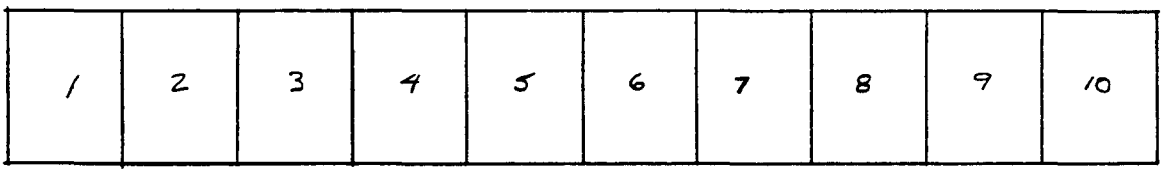

Bottom Floor Beam

Figure 6: Numbering of Floor Beams

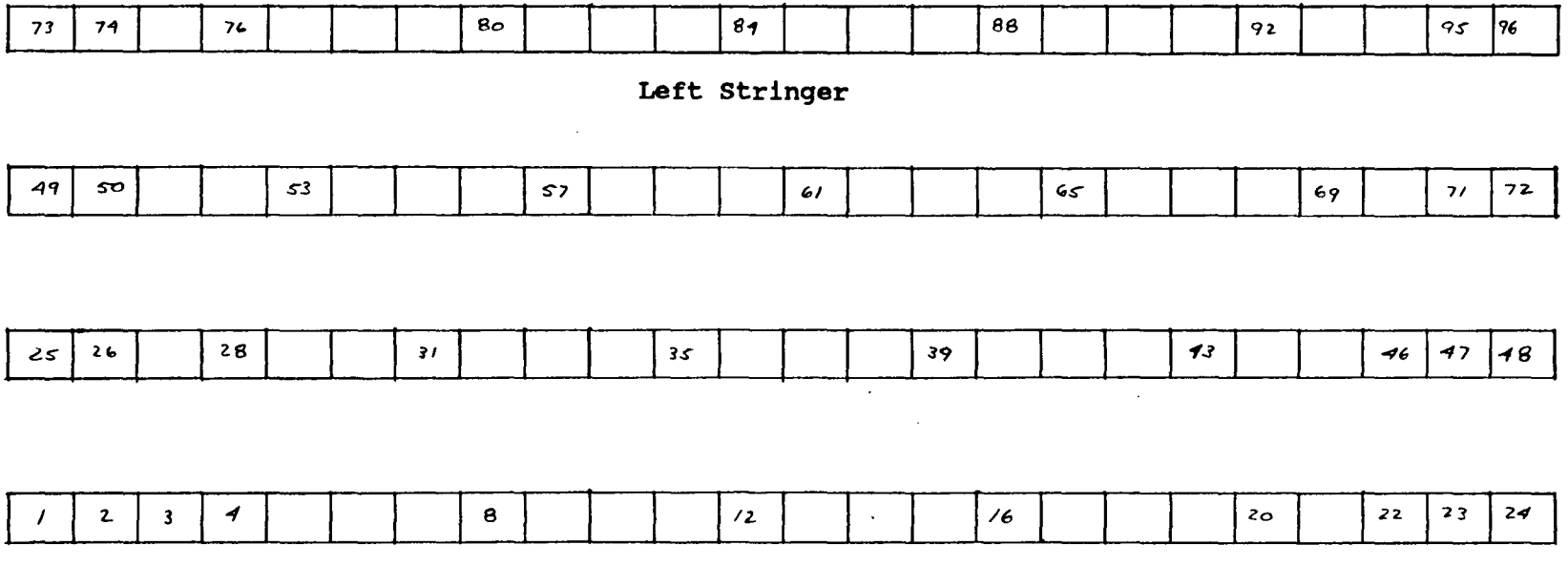

Figure 7: Numbering of Stringers

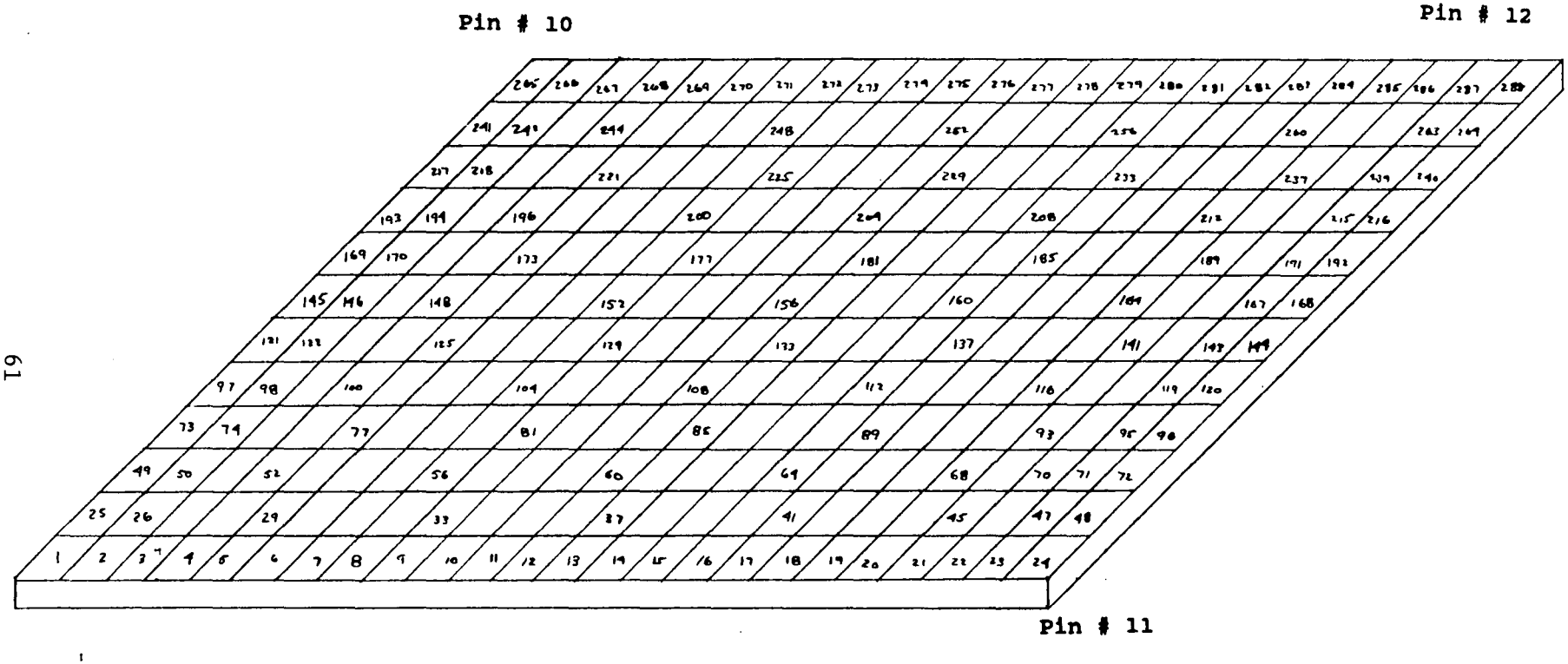

Figure 8: Numbering of Deck

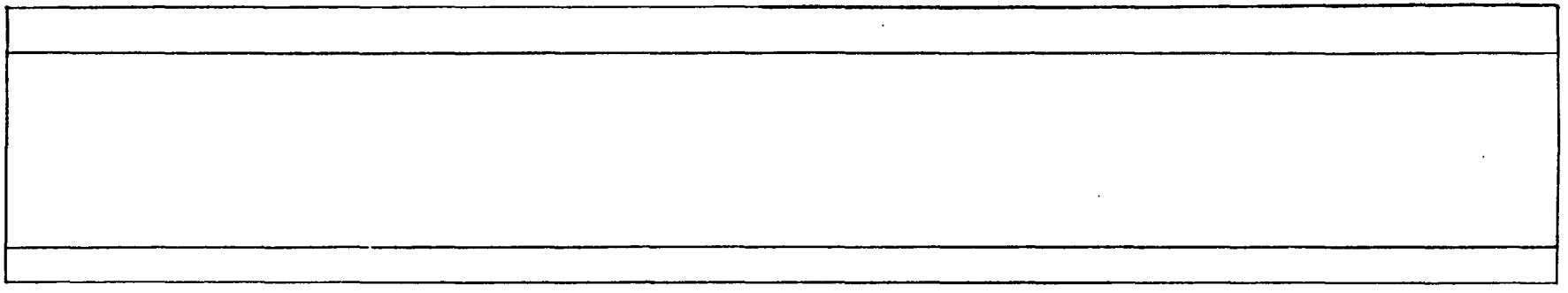

Intact Girder

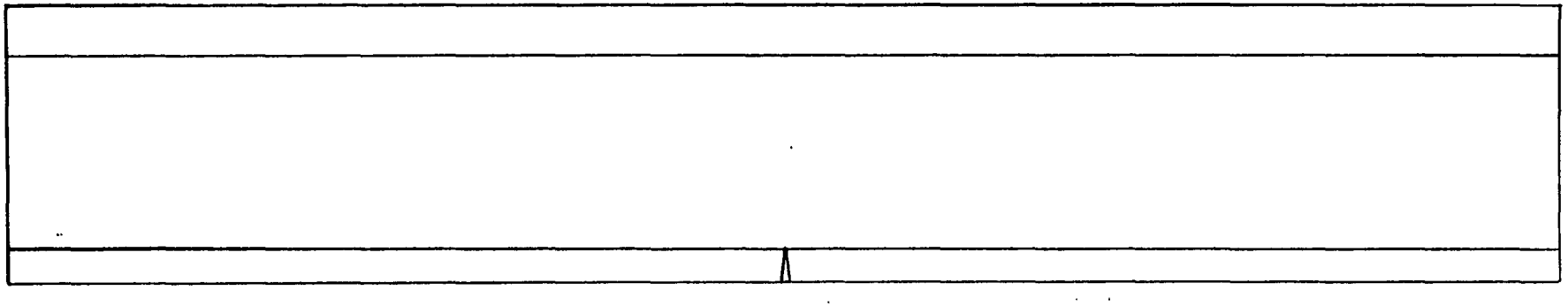

Crack Level 1

Figure 9: Intact and Crack Level 1 Conditions

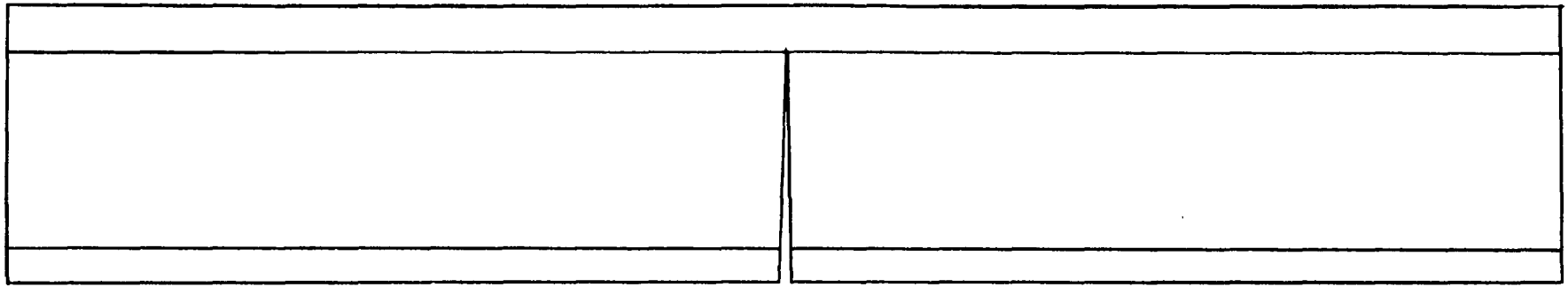

Crack Level 2

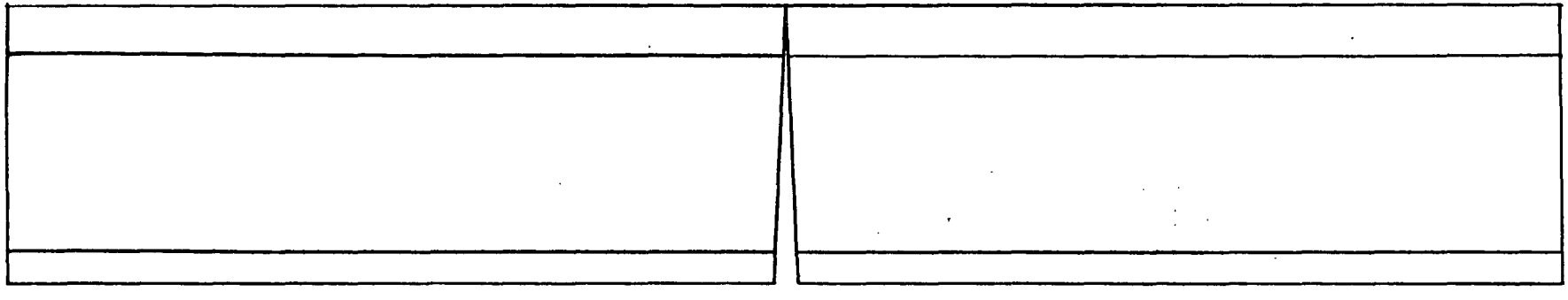

Crack Level 3

Figure 10: Crack Level 2 and 3

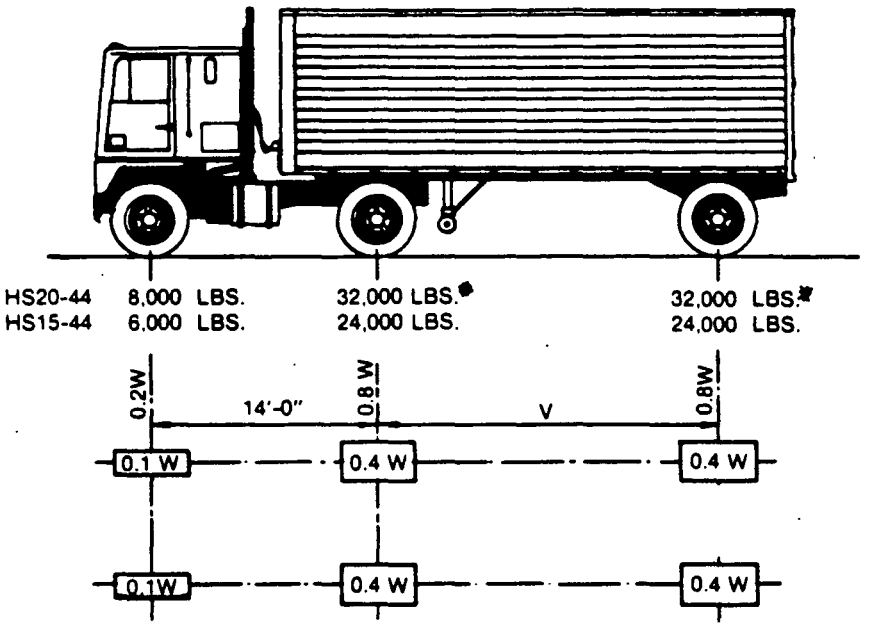

W = COMBINED WEIGHT ON THE FIRST TWO AXLES WHICH IS THE SAME AS FOR THE CORRESPONDING H (M) TRUCK.

V = VARIABLE SPACING — 14 FEET TO 30 FEET INCLUSIVE. SPACING TO BE USED IS THAT WHICH PRODUCES MAXIMUM STRESSES.

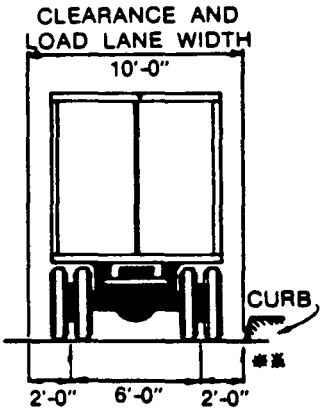

Figure 11: AASHTO HS20-44 Loading

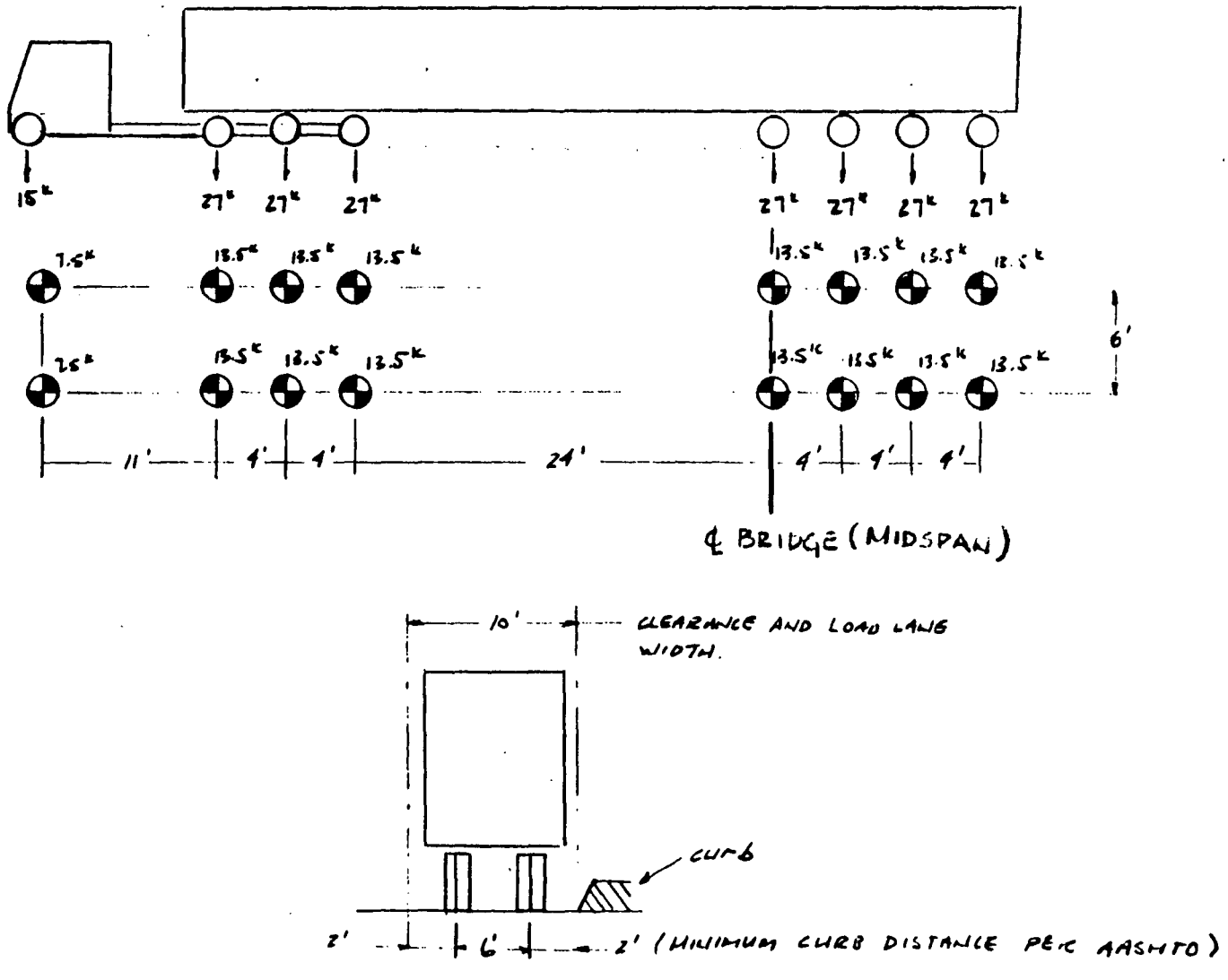

Figure 12: PennDOT 204 kip Permit Vehicle

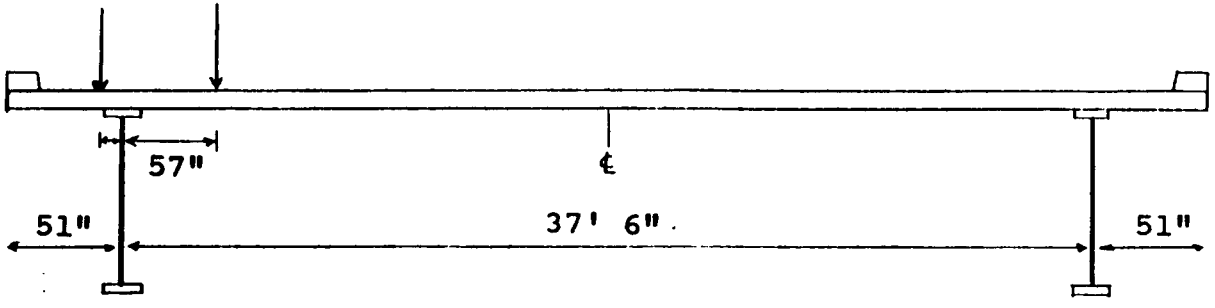

Load Condition 1

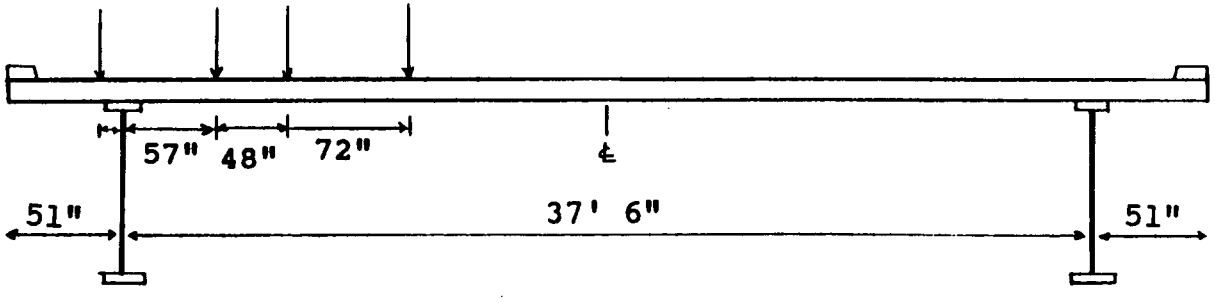

Load Condition 2

Figure 13: Load Conditions 1 and 2

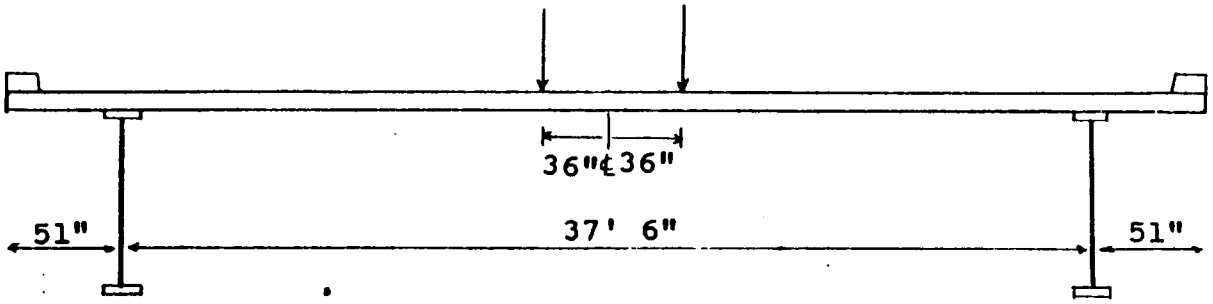

Load Condition 3

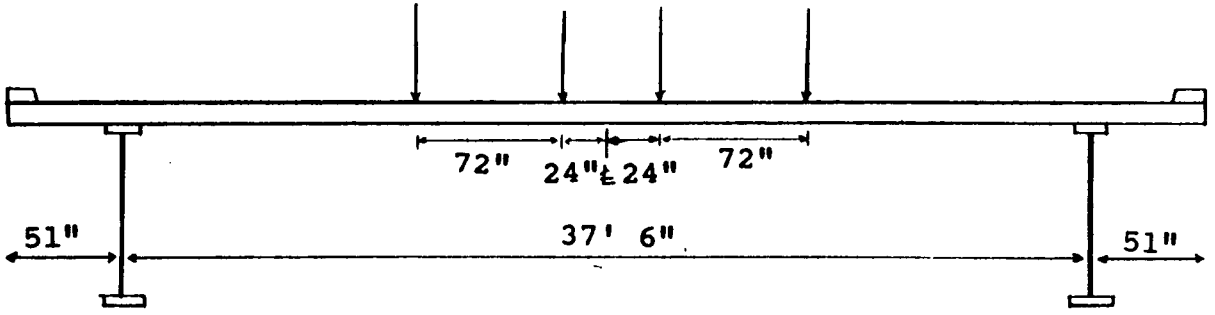

Load Condition 4

Figure 14: Load Conditions 3 and 4

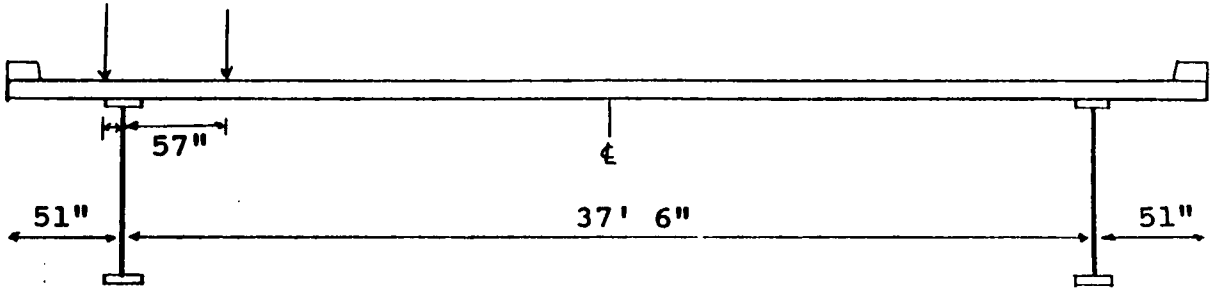

Load Condition 5

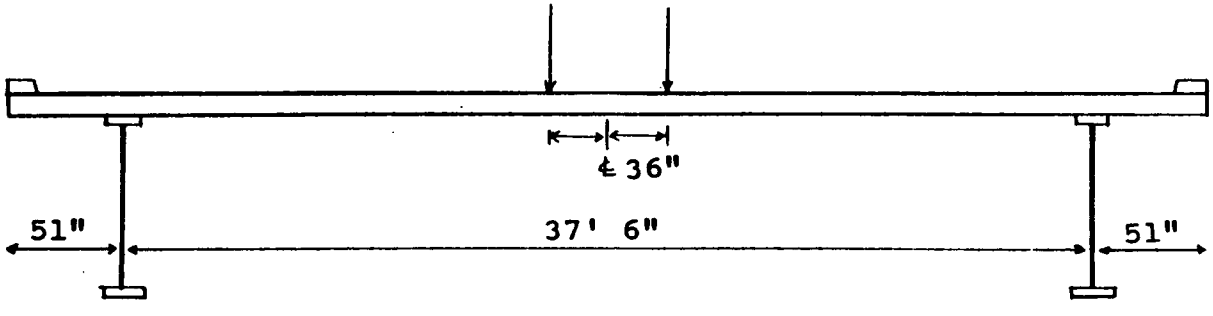

Load Condition 6

Figure 15: Load Conditions 5 and 6

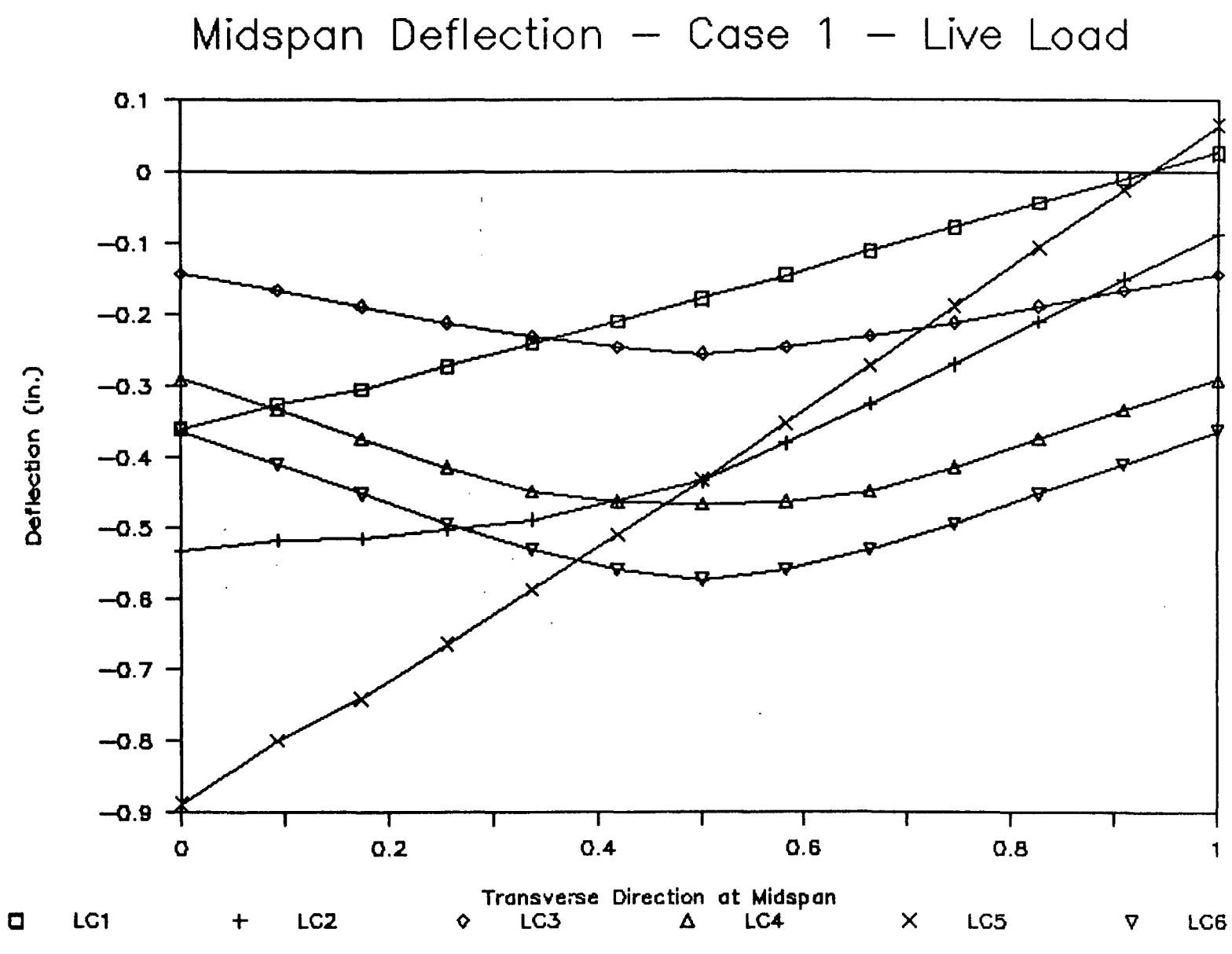
Midspan Deflection – Case 1 – Live Load
Deflection (in.)
0.1
0
-0.1
-0.2
-0.3
-0.4
-0.5
-0.6
-0.7
-0.8
-0.9
0
0.2
0.4
0.6
0.8
1
Transverse Direction at Midspan
LC1
LC2
LC3
LC4
LC5
LC6

Figure 16

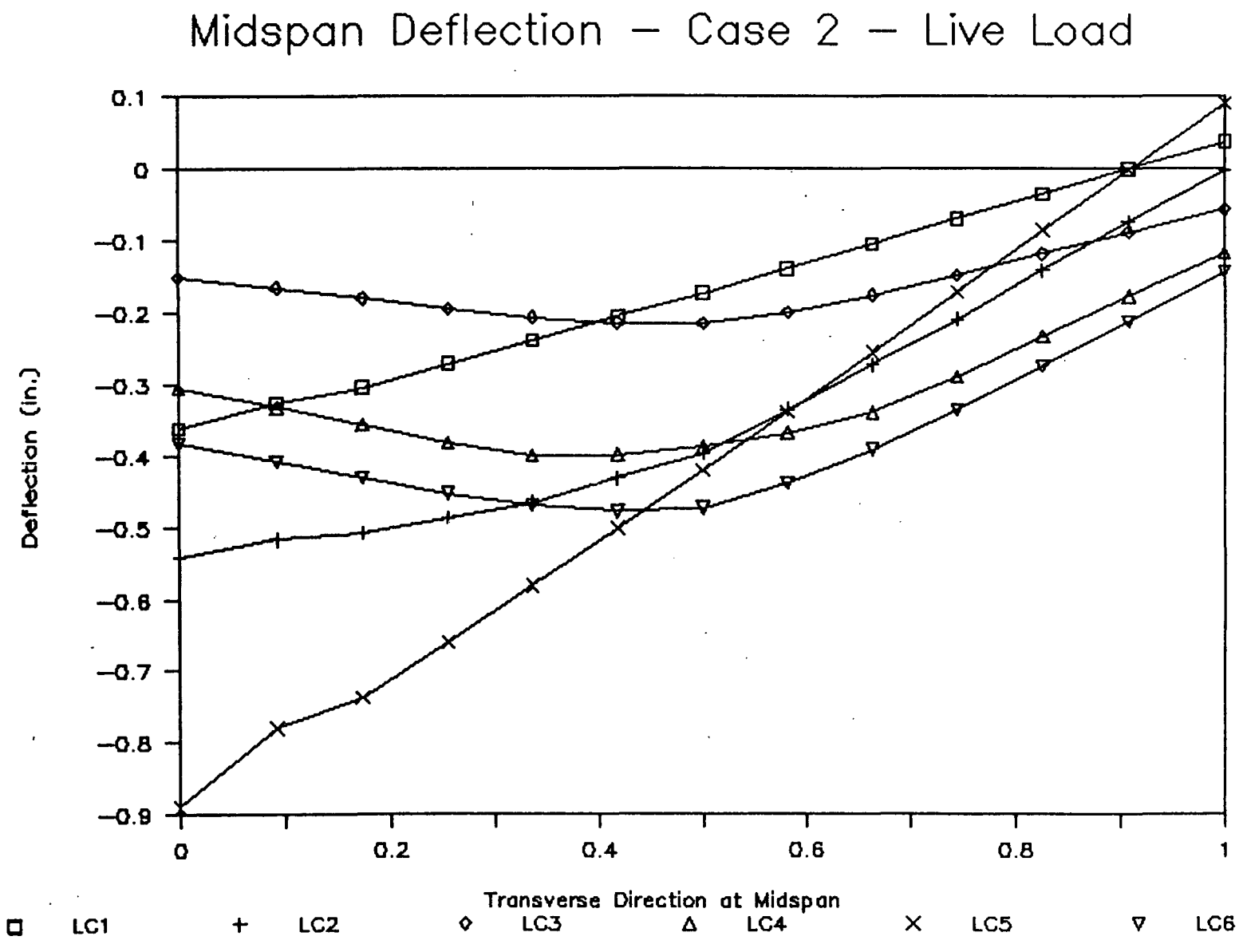
Midspan Deflection – Case 2 – Live Load
Deflection (in.)
0.1
0
-0.1
-0.2
-0.3
-0.4
-0.5
-0.6
-0.7
-0.8
-0.9
0
0.2
0.4
0.6
0.8
1
Transverse Direction at Midspan
LC1
LC2
LC3
LC4
LC5
LC6

Figure 17

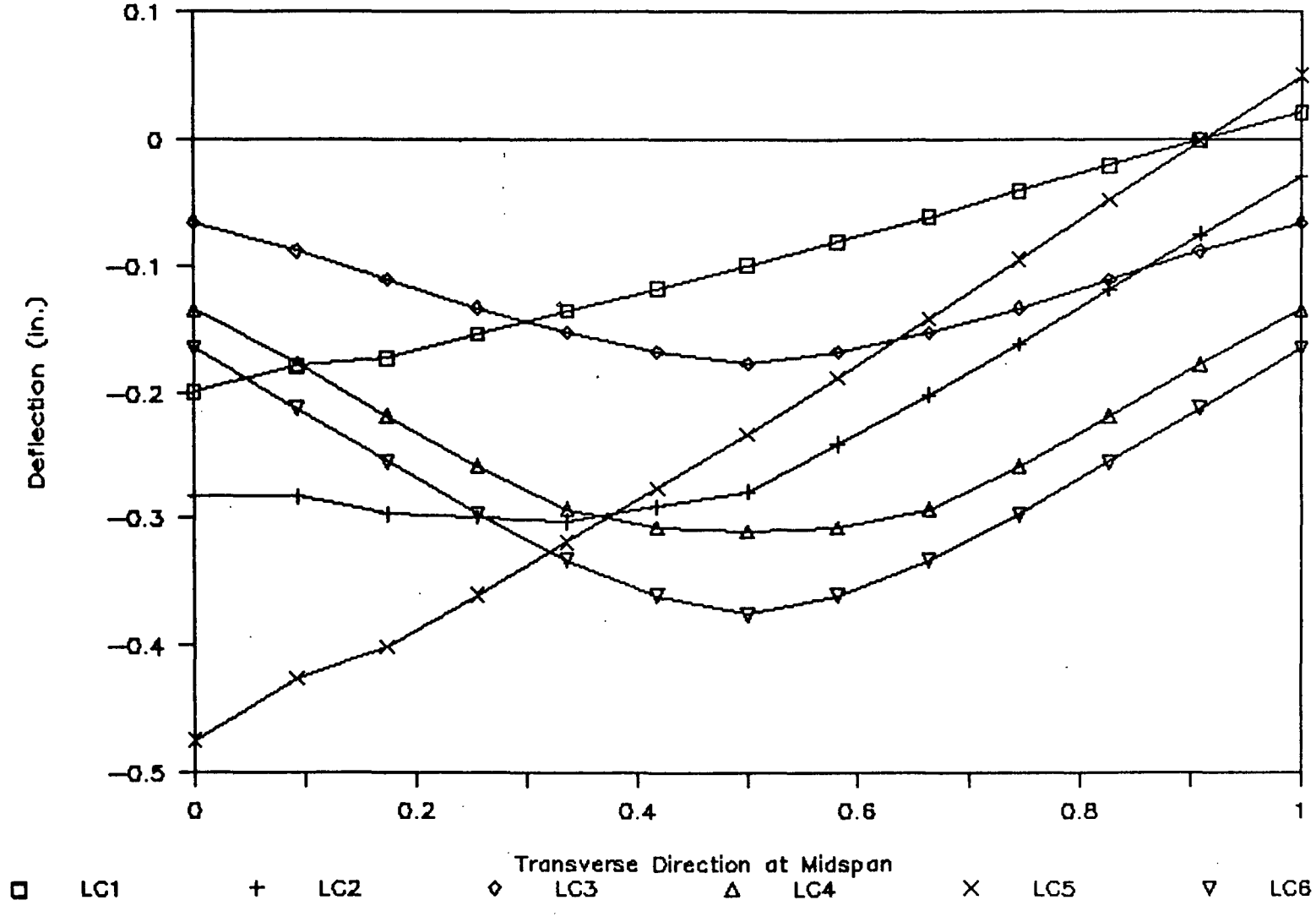
Midspan Deflection – Case 3 – Live Load
Deflection (in.)
0.1
0
-0.1
-0.2
-0.3
-0.4
-0.5
0
0.2
0.4
0.6
0.8
1
Transverse Direction at Midspan
LC1
LC2
LC3
LC4
LC5
LC6

Figure 18

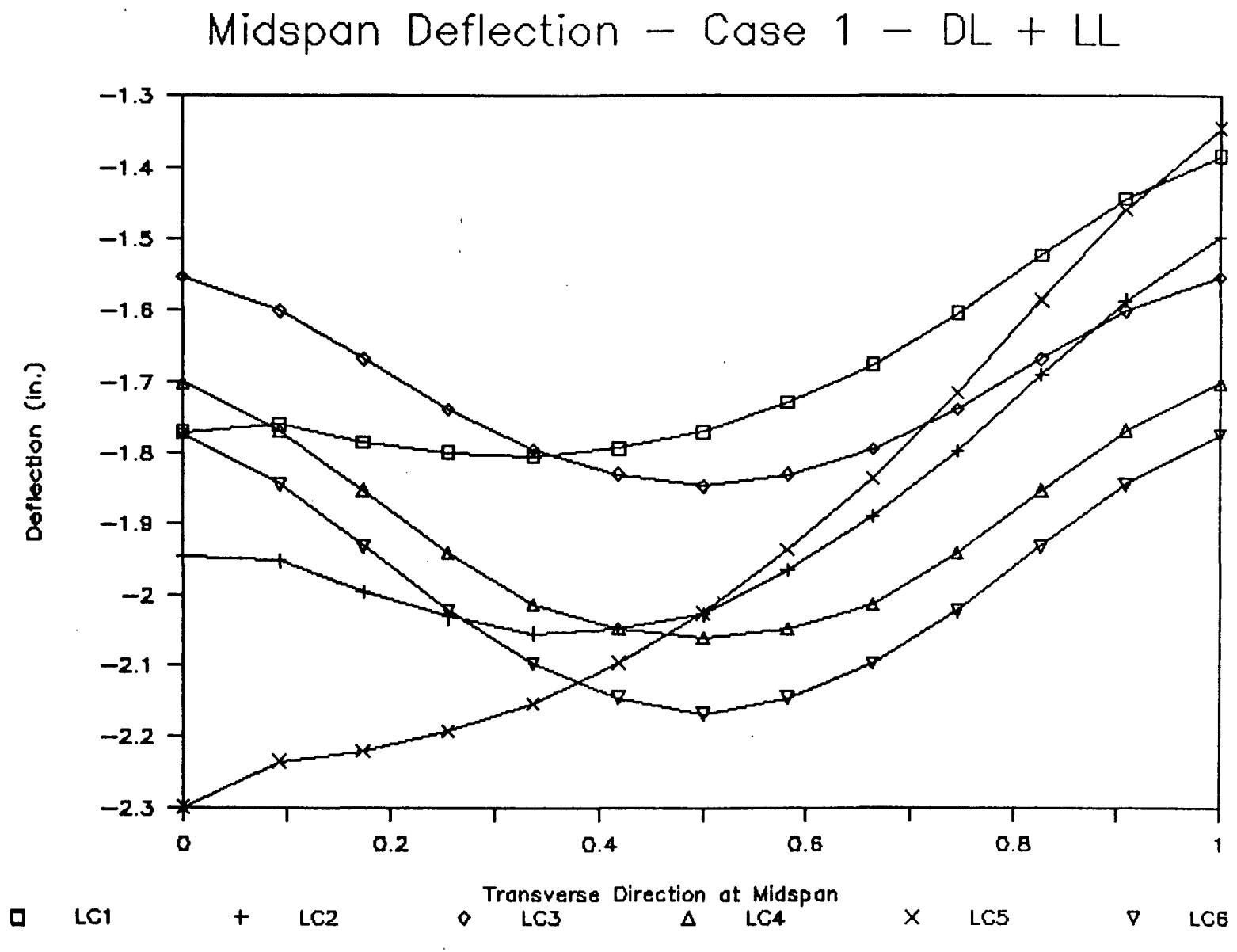
Midspan Deflection – Case 1 – DL + LL
Deflection (in.)
-1.3
-1.4
-1.5
-1.6
-1.7
-1.8
-1.9
-2
-2.1
-2.2
-2.3
0
0.2
0.4
0.6
0.8
1
Transverse Direction at Midspan
LC1
LC2
LC3
LC4
LC5
LC6

Figure 19

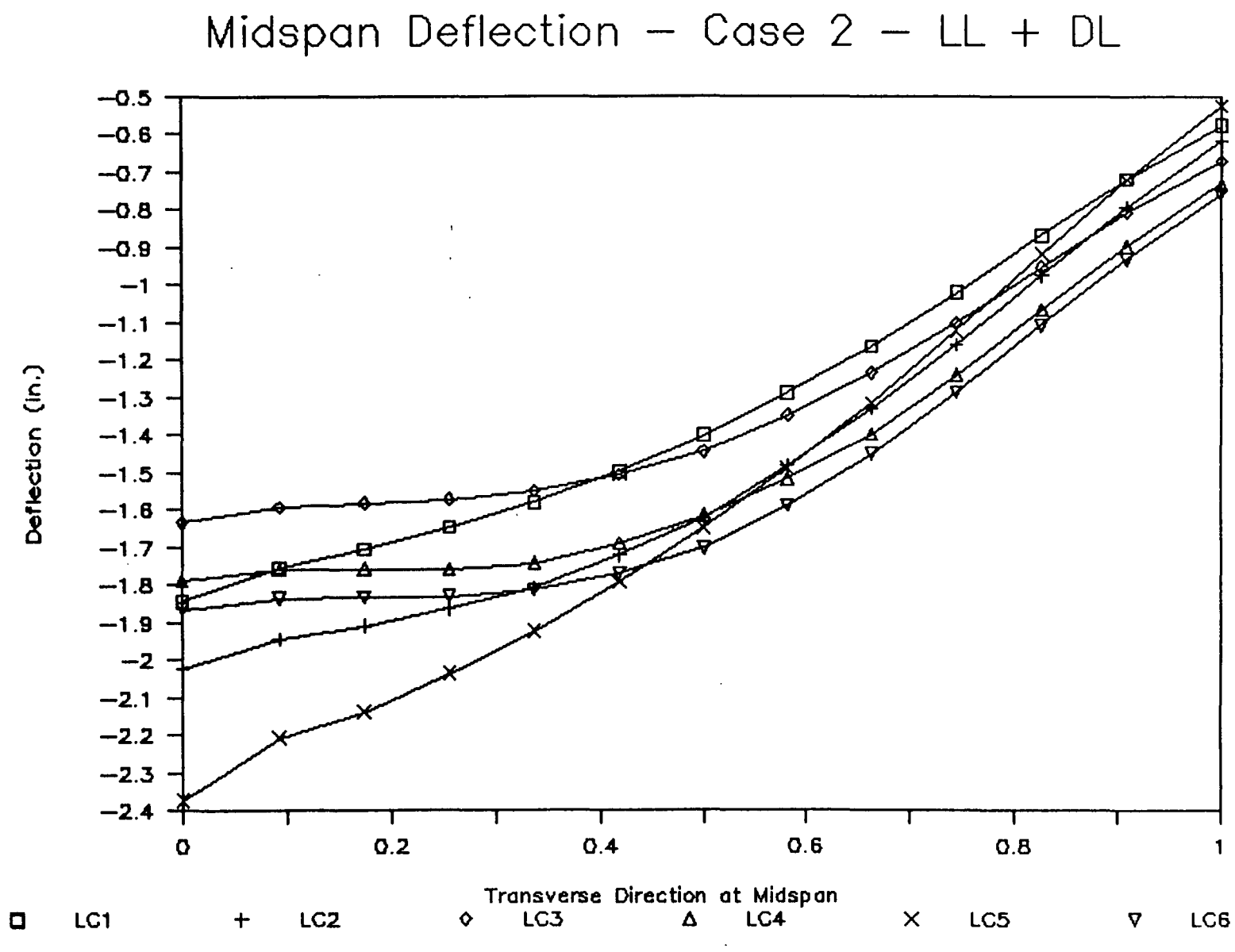
Midspan Deflection – Case 2 – LL + DL
Deflection (in.)
-0.5
-0.6
-0.7
-0.8
-0.9
-1
-1.1
-1.2
-1.3
-1.4
-1.5
-1.6
-1.7
-1.8
-1.9
-2
-2.1
-2.2
-2.3
-2.4
0
0.2
0.4
0.6
0.8
1
Transverse Direction at Midspan
LC1
LC2
LC3
LC4
LC5
LC6

Figure 20

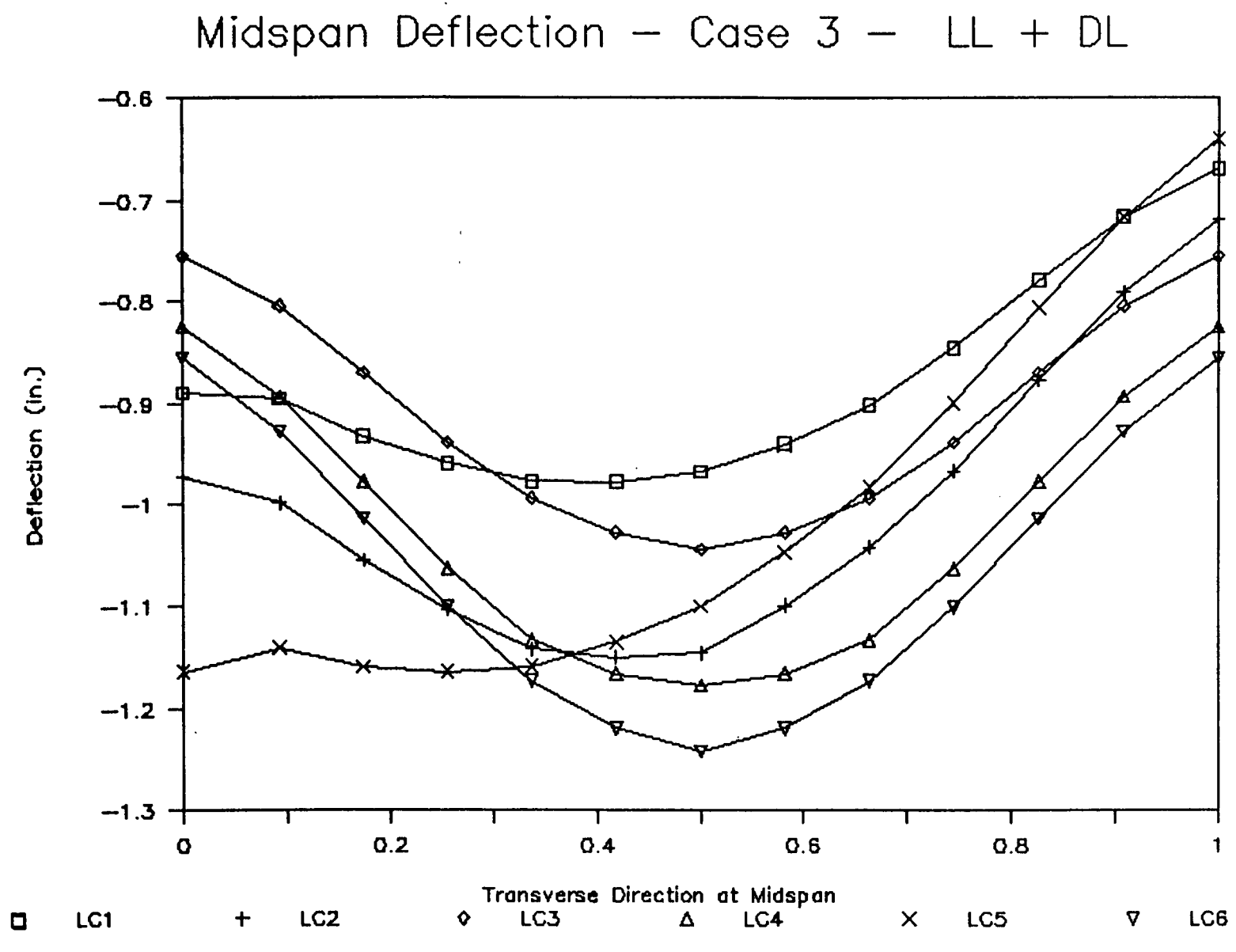
Midspan Deflection – Case 3 – LL + DL
Deflection (in.)
-0.6
-0.7
-0.8
-0.9
-1
-1.1
-1.2
-1.3
0
0.2
0.4
0.6
0.8
1
Transverse Direction at Midspan
LC1
LC2
LC3
LC4
LC5
LC6

Figure 21

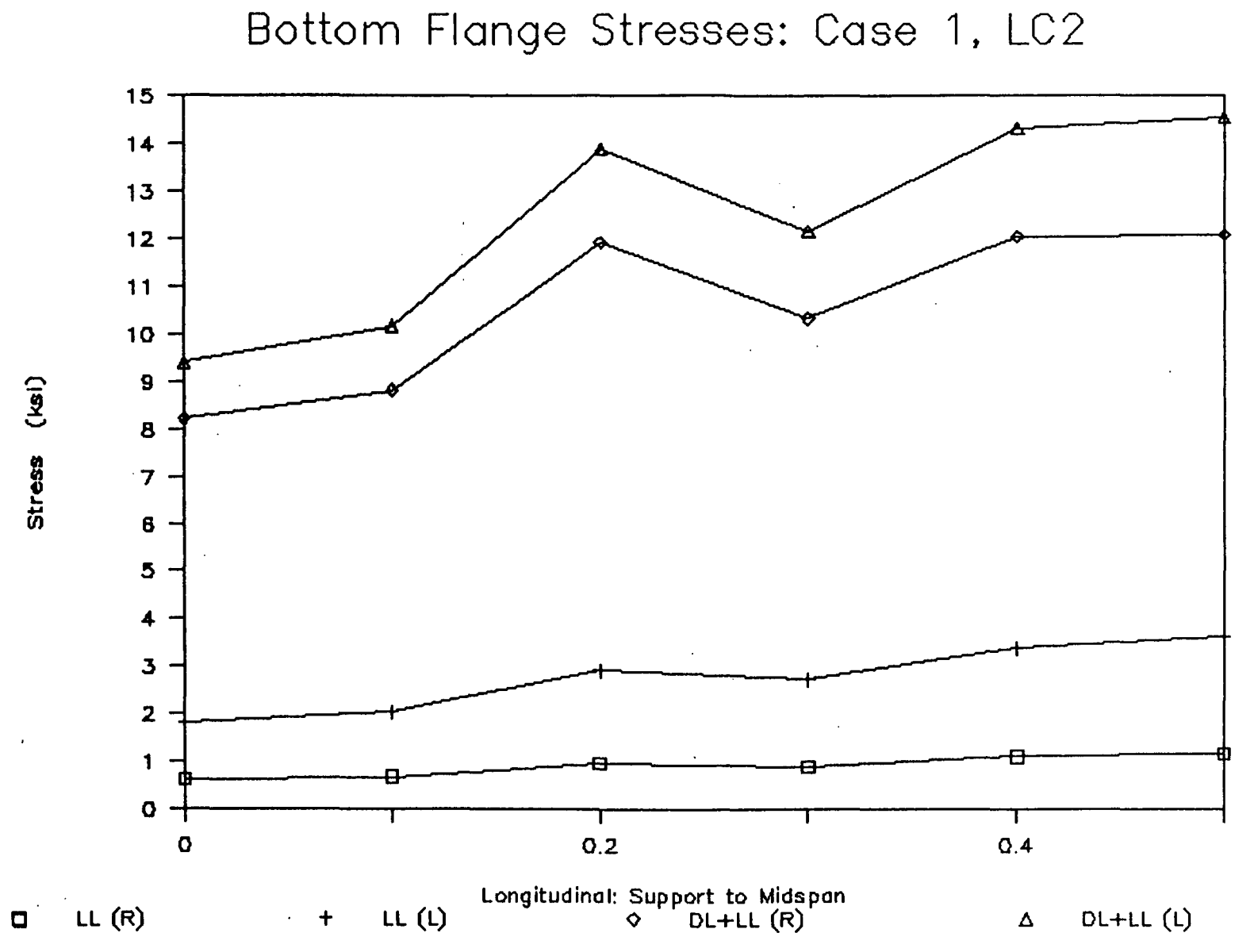
Bottom Flange Stresses: Case 1, LC2
Stress (ksi)
15
14
13
12
11
10
9
8
7
6
5
4
3
2
1
0
0
0.2
0.4
Longitudinal: Support to Midspan
LL (R)
LL (L)
DL+LL (R)
DL+LL (L)

Figure 22

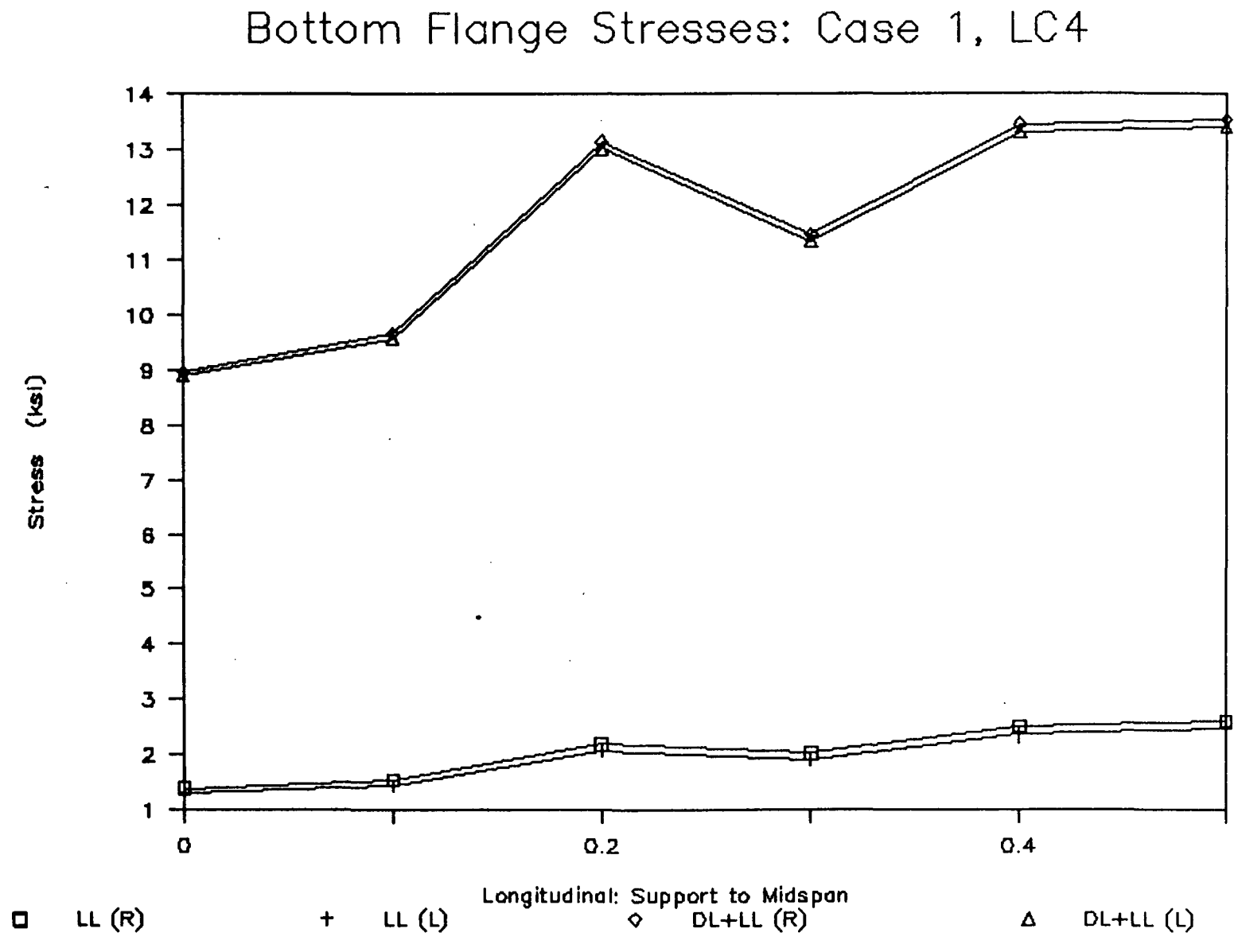
Bottom Flange Stresses: Case 1, LC4
Stress (ksi)
14
13
12
11
10
9
8
7
6
5
4
3
2
1
0
0.2
0.4
Longitudinal: Support to Midspan
LL (R)
LL (L)
DL+LL (R)
DL+LL (L)

Figure 23

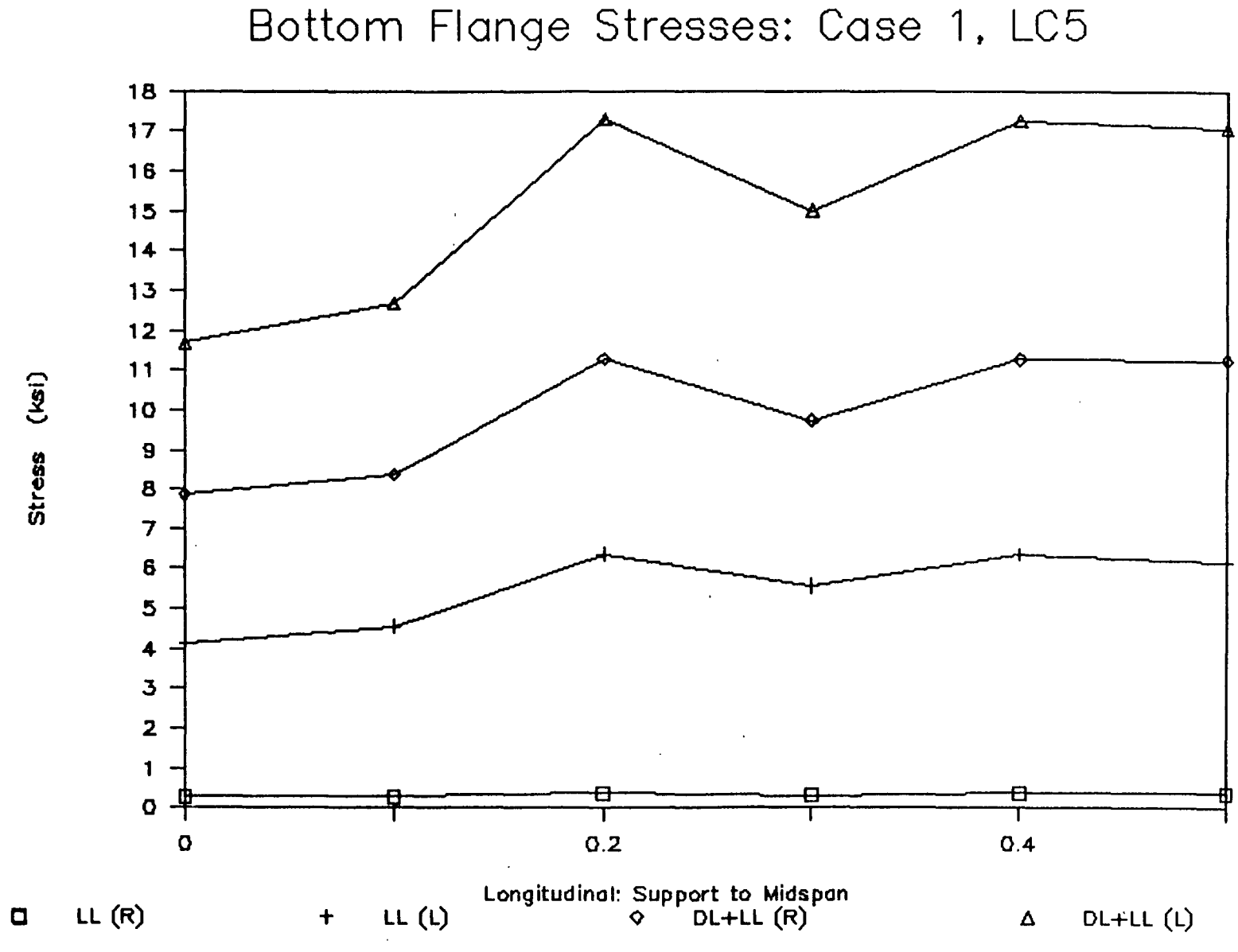
Bottom Flange Stresses: Case 1, LC5
Stress (ksi)
18
17
16
15
14
13
12
11
10
9
8
7
6
5
4
3
2
1
0
0
0.2
0.4
Longitudinal: Support to Midspan
LL (R)
LL (L)
DL+LL (R)
DL+LL (L)

Figure 24

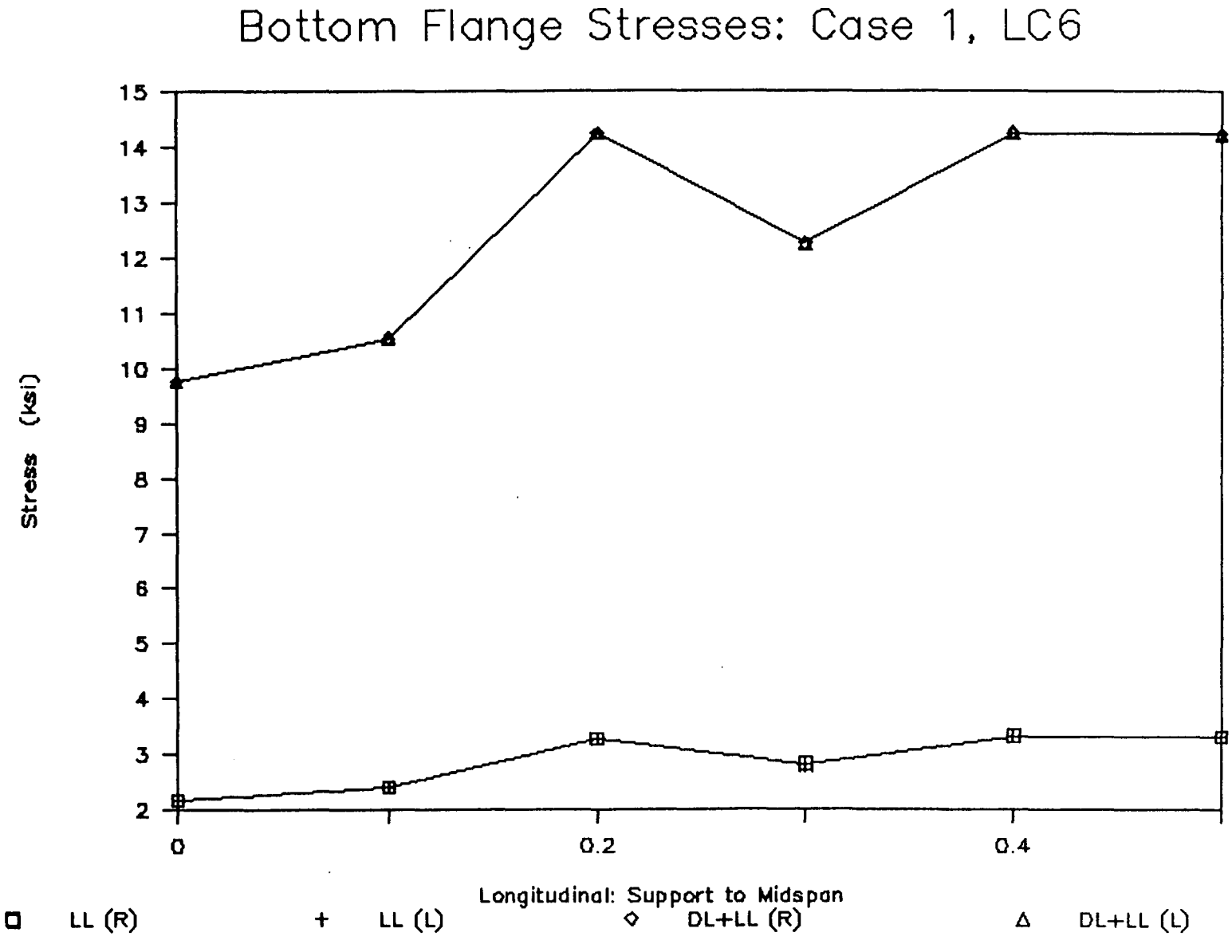
Bottom Flange Stresses: Case 1, LC6
Stress (ksi)
15
14
13
12
11
10
9
8
7
6
5
4
3
2
0
0.2
0.4
Longitudinal: Support to Midspan
LL (R)
LL (L)
DL+LL (R)
DL+LL (L)

Figure 25

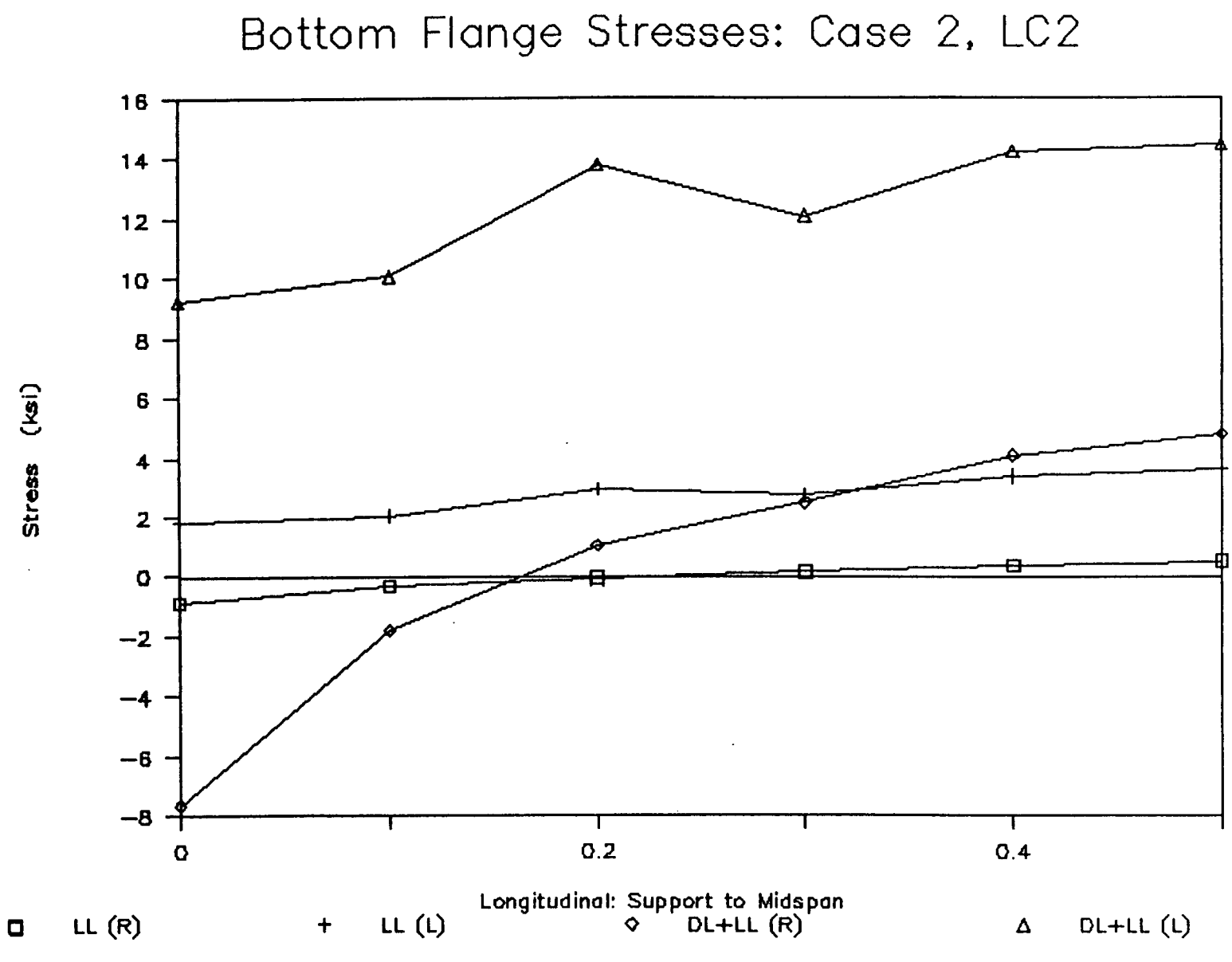
Bottom Flange Stresses: Case 2, LC2
Stress (ksi)
16
14
12
10
8
6
4
2
0
−2
−4
−6
−8
0
0.2
0.4
Longitudinal: Support to Midspan
LL (R)
LL (L)
DL+LL (R)
DL+LL (L)

Figure 26

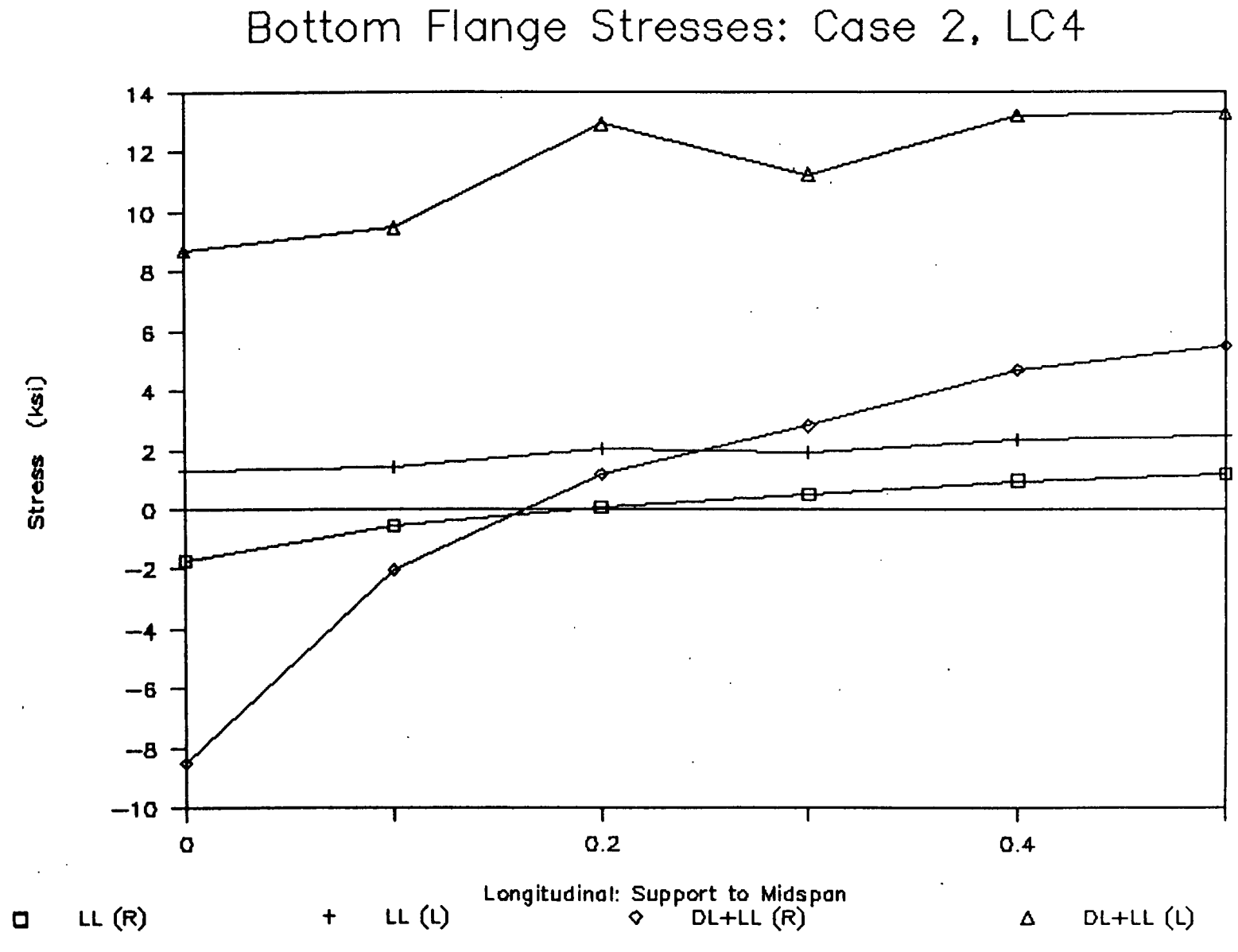
Bottom Flange Stresses: Case 2, LC4
Stress (ksi)
14
12
10
8
6
4
2
0
−2
−4
−6
−8
−10
0
0.2
0.4
Longitudinal: Support to Midspan
LL (R)
LL (L)
DL+LL (R)
DL+LL (L)

Figure 27

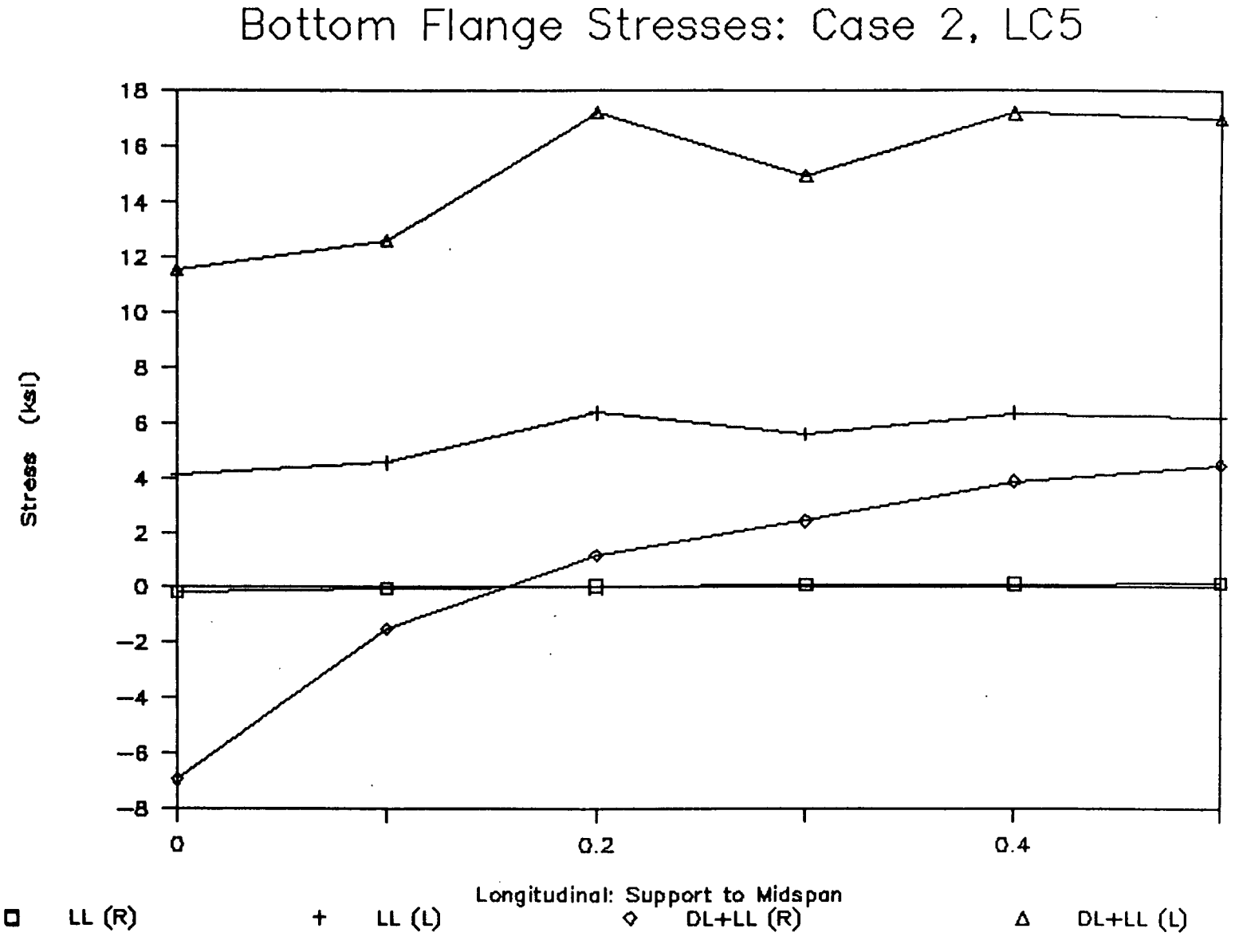
Bottom Flange Stresses: Case 2, LC5
Stress (ksi)
18
16
14
12
10
8
6
4
2
0
−2
−4
−6
−8
0
0.2
0.4
Longitudinal: Support to Midspan
LL (R)
LL (L)
DL+LL (R)
DL+LL (L)

Figure 28

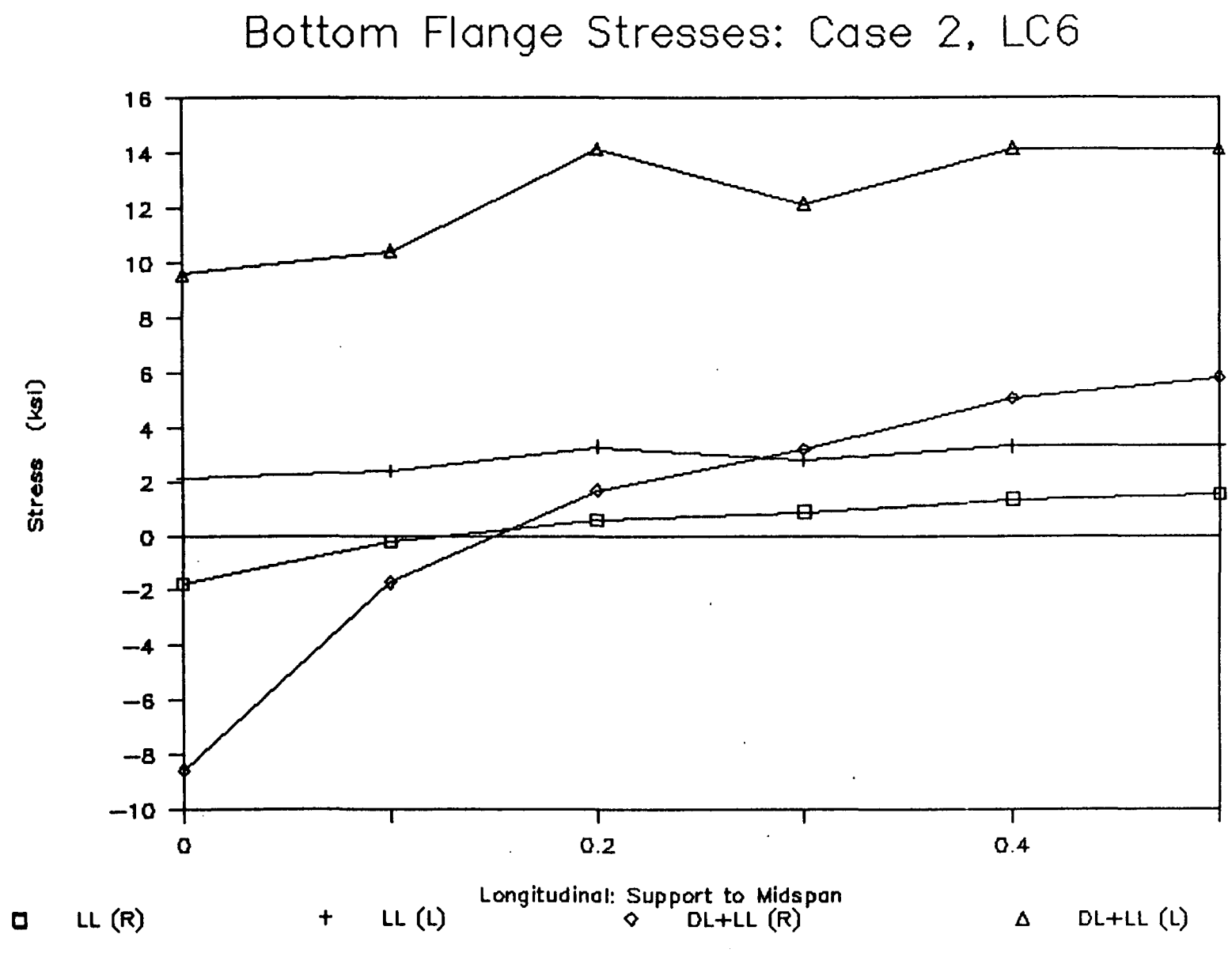
Bottom Flange Stresses: Case 2, LC6
Stress (ksi)
16
14
12
10
8
6
4
2
0
−2
−4
−6
−8
−10
0
0.2
0.4
Longitudinal: Support to Midspan
LL (R)
LL (L)
DL+LL (R)
DL+LL (L)

Figure 29

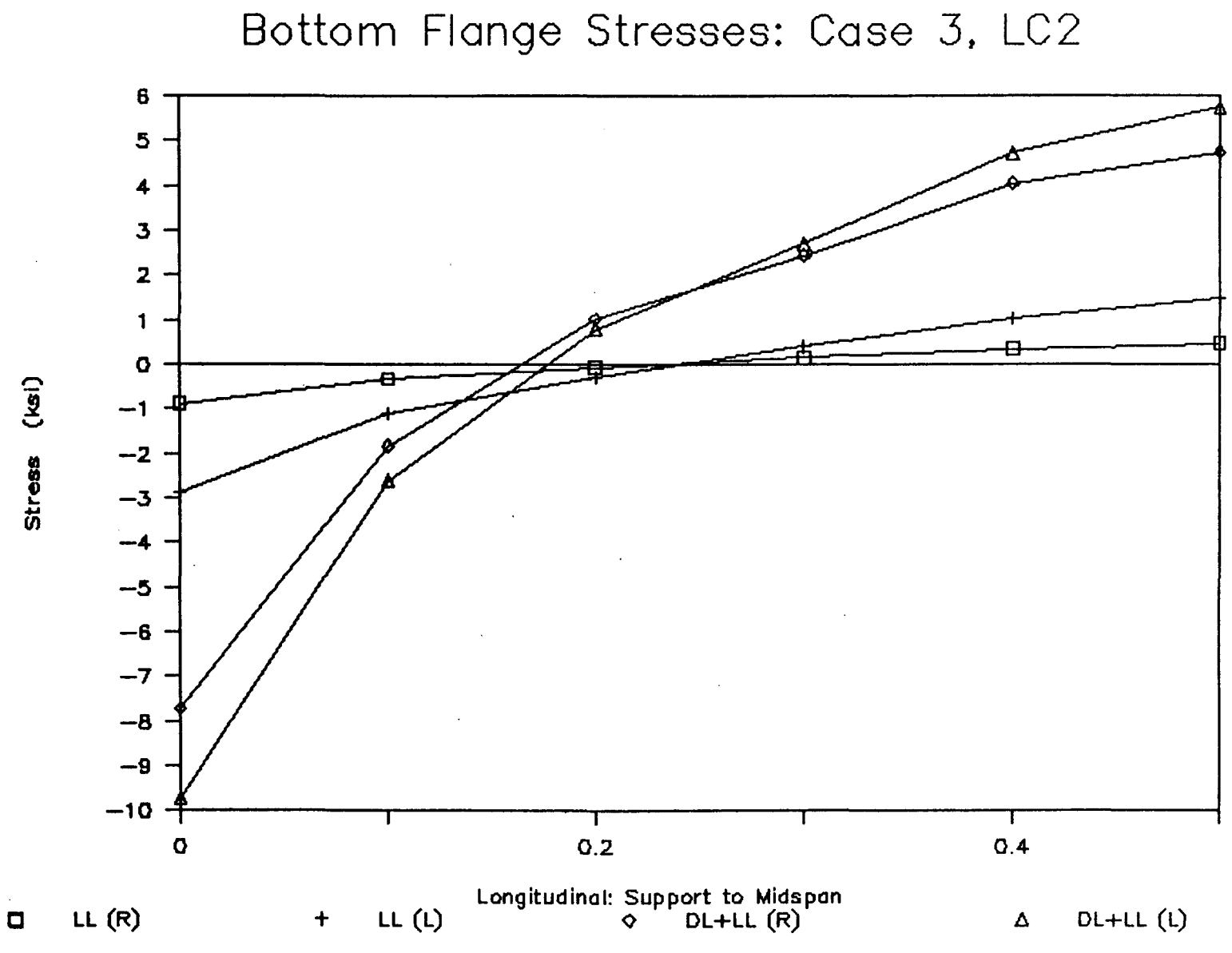
Bottom Flange Stresses: Case 3, LC2
Stress (ksi)
6
5
4
3
2
1
0
−1
−2
−3
−4
−5
−6
−7
−8
−9
−10
0
0.2
0.4
Longitudinal: Support to Midspan
LL (R)
LL (L)
DL+LL (R)
DL+LL (L)

Figure 30

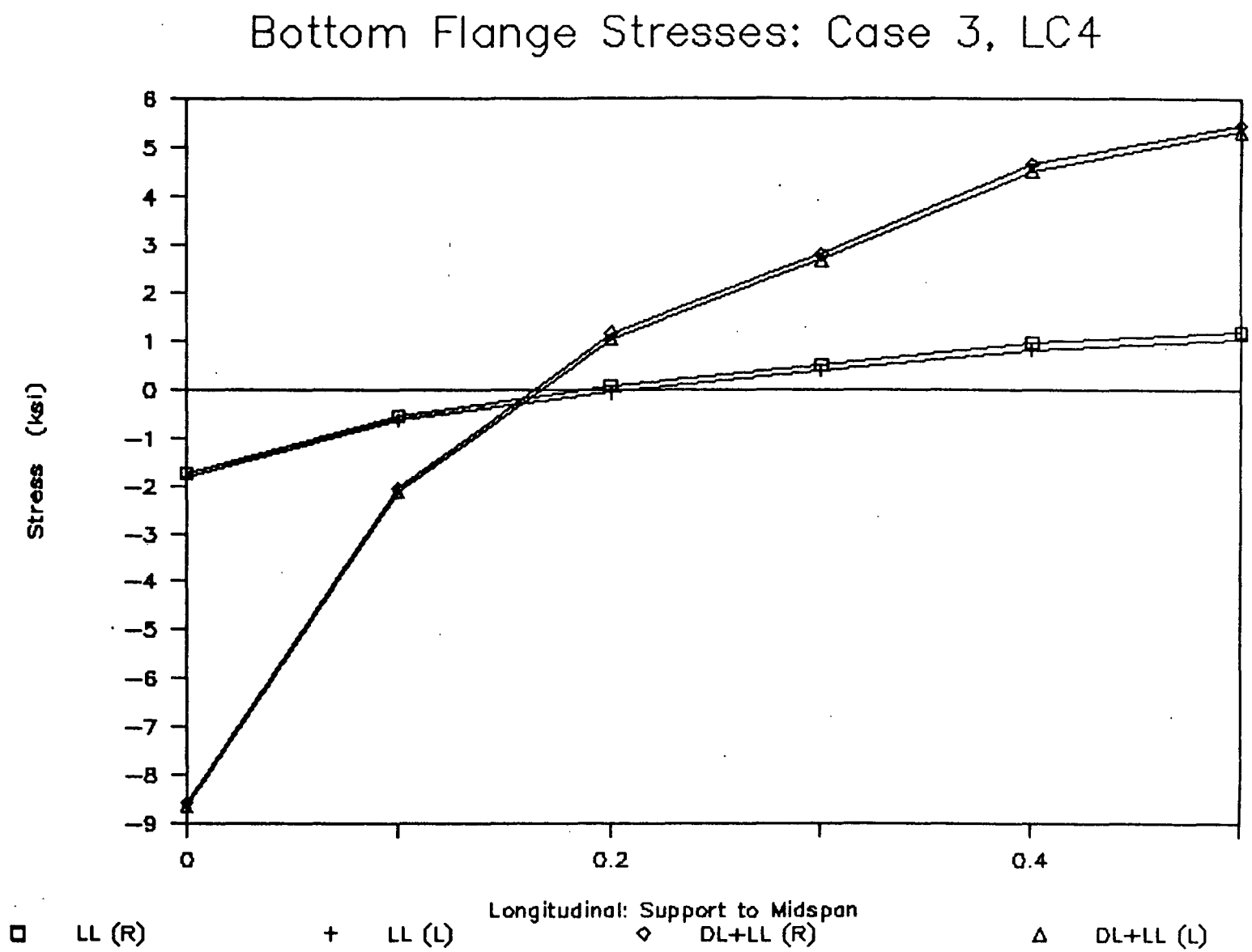
Bottom Flange Stresses: Case 3, LC4
Stress (ksi)
6
5
4
3
2
1
0
-1
-2
-3
-4
-5
-6
-7
-8
-9
0
0.2
0.4
Longitudinal: Support to Midspan
LL (R)
LL (L)
DL+LL (R)
DL+LL (L)

Figure 31

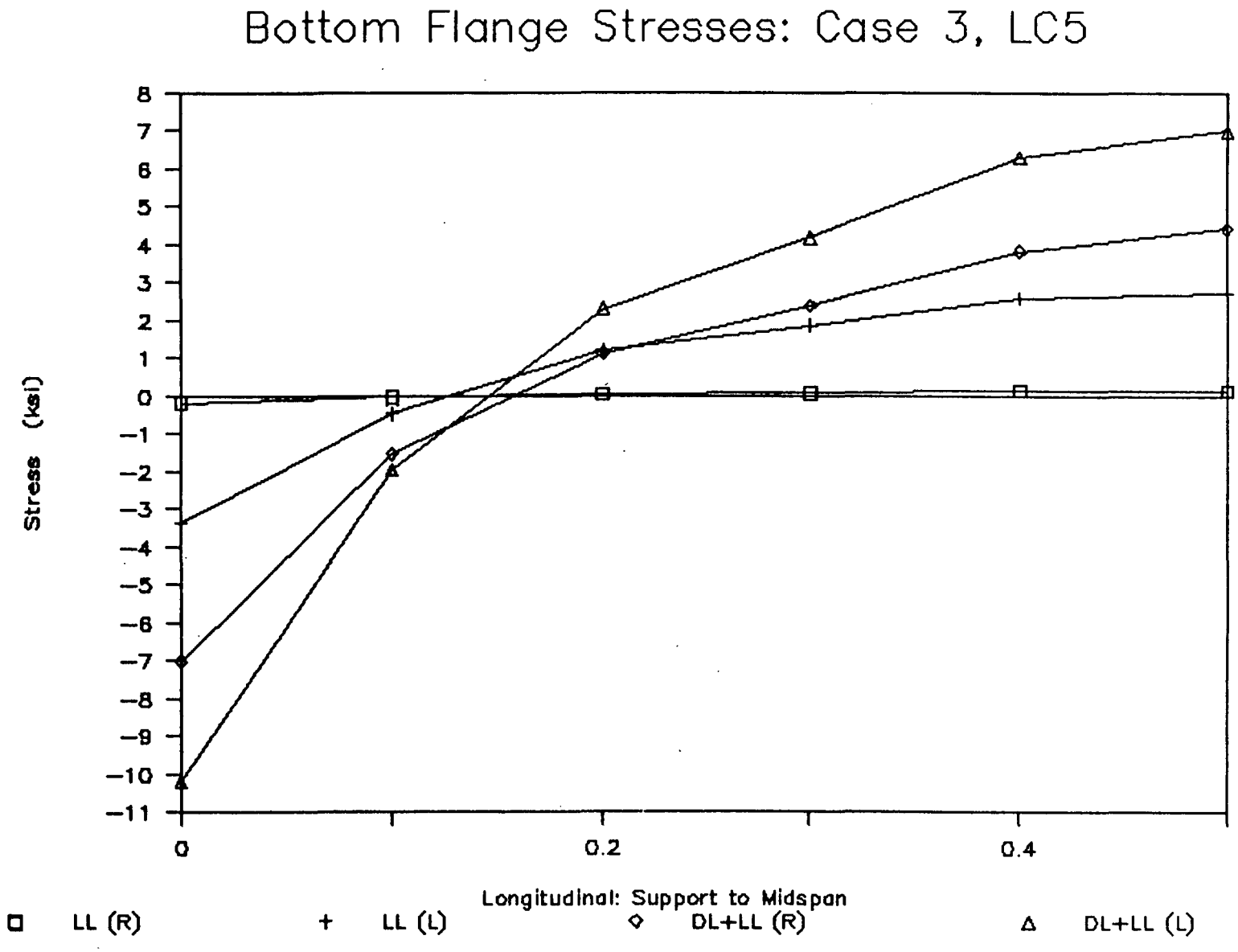
Bottom Flange Stresses: Case 3, LC5
Stress (ksi)
8
7
6
5
4
3
2
1
0
-1
-2
-3
-4
-5
-6
-7
-8
-9
-10
-11
0
0.2
0.4
Longitudinal: Support to Midspan
LL (R)
LL (L)
DL+LL (R)
DL+LL (L)

Figure 32

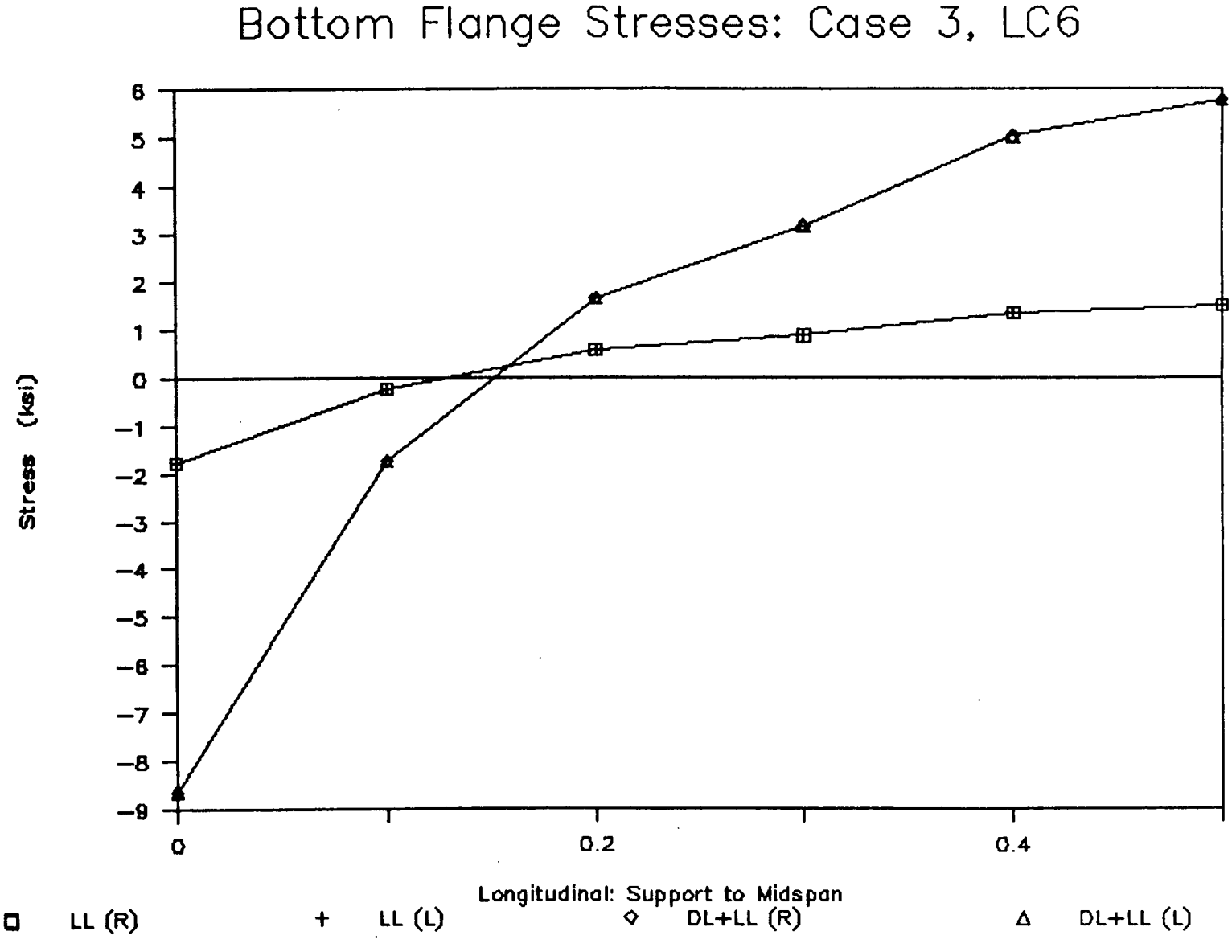
Bottom Flange Stresses: Case 3, LC6
Stress (ksi)
6
5
4
3
2
1
0
-1
-2
-3
-4
-5
-6
-7
-8
-9
0
0.2
0.4
Longitudinal: Support to Midspan
LL (R)
LL (L)
DL+LL (R)
DL+LL (L)

Figure 33

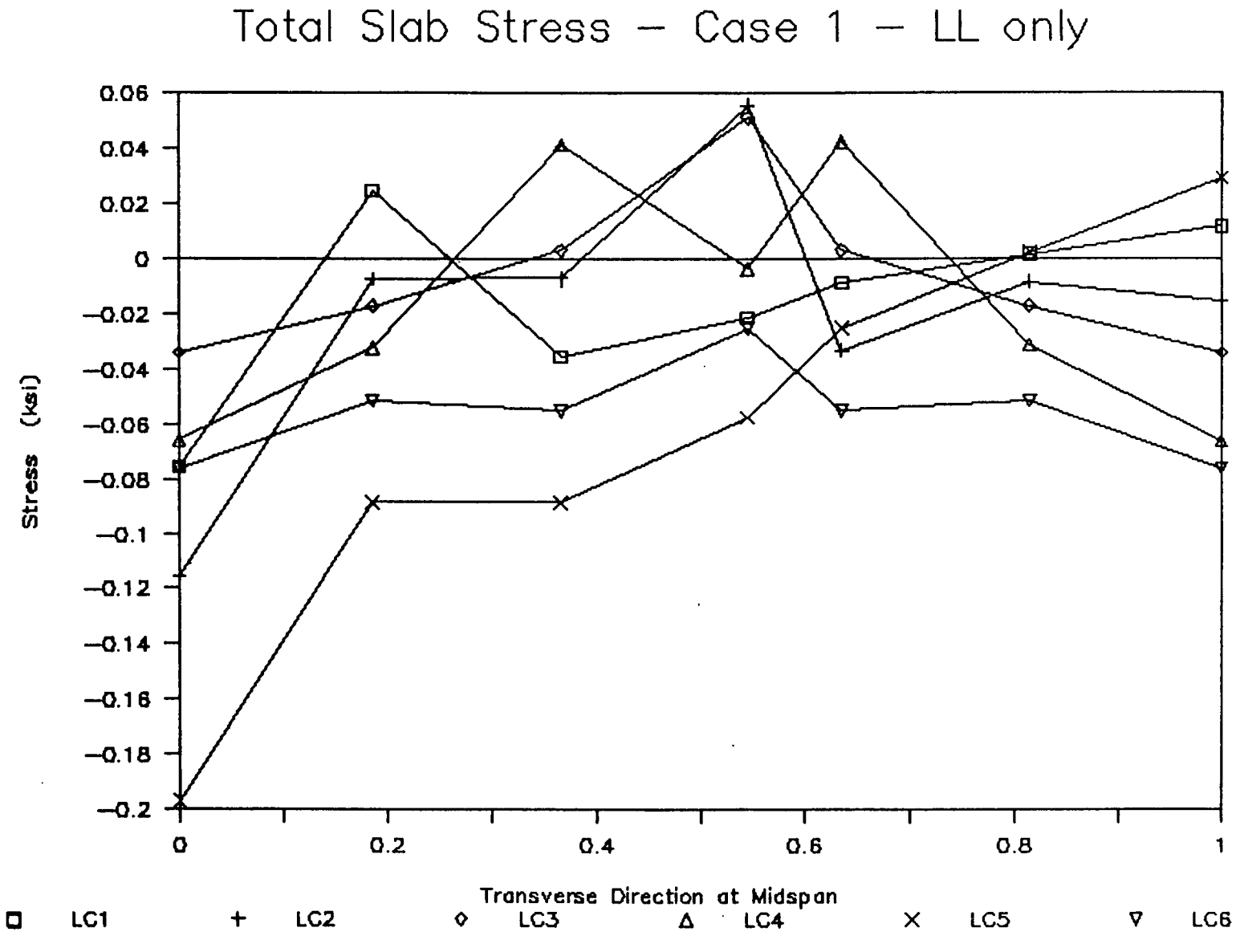
Total Slab Stress – Case 1 – LL only
Stress (ksi)
0.06
0.04
0.02
0
−0.02
−0.04
−0.06
−0.08
−0.1
−0.12
−0.14
−0.16
−0.18
−0.2
0
0.2
0.4
0.6
0.8
1
Transverse Direction at Midspan
LC1
LC2
LC3
LC4
LC5
LC6

Figure 34

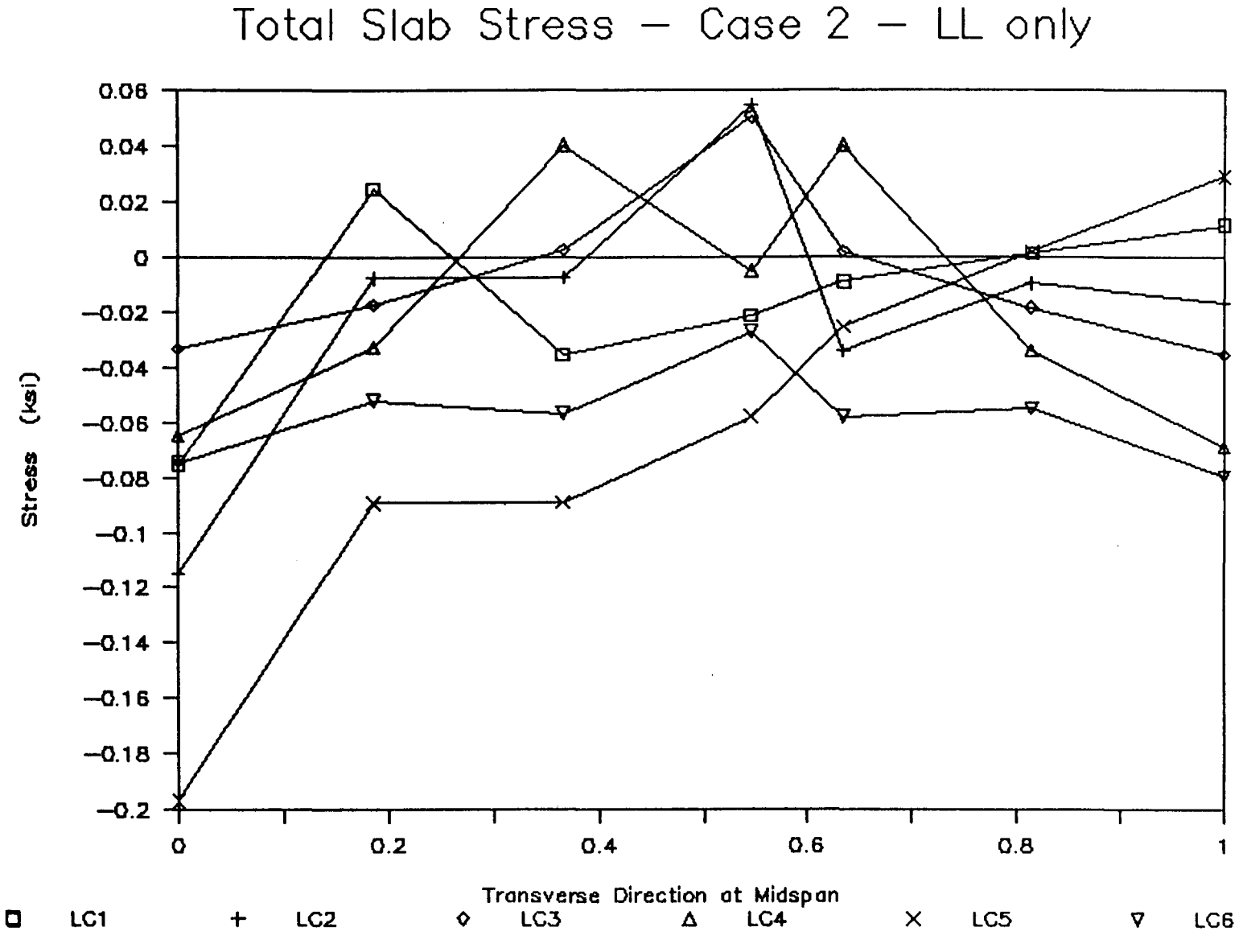
Total Slab Stress – Case 2 – LL only
Stress (ksi)
0.06
0.04
0.02
0
-0.02
-0.04
-0.06
-0.08
-0.1
-0.12
-0.14
-0.16
-0.18
-0.2
0
0.2
0.4
0.6
0.8
1
Transverse Direction at Midspan
LC1
LC2
LC3
LC4
LC5
LC6

Figure 35

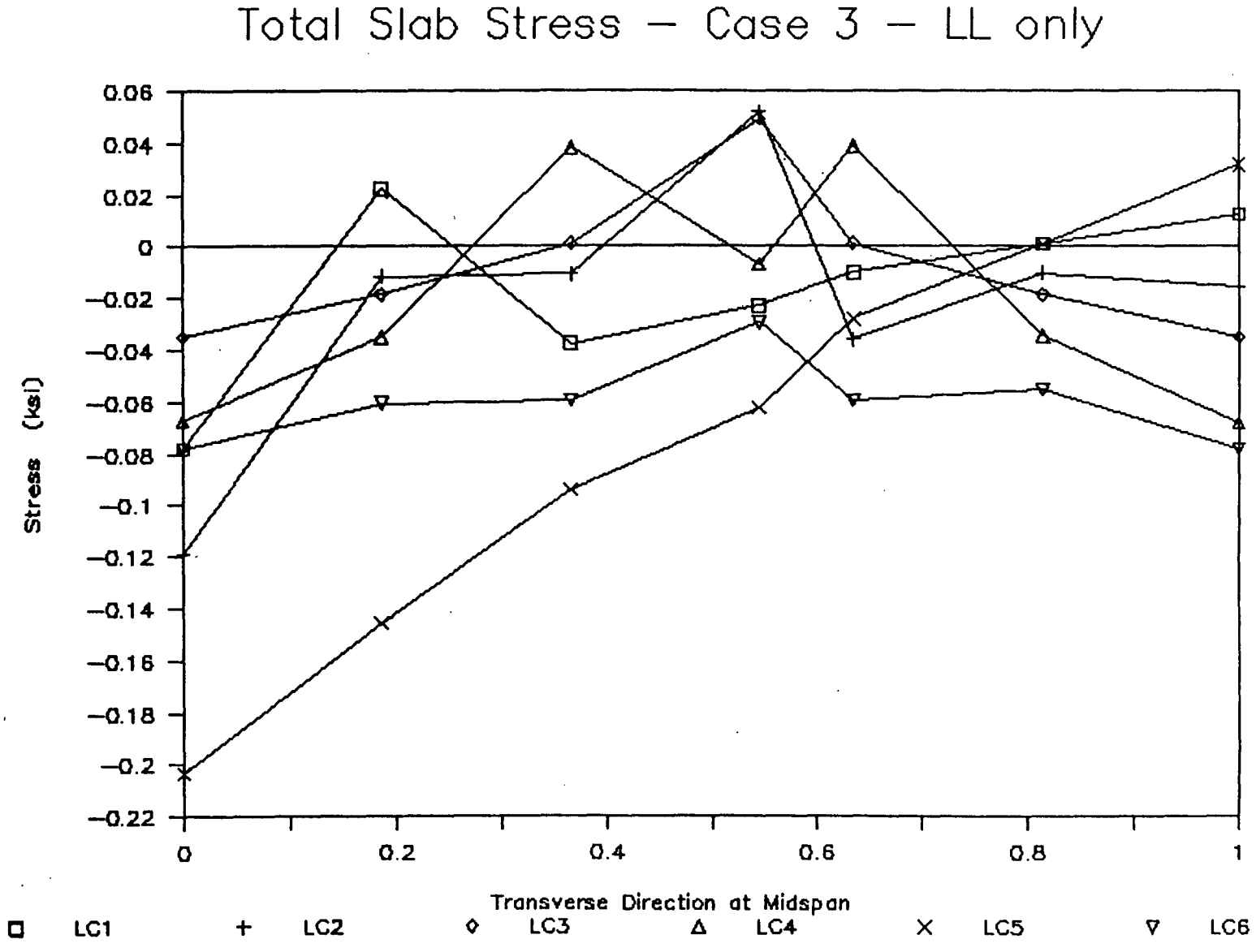
Total Slab Stress – Case 3 – LL only
0.06
0.04
0.02
0
−0.02
−0.04
−0.06
−0.08
−0.1
−0.12
−0.14
−0.16
−0.18
−0.2
−0.22
Stress (ksi)
0
0.2
0.4
0.6
0.8
1
Transverse Direction at Midspan
LC1
LC2
LC3
LC4
LC5
LC6

Figure 36

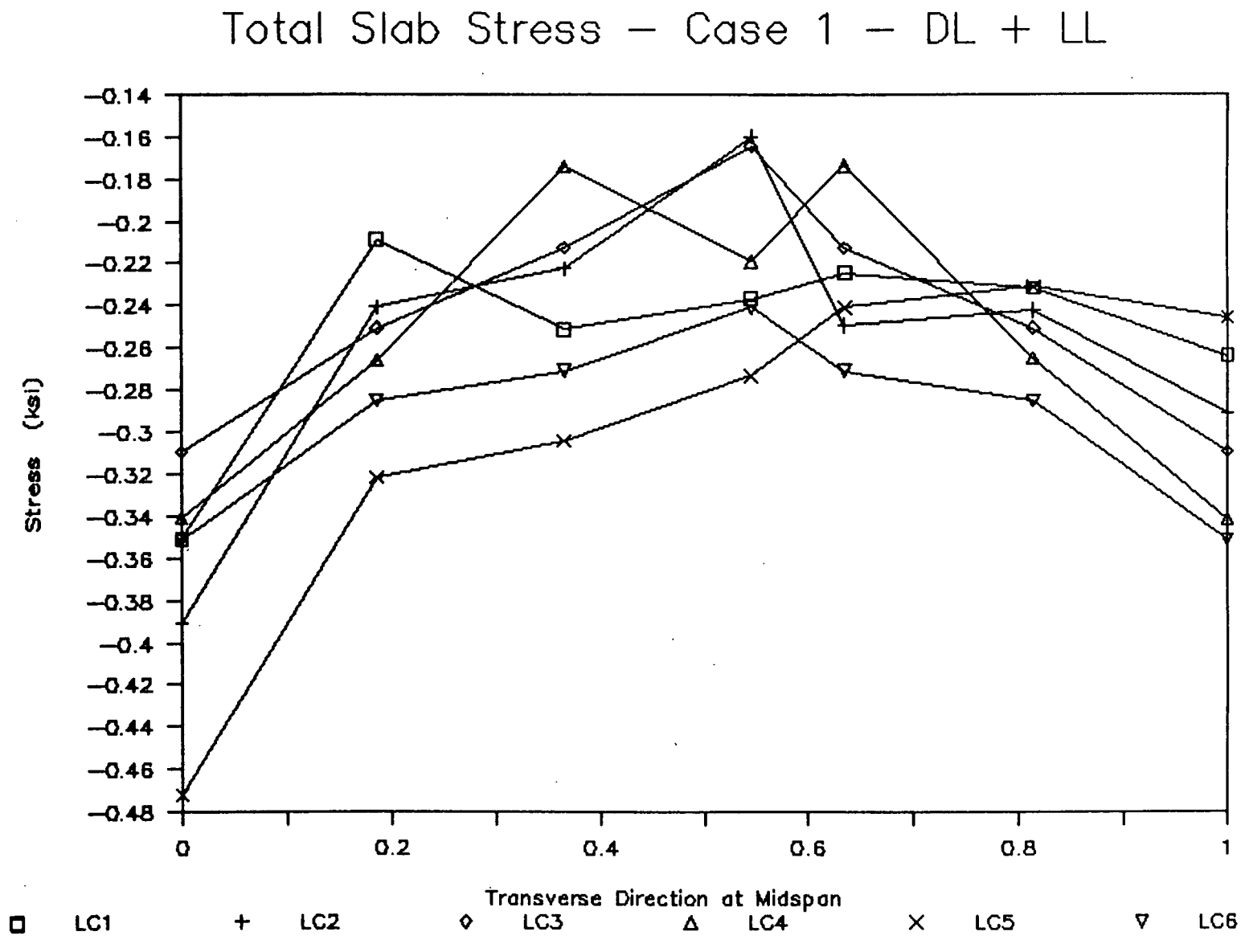
Total Slab Stress – Case 1 – DL + LL
Stress (ksi)
-0.14
-0.16
-0.18
-0.2
-0.22
-0.24
-0.26
-0.28
-0.3
-0.32
-0.34
-0.36
-0.38
-0.4
-0.42
-0.44
-0.46
-0.48
0
0.2
0.4
0.6
0.8
1
Transverse Direction at Midspan
LC1
LC2
LC3
LC4
LC5
LC6

Figure 37

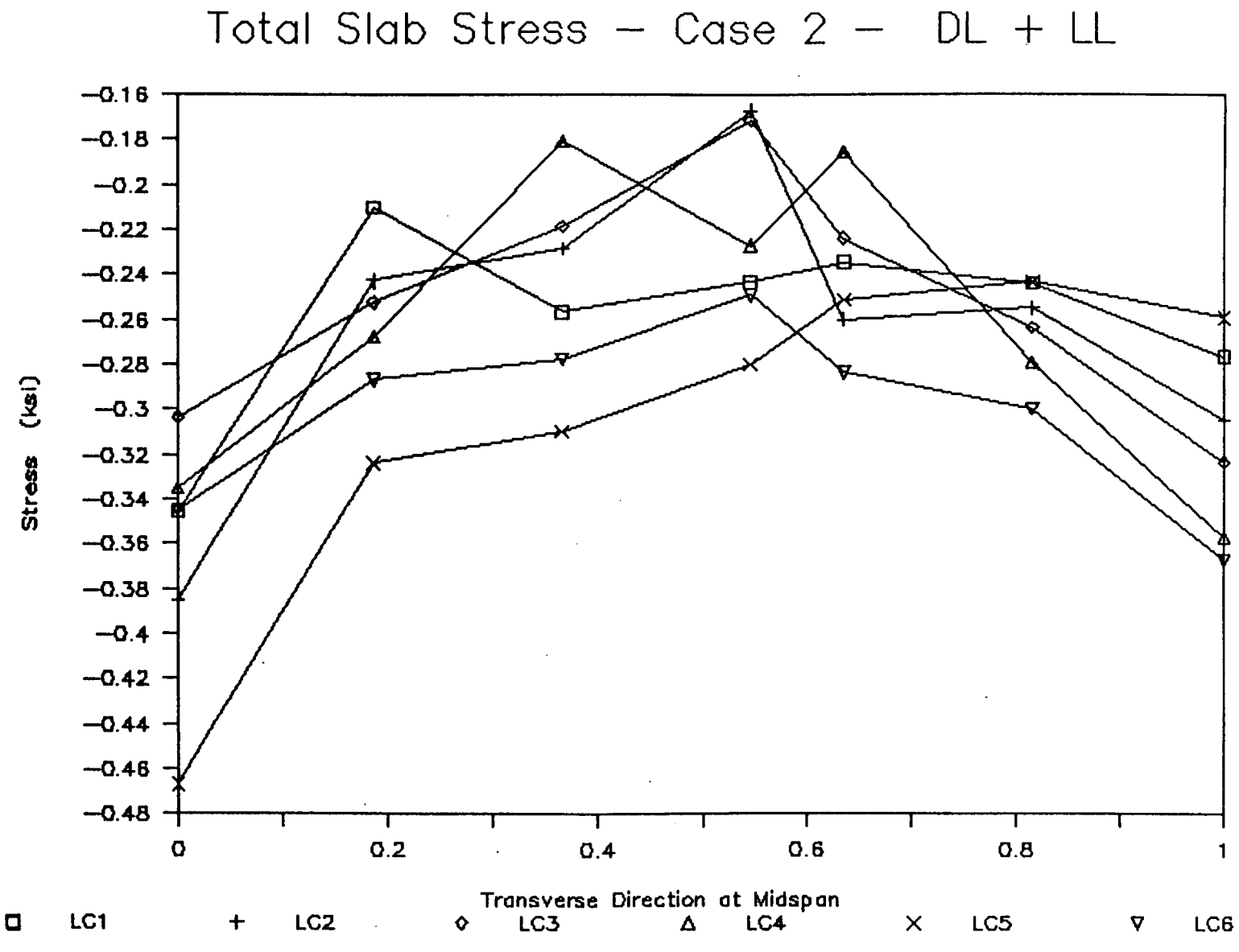
Total Slab Stress – Case 2 – DL + LL
Stress (ksi)
-0.16
-0.18
-0.2
-0.22
-0.24
-0.26
-0.28
-0.3
-0.32
-0.34
-0.36
-0.38
-0.4
-0.42
-0.44
-0.46
-0.48
0
0.2
0.4
0.6
0.8
1
Transverse Direction at Midspan
LC1
LC2
LC3
LC4
LC5
LC6

Figure 38

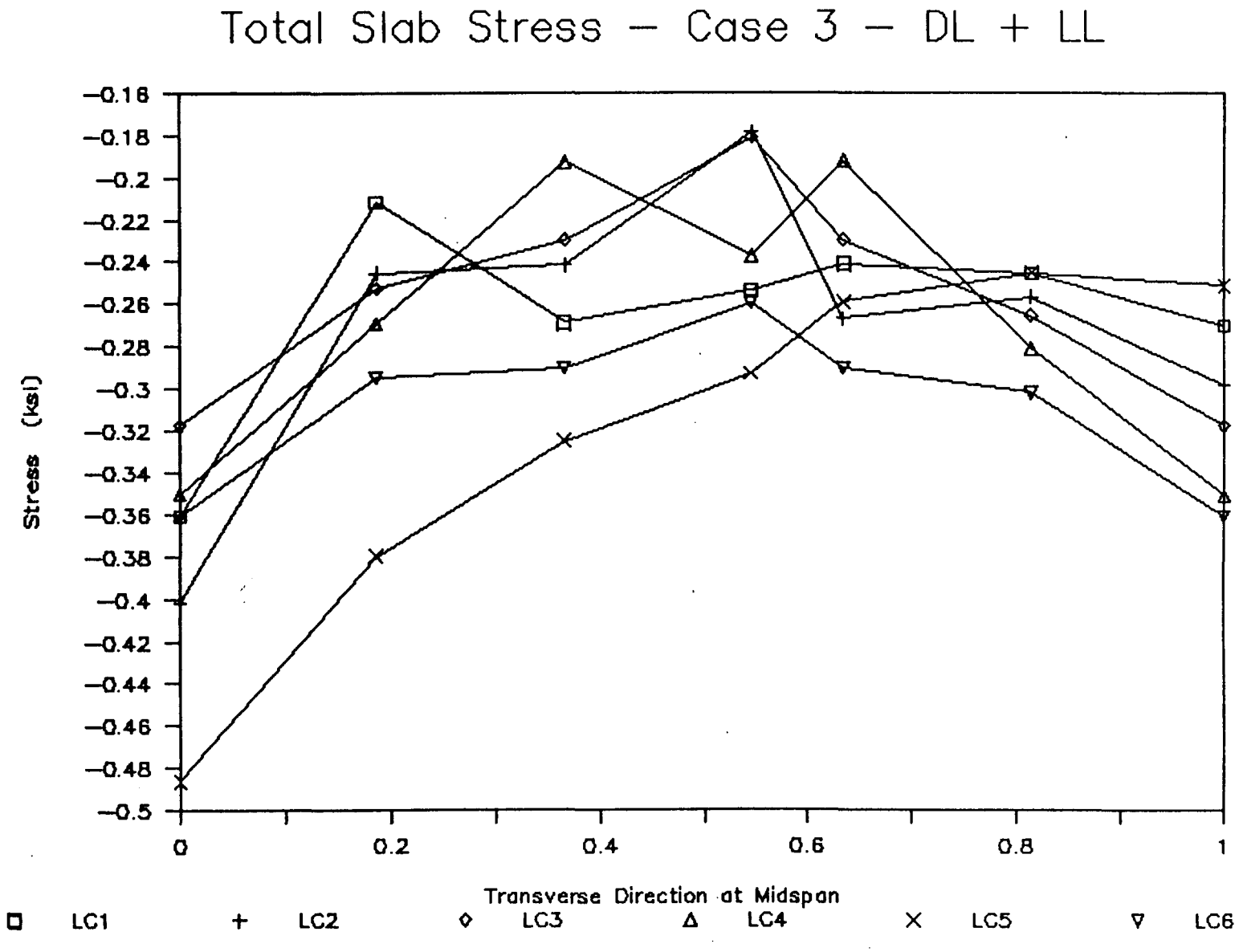
Total Slab Stress – Case 3 – DL + LL
Stress (ksi)
-0.16
-0.18
-0.2
-0.22
-0.24
-0.26
-0.28
-0.3
-0.32
-0.34
-0.36
-0.38
-0.4
-0.42
-0.44
-0.46
-0.48
-0.5
0
0.2
0.4
0.6
0.8
1
Transverse Direction at Midspan
LC1
LC2
LC3
LC4
LC5
LC6

Figure 39

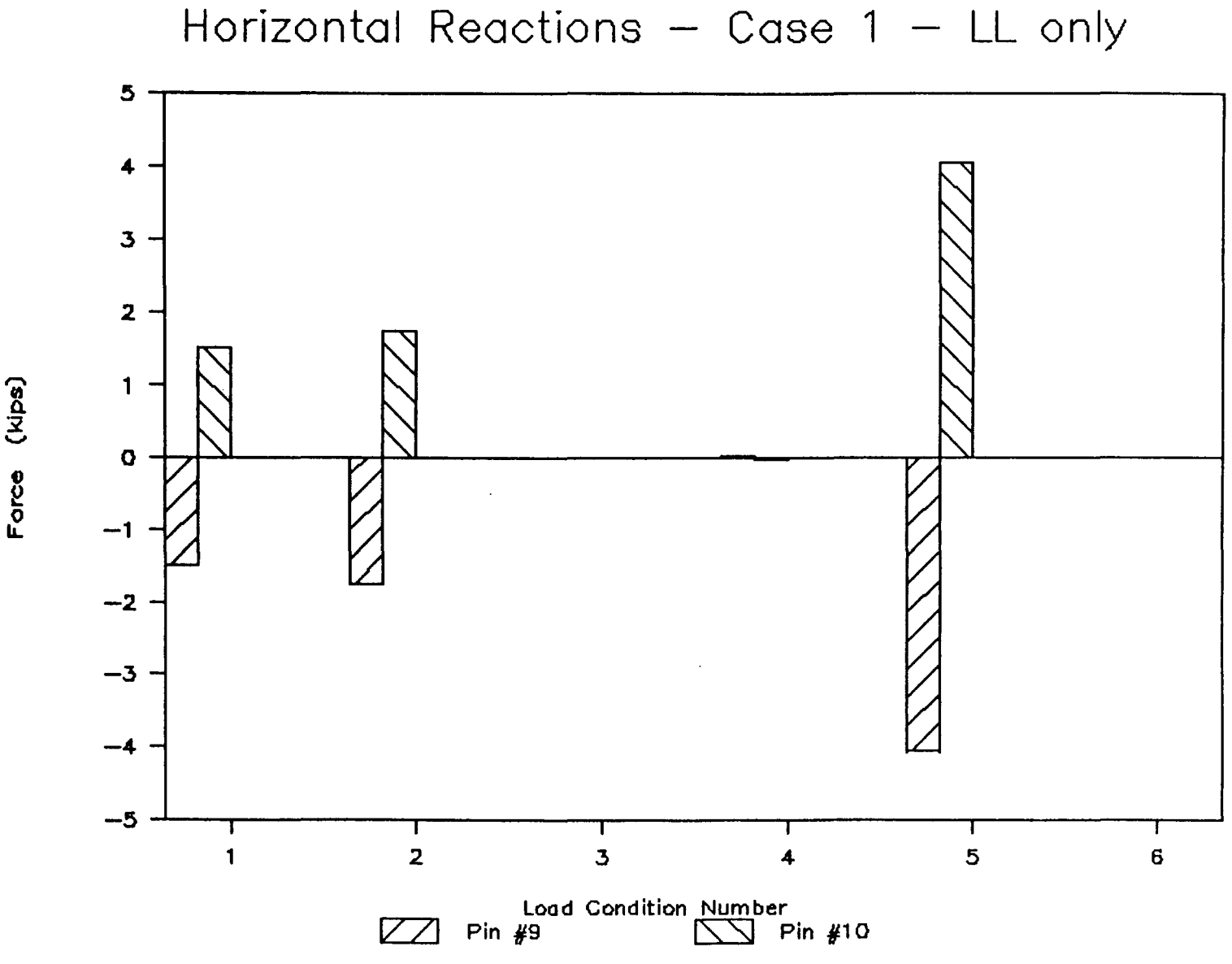
Horizontal Reactions – Case 1 – LL only
Force (kips)
5
4
3
2
1
0
−1
−2
−3
−4
−5
1
2
3
4
5
6
Load Condition Number
Pin #9
Pin #10

Figure 40

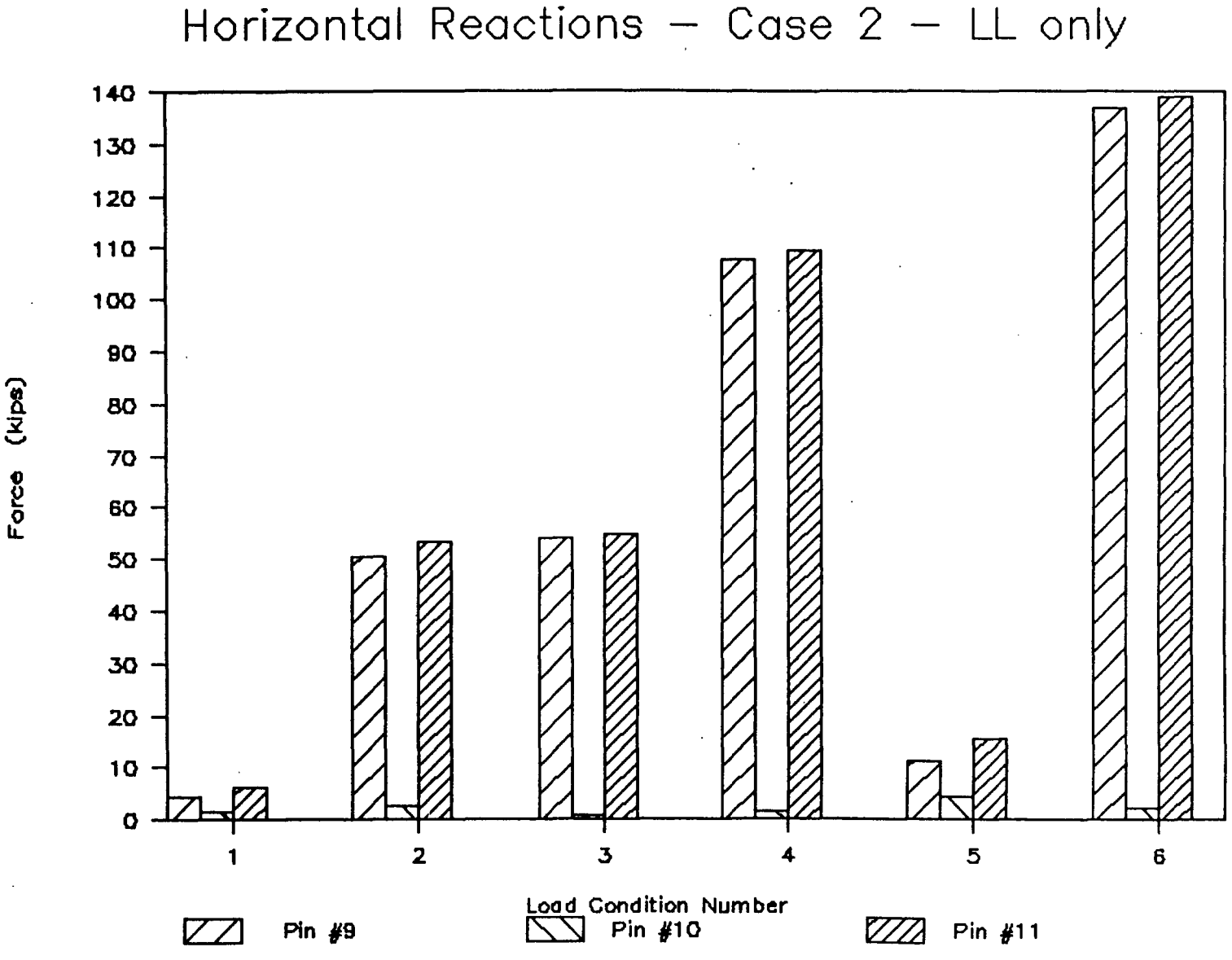
Horizontal Reactions – Case 2 – LL only
Force (kips)
140
130
120
110
100
90
80
70
60
50
40
30
20
10
0
1
2
3
4
5
6
Load Condition Number
Pin #9
Pin #10
Pin #11

Figure 41

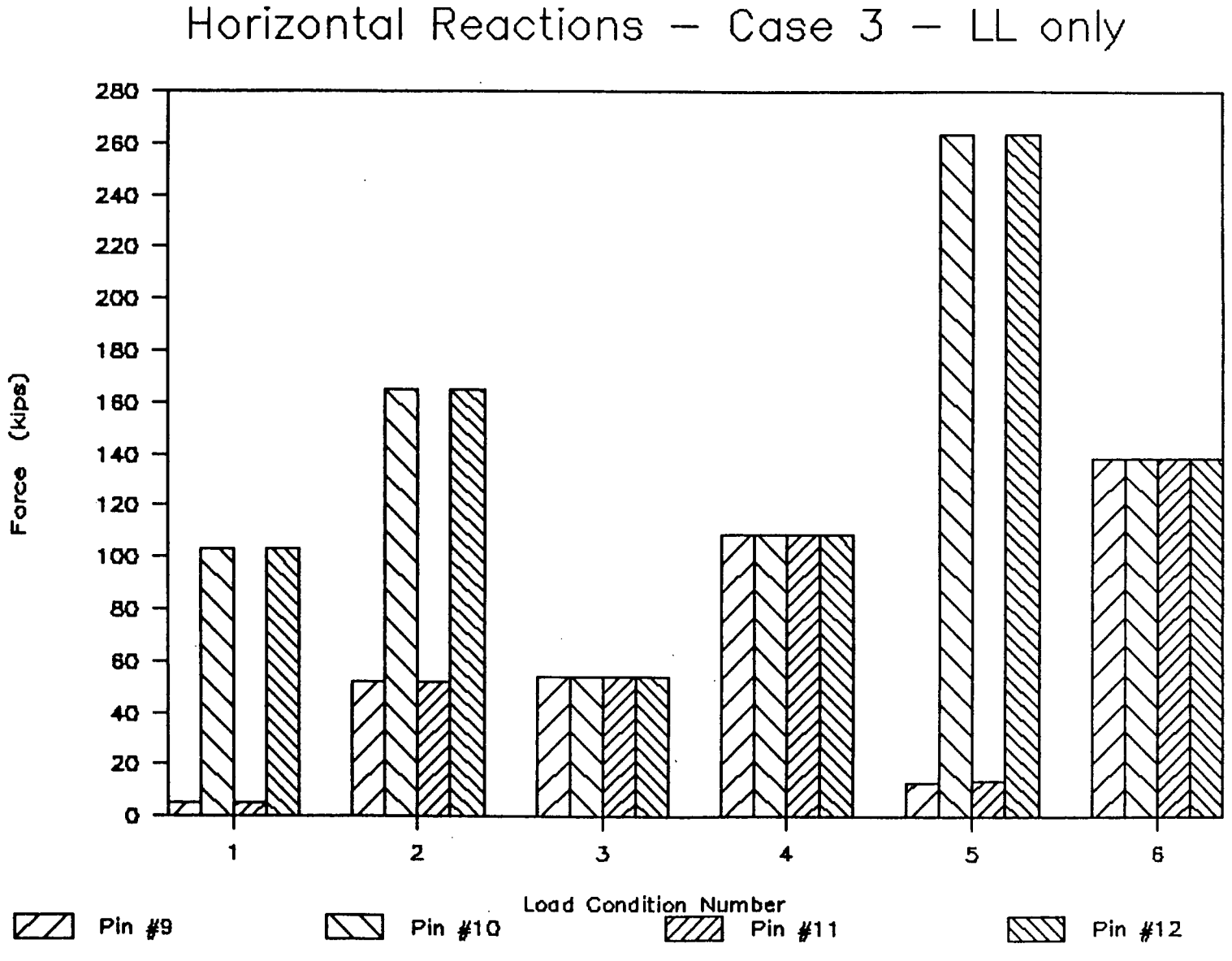
Horizontal Reactions – Case 3 – LL only
Force (kips)
280
260
240
220
200
180
160
140
120
100
80
60
40
20
0
1
2
3
4
5
6
Load Condition Number
Pin #9
Pin #10
Pin #11
Pin #12

Figure 42

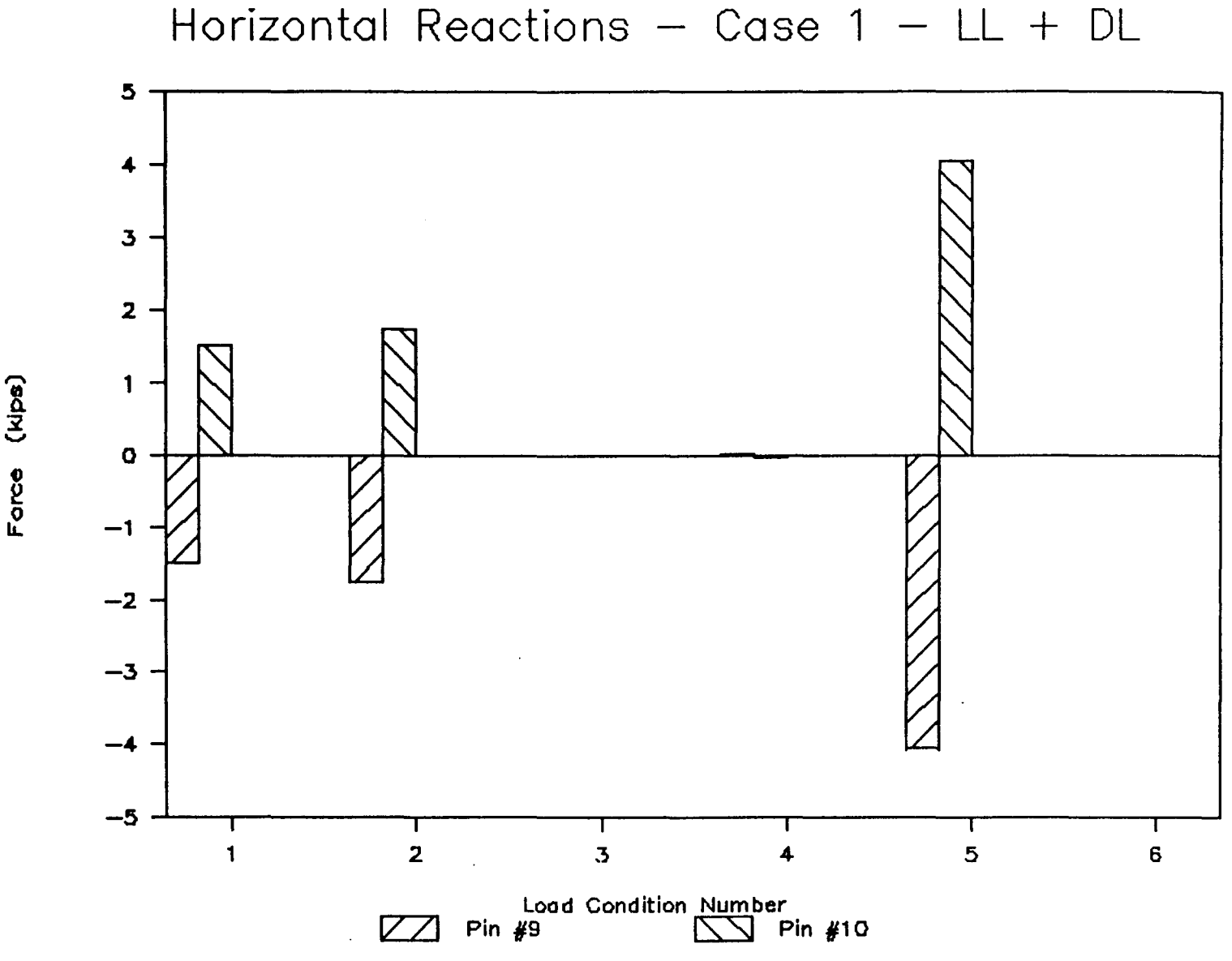
Horizontal Reactions – Case 1 – LL + DL
Force (kips)
5
4
3
2
1
0
-1
-2
-3
-4
-5
1
2
3
4
5
6
Load Condition Number
Pin #9
Pin #10

Figure 43

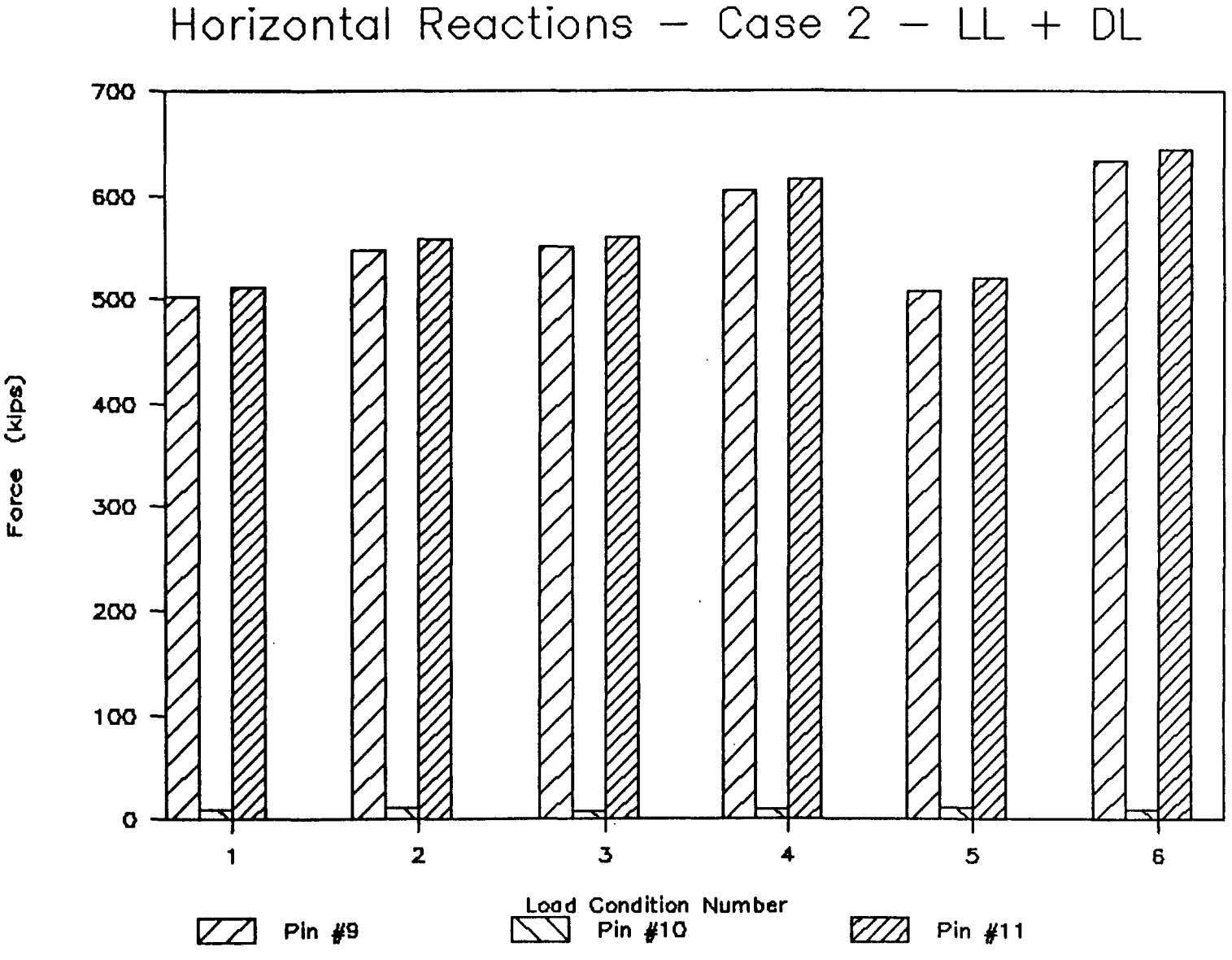
Horizontal Reactions – Case 2 – LL + DL
Force (kips)
700
600
500
400
300
200
100
0
1
2
3
4
5
6
Load Condition Number
Pin #9
Pin #10
Pin #11

Figure 44

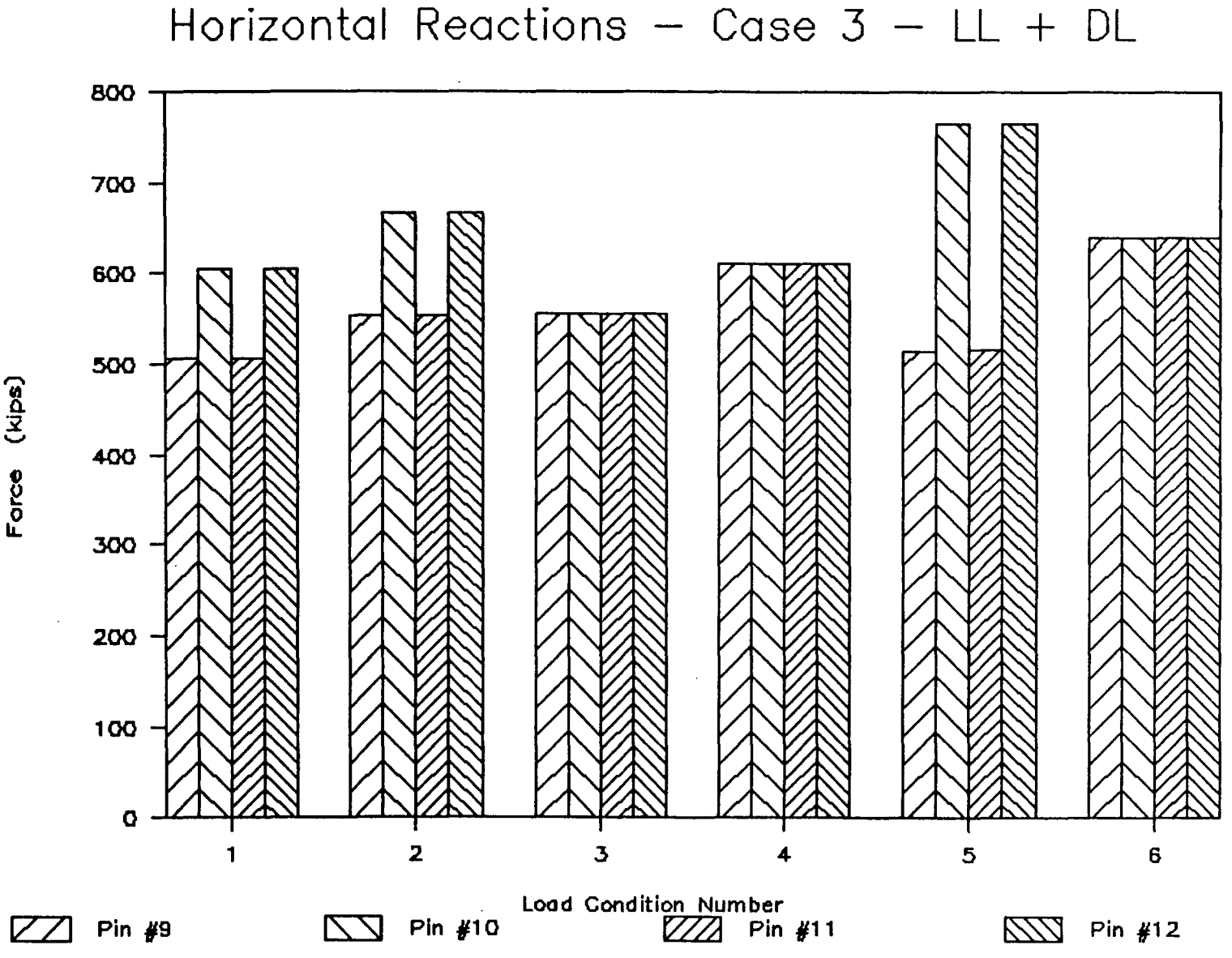
Horizontal Reactions – Case 3 – LL + DL
800
700
600
500
400
300
200
100
0
Force (kips)
1
2
3
4
5
6
Load Condition Number
Pin #9
Pin #10
Pin #11
Pin #12

Figure 45

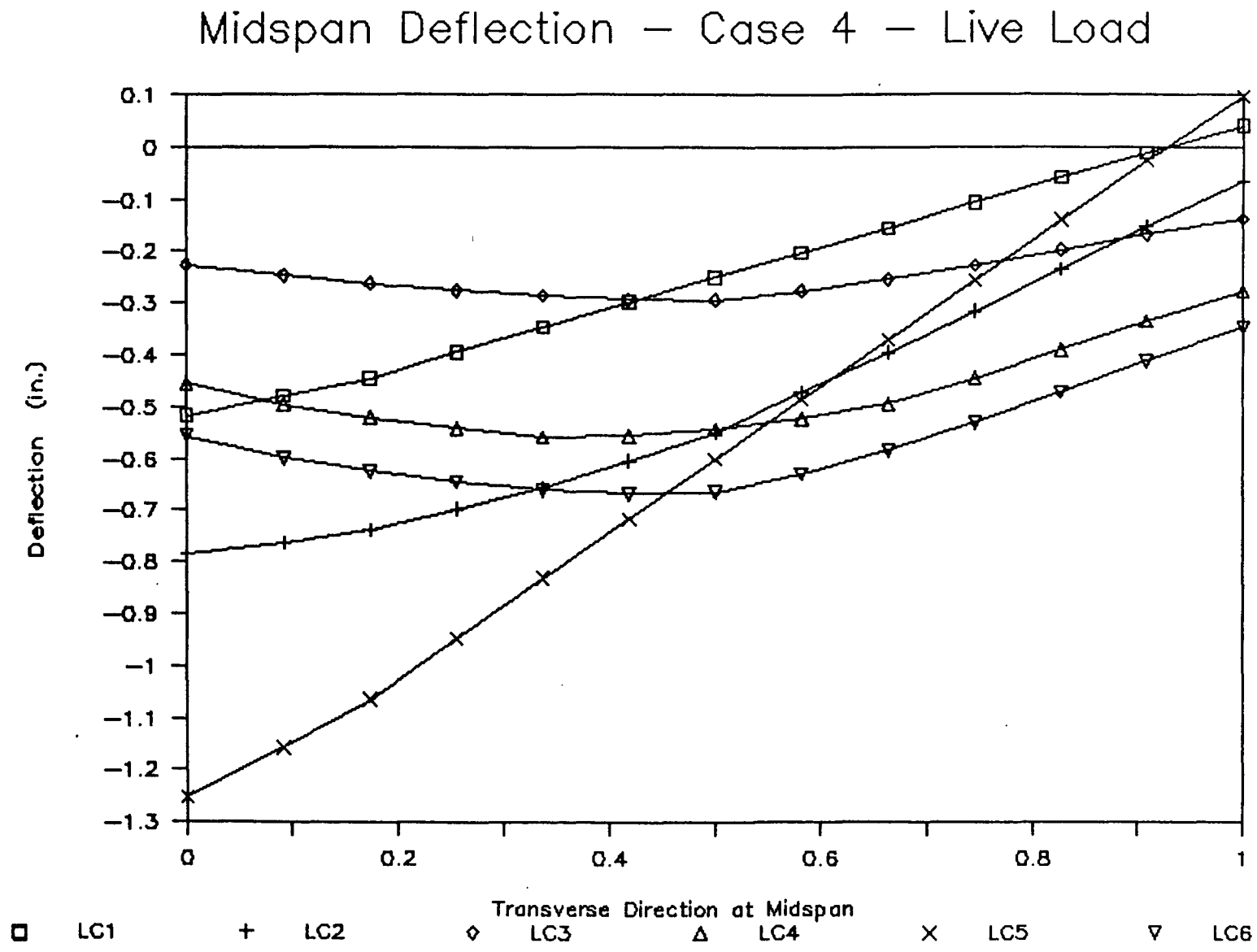
Midspan Deflection – Case 4 – Live Load
Deflection (in.)
0.1
0
-0.1
-0.2
-0.3
-0.4
-0.5
-0.6
-0.7
-0.8
-0.9
-1
-1.1
-1.2
-1.3
0
0.2
0.4
0.6
0.8
1
Transverse Direction at Midspan
LC1
LC2
LC3
LC4
LC5
LC6

Figure 46

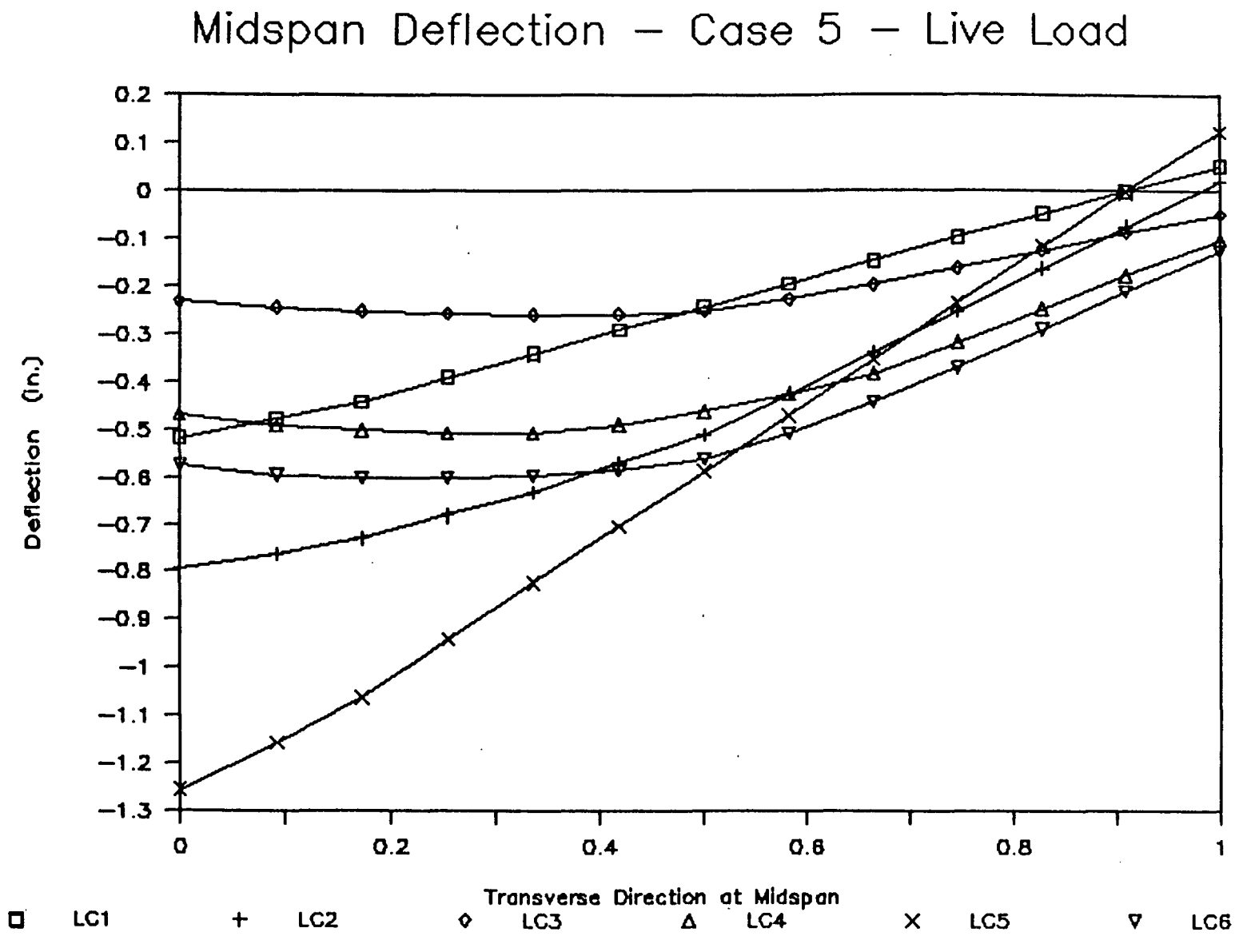
Midspan Deflection – Case 5 – Live Load
Deflection (in.)
0.2
0.1
0
-0.1
-0.2
-0.3
-0.4
-0.5
-0.6
-0.7
-0.8
-0.9
-1
-1.1
-1.2
-1.3
0
0.2
0.4
0.6
0.8
1
Transverse Direction at Midspan
LC1
LC2
LC3
LC4
LC5
LC6

Figure 47

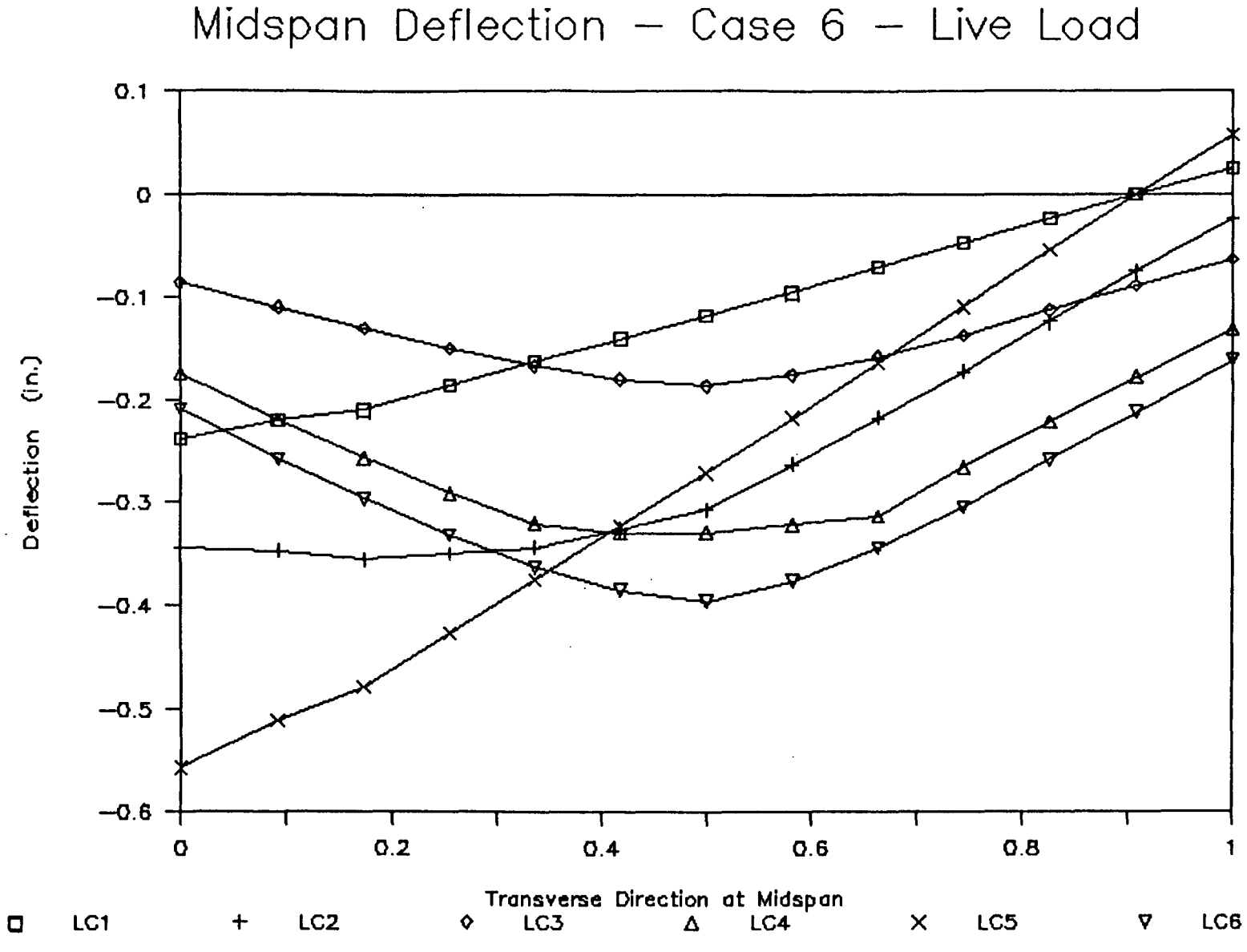
Midspan Deflection – Case 6 – Live Load
0.1
0
−0.1
−0.2
−0.3
−0.4
−0.5
−0.6
Deflection (in.)
0
0.2
0.4
0.6
0.8
1
Transverse Direction at Midspan
LC1
LC2
LC3
LC4
LC5
LC6

Figure 48

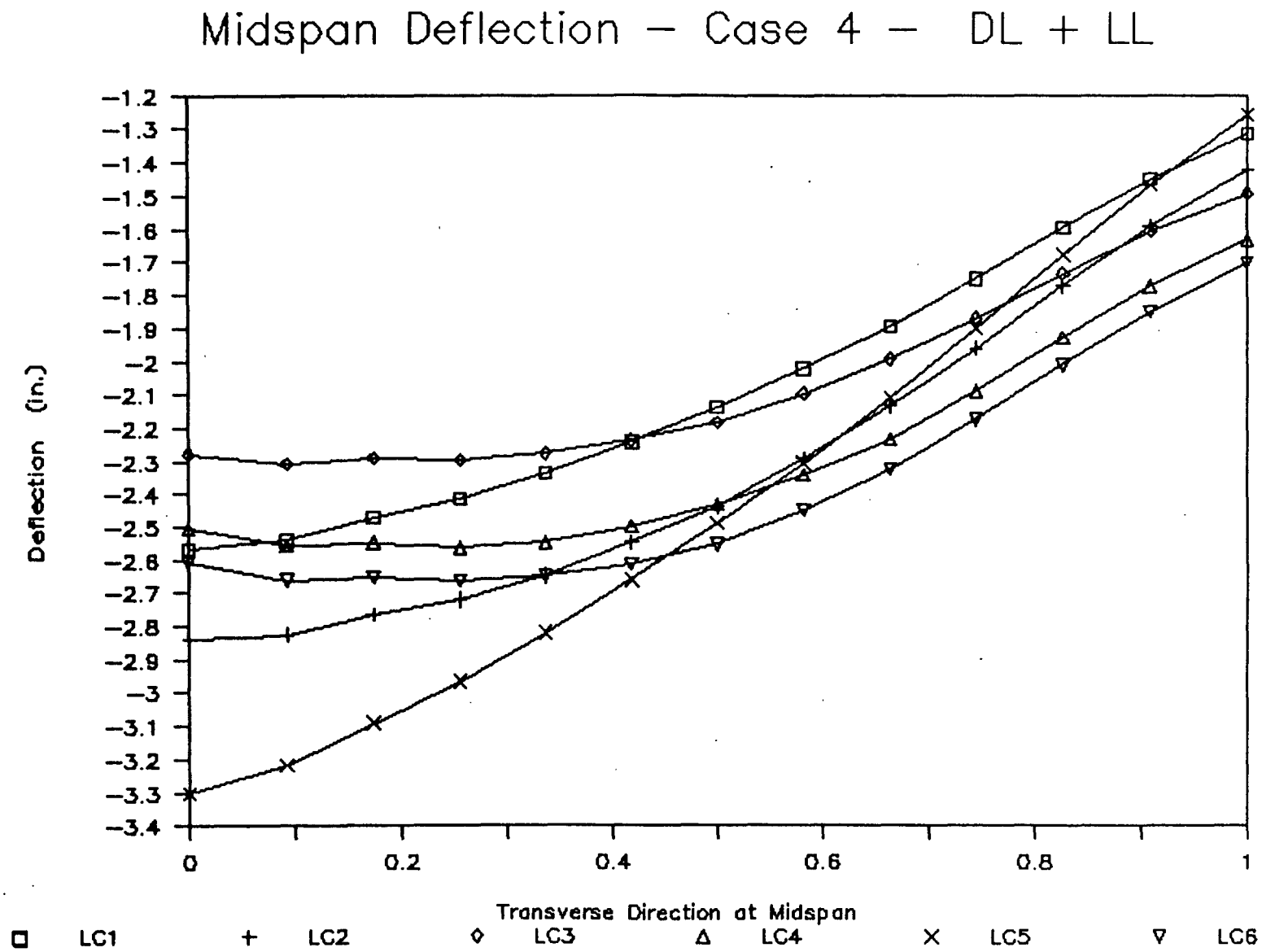
Midspan Deflection – Case 4 – DL + LL
Deflection (in.)
-1.2
-1.3
-1.4
-1.5
-1.6
-1.7
-1.8
-1.9
-2
-2.1
-2.2
-2.3
-2.4
-2.5
-2.6
-2.7
-2.8
-2.9
-3
-3.1
-3.2
-3.3
-3.4
0
0.2
0.4
0.6
0.8
1
Transverse Direction at Midspan
LC1
LC2
LC3
LC4
LC5
LC6

Figure 49

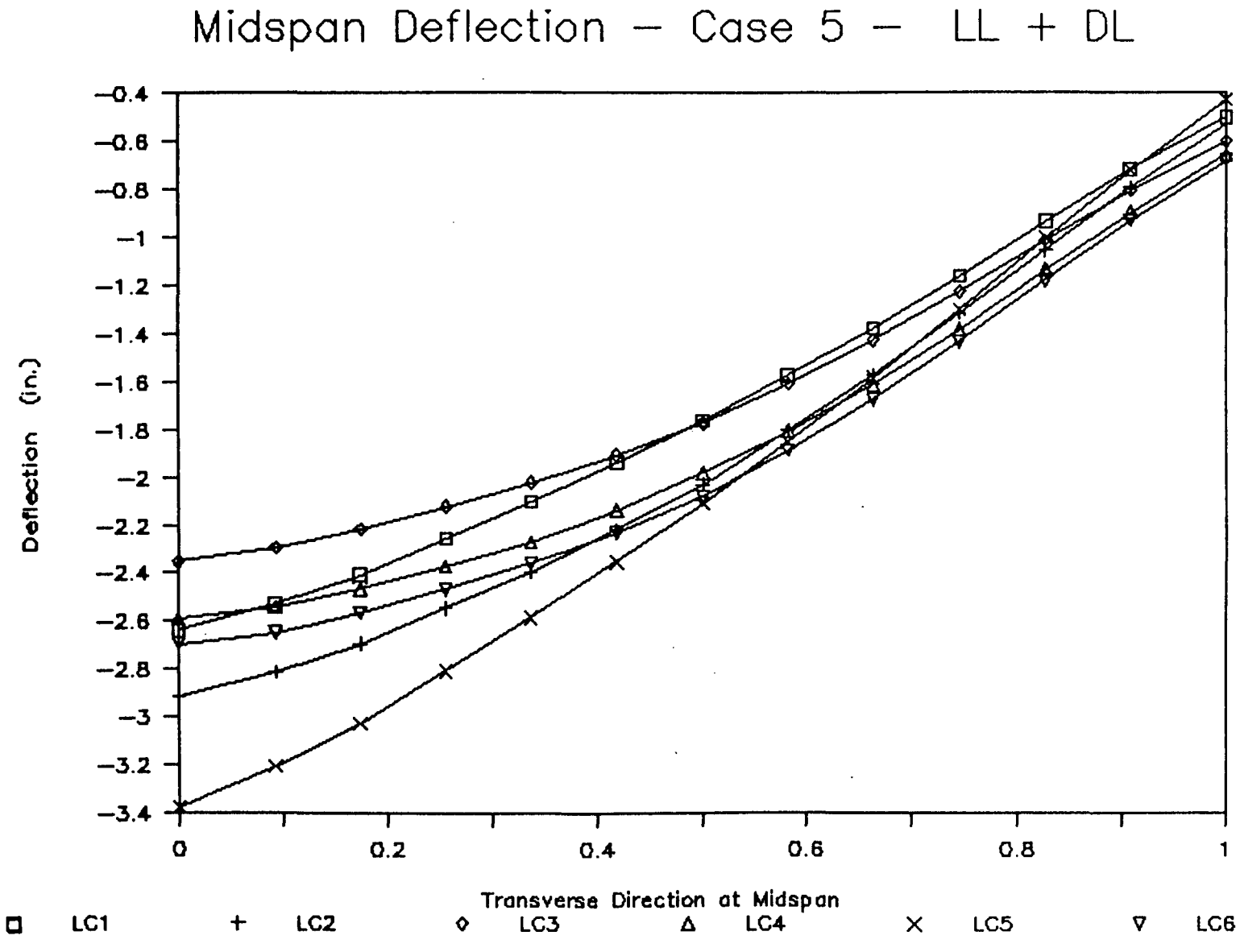
Midspan Deflection – Case 5 – LL + DL
Deflection (in.)
-0.4
-0.6
-0.8
-1
-1.2
-1.4
-1.6
-1.8
-2
-2.2
-2.4
-2.6
-2.8
-3
-3.2
-3.4
0
0.2
0.4
0.6
0.8
1
Transverse Direction at Midspan
LC1
LC2
LC3
LC4
LC5
LC6

Figure 50

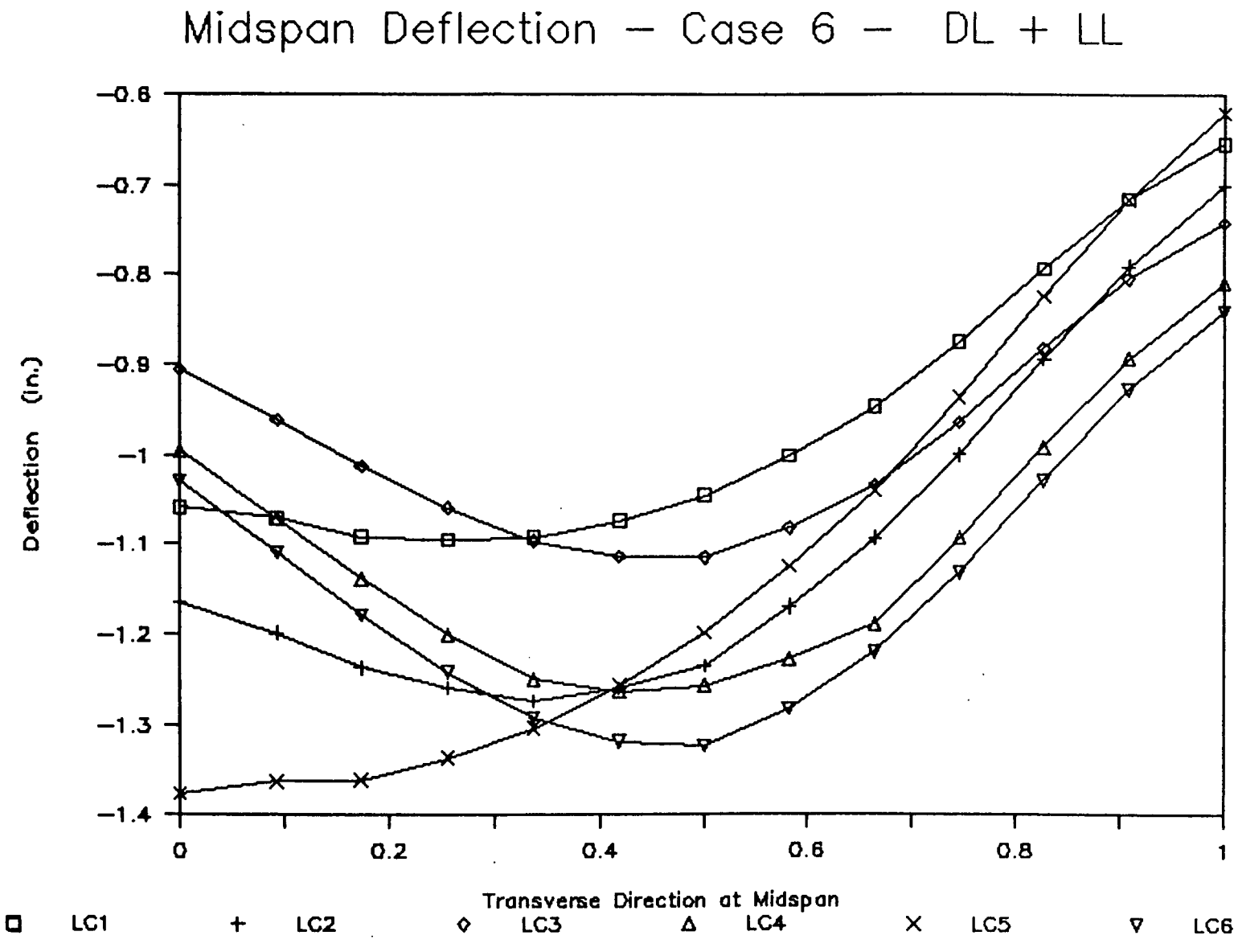
Midspan Deflection – Case 6 – DL + LL
Deflection (in.)
-0.6
-0.7
-0.8
-0.9
-1
-1.1
-1.2
-1.3
-1.4
0
0.2
0.4
0.6
0.8
1
Transverse Direction at Midspan
LC1
LC2
LC3
LC4
LC5
LC6

Figure 51

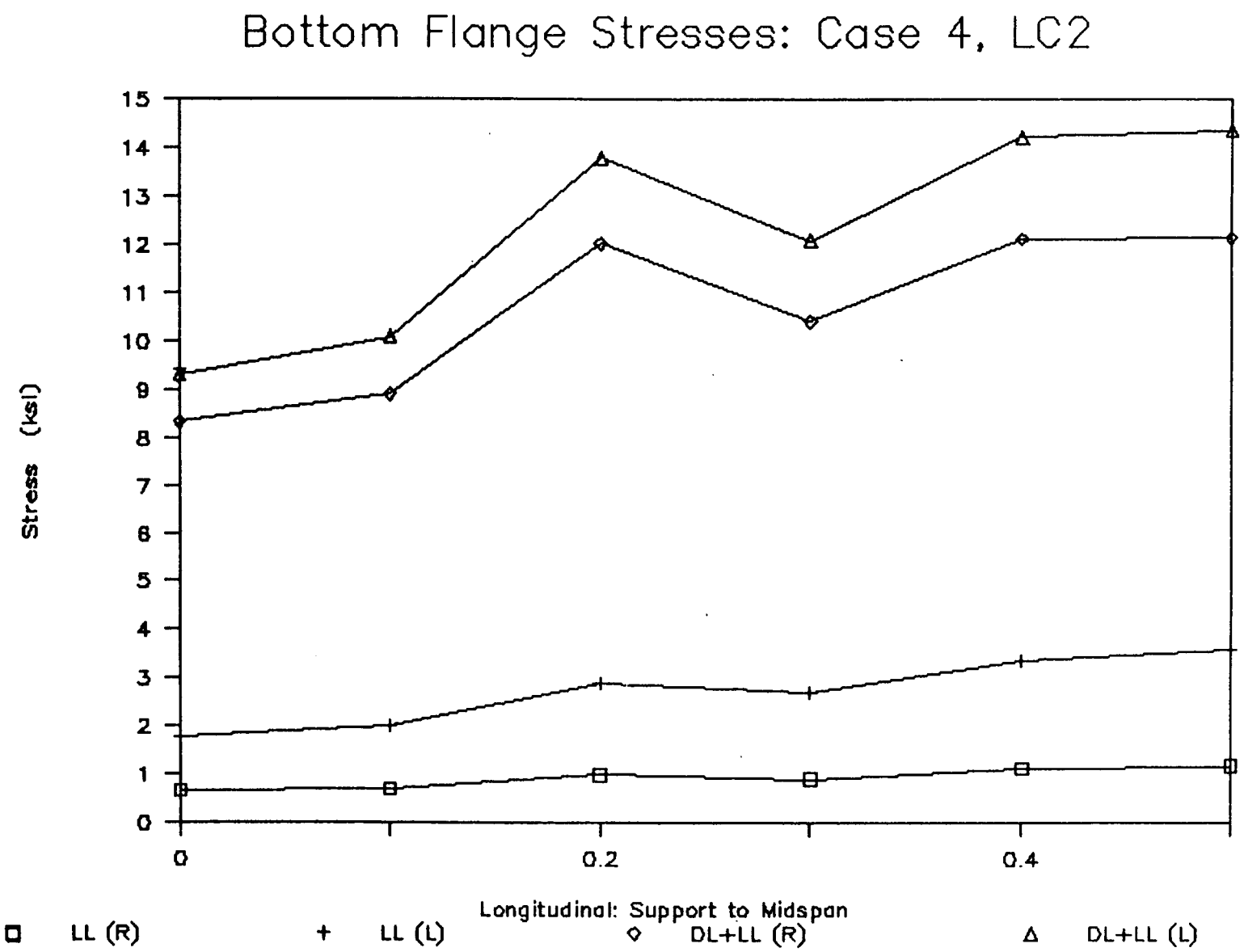
Bottom Flange Stresses: Case 4, LC2
Stress (ksi)
15
14
13
12
11
10
9
8
7
6
5
4
3
2
1
0
0
0.2
0.4
Longitudinal: Support to Midspan
LL (R)
LL (L)
DL+LL (R)
DL+LL (L)

Figure 52

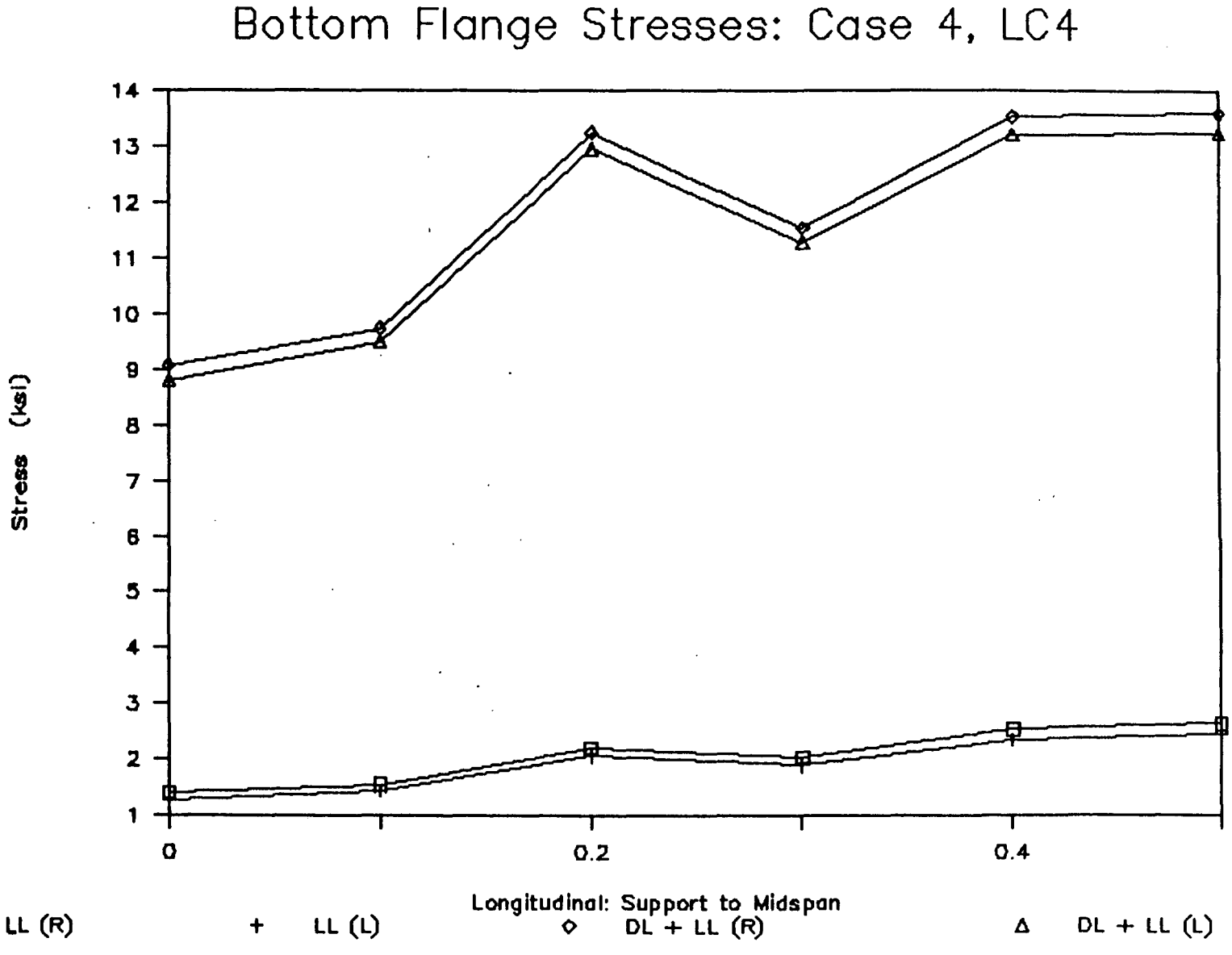
Bottom Flange Stresses: Case 4, LC4
Stress (ksi)
14
13
12
11
10
9
8
7
6
5
4
3
2
1
0
0.2
0.4
Longitudinal: Support to Midspan
LL (R)
+ LL (L)
◇ DL + LL (R)
Δ DL + LL (L)

Figure 53

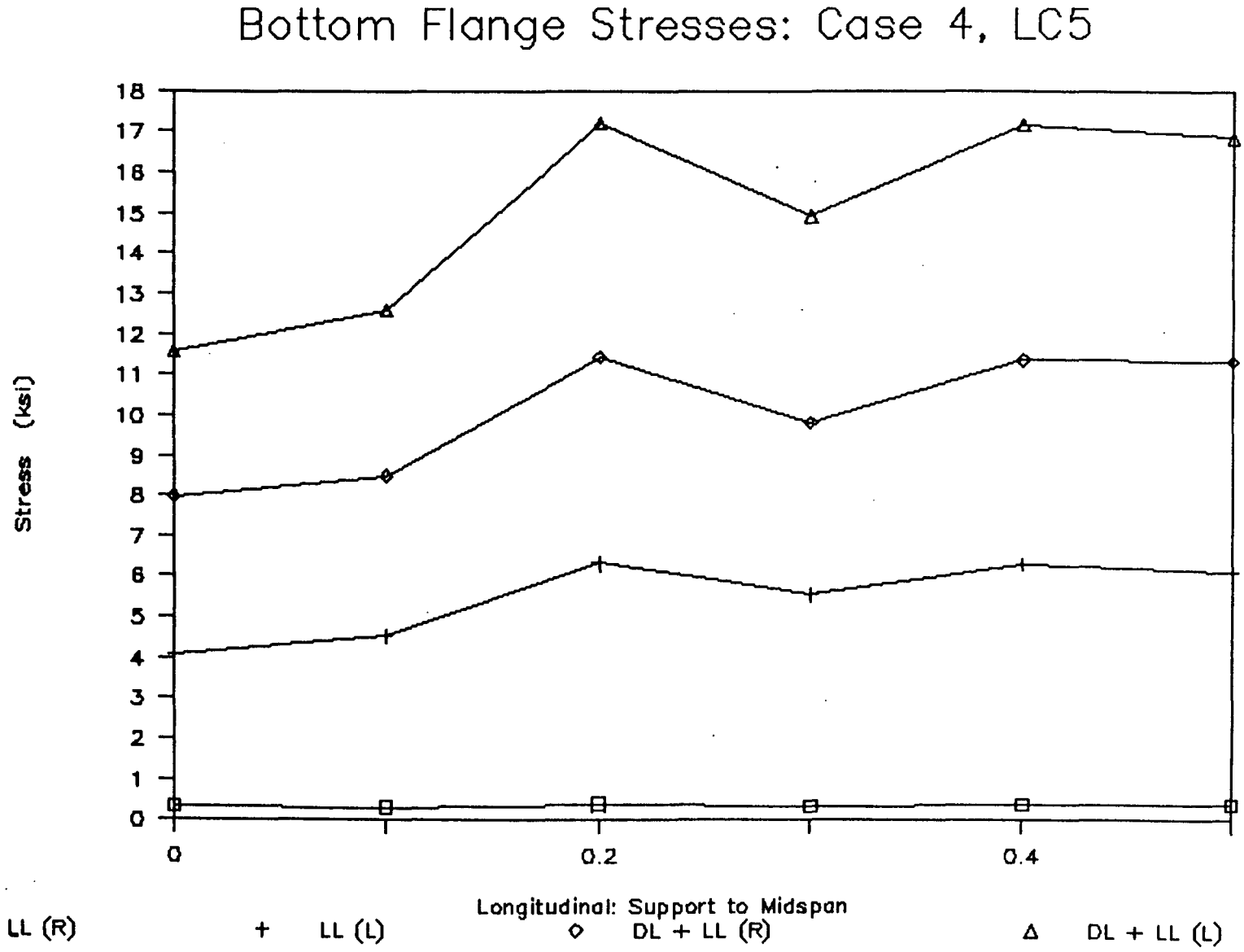
Bottom Flange Stresses: Case 4, LC5
Stress (ksi)
18
17
16
15
14
13
12
11
10
9
8
7
6
5
4
3
2
1
0
0
0.2
0.4
Longitudinal: Support to Midspan
LL (R)
+ LL (L)
◇ DL + LL (R)
Δ DL + LL (L)

Figure 54

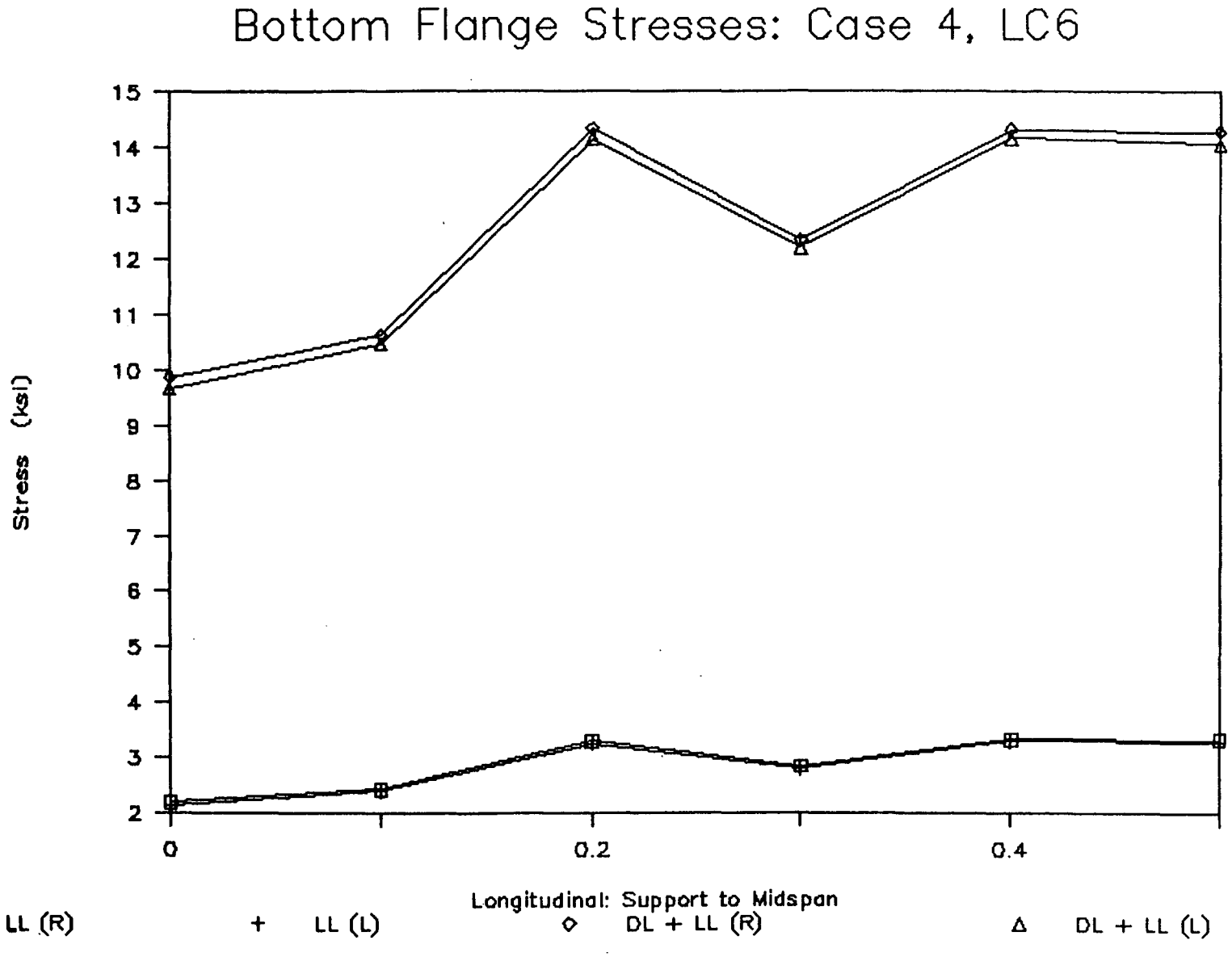
Bottom Flange Stresses: Case 4, LC6
Stress (ksi)
15
14
13
12
11
10
9
8
7
6
5
4
3
2
0
0.2
0.4
Longitudinal: Support to Midspan
LL (R)
+ LL (L)
◇ DL + LL (R)
△ DL + LL (L)

Figure 55

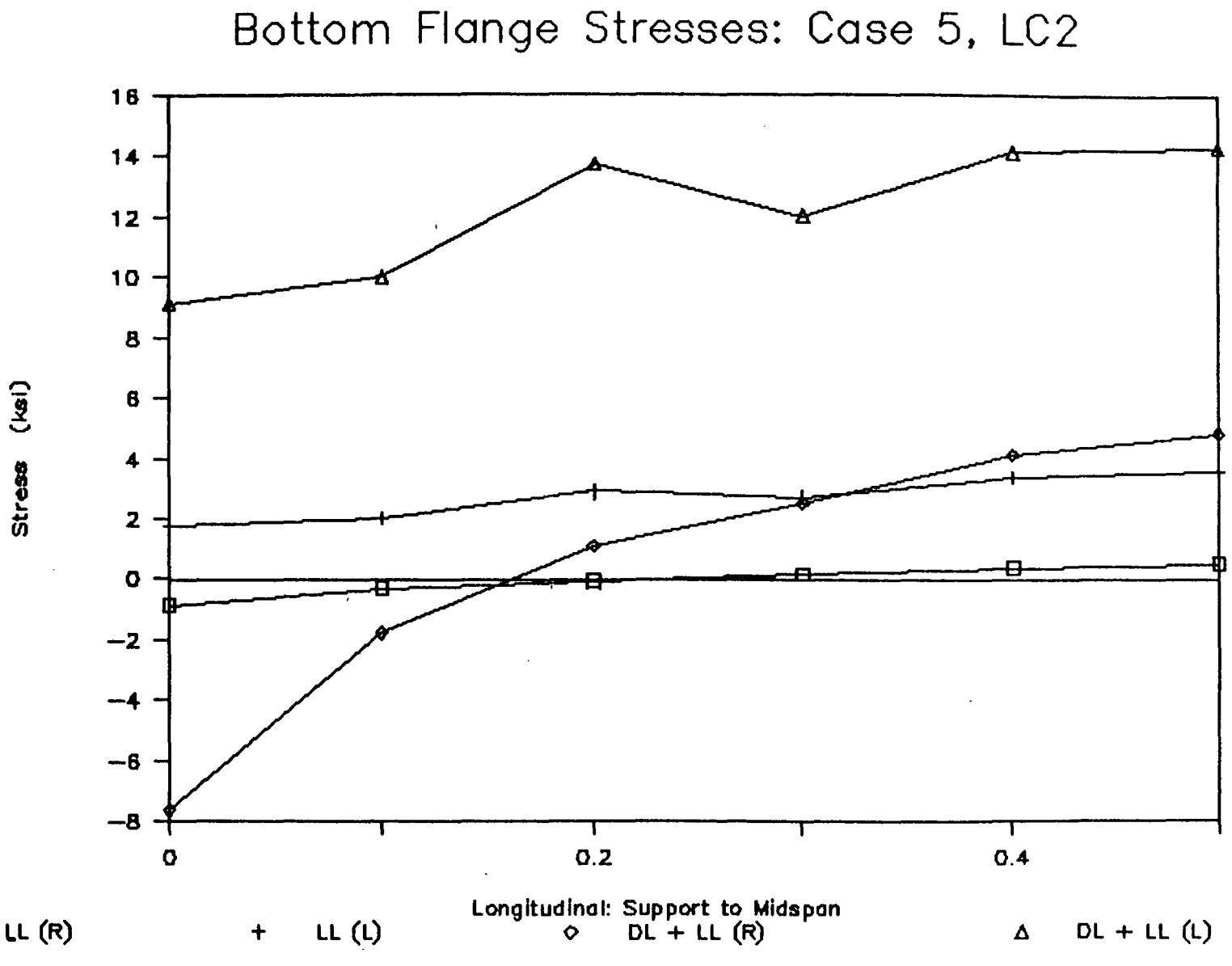
Bottom Flange Stresses: Case 5, LC2
16
14
12
10
8
6
4
2
0
−2
−4
−6
−8
Stress (ksi)
0
0.2
0.4
Longitudinal: Support to Midspan
LL (R)
+ LL (L)
◇ DL + LL (R)
Δ DL + LL (L)

Figure 56

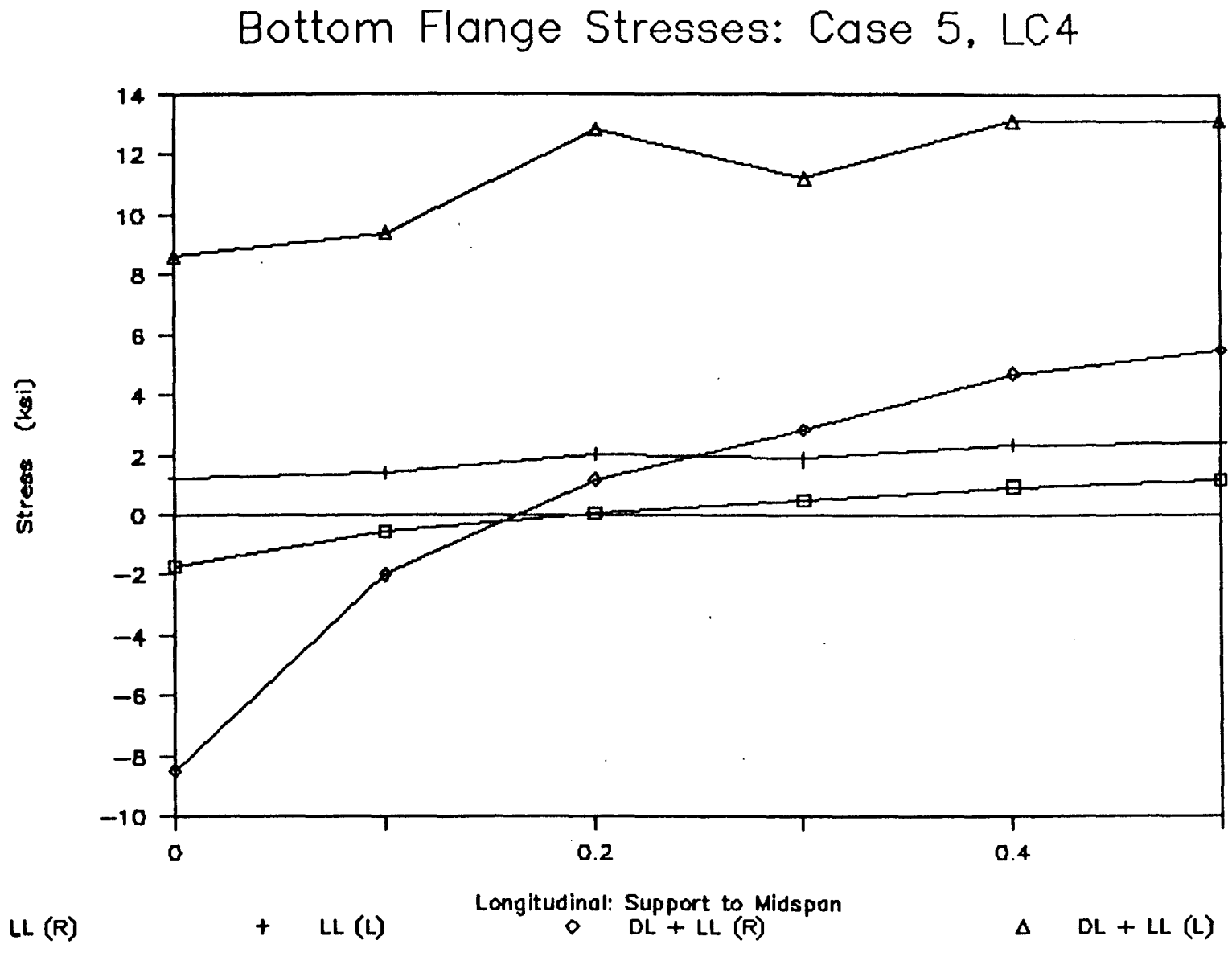
Bottom Flange Stresses: Case 5, LC4
14
12
10
8
6
4
2
0
−2
−4
−6
−8
−10
Stress (ksi)
0
0.2
0.4
Longitudinal: Support to Midspan
LL (R)
LL (L)
DL + LL (R)
DL + LL (L)

Figure 57

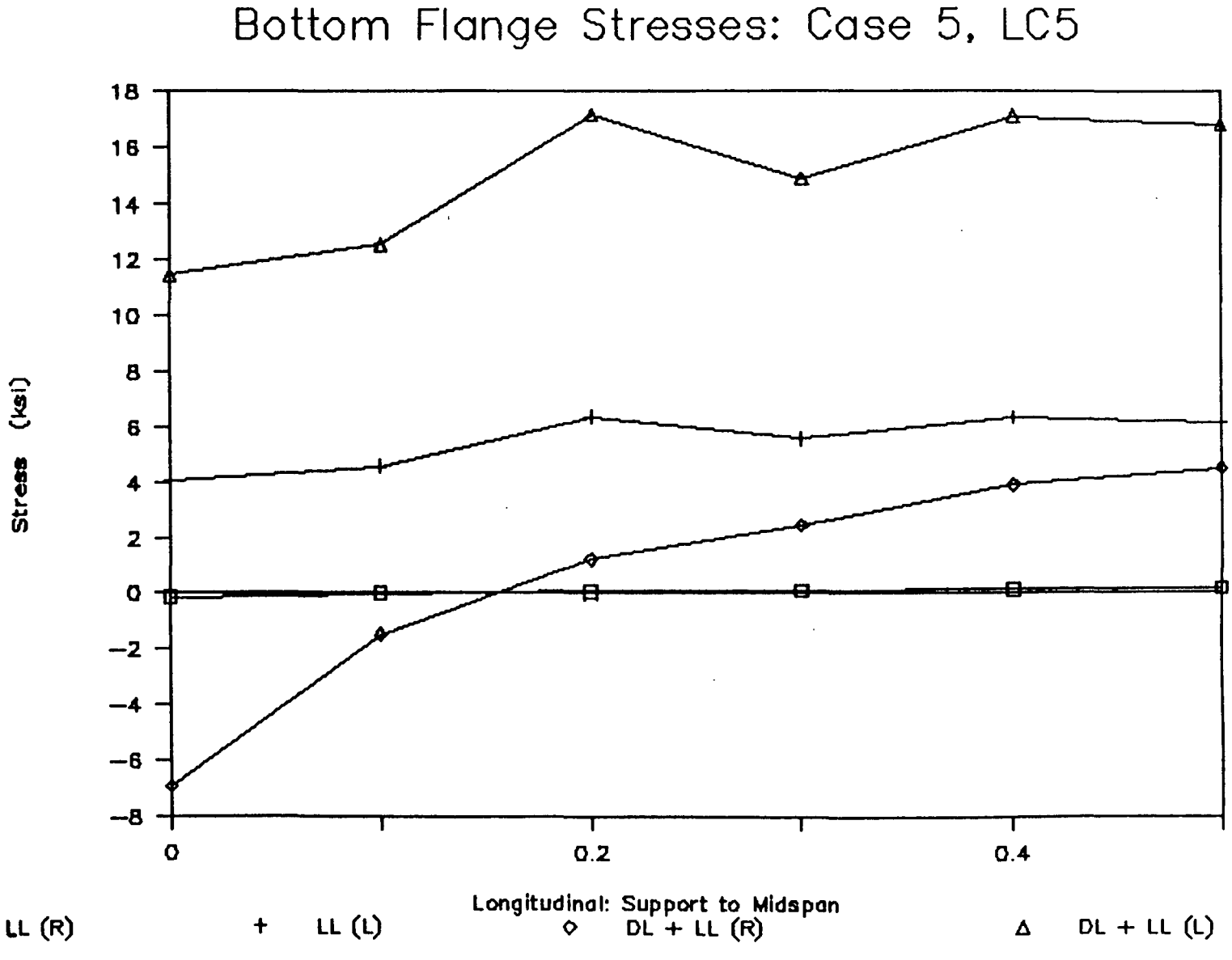
Bottom Flange Stresses: Case 5, LC5
Stress (ksi)
18
16
14
12
10
8
6
4
2
0
−2
−4
−6
−8
0
0.2
0.4
Longitudinal: Support to Midspan
LL (R)
+ LL (L)
◇ DL + LL (R)
△ DL + LL (L)

Figure 58

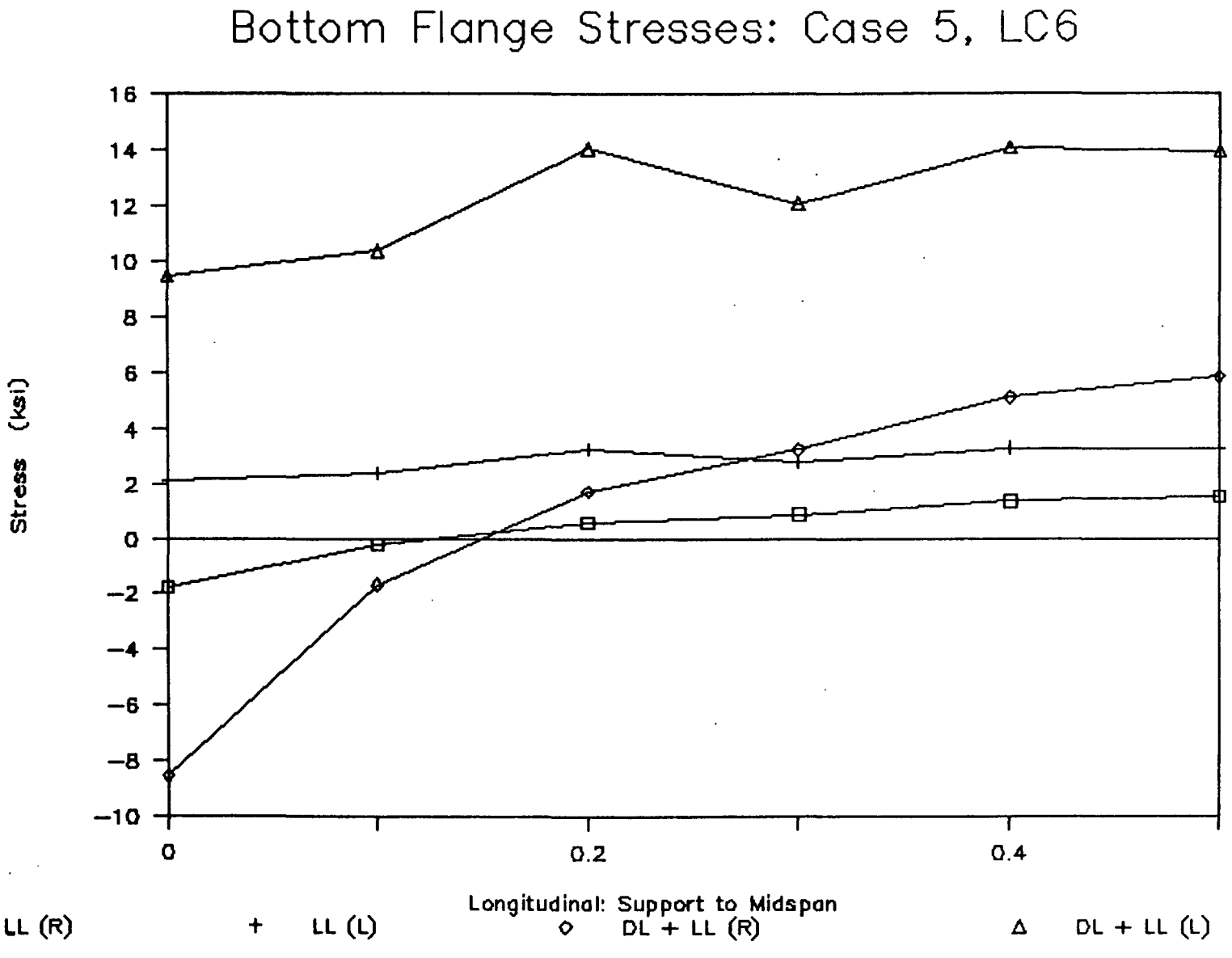
Bottom Flange Stresses: Case 5, LC6
16
14
12
10
8
6
4
2
0
−2
−4
−6
−8
−10
Stress (ksi)
0
0.2
0.4
Longitudinal: Support to Midspan
LL (R)
+ LL (L)
◇ DL + LL (R)
△ DL + LL (L)

Figure 59

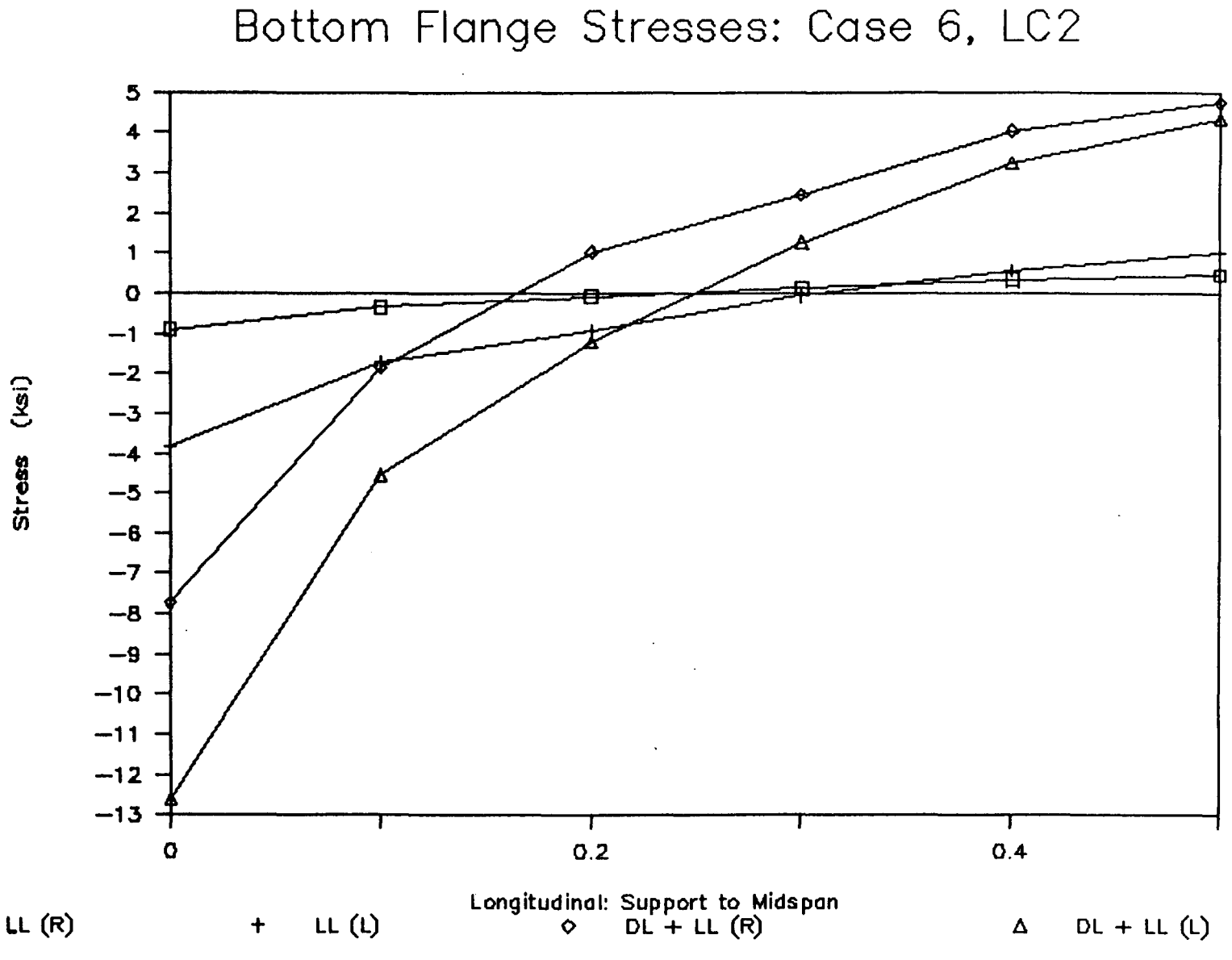
Bottom Flange Stresses: Case 6, LC2
Stress (ksi)
5
4
3
2
1
0
-1
-2
-3
-4
-5
-6
-7
-8
-9
-10
-11
-12
-13
0
0.2
0.4
Longitudinal: Support to Midspan
LL (R)
+ LL (L)
◇ DL + LL (R)
Δ DL + LL (L)

Figure 60

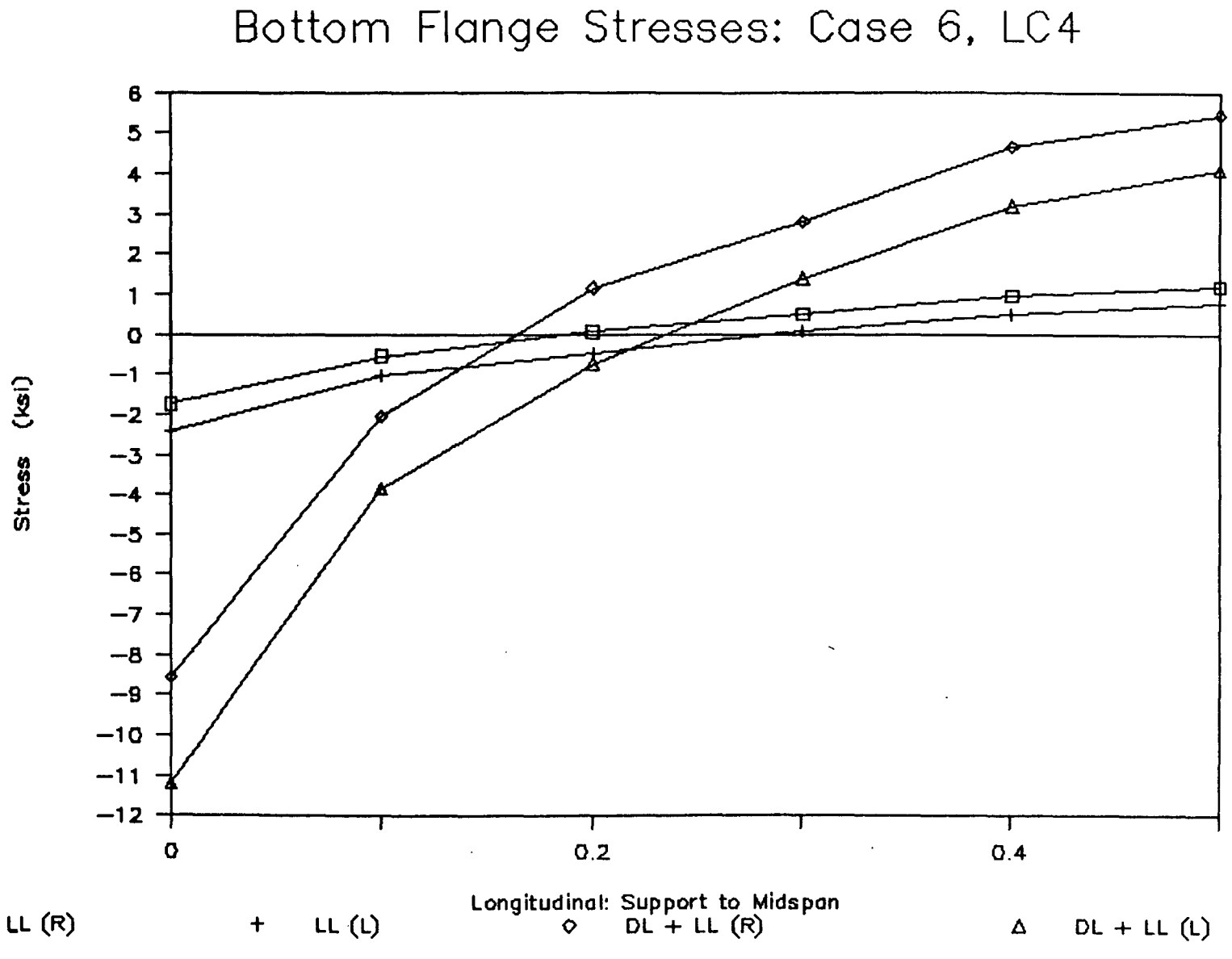
Bottom Flange Stresses: Case 6, LC4
Stress (ksi)
6
5
4
3
2
1
0
−1
−2
−3
−4
−5
−6
−7
−8
−9
−10
−11
−12
0
0.2
0.4
Longitudinal: Support to Midspan
LL (R)
+ LL (L)
◇ DL + LL (R)
Δ DL + LL (L)

Figure 61

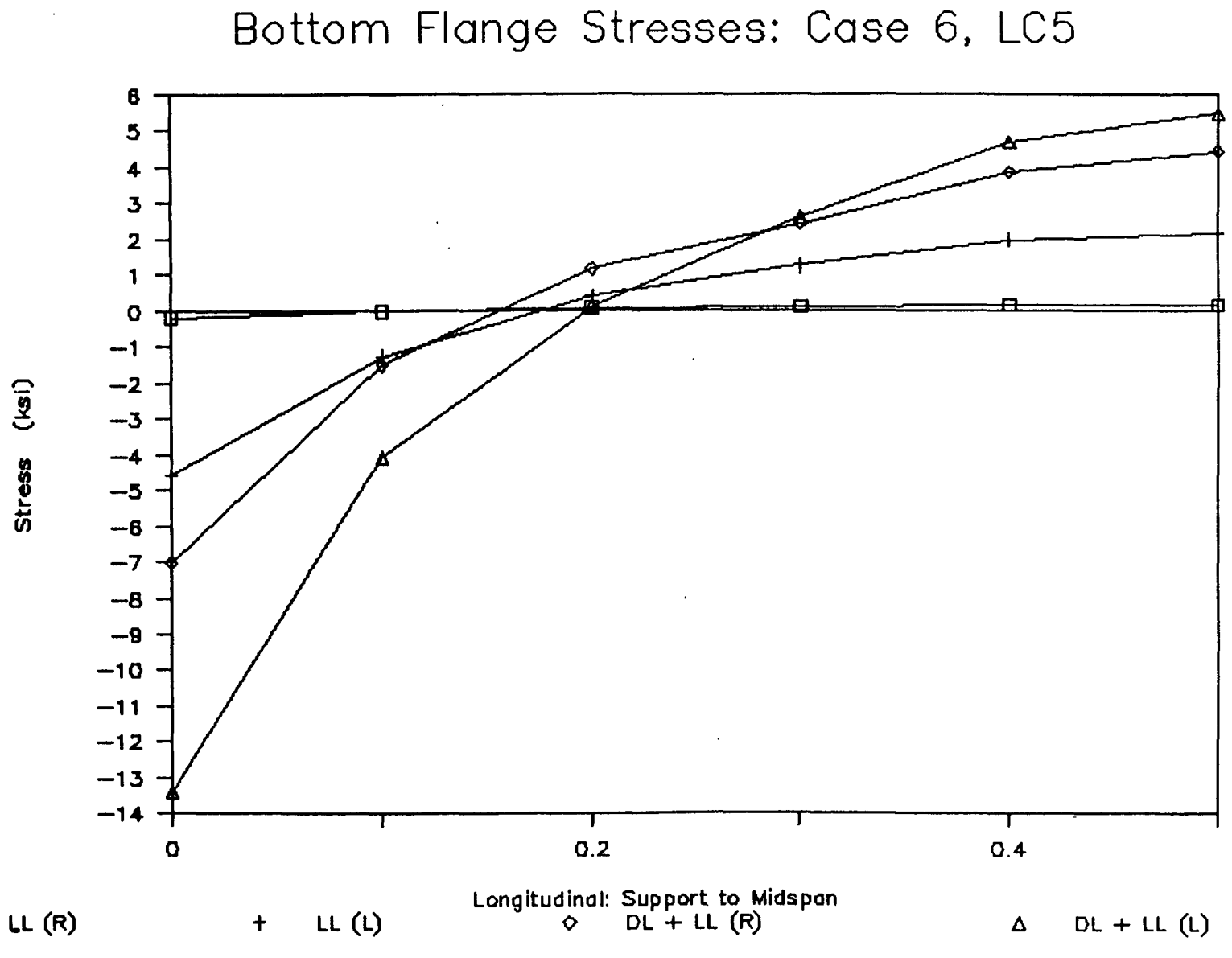
Bottom Flange Stresses: Case 6, LC5
Stress (ksi)
6
5
4
3
2
1
0
-1
-2
-3
-4
-5
-6
-7
-8
-9
-10
-11
-12
-13
-14
0
0.2
0.4
Longitudinal: Support to Midspan
LL (R)
+ LL (L)
◇ DL + LL (R)
Δ DL + LL (L)

Figure 62

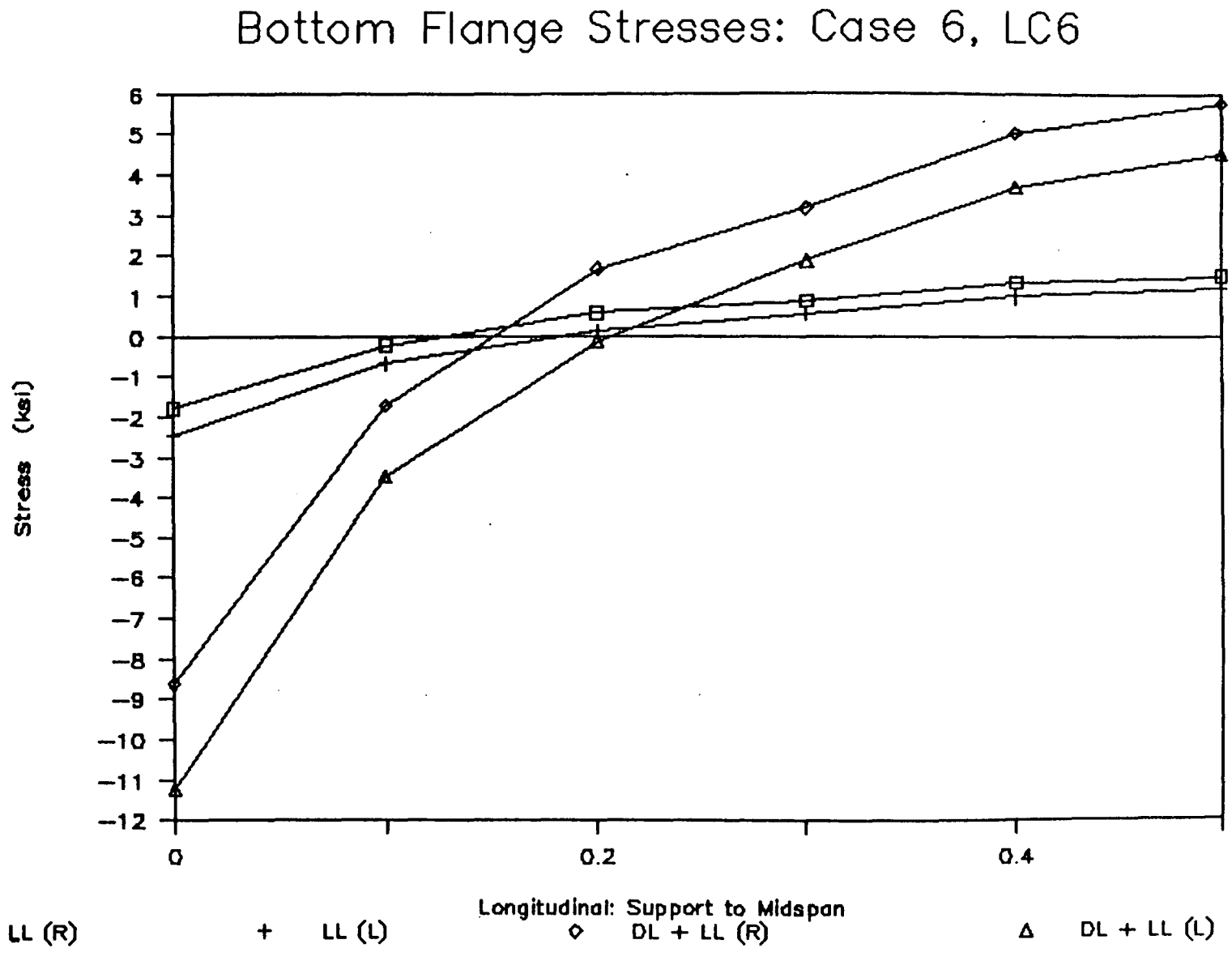
Bottom Flange Stresses: Case 6, LC6
Stress (ksi)
6
5
4
3
2
1
0
−1
−2
−3
−4
−5
−6
−7
−8
−9
−10
−11
−12
0
0.2
0.4
Longitudinal: Support to Midspan
LL (R)
+ LL (L)
◇ DL + LL (R)
Δ DL + LL (L)

Figure 63

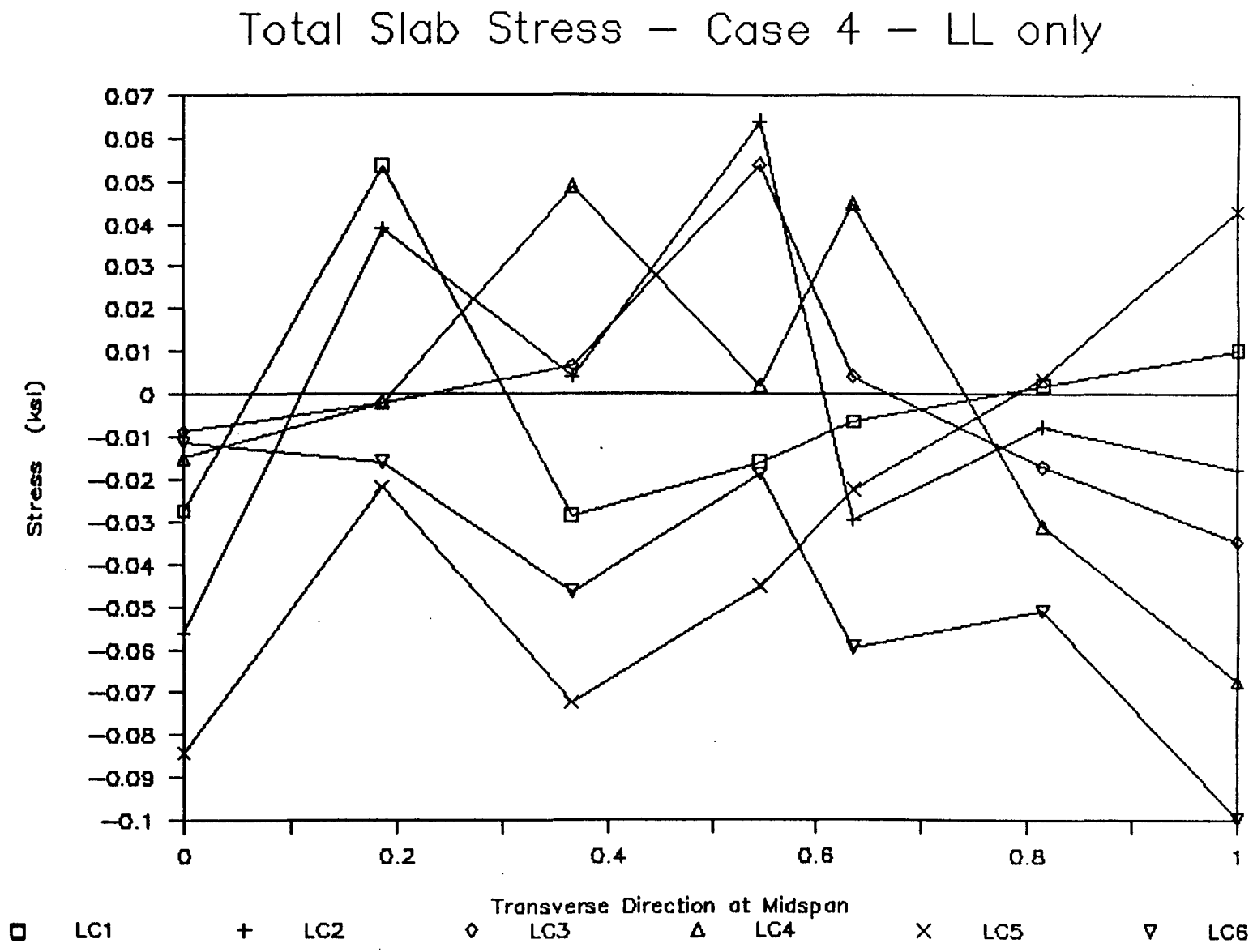
Total Slab Stress – Case 4 – LL only
Stress (ksi)
0.07
0.06
0.05
0.04
0.03
0.02
0.01
0
-0.01
-0.02
-0.03
-0.04
-0.05
-0.06
-0.07
-0.08
-0.09
-0.1
0
0.2
0.4
0.6
0.8
1
Transverse Direction at Midspan
LC1
LC2
LC3
LC4
LC5
LC6

Figure 64

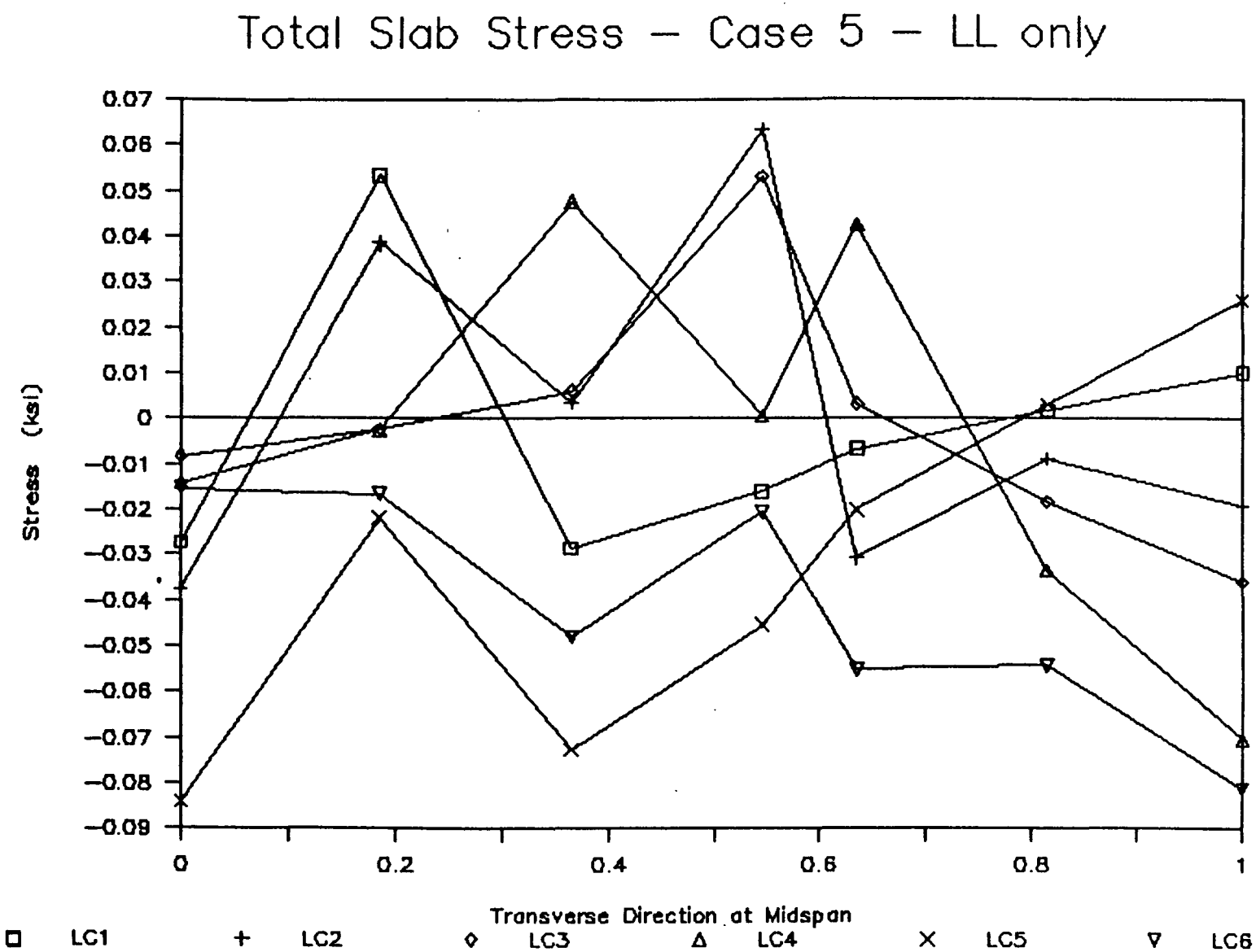
Total Slab Stress – Case 5 – LL only
Stress (ksi)
0.07
0.06
0.05
0.04
0.03
0.02
0.01
0
-0.01
-0.02
-0.03
-0.04
-0.05
-0.06
-0.07
-0.08
-0.09
0
0.2
0.4
0.6
0.8
1
Transverse Direction at Midspan
LC1
LC2
LC3
LC4
LC5
LC6

Figure 65

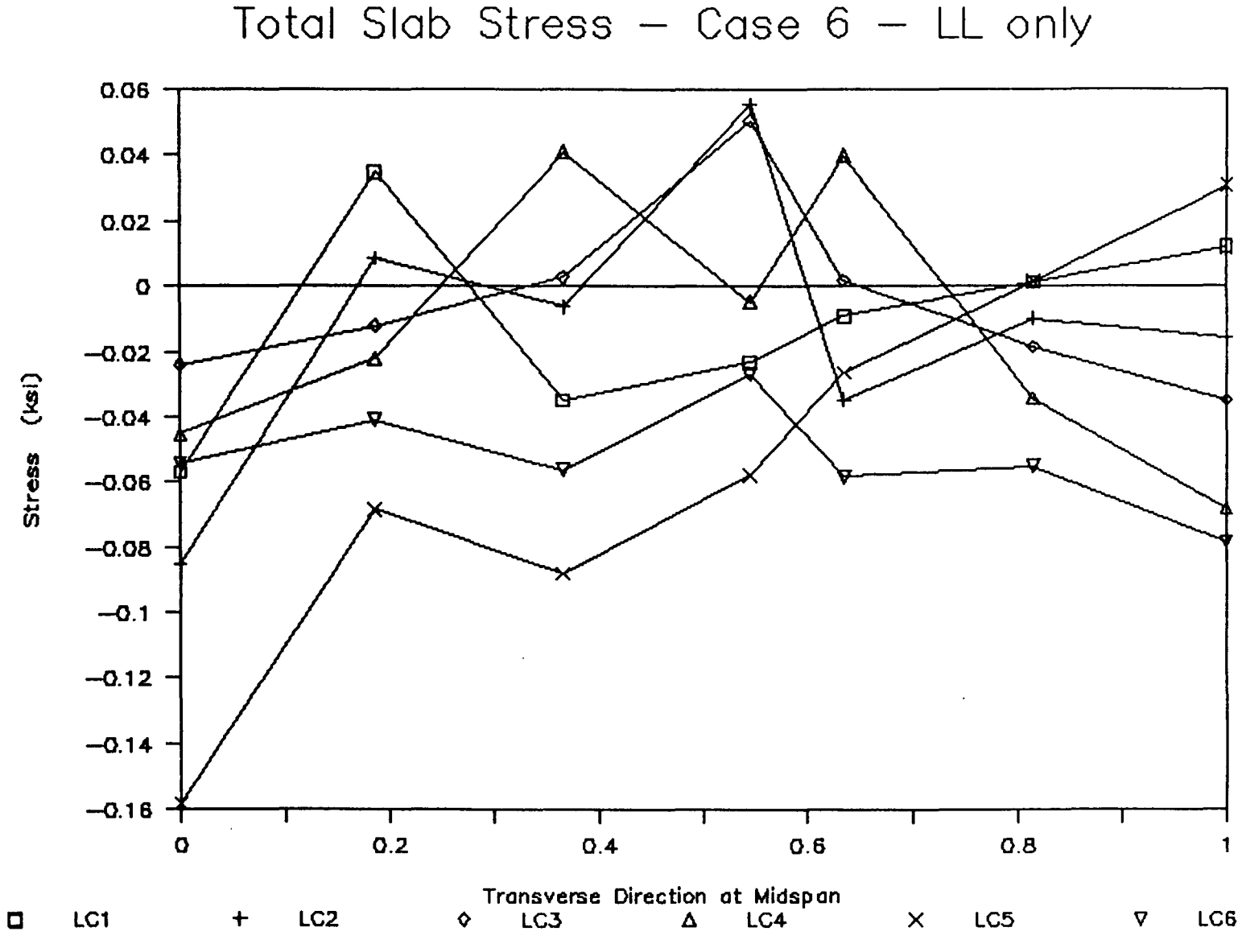
Total Slab Stress – Case 6 – LL only
0.06
0.04
0.02
0
−0.02
−0.04
−0.06
−0.08
−0.1
−0.12
−0.14
−0.16
Stress (ksi)
0
0.2
0.4
0.6
0.8
1
Transverse Direction at Midspan
LC1
LC2
LC3
LC4
LC5
LC6

Figure 66

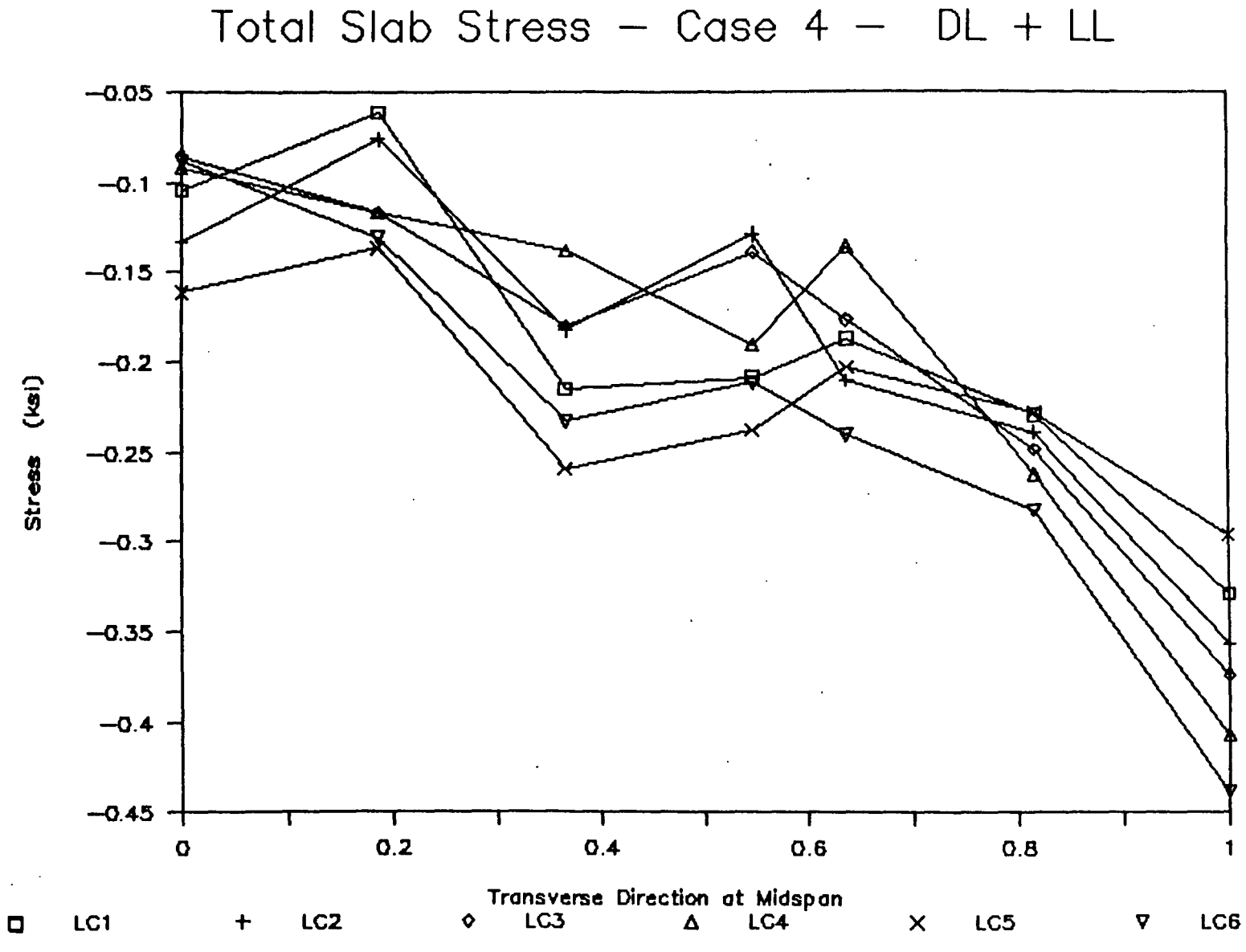
Total Slab Stress – Case 4 – DL + LL
Stress (ksi)
-0.05
-0.1
-0.15
-0.2
-0.25
-0.3
-0.35
-0.4
-0.45
0
0.2
0.4
0.6
0.8
1
Transverse Direction at Midspan
LC1
LC2
LC3
LC4
LC5
LC6

Figure 67

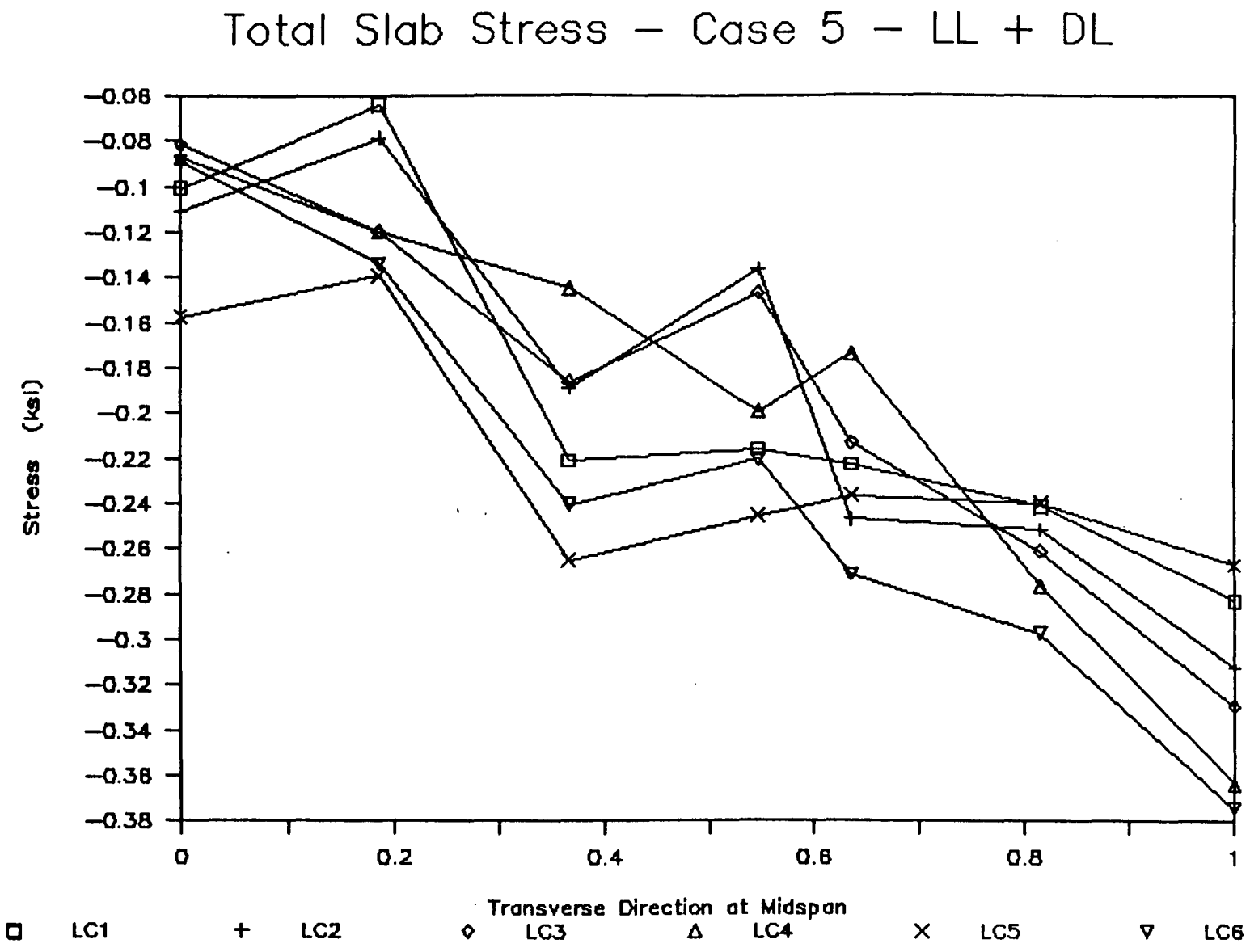
Total Slab Stress – Case 5 – LL + DL
Stress (ksi)
-0.06
-0.08
-0.1
-0.12
-0.14
-0.16
-0.18
-0.2
-0.22
-0.24
-0.26
-0.28
-0.3
-0.32
-0.34
-0.36
-0.38
0
0.2
0.4
0.6
0.8
1
Transverse Direction at Midspan
LC1
LC2
LC3
LC4
LC5
LC6

Figure 68

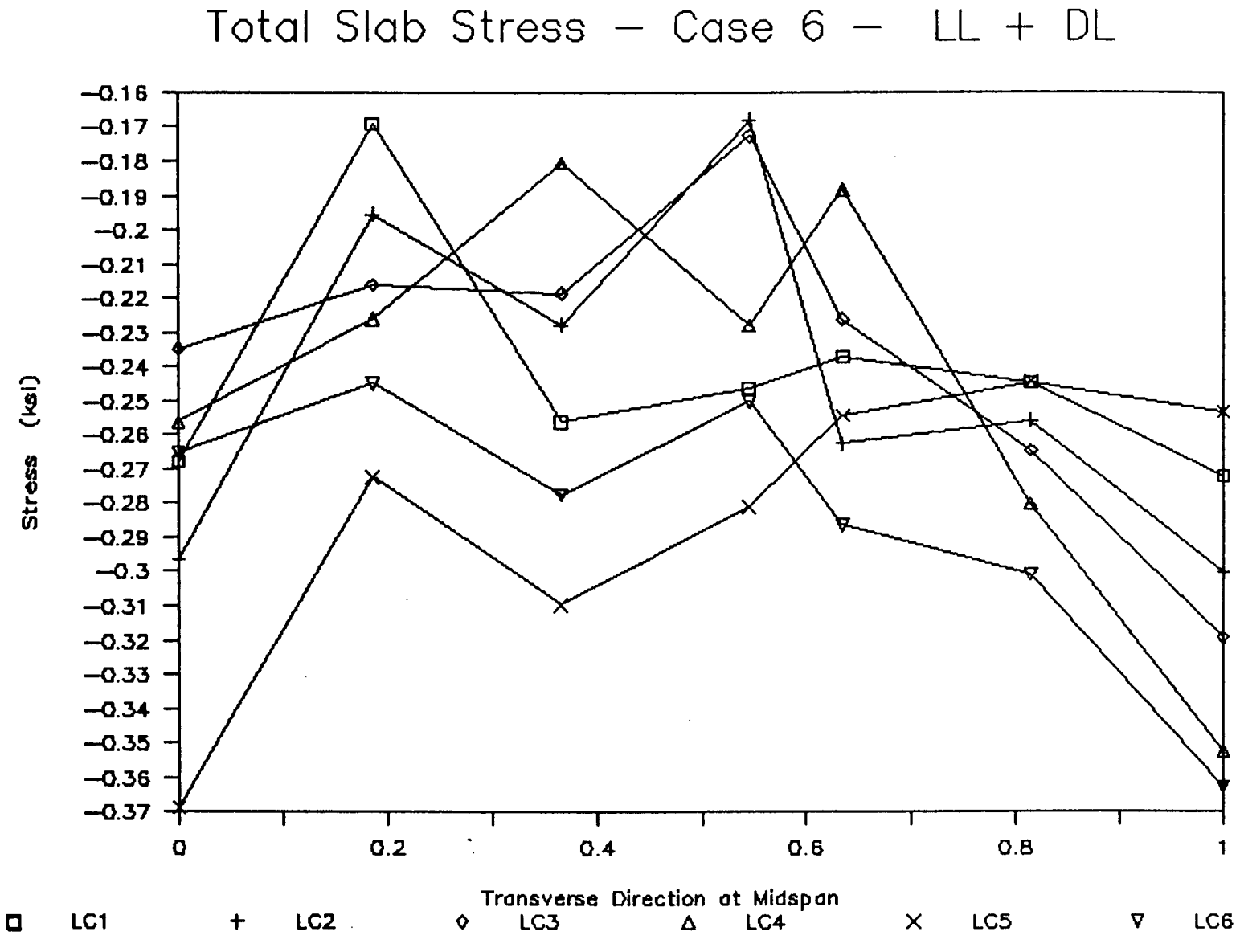
Total Slab Stress – Case 6 – LL + DL
Stress (ksi)
-0.16
-0.17
-0.18
-0.19
-0.2
-0.21
-0.22
-0.23
-0.24
-0.25
-0.26
-0.27
-0.28
-0.29
-0.3
-0.31
-0.32
-0.33
-0.34
-0.35
-0.36
-0.37
0
0.2
0.4
0.6
0.8
1
Transverse Direction at Midspan
LC1
LC2
LC3
LC4
LC5
LC6

Figure 69

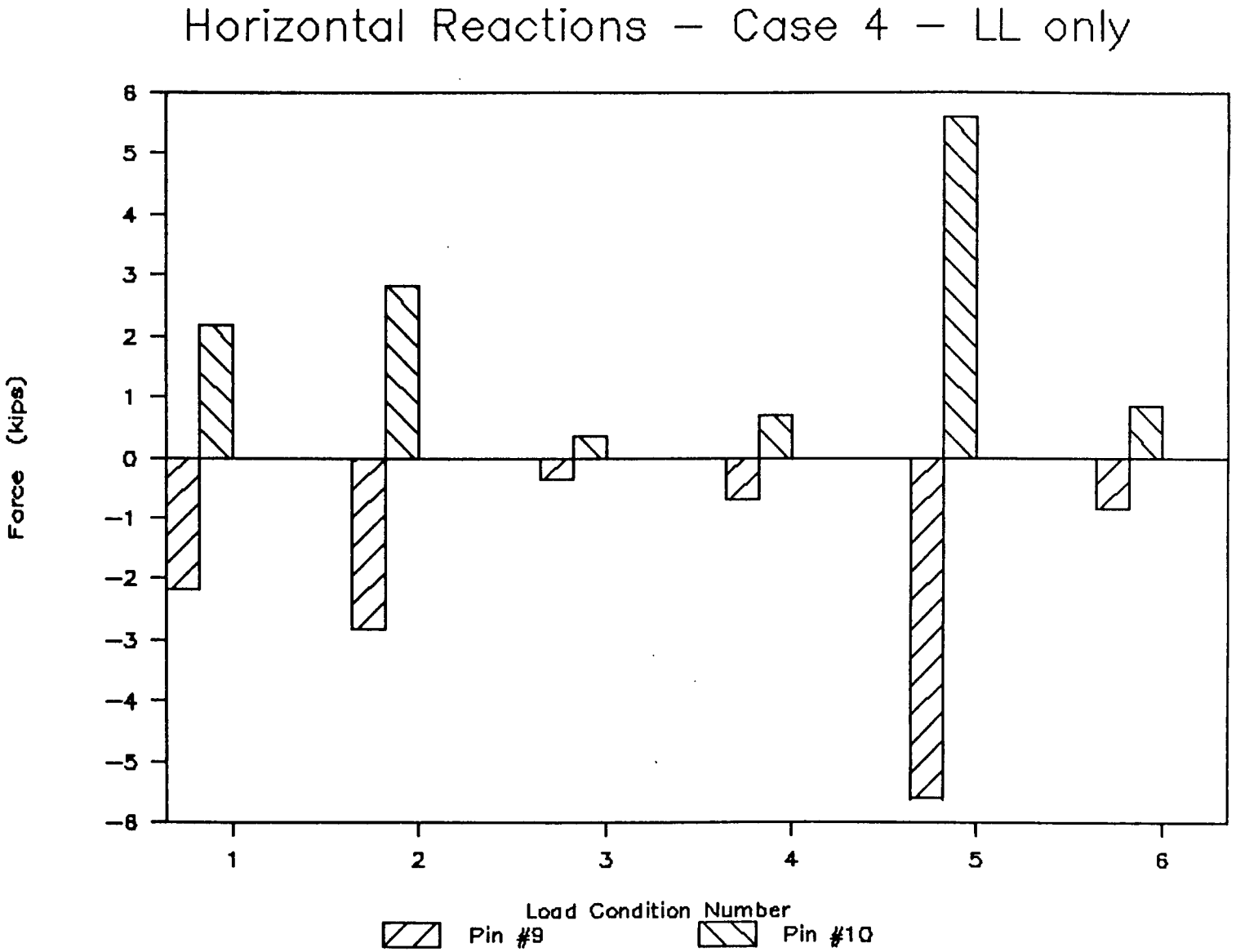
Horizontal Reactions – Case 4 – LL only
Force (kips)
6
5
4
3
2
1
0
-1
-2
-3
-4
-5
-6
1
2
3
4
5
6
Load Condition Number
Pin #9
Pin #10

Figure 70

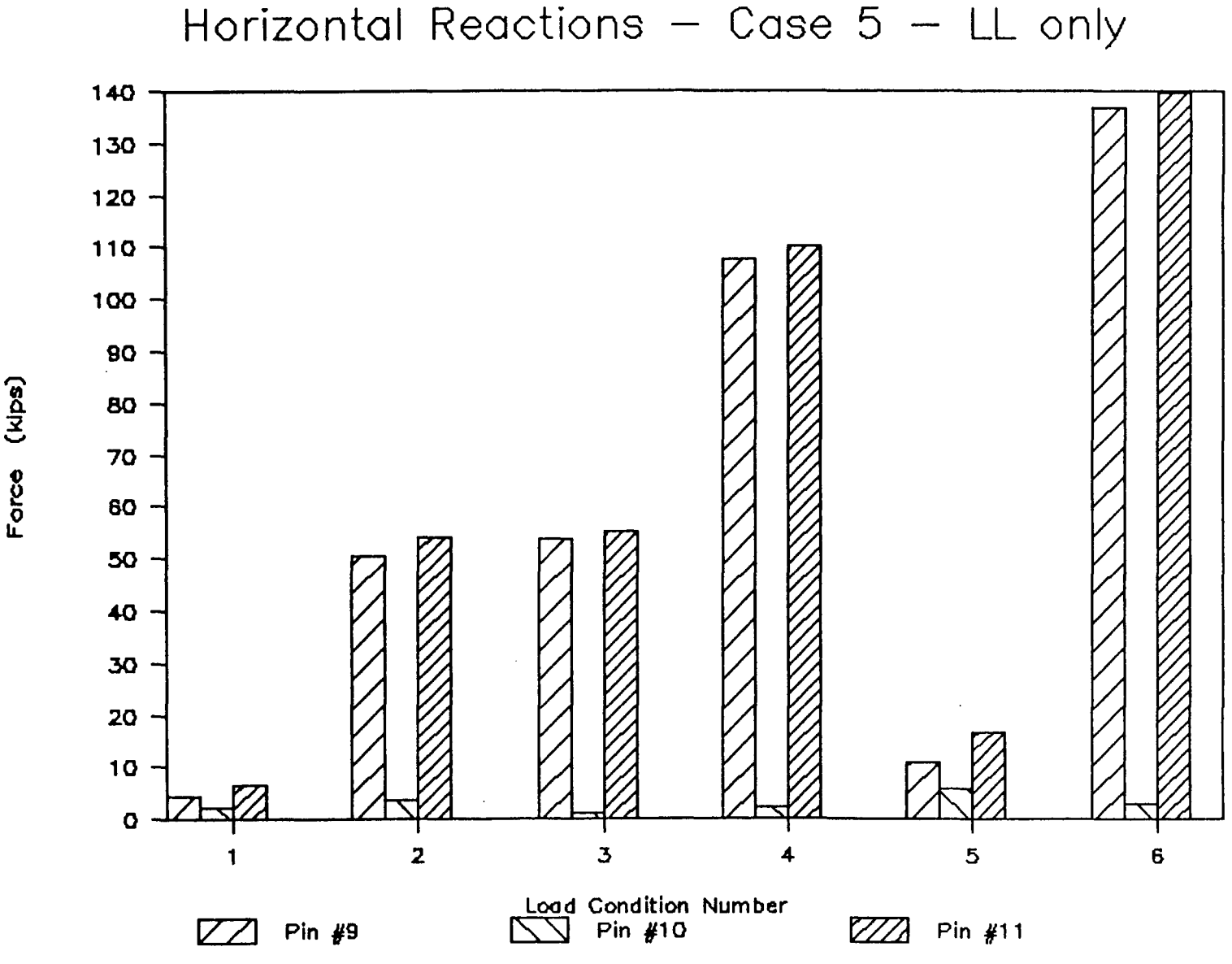
Horizontal Reactions – Case 5 – LL only
Force (kips)
140
130
120
110
100
90
80
70
60
50
40
30
20
10
0
1
2
3
4
5
6
Load Condition Number
Pin #9
Pin #10
Pin #11

Figure 71

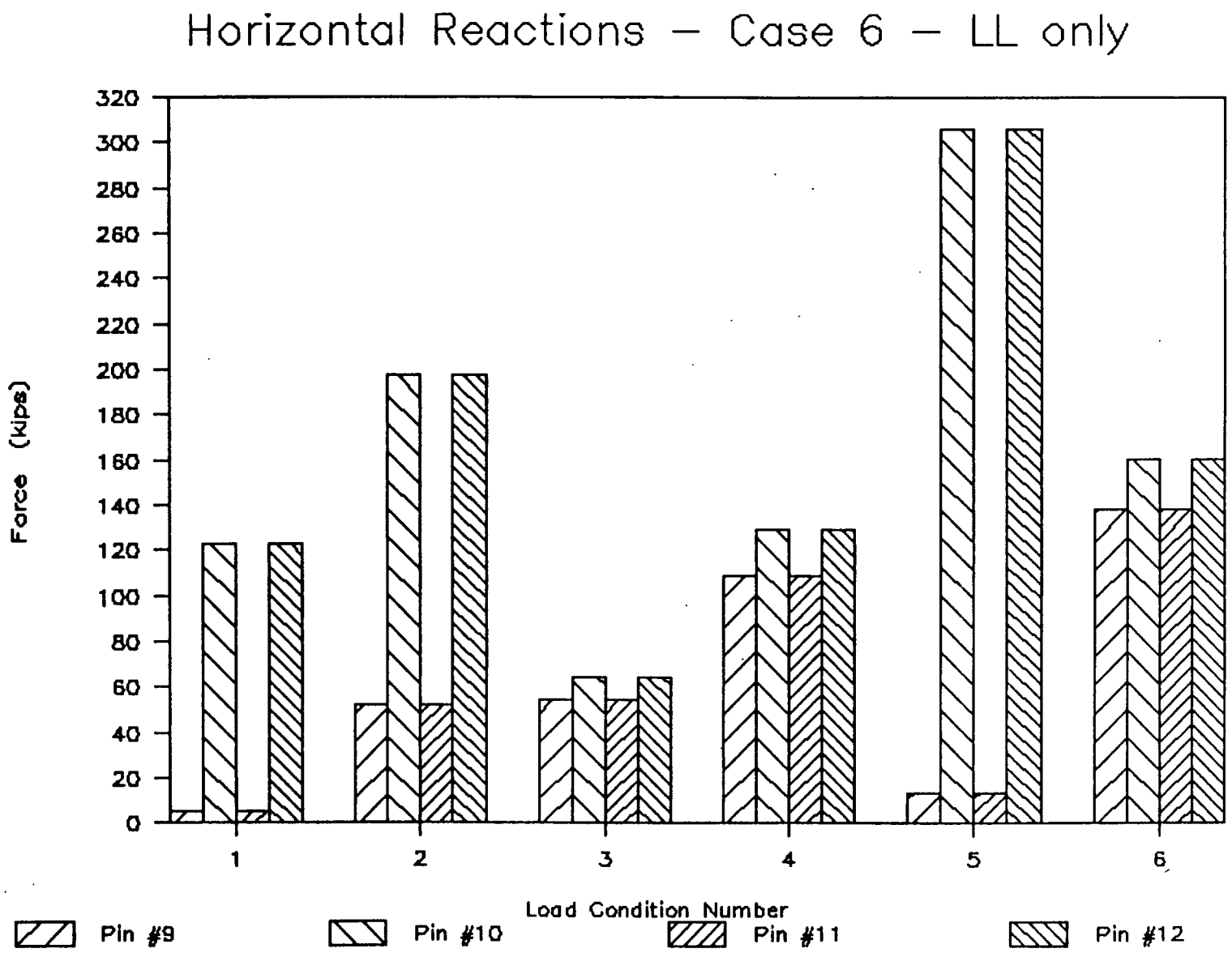
Horizontal Reactions – Case 6 – LL only
Force (kips)
320
300
280
260
240
220
200
180
160
140
120
100
80
60
40
20
0
1
2
3
4
5
6
Load Condition Number
Pin #9
Pin #10
Pin #11
Pin #12

Figure 72

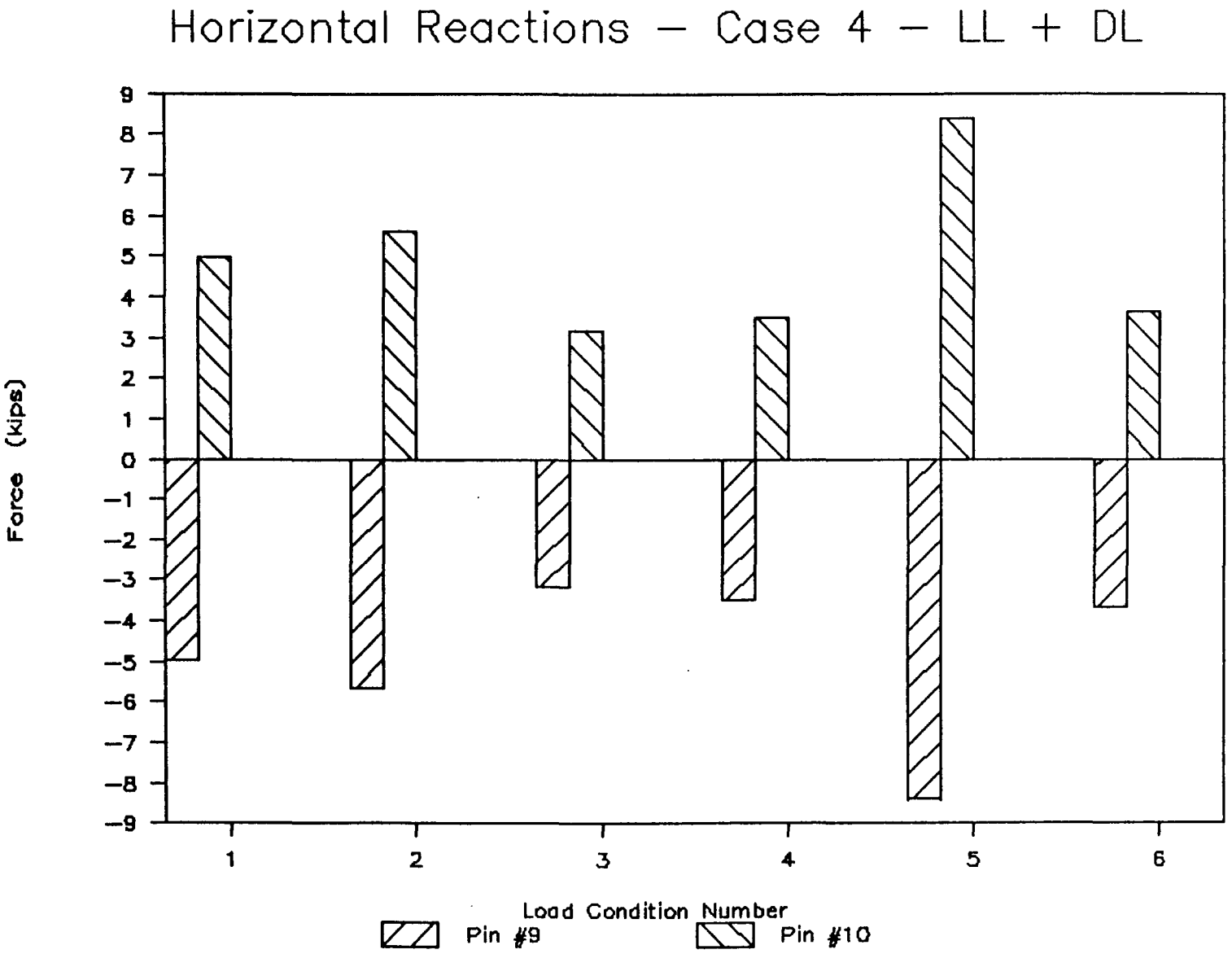
Horizontal Reactions – Case 4 – LL + DL
Force (kips)
9
8
7
6
5
4
3
2
1
0
-1
-2
-3
-4
-5
-6
-7
-8
-9
1
2
3
4
5
6
Load Condition Number
Pin #9
Pin #10

Figure 73

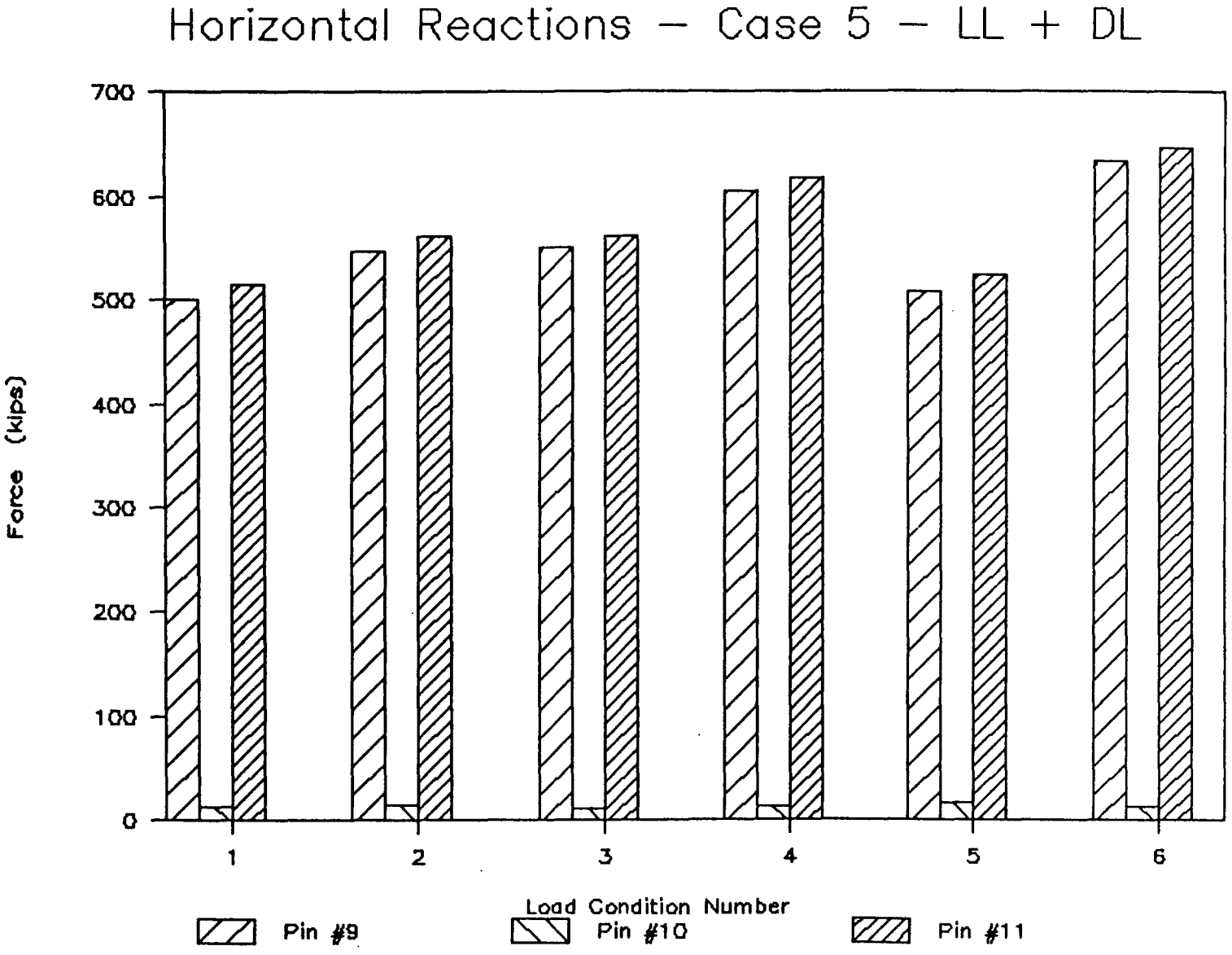
Horizontal Reactions – Case 5 – LL + DL
Force (kips)
700
600
500
400
300
200
100
0
1
2
3
4
5
6
Load Condition Number
Pin #9
Pin #10
Pin #11

Figure 74

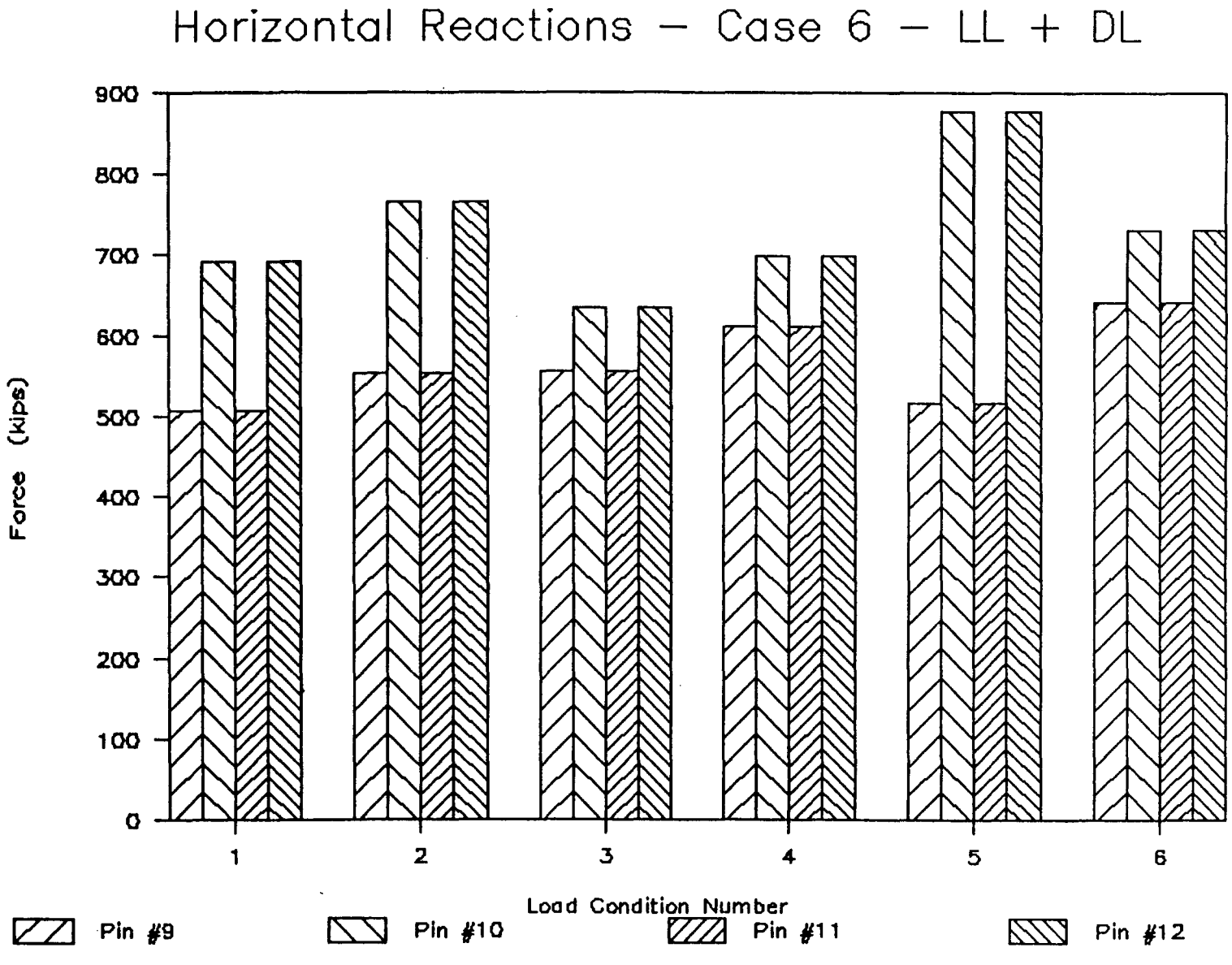
Horizontal Reactions – Case 6 – LL + DL
900
800
700
600
500
400
300
200
100
0
Force (kips)
1
2
3
4
5
6
Load Condition Number
Pin #9
Pin #10
Pin #11
Pin #12

Figure 75

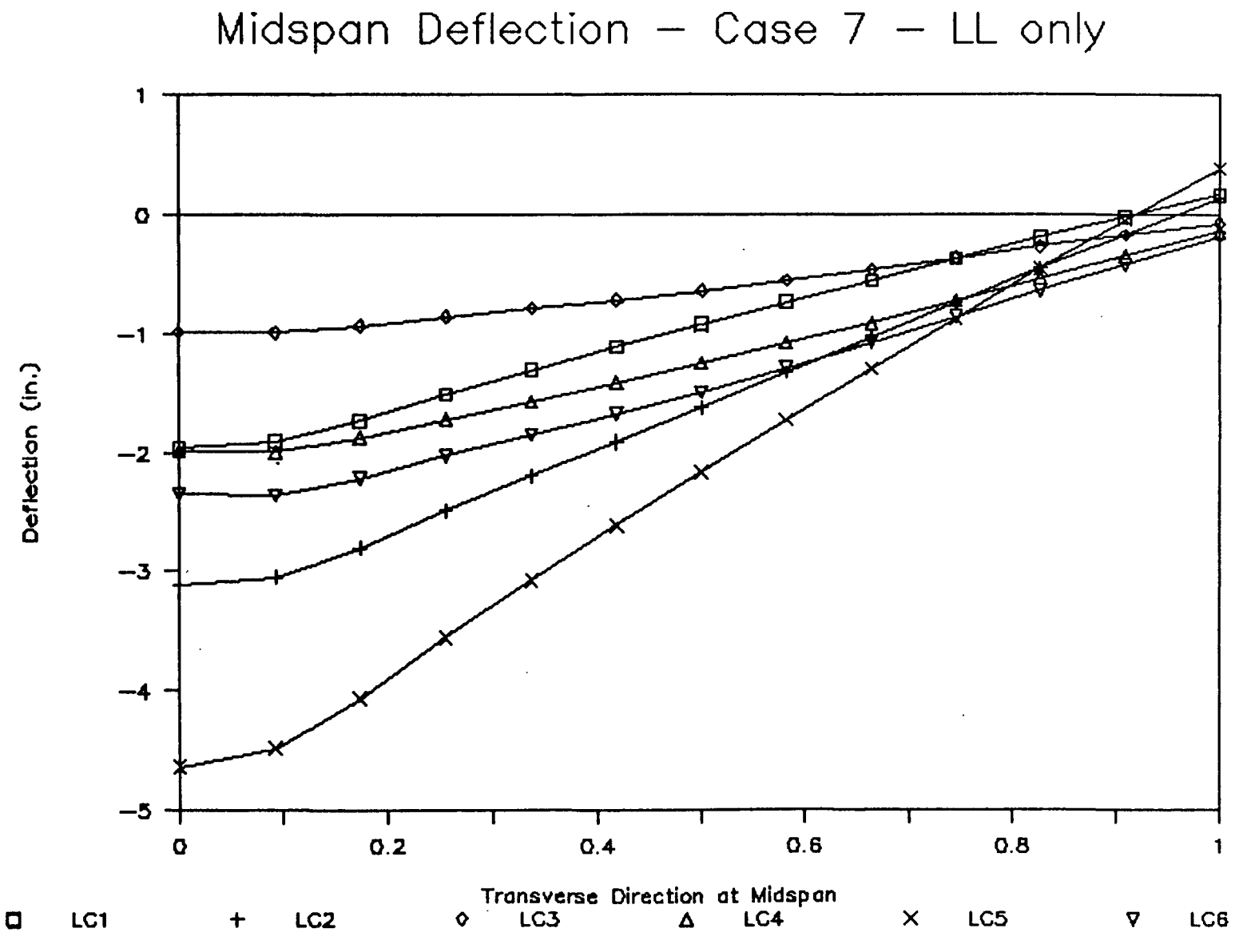
Midspan Deflection – Case 7 – LL only
Deflection (in.)
1
0
-1
-2
-3
-4
-5
0
0.2
0.4
0.6
0.8
1
Transverse Direction at Midspan
LC1
LC2
LC3
LC4
LC5
LC6

Figure 76

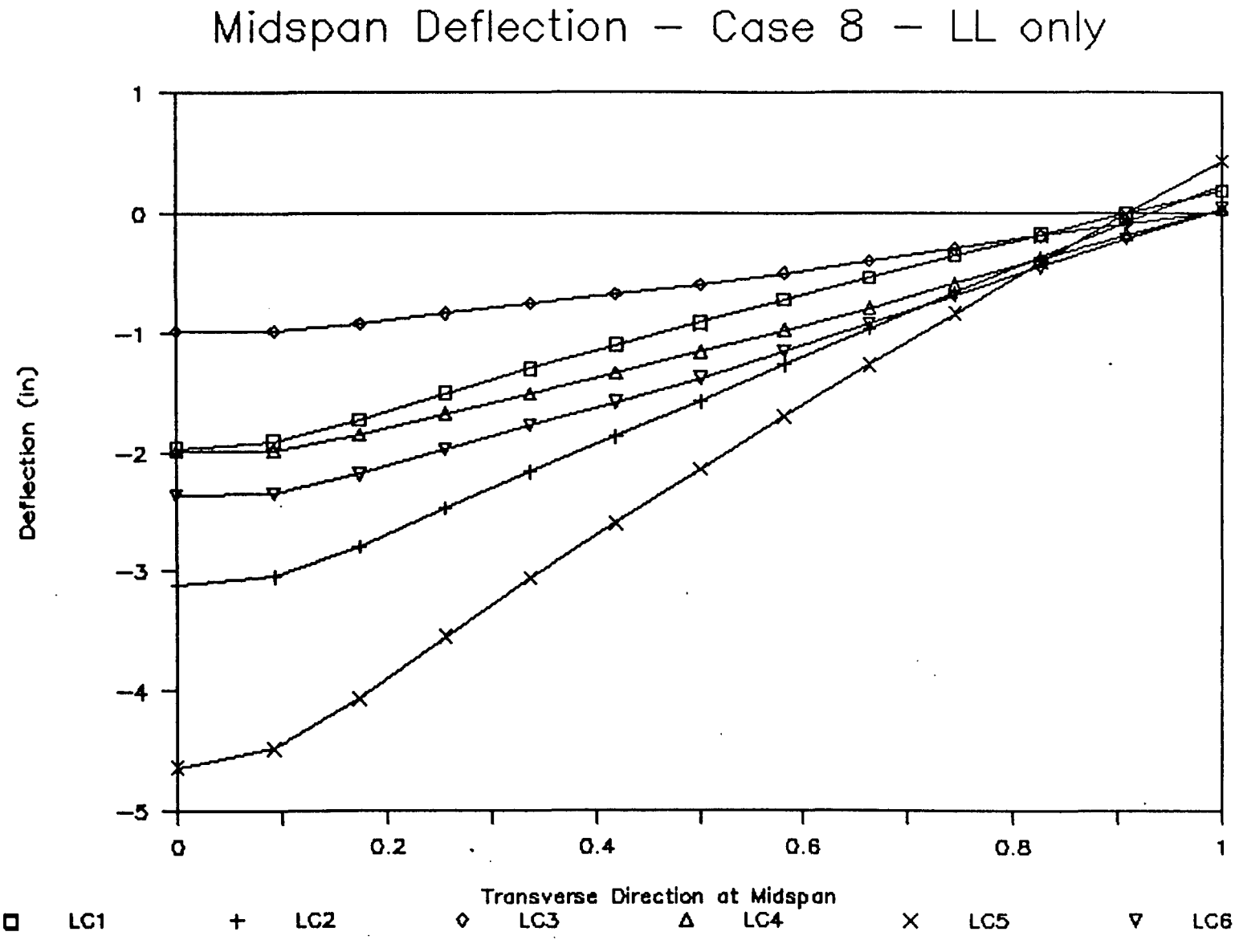
Midspan Deflection – Case 8 – LL only
Deflection (in)
1
0
-1
-2
-3
-4
-5
0
0.2
0.4
0.6
0.8
1
Transverse Direction at Midspan
LC1
LC2
LC3
LC4
LC5
LC6

Figure 77

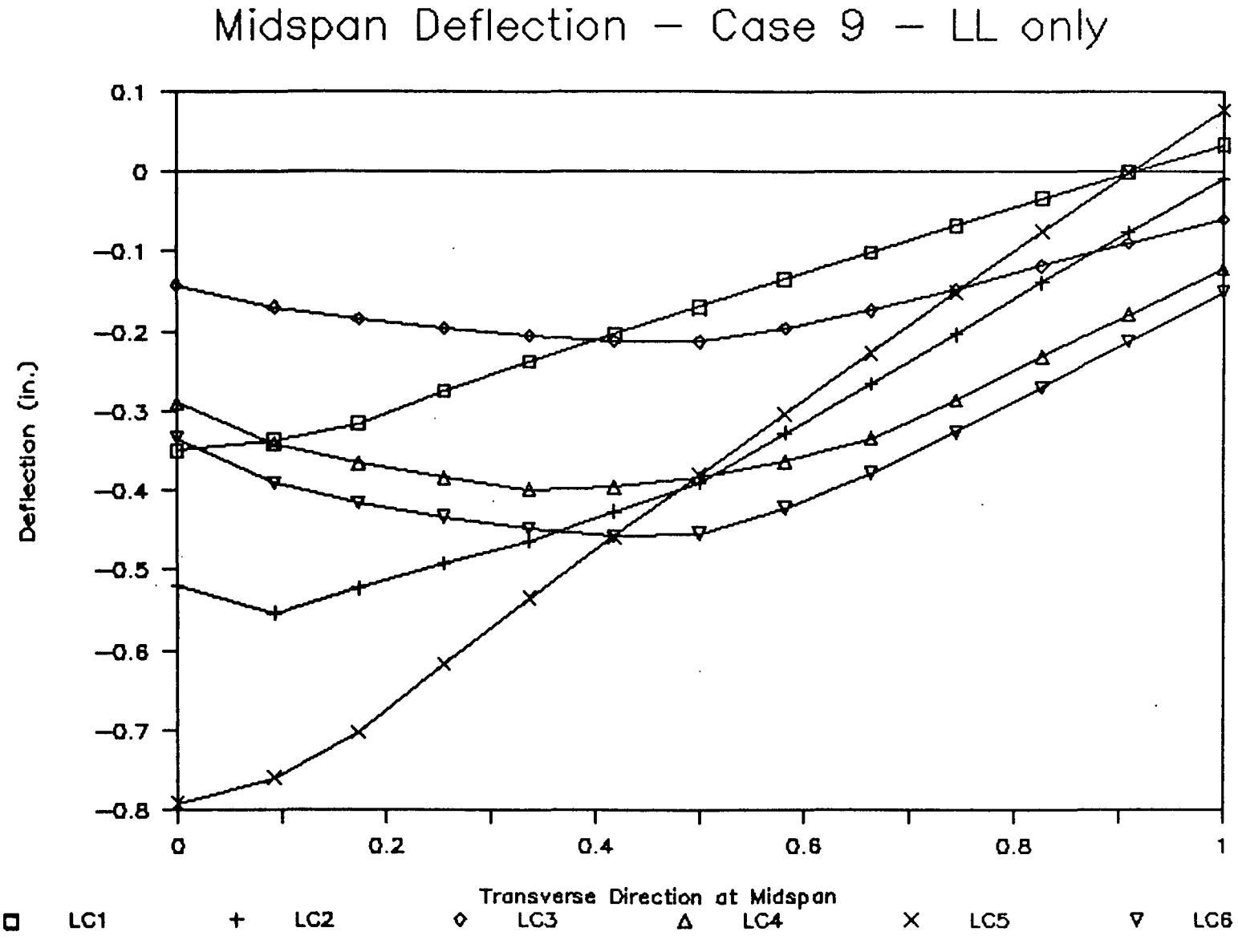
Midspan Deflection – Case 9 – LL only
0.1
0
-0.1
-0.2
-0.3
-0.4
-0.5
-0.6
-0.7
-0.8
Deflection (in.)
0
0.2
0.4
0.6
0.8
1
Transverse Direction at Midspan
LC1
LC2
LC3
LC4
LC5
LC6

Figure 78

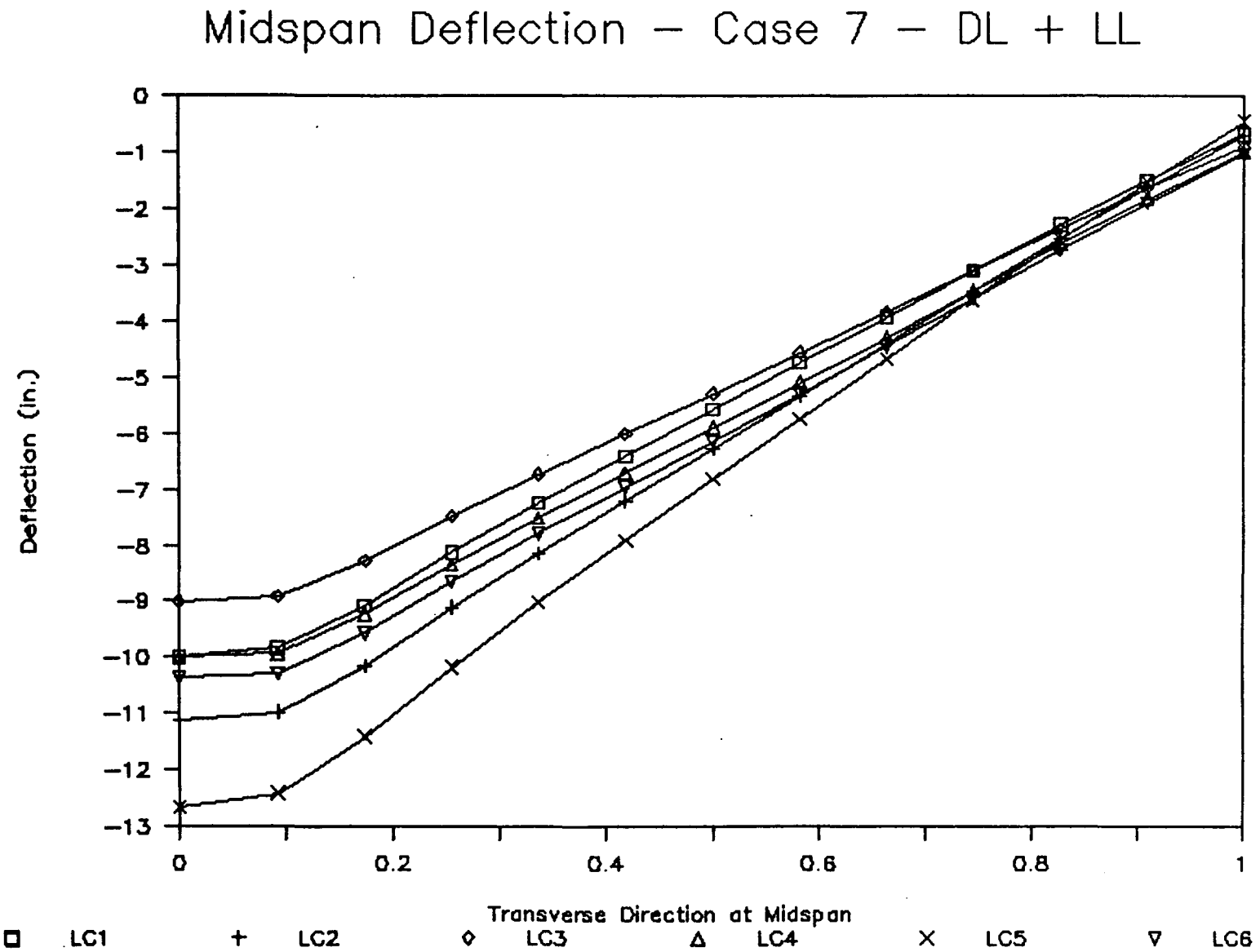
Midspan Deflection – Case 7 – DL + LL
Deflection (in.)
0
-1
-2
-3
-4
-5
-6
-7
-8
-9
-10
-11
-12
-13
0
0.2
0.4
0.6
0.8
1
Transverse Direction at Midspan
LC1
LC2
LC3
LC4
LC5
LC6

Figure 79

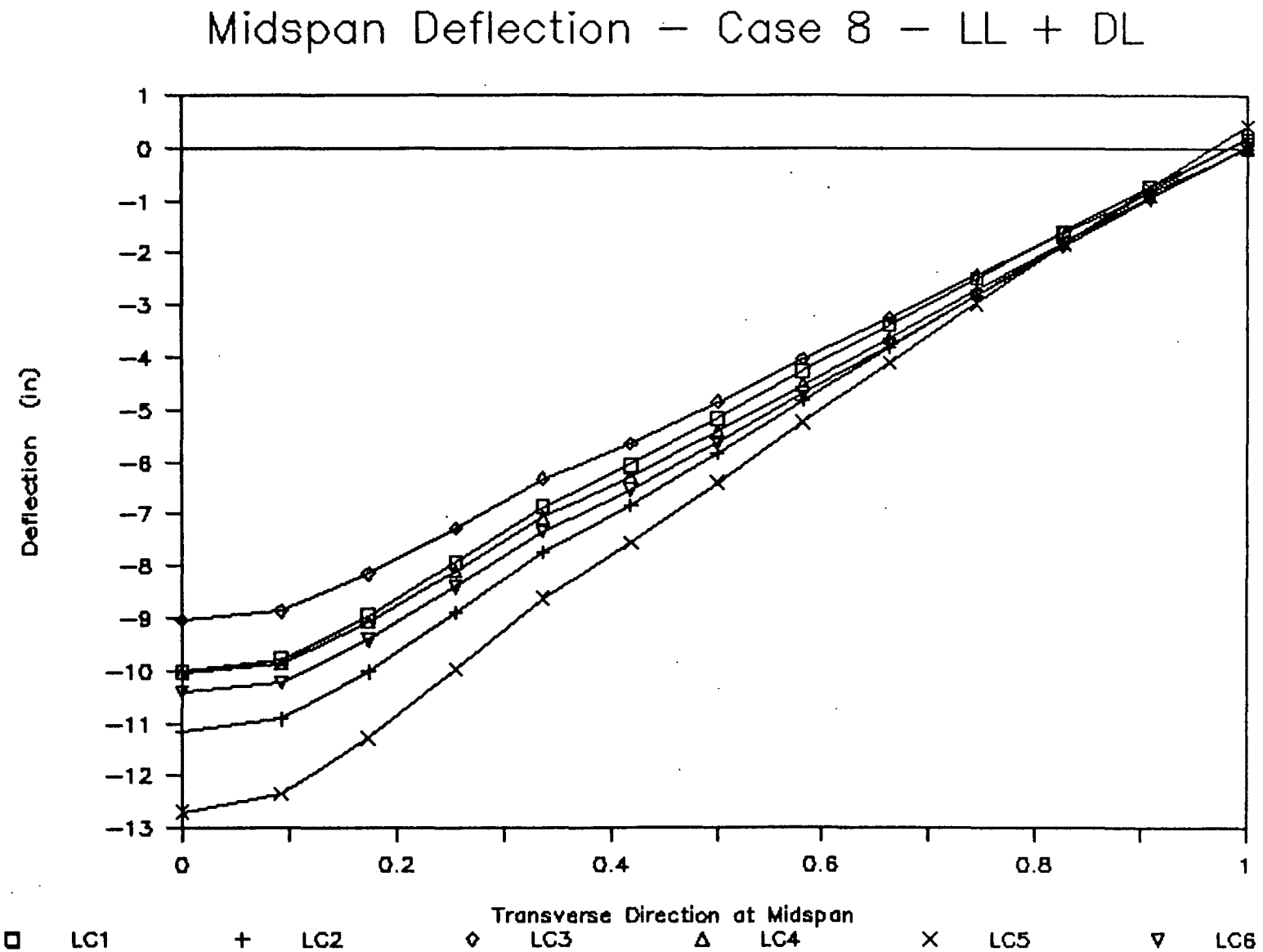
Midspan Deflection – Case 8 – LL + DL
Deflection (in)
1
0
-1
-2
-3
-4
-5
-6
-7
-8
-9
-10
-11
-12
-13
0
0.2
0.4
0.6
0.8
1
Transverse Direction at Midspan
LC1
LC2
LC3
LC4
LC5
LC6

Figure 80

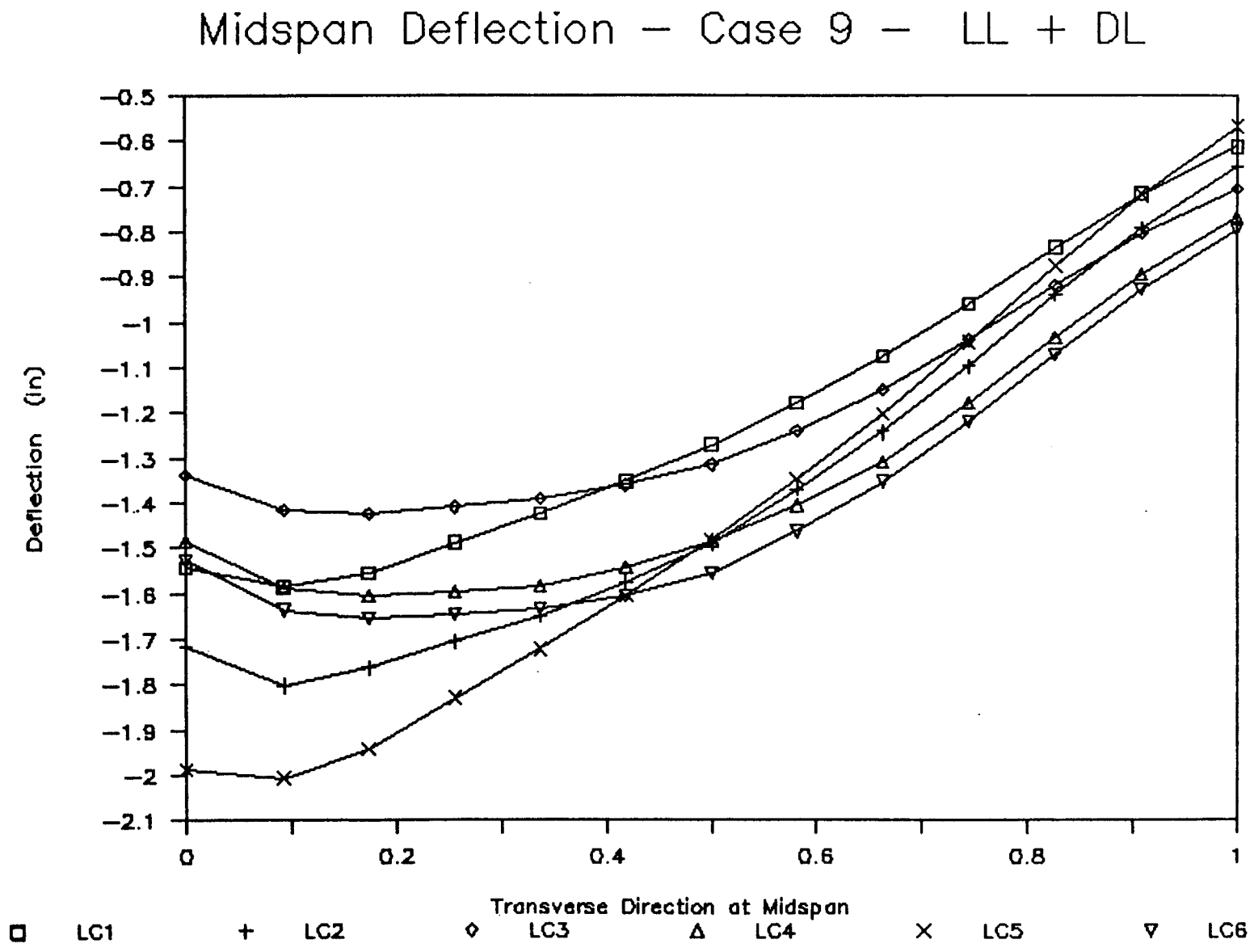
Midspan Deflection – Case 9 – LL + DL
Deflection (in)
-0.5
-0.6
-0.7
-0.8
-0.9
-1
-1.1
-1.2
-1.3
-1.4
-1.5
-1.6
-1.7
-1.8
-1.9
-2
-2.1
0
0.2
0.4
0.6
0.8
1
Transverse Direction at Midspan
LC1
LC2
LC3
LC4
LC5
LC6

Figure 81

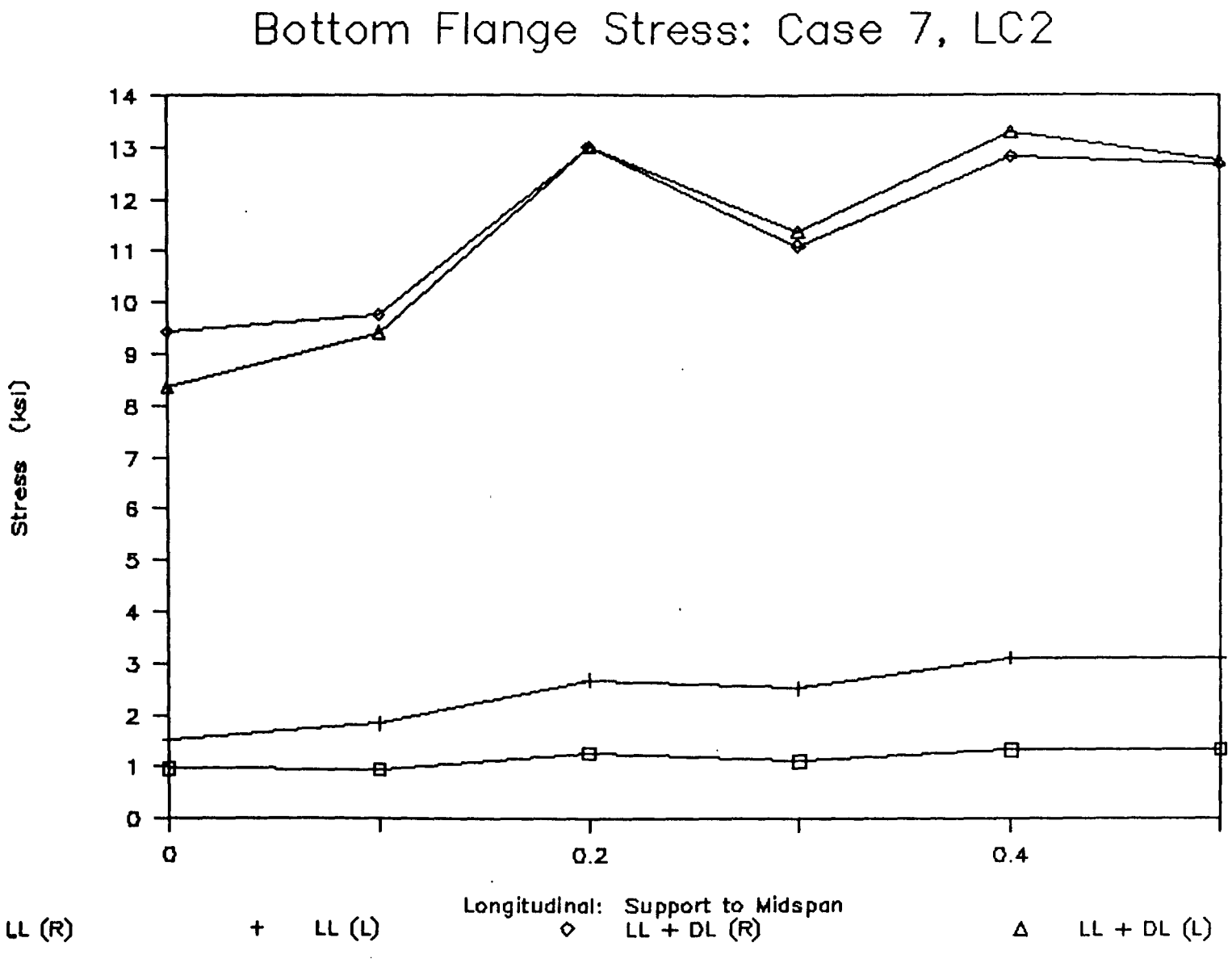
Bottom Flange Stress: Case 7, LC2
Stress (ksi)
14
13
12
11
10
9
8
7
6
5
4
3
2
1
0
0
0.2
0.4
Longitudinal: Support to Midspan
LL (R)
+ LL (L)
◇ LL + DL (R)
Δ LL + DL (L)

Figure 82

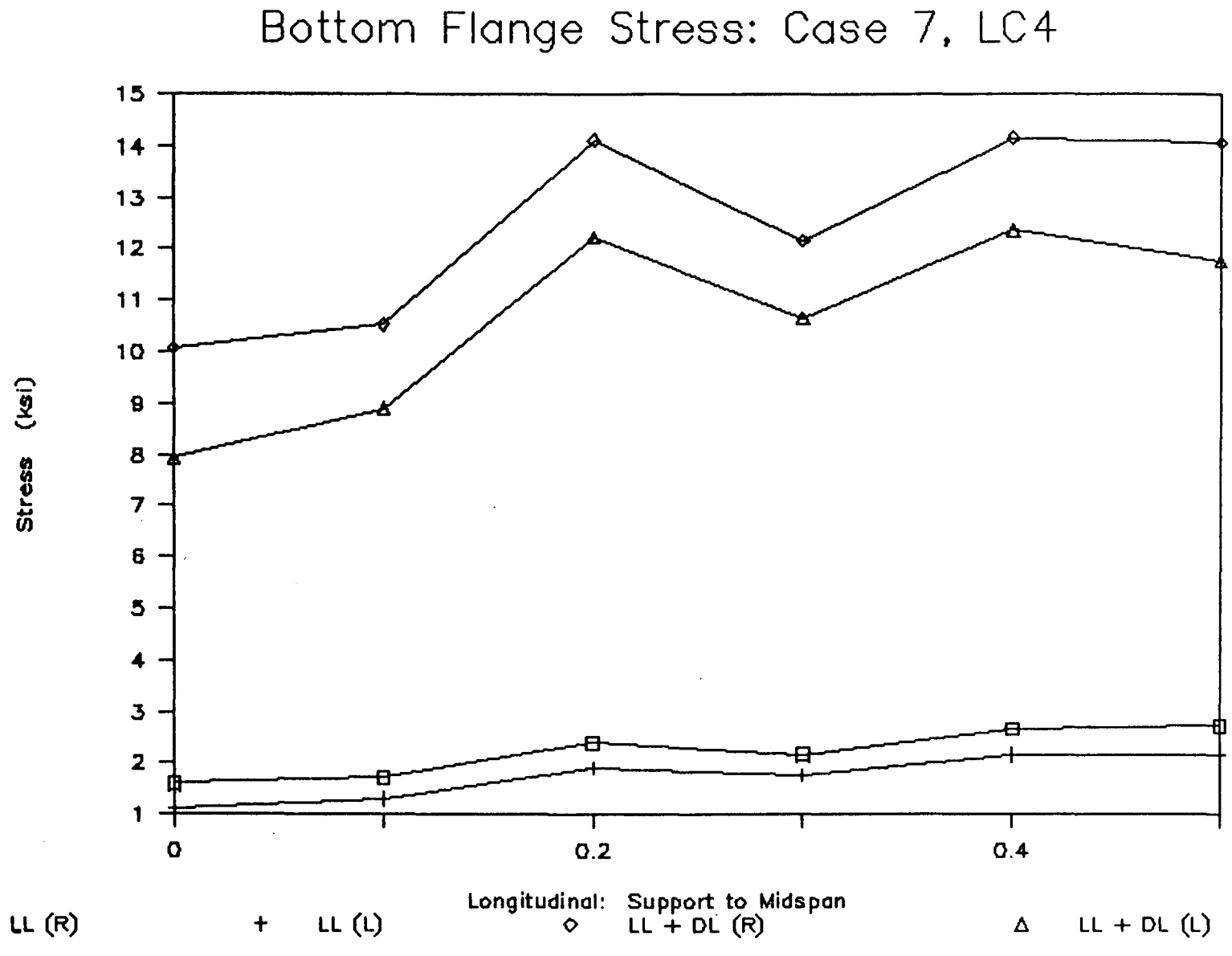
Bottom Flange Stress: Case 7, LC4
Stress (ksi)
15
14
13
12
11
10
9
8
7
6
5
4
3
2
1
0
0.2
0.4
Longitudinal: Support to Midspan
LL (R)
+ LL (L)
◇ LL + DL (R)
△ LL + DL (L)

Figure 83

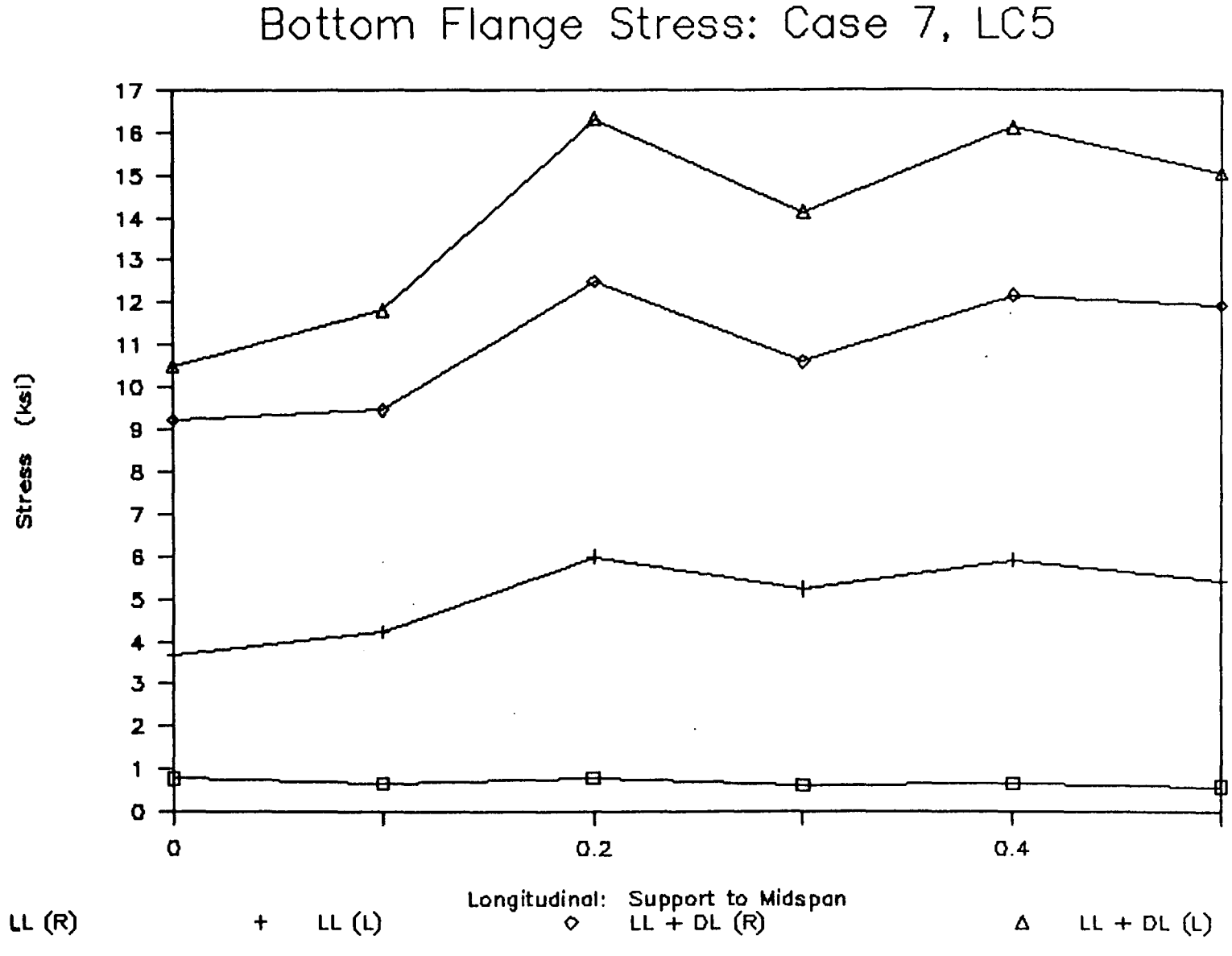
Bottom Flange Stress: Case 7, LC5
Stress (ksi)
17
16
15
14
13
12
11
10
9
8
7
6
5
4
3
2
1
0
0
0.2
0.4
Longitudinal: Support to Midspan
LL (R)
+ LL (L)
◇ LL + DL (R)
Δ LL + DL (L)

Figure 84

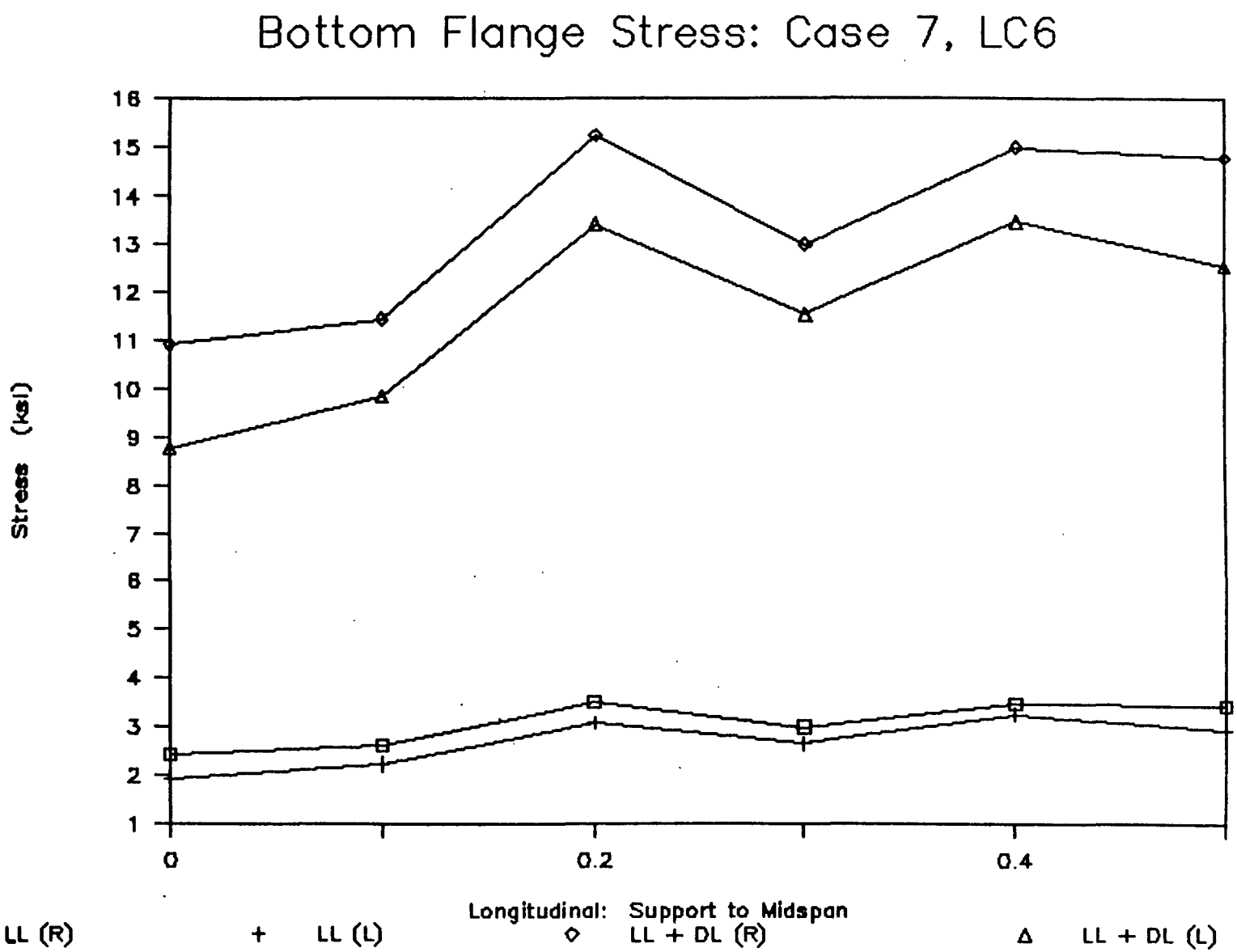
Bottom Flange Stress: Case 7, LC6
Stress (ksi)
16
15
14
13
12
11
10
9
8
7
6
5
4
3
2
1
0
0.2
0.4
Longitudinal: Support to Midspan
LL (R)
+ LL (L)
◇ LL + DL (R)
Δ LL + DL (L)

Figure 85

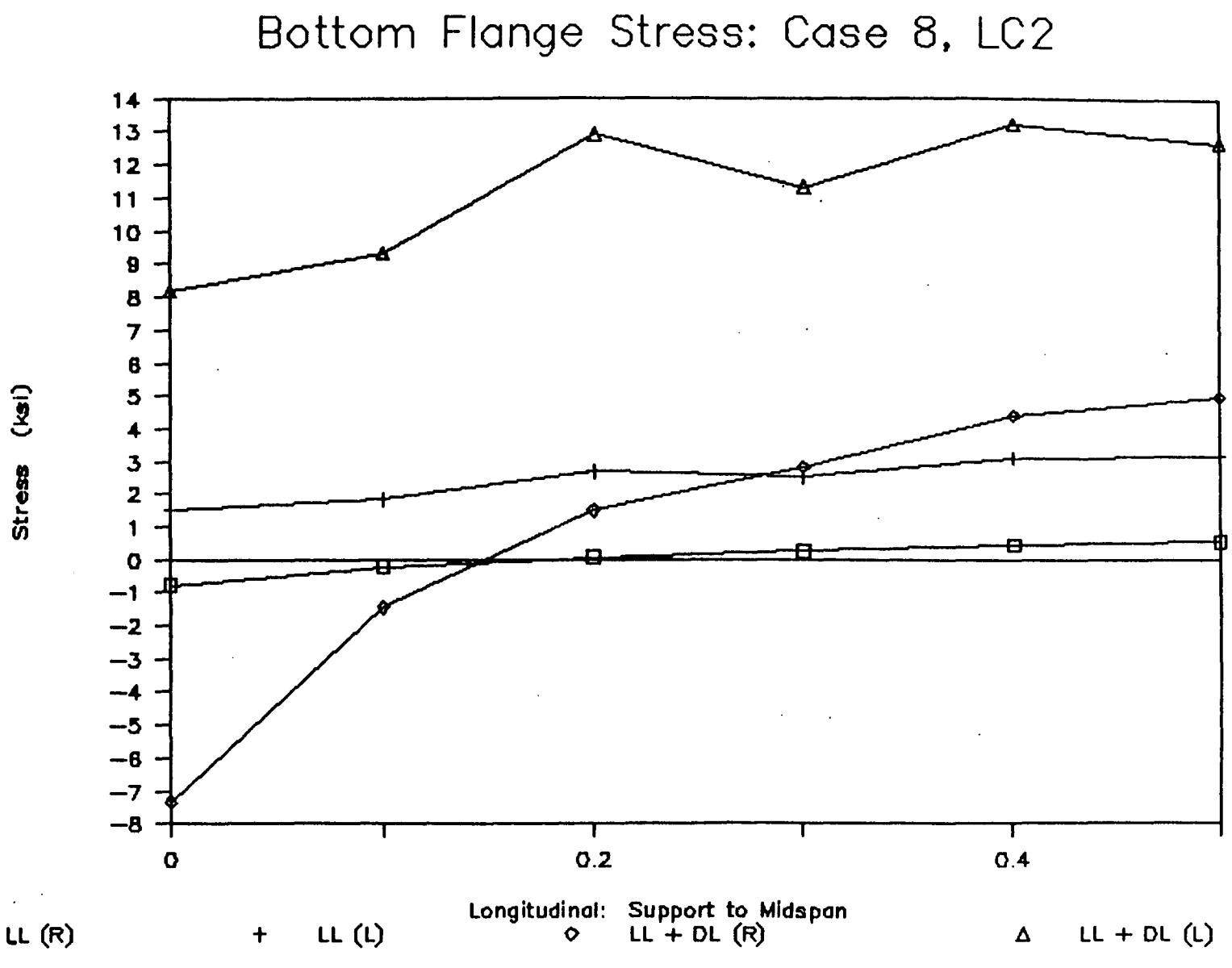
Bottom Flange Stress: Case 8, LC2
Stress (ksi)
14
13
12
11
10
9
8
7
6
5
4
3
2
1
0
−1
−2
−3
−4
−5
−6
−7
−8
0
0.2
0.4
Longitudinal: Support to Midspan
LL (R)
+ LL (L)
◇ LL + DL (R)
Δ LL + DL (L)

Figure 86

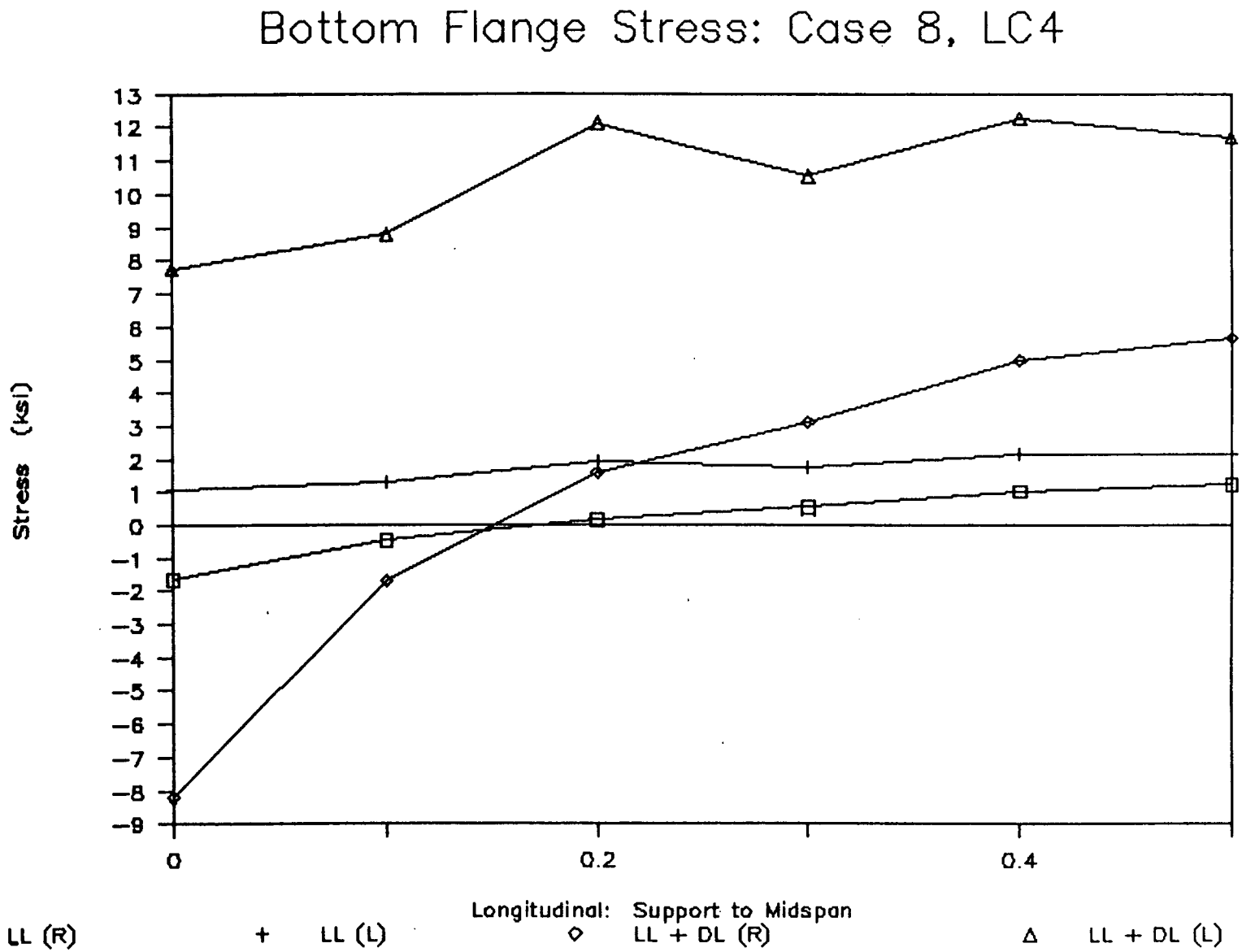
Bottom Flange Stress: Case 8, LC4
Stress (ksi)
13
12
11
10
9
8
7
6
5
4
3
2
1
0
-1
-2
-3
-4
-5
-6
-7
-8
-9
0
0.2
0.4
Longitudinal: Support to Midspan
LL (R)
+ LL (L)
◇ LL + DL (R)
Δ LL + DL (L)

Figure 87

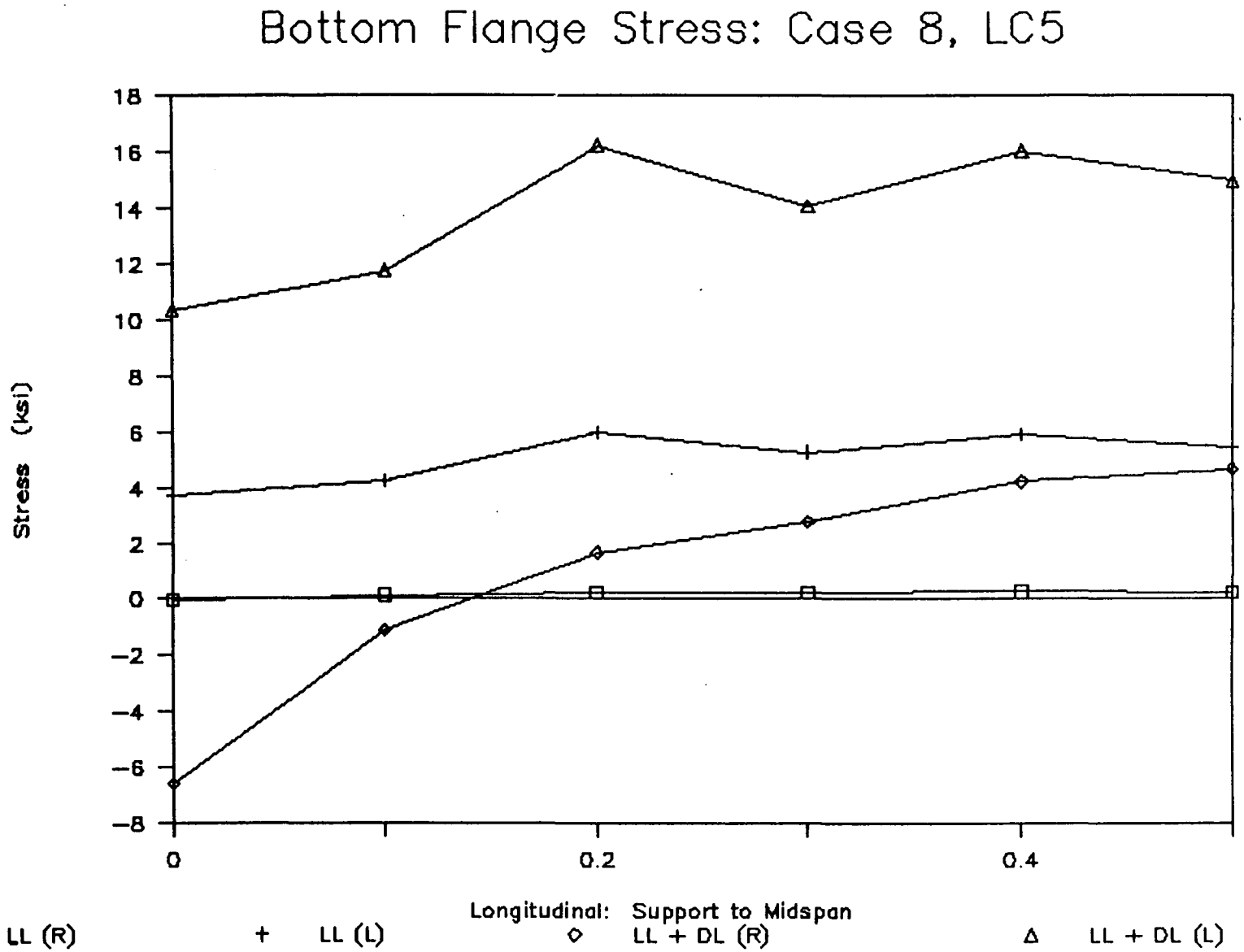
Bottom Flange Stress: Case 8, LC5
Stress (ksi)
18
16
14
12
10
8
6
4
2
0
−2
−4
−6
−8
0
0.2
0.4
Longitudinal: Support to Midspan
LL (R)
LL (L)
LL + DL (R)
LL + DL (L)

Figure 88

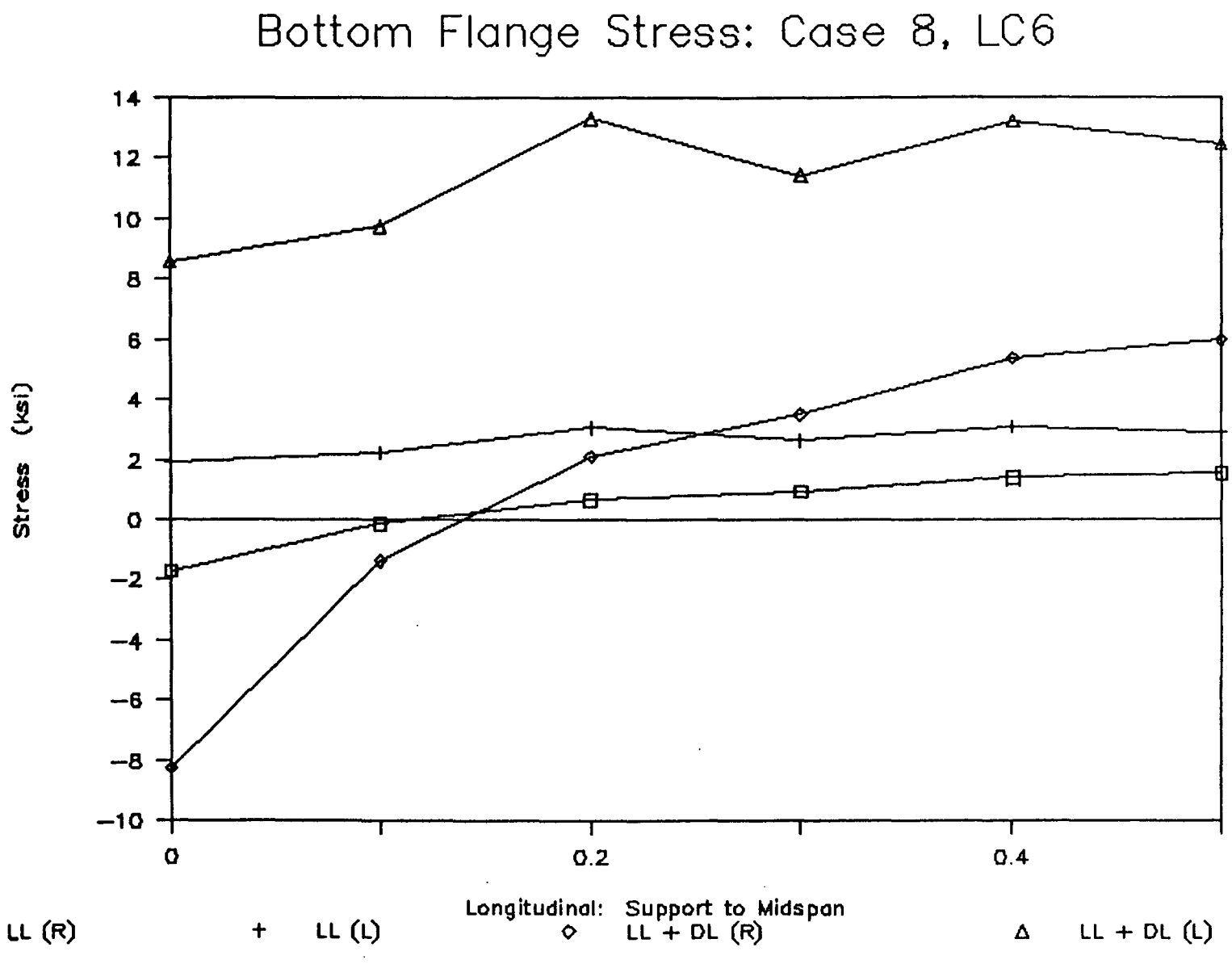
Bottom Flange Stress: Case 8, LC6
Stress (ksi)
14
12
10
8
6
4
2
0
−2
−4
−6
−8
−10
0
0.2
0.4
Longitudinal: Support to Midspan
LL (R)
+ LL (L)
◇ LL + DL (R)
Δ LL + DL (L)

Figure 89

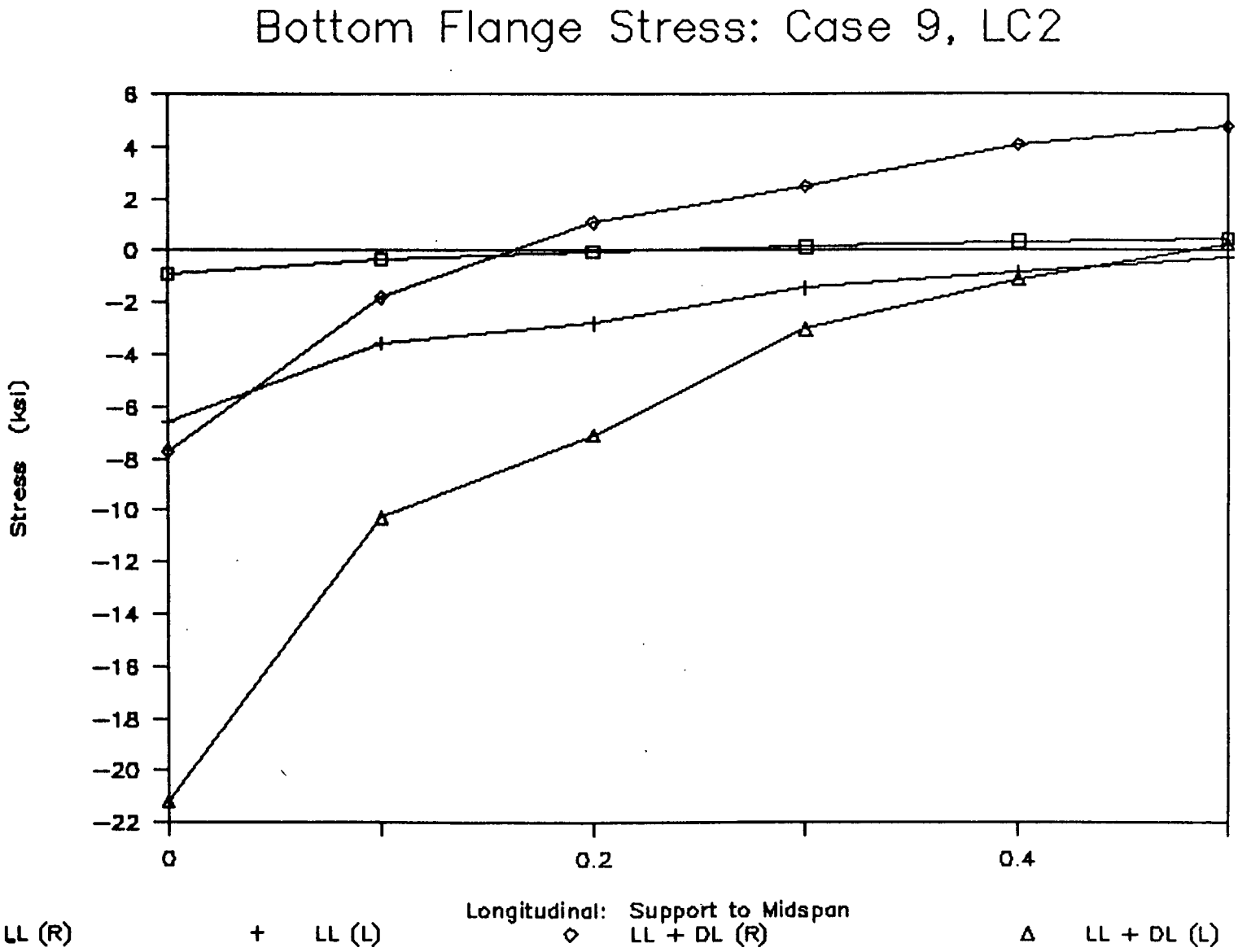
Bottom Flange Stress: Case 9, LC2
Stress (ksi)
6
4
2
0
-2
-4
-6
-8
-10
-12
-14
-16
-18
-20
-22
0
0.2
0.4
Longitudinal: Support to Midspan
LL (R)
+ LL (L)
◇ LL + DL (R)
Δ LL + DL (L)

Figure 90

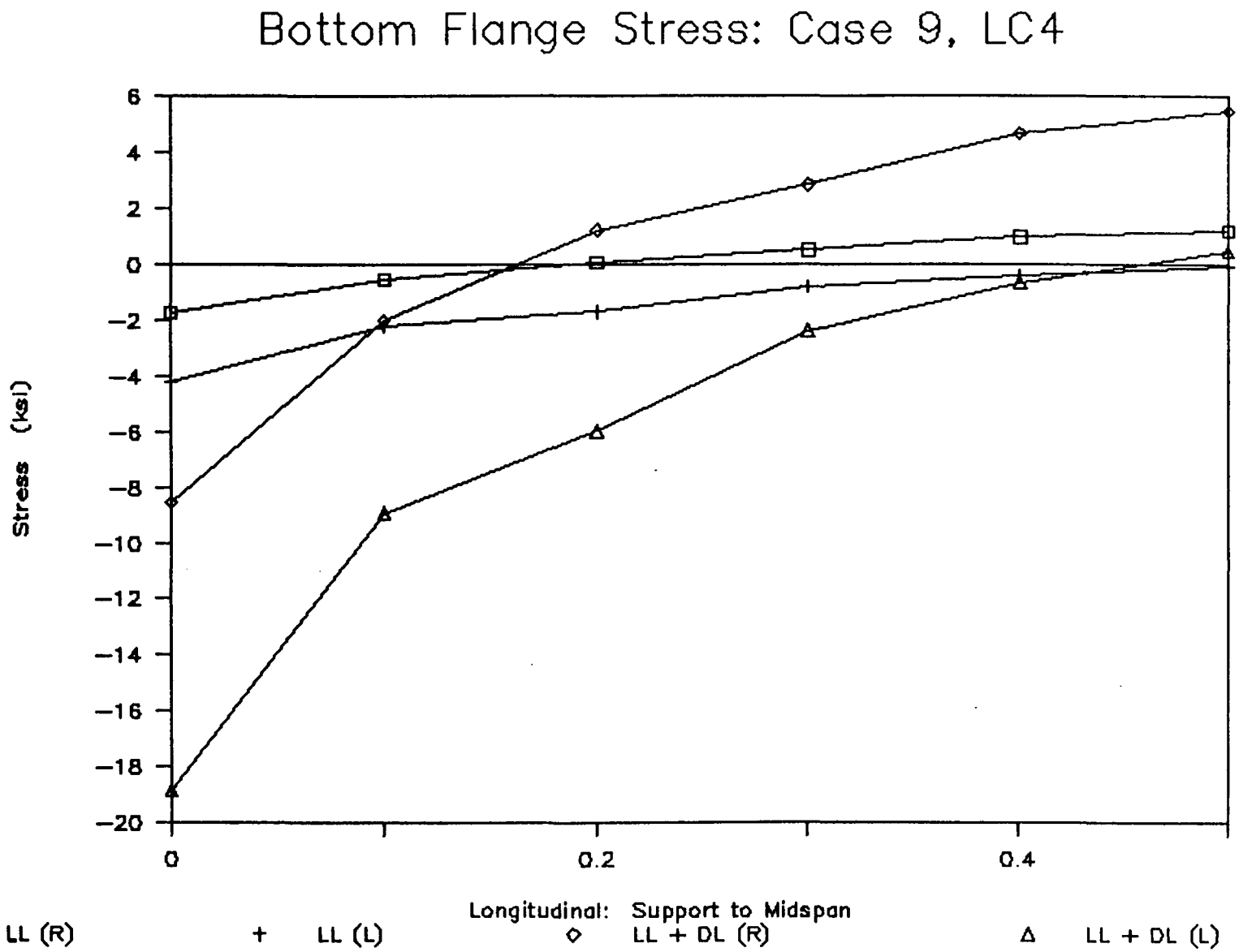
Bottom Flange Stress: Case 9, LC4
Stress (ksi)
6
4
2
0
-2
-4
-6
-8
-10
-12
-14
-16
-18
-20
0
0.2
0.4
Longitudinal: Support to Midspan
LL (R)
LL (L)
LL + DL (R)
LL + DL (L)

Figure 91

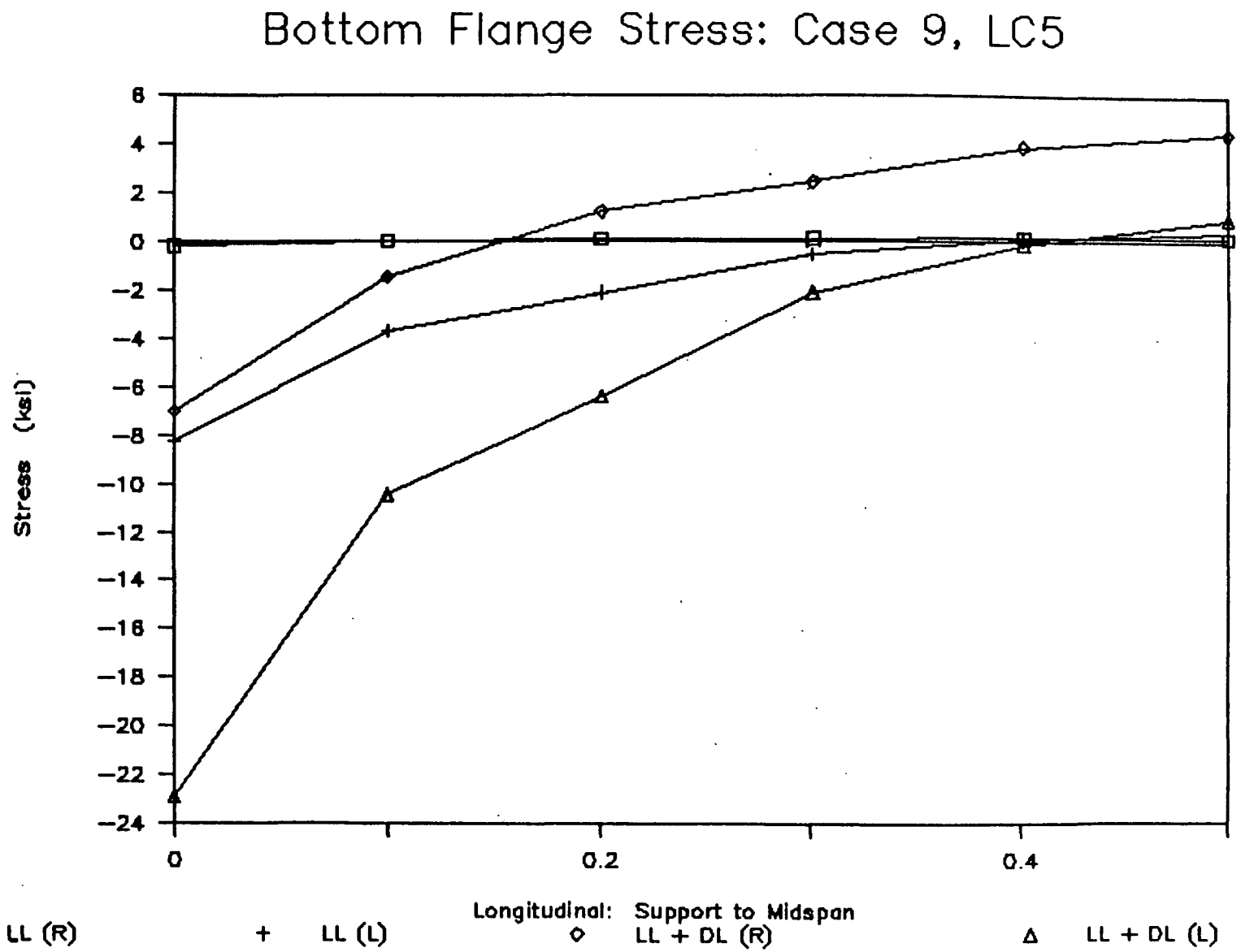
Bottom Flange Stress: Case 9, LC5
Stress (ksi)
6
4
2
0
-2
-4
-6
-8
-10
-12
-14
-16
-18
-20
-22
-24
0
0.2
0.4
Longitudinal: Support to Midspan
LL (R)
+ LL (L)
◇ LL + DL (R)
Δ LL + DL (L)

Figure 92

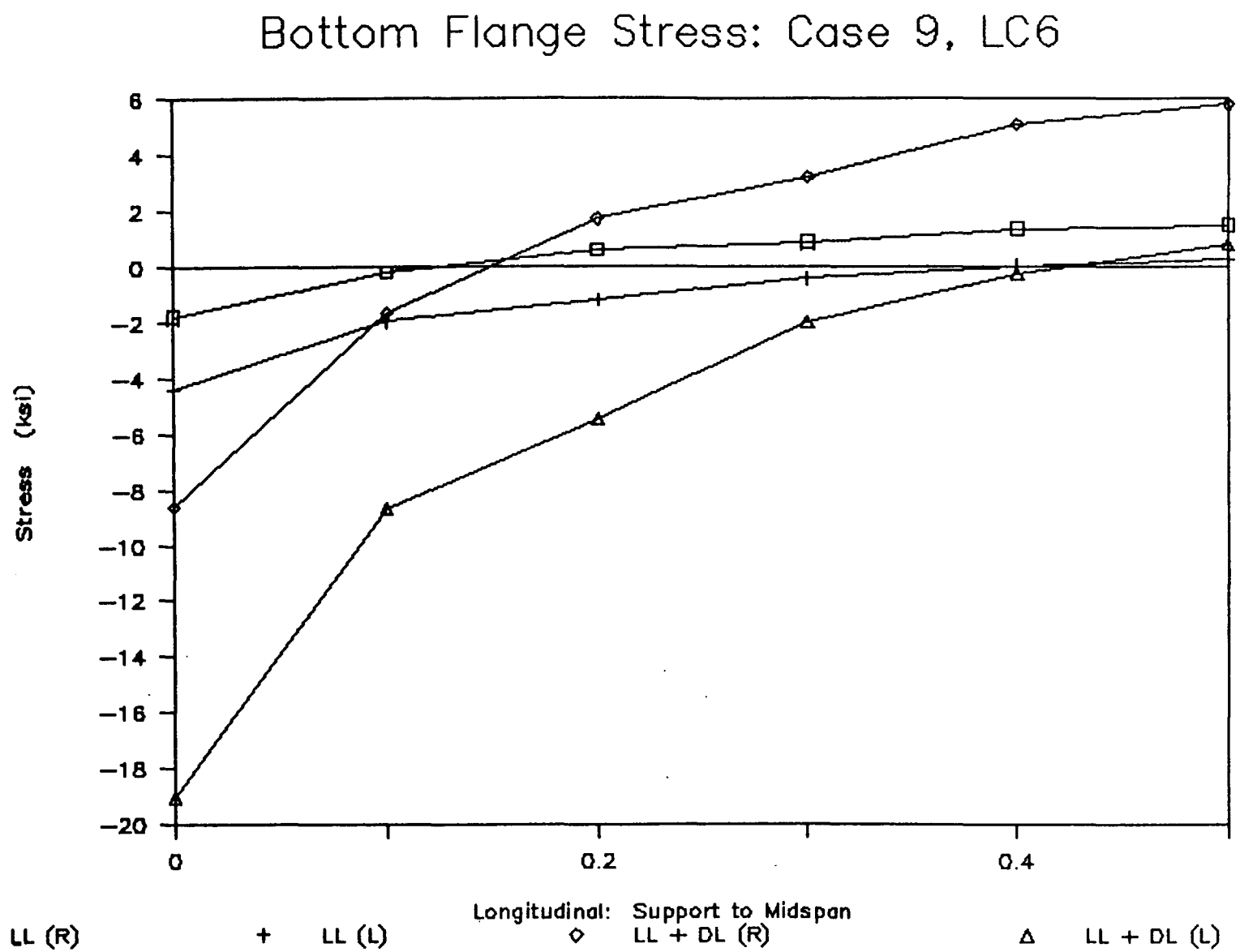
Bottom Flange Stress: Case 9, LC6
Stress (ksi)
6
4
2
0
-2
-4
-6
-8
-10
-12
-14
-16
-18
-20
0
0.2
0.4
Longitudinal: Support to Midspan
LL (R)
+ LL (L)
◇ LL + DL (R)
Δ LL + DL (L)

Figure 93

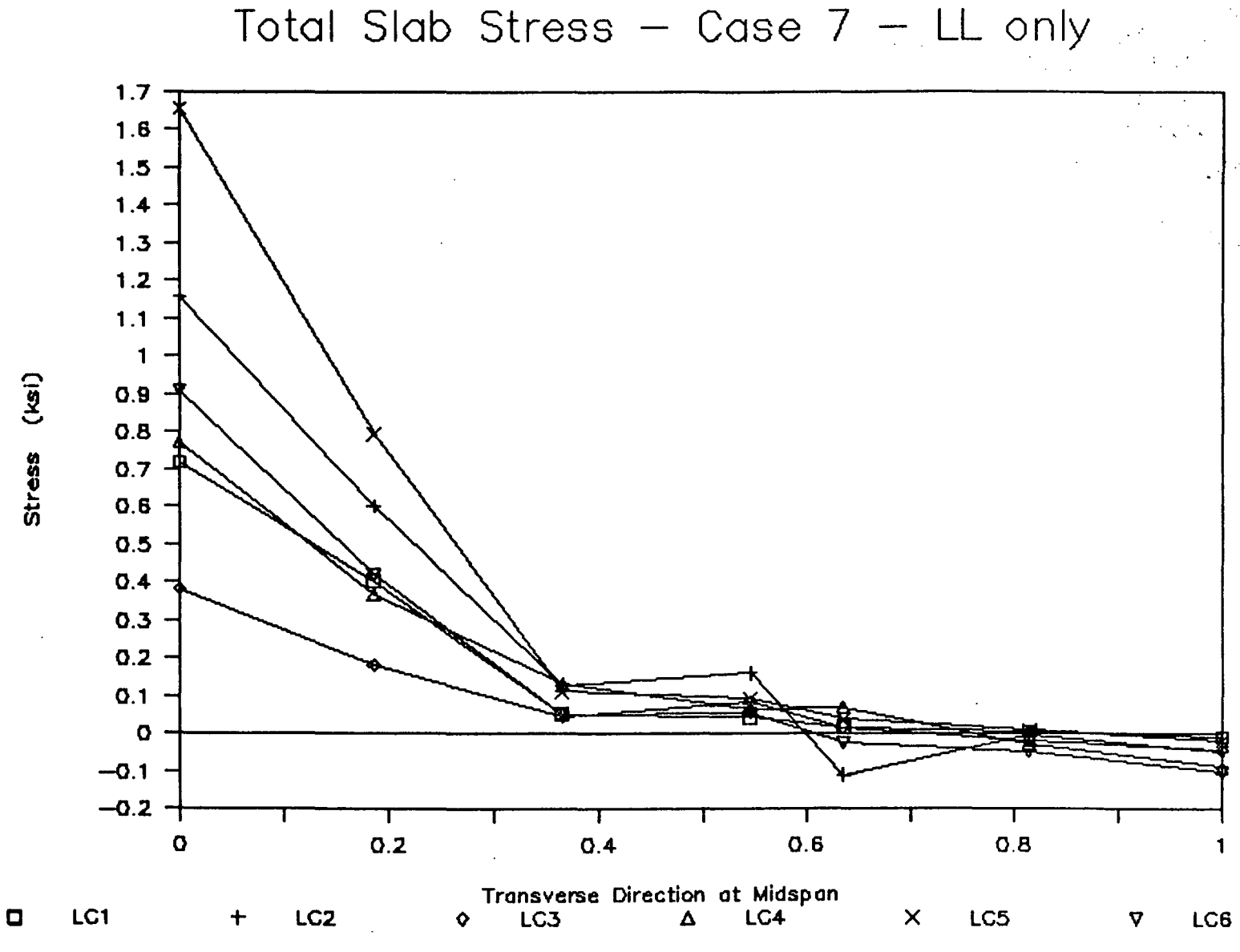
Total Slab Stress – Case 7 – LL only
Stress (ksi)
1.7
1.6
1.5
1.4
1.3
1.2
1.1
1
0.9
0.8
0.7
0.6
0.5
0.4
0.3
0.2
0.1
0
−0.1
−0.2
0
0.2
0.4
0.6
0.8
1
Transverse Direction at Midspan
LC1
LC2
LC3
LC4
LC5
LC6

Figure 94

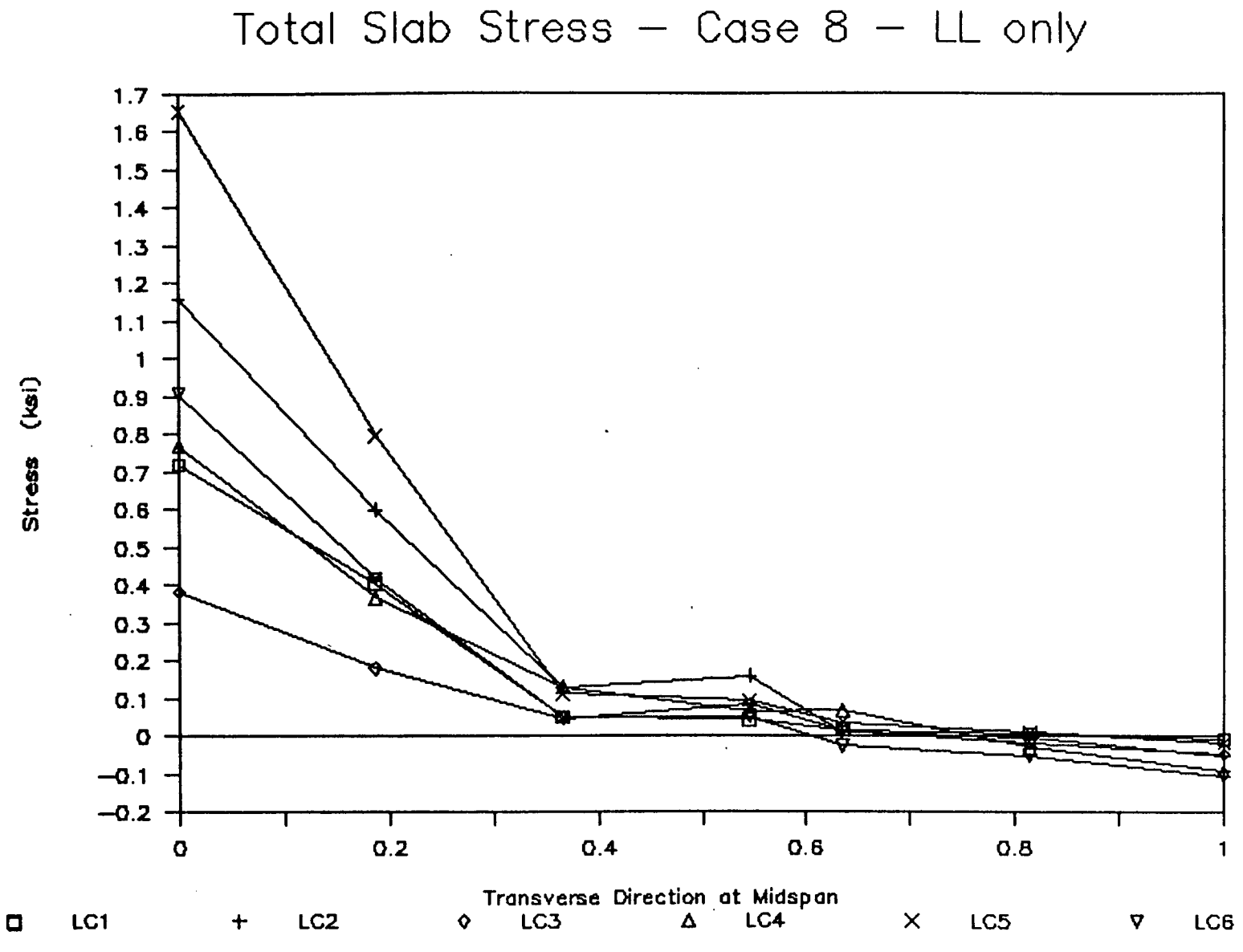
Total Slab Stress – Case 8 – LL only
Stress (ksi)
1.7
1.6
1.5
1.4
1.3
1.2
1.1
1
0.9
0.8
0.7
0.6
0.5
0.4
0.3
0.2
0.1
0
-0.1
-0.2
0
0.2
0.4
0.6
0.8
1
Transverse Direction at Midspan
LC1
LC2
LC3
LC4
LC5
LC6

Figure 95

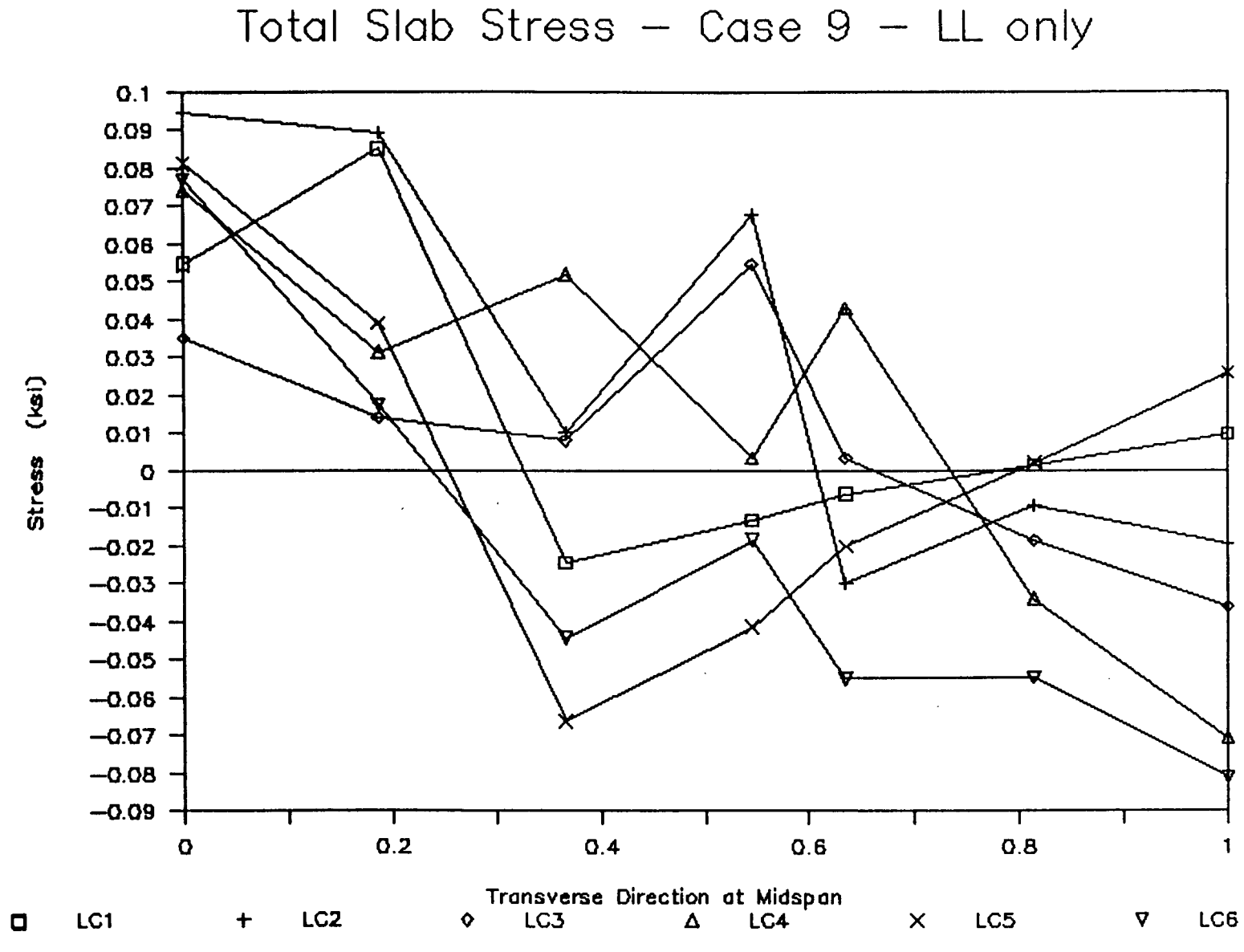
Total Slab Stress – Case 9 – LL only
Stress (ksi)
0.1
0.09
0.08
0.07
0.06
0.05
0.04
0.03
0.02
0.01
0
−0.01
−0.02
−0.03
−0.04
−0.05
−0.06
−0.07
−0.08
−0.09
0
0.2
0.4
0.6
0.8
1
Transverse Direction at Midspan
LC1
LC2
LC3
LC4
LC5
LC6

Figure 96

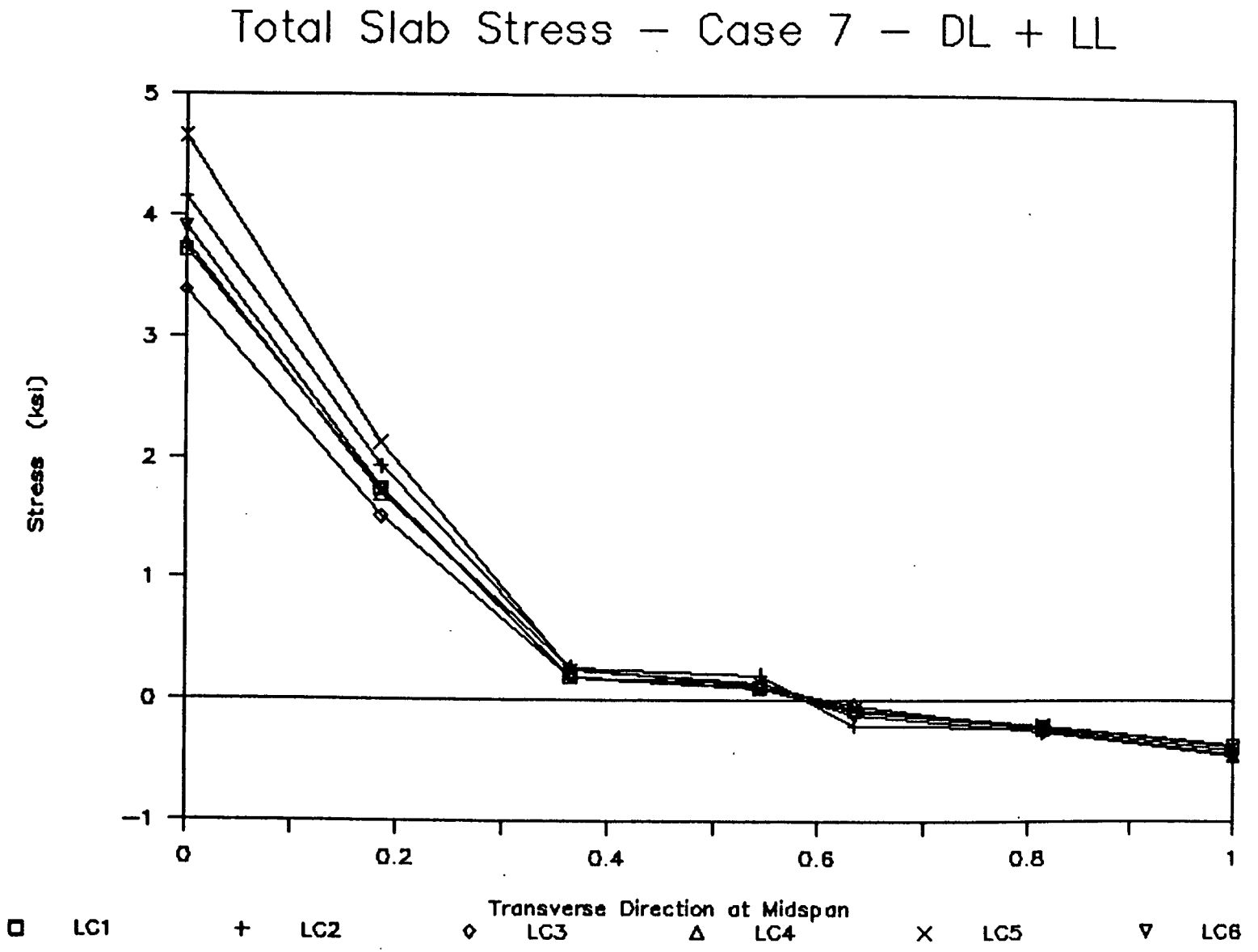
Total Slab Stress – Case 7 – DL + LL
Stress (ksi)
5
4
3
2
1
0
-1
0
0.2
0.4
0.6
0.8
1
Transverse Direction at Midspan
LC1
LC2
LC3
LC4
LC5
LC6

Figure 97

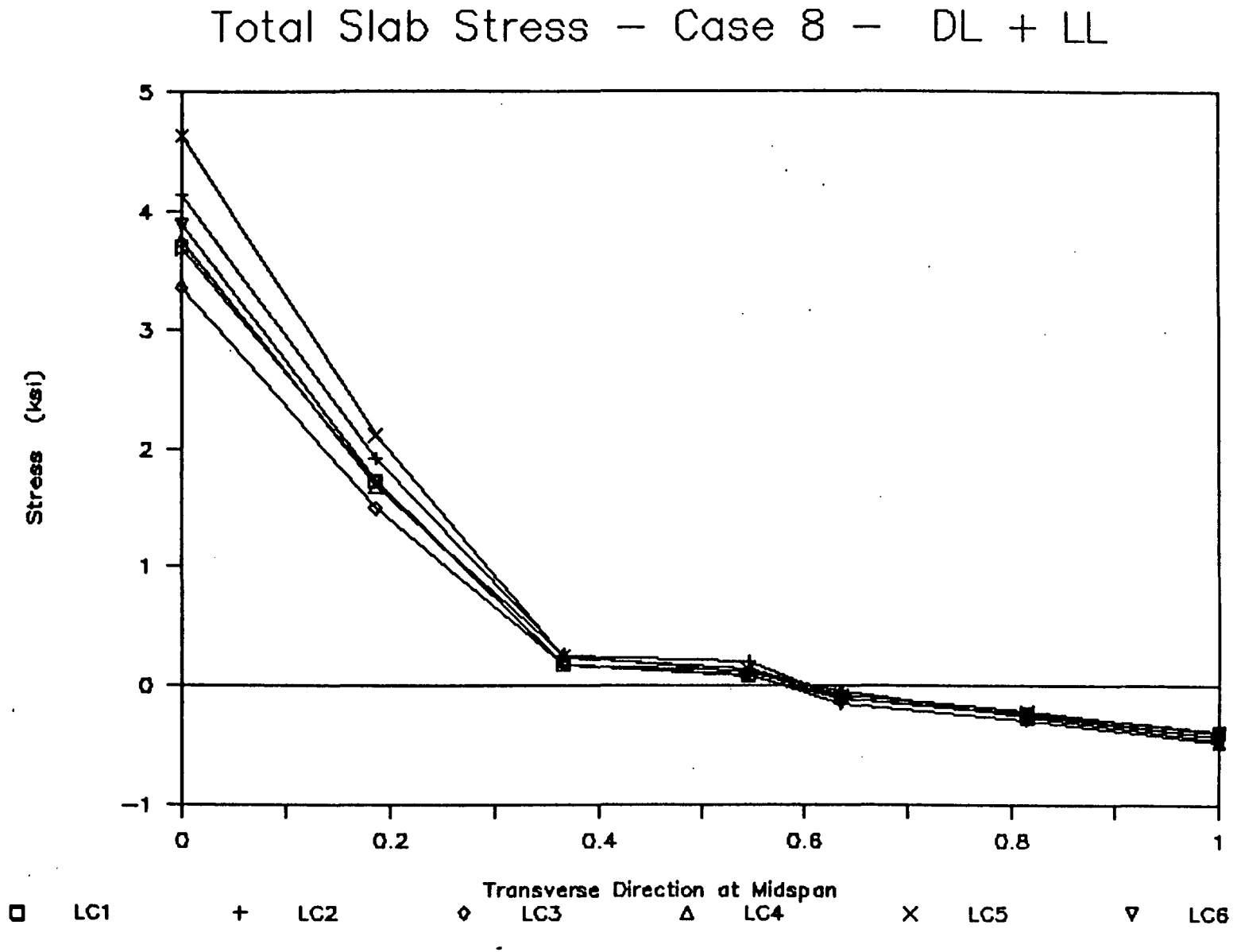
Total Slab Stress – Case 8 – DL + LL
Stress (ksi)
5
4
3
2
1
0
−1
0
0.2
0.4
0.6
0.8
1
Transverse Direction at Midspan
LC1
LC2
LC3
LC4
LC5
LC6

Figure 98

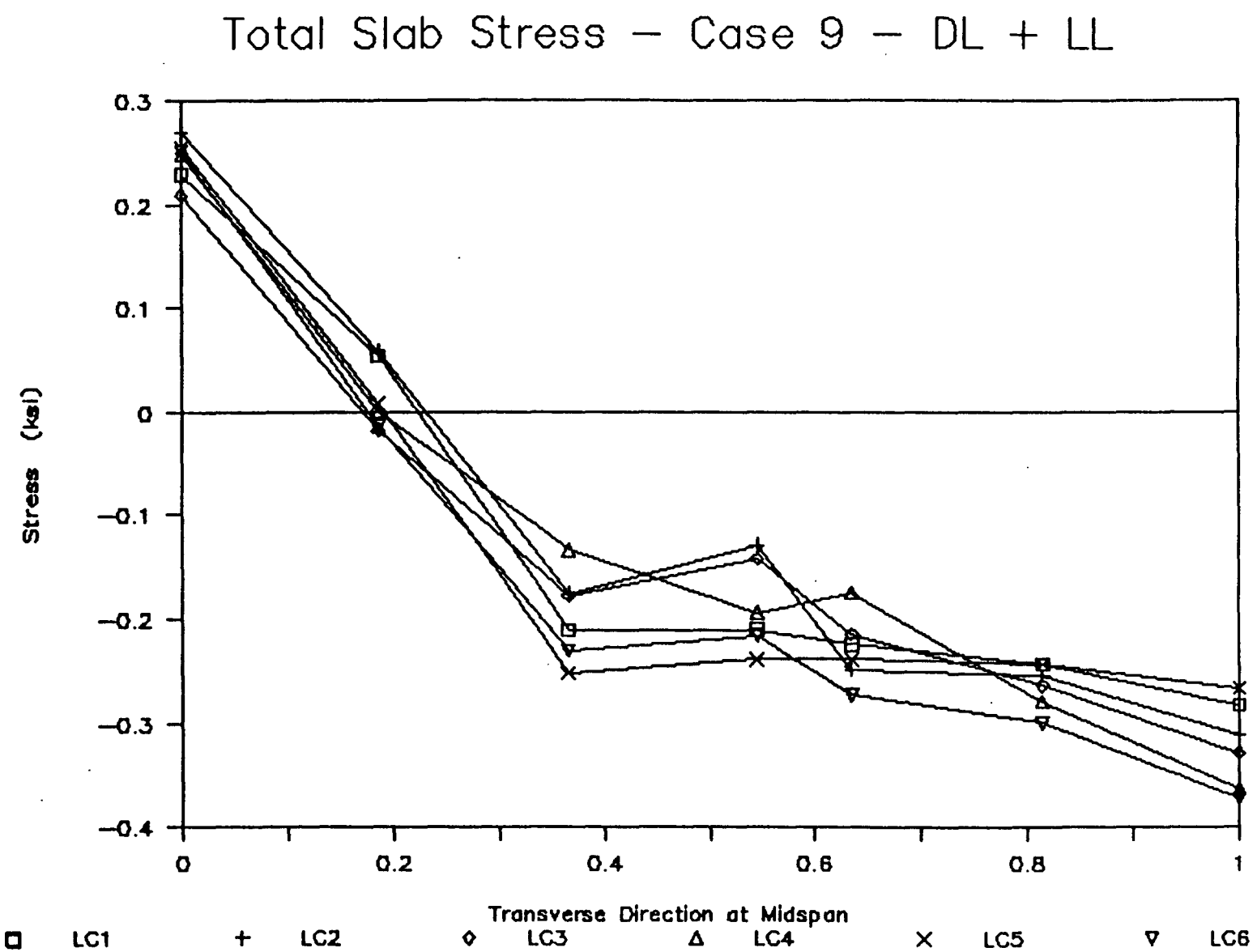
Total Slab Stress – Case 9 – DL + LL
Stress (ksi)
0.3
0.2
0.1
0
-0.1
-0.2
-0.3
-0.4
0
0.2
0.4
0.6
0.8
1
Transverse Direction at Midspan
LC1
LC2
LC3
LC4
LC5
LC6

Figure 99

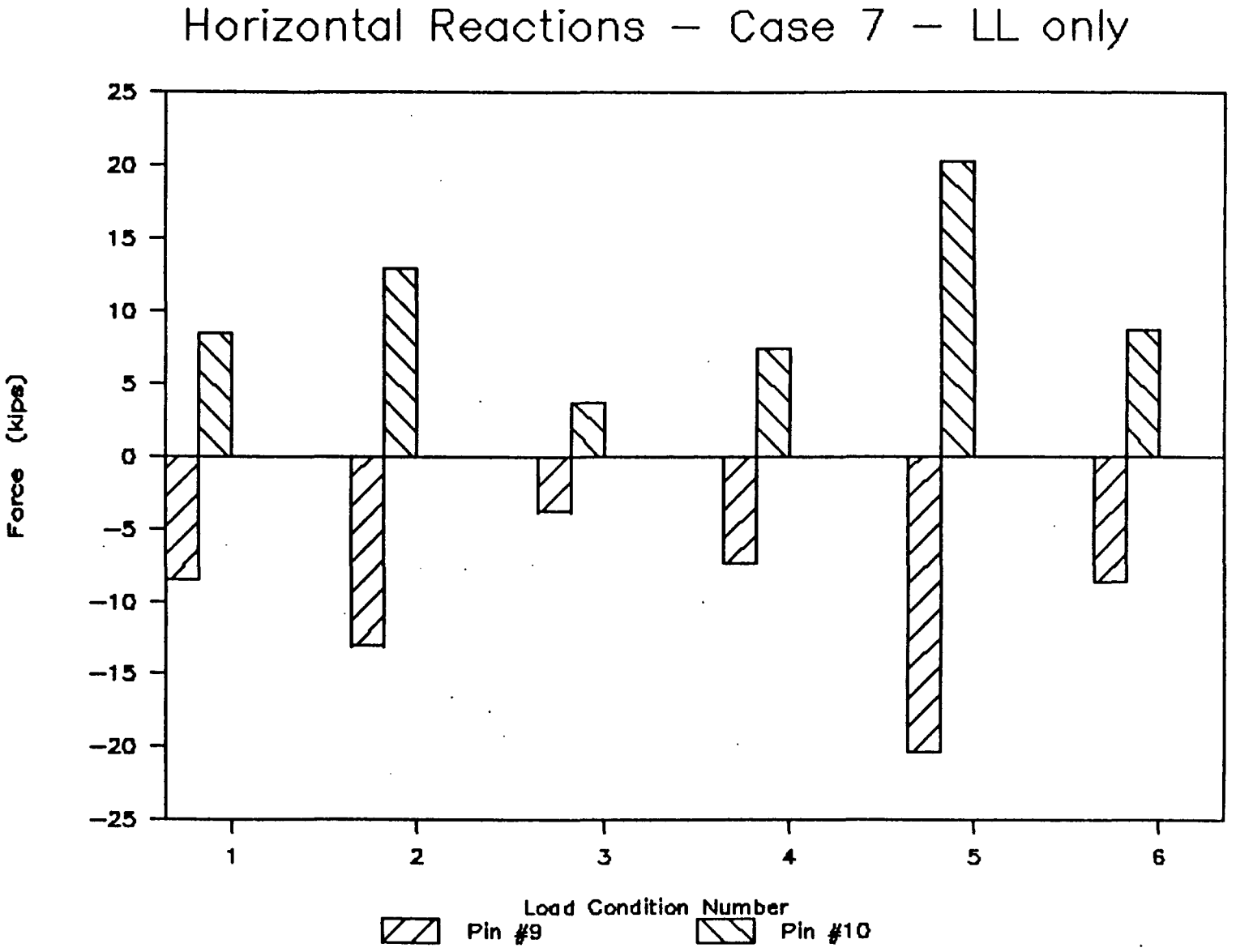
Horizontal Reactions – Case 7 – LL only
Force (kips)
25
20
15
10
5
0
-5
-10
-15
-20
-25
1
2
3
4
5
6
Load Condition Number
Pin #9
Pin #10

Figure 100

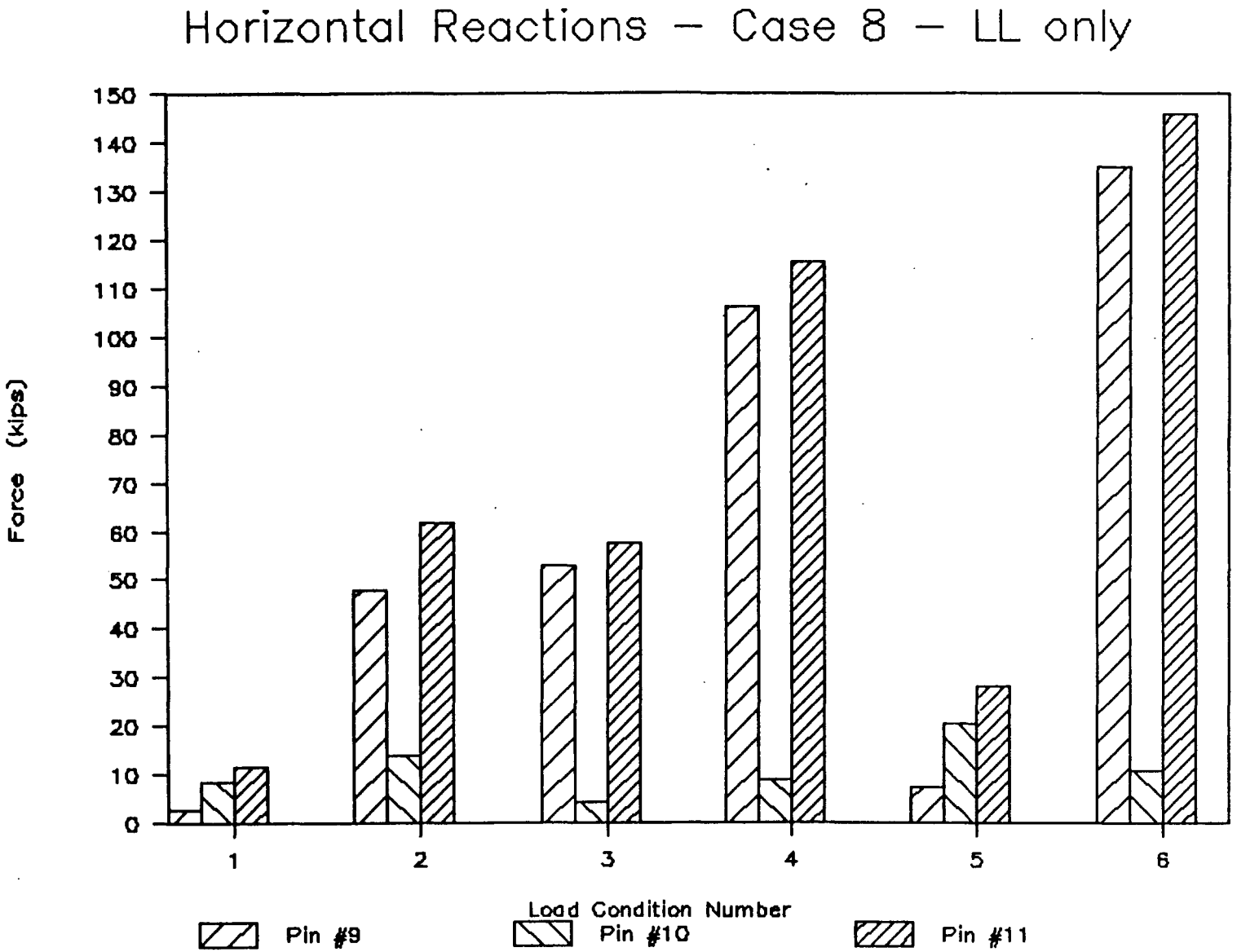
Horizontal Reactions – Case 8 – LL only
Force (kips)
150
140
130
120
110
100
90
80
70
60
50
40
30
20
10
0
1
2
3
4
5
6
Load Condition Number
Pin #9
Pin #10
Pin #11

Figure 101

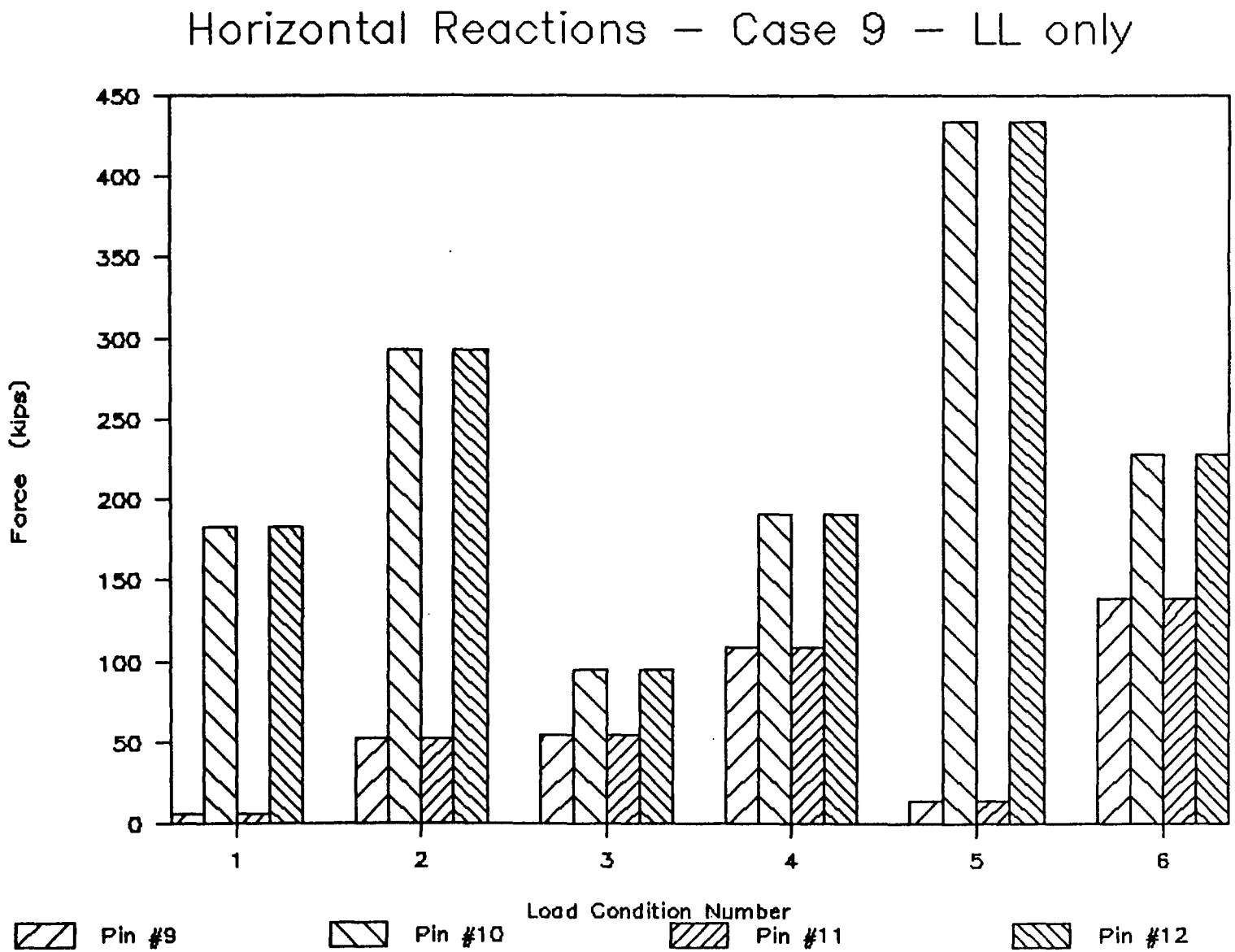
Horizontal Reactions – Case 9 – LL only
Force (kips)
450
400
350
300
250
200
150
100
50
0
1
2
3
4
5
6
Load Condition Number
Pin #9
Pin #10
Pin #11
Pin #12

Figure 102

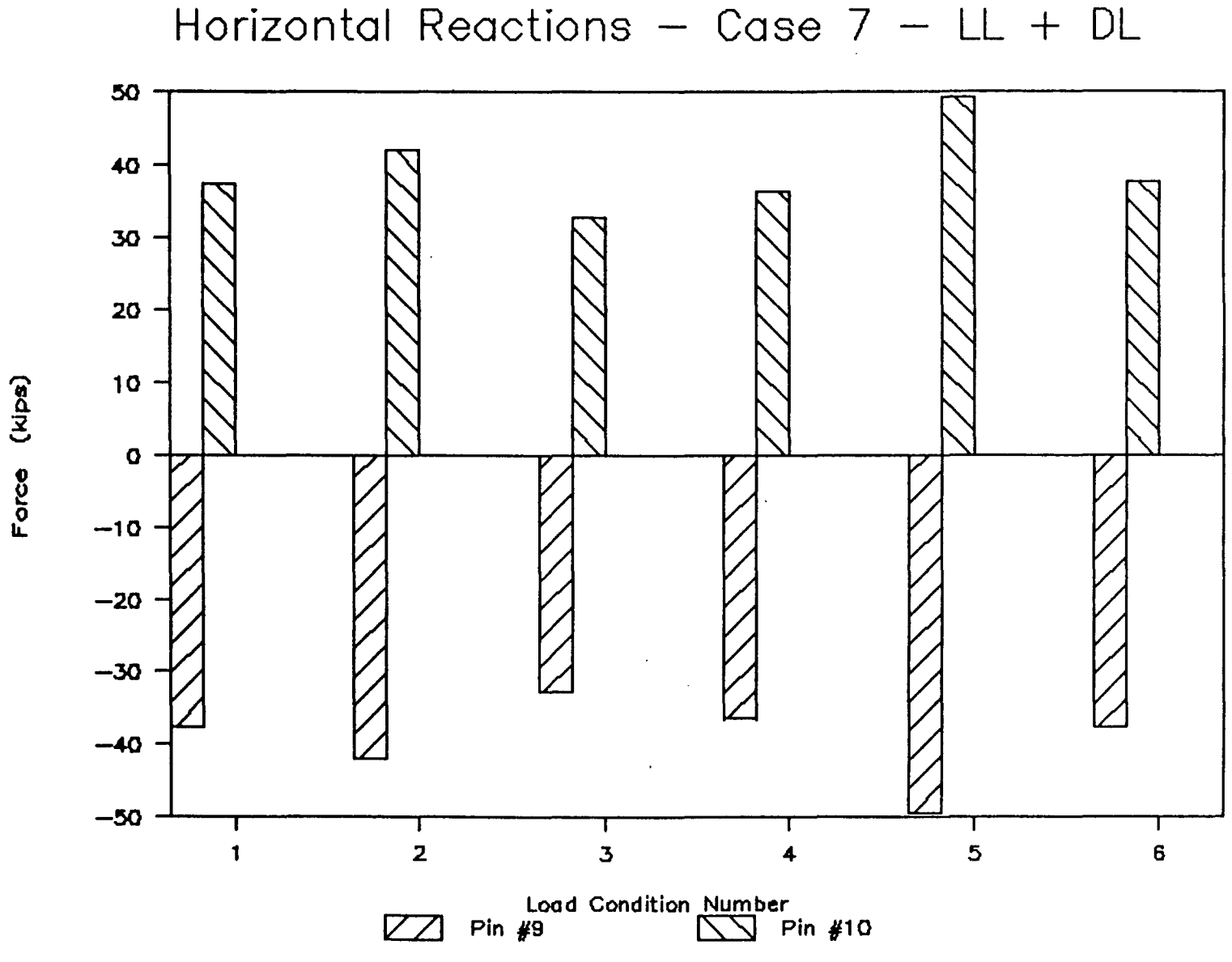
Horizontal Reactions – Case 7 – LL + DL
Force (kips)
50
40
30
20
10
0
-10
-20
-30
-40
-50
1
2
3
4
5
6
Load Condition Number
Pin #9
Pin #10

Figure 103

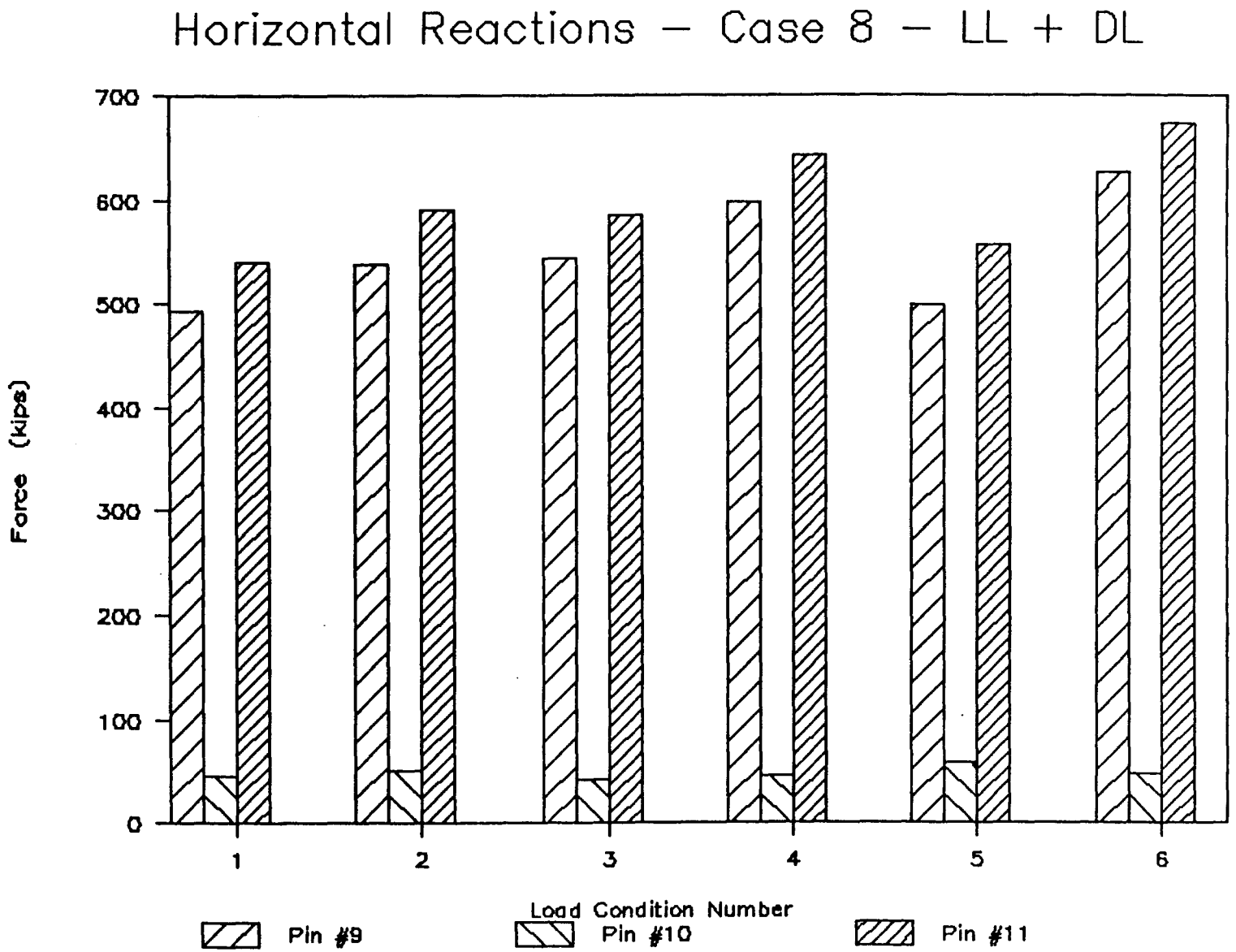
Horizontal Reactions – Case 8 – LL + DL
Force (kips)
700
600
500
400
300
200
100
0
1
2
3
4
5
6
Load Condition Number
Pin #9
Pin #10
Pin #11

Figure 104

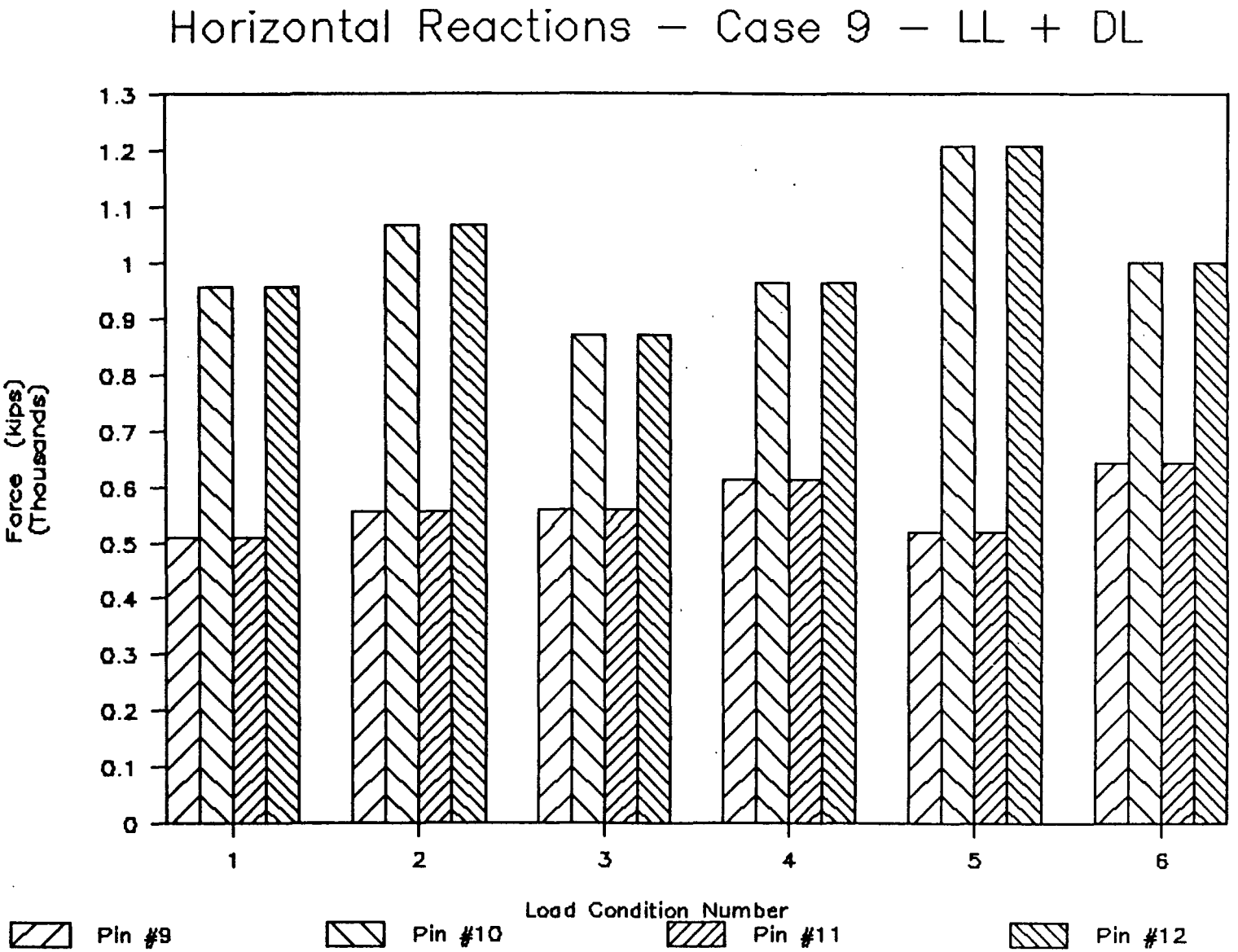
Horizontal Reactions – Case 9 – LL + DL
Force (kips)
(Thousands)
1.3
1.2
1.1
1
0.9
0.8
0.7
0.6
0.5
0.4
0.3
0.2
0.1
0
1
2
3
4
5
6
Load Condition Number
Pin #9
Pin #10
Pin #11
Pin #12

Figure 105

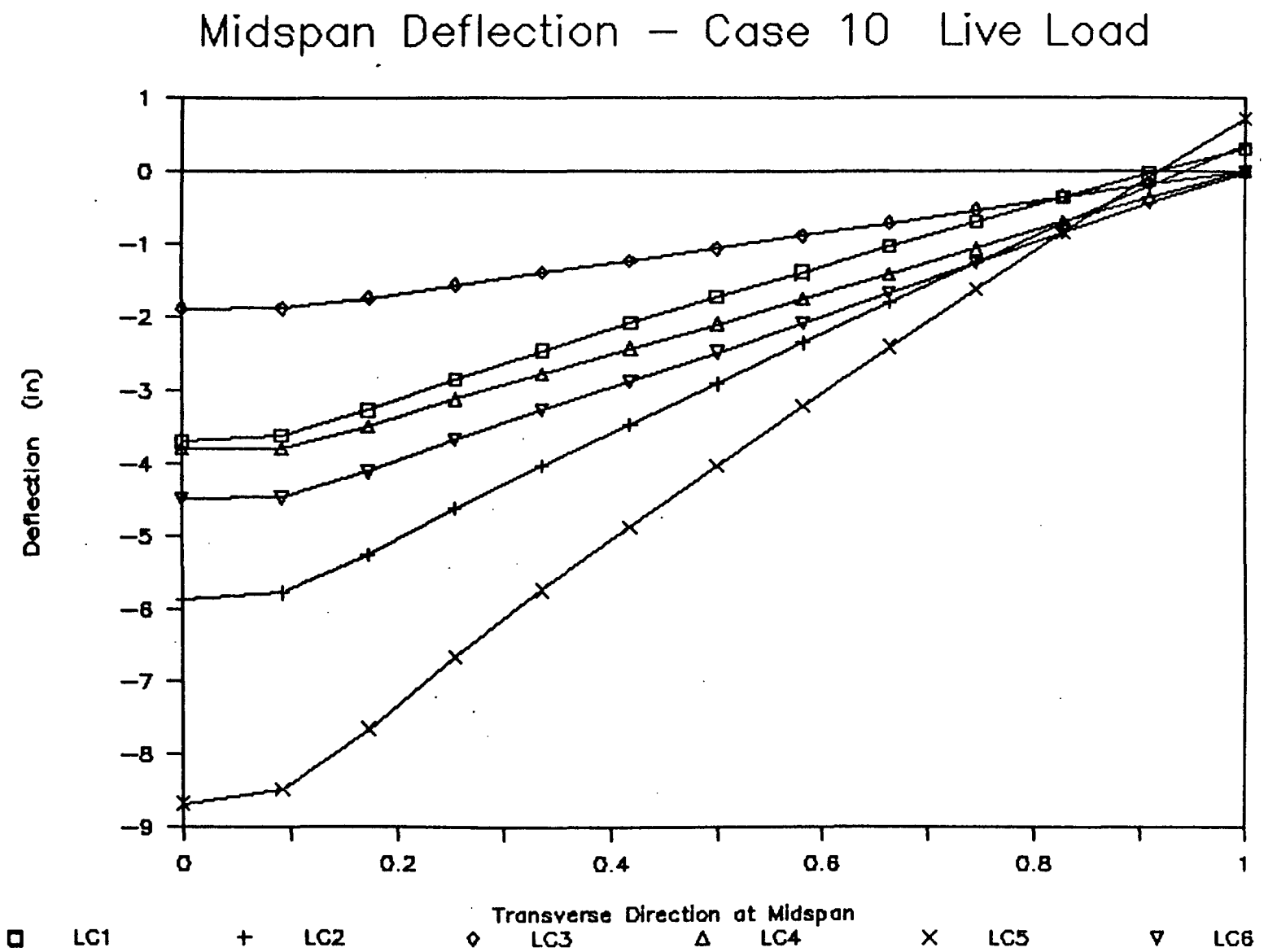
Midspan Deflection – Case 10 Live Load
Deflection (in)
1
0
-1
-2
-3
-4
-5
-6
-7
-8
-9
0
0.2
0.4
0.6
0.8
1
Transverse Direction at Midspan
LC1
LC2
LC3
LC4
LC5
LC6

Figure 106

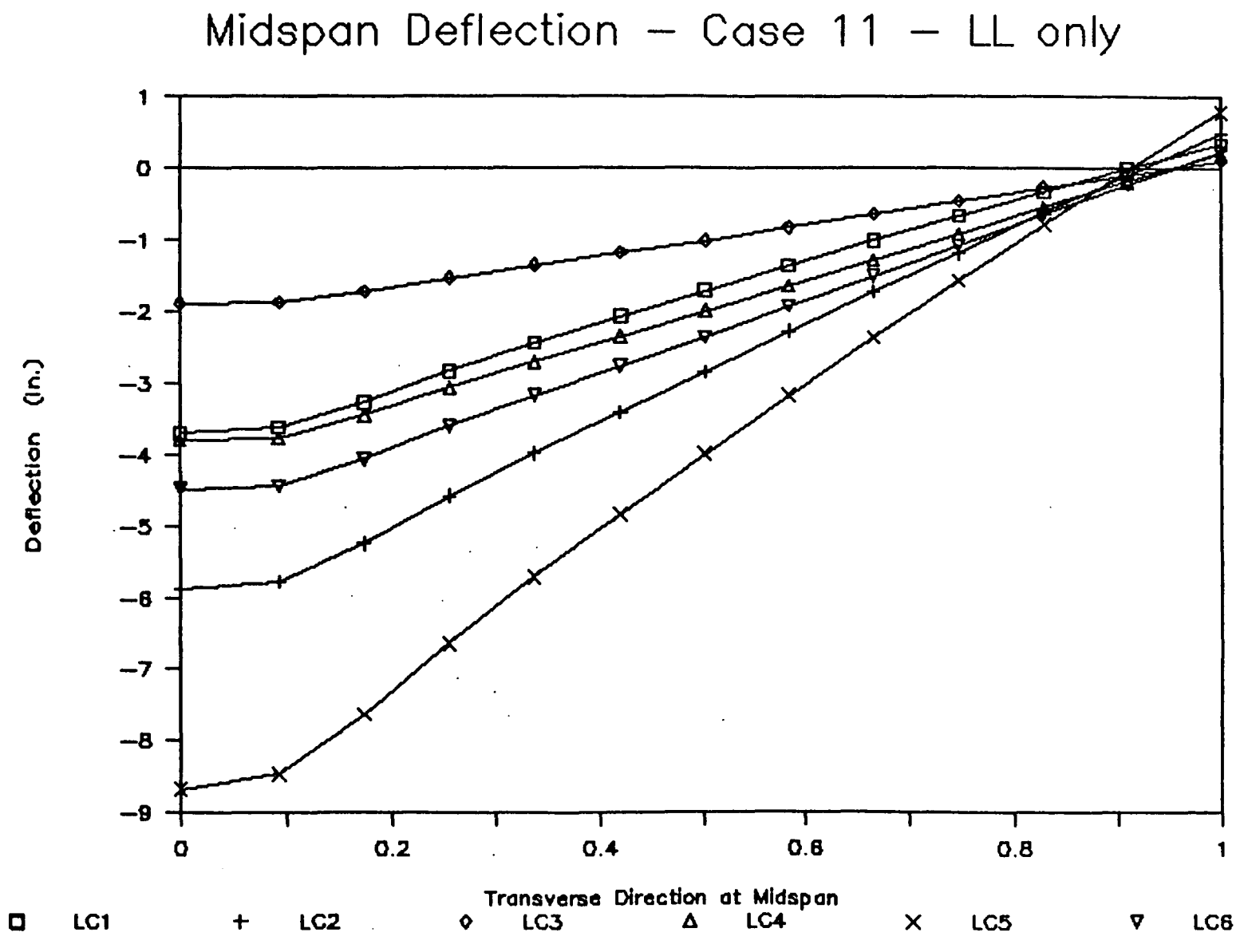
Midspan Deflection – Case 11 – LL only
Deflection (in.)
1
0
-1
-2
-3
-4
-5
-6
-7
-8
-9
0
0.2
0.4
0.6
0.8
1
Transverse Direction at Midspan
LC1
LC2
LC3
LC4
LC5
LC6

Figure 107

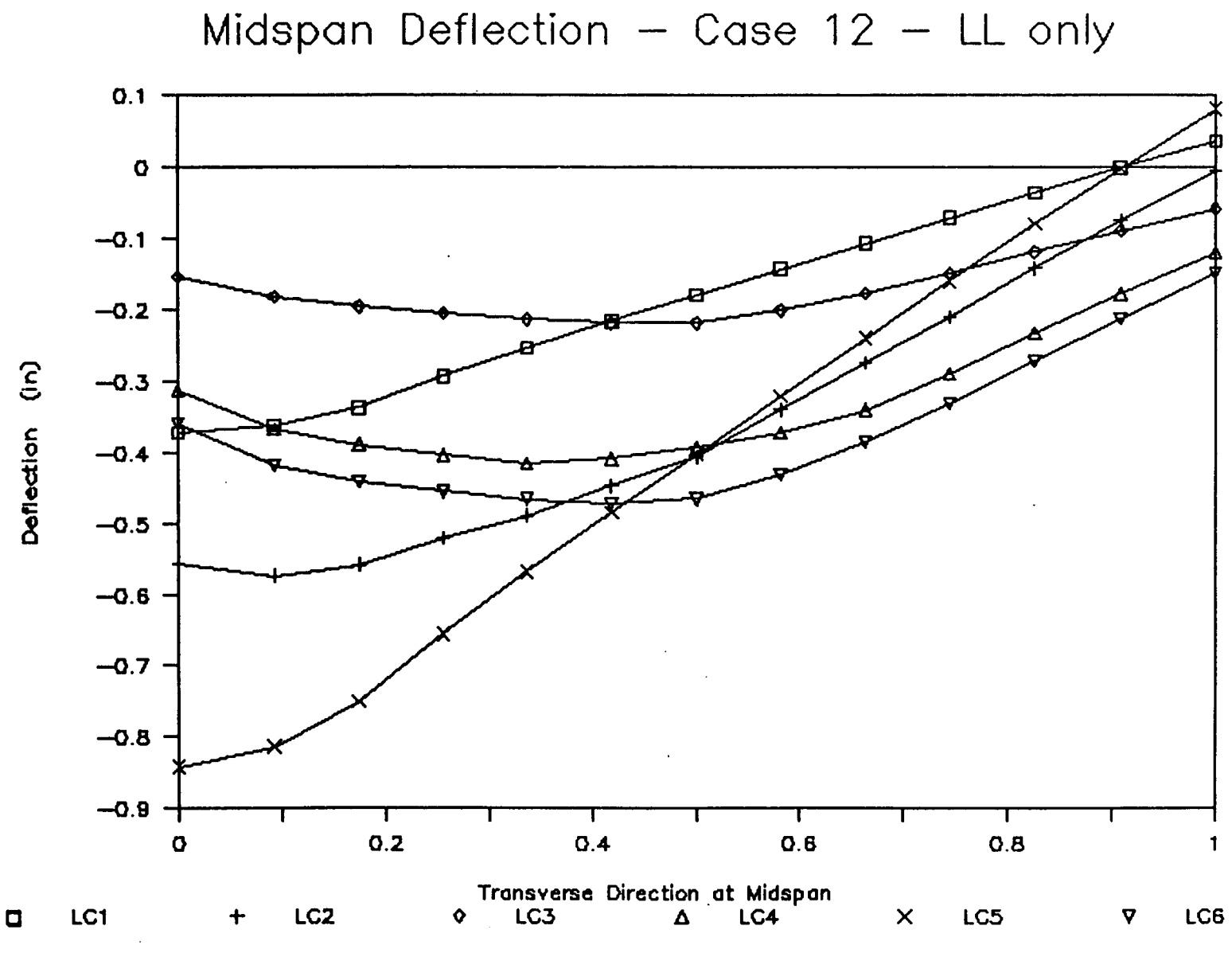
Midspan Deflection – Case 12 – LL only
Deflection (in)
0.1
0
-0.1
-0.2
-0.3
-0.4
-0.5
-0.6
-0.7
-0.8
-0.9
0
0.2
0.4
0.6
0.8
1
Transverse Direction at Midspan
LC1
LC2
LC3
LC4
LC5
LC6

Figure 108

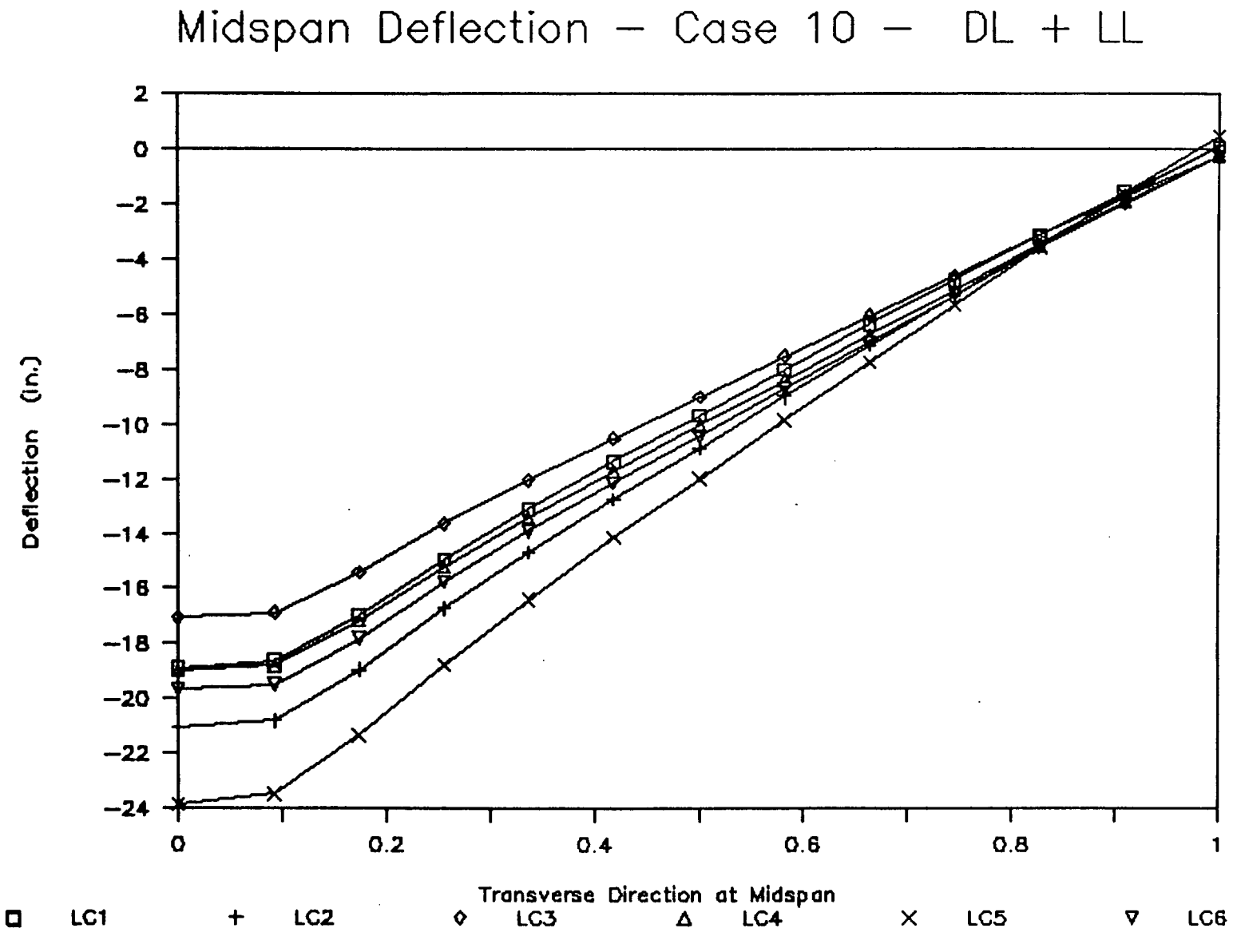
Midspan Deflection – Case 10 – DL + LL
Deflection (in.)
2
0
-2
-4
-6
-8
-10
-12
-14
-16
-18
-20
-22
-24
0
0.2
0.4
0.6
0.8
1
Transverse Direction at Midspan
LC1
LC2
LC3
LC4
LC5
LC6

Figure 109

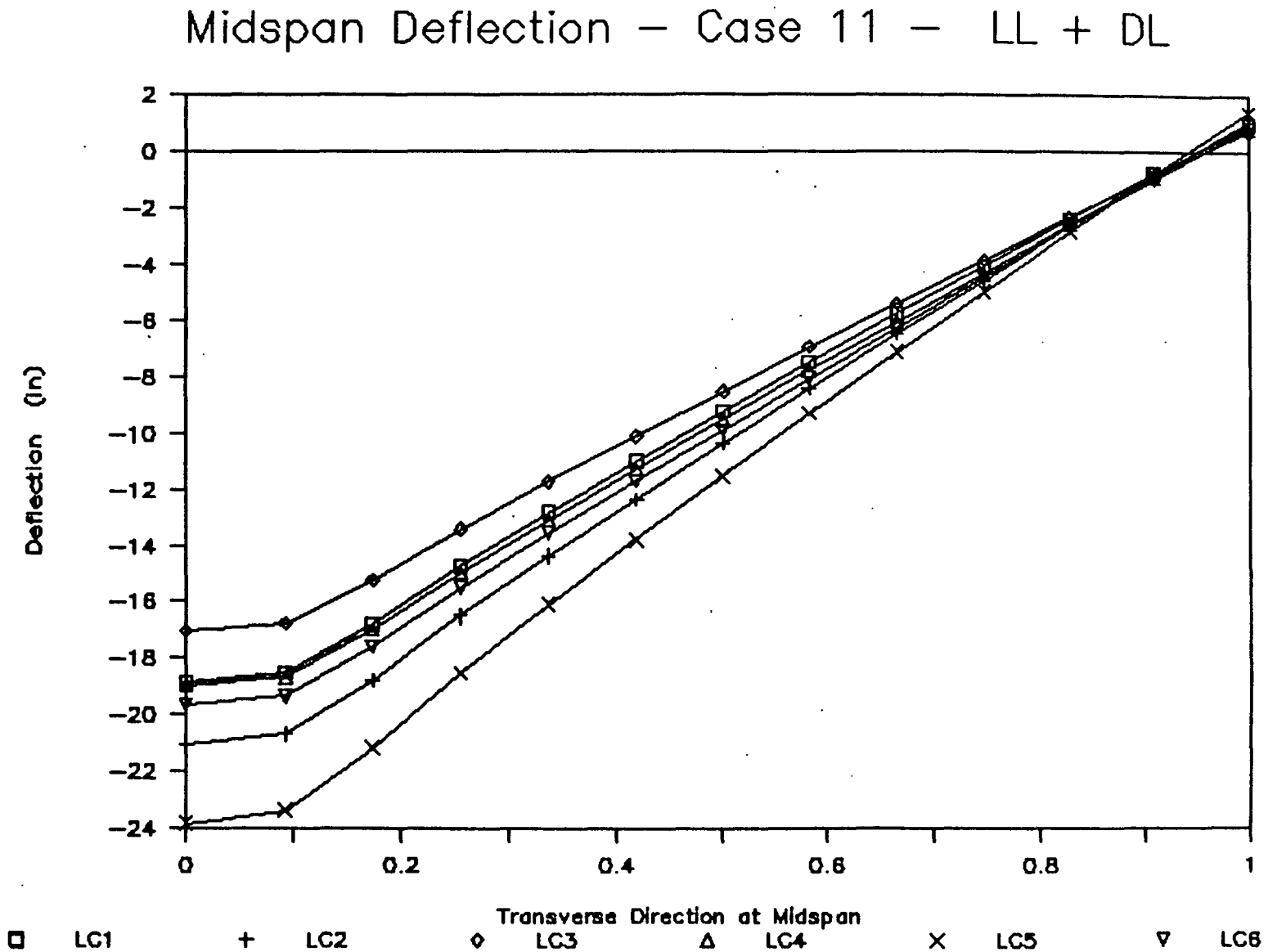
Midspan Deflection – Case 11 – LL + DL
Deflection (in)
2
0
-2
-4
-6
-8
-10
-12
-14
-16
-18
-20
-22
-24
0
0.2
0.4
0.6
0.8
1
Transverse Direction at Midspan
LC1
LC2
LC3
LC4
LC5
LC6

Figure 110

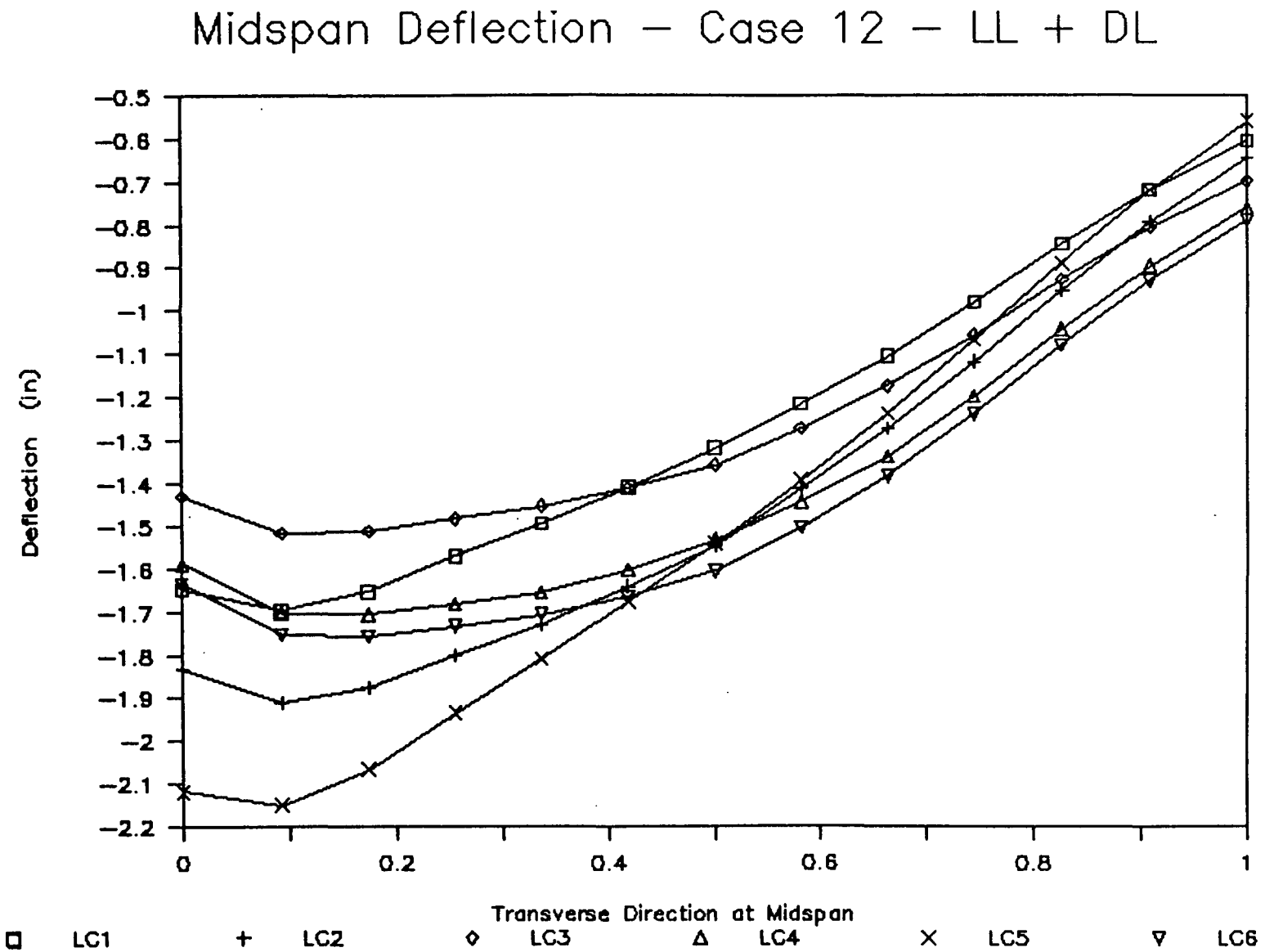
Midspan Deflection – Case 12 – LL + DL
Deflection (in)
-0.5
-0.6
-0.7
-0.8
-0.9
-1
-1.1
-1.2
-1.3
-1.4
-1.5
-1.6
-1.7
-1.8
-1.9
-2
-2.1
-2.2
0
0.2
0.4
0.6
0.8
1
Transverse Direction at Midspan
LC1
LC2
LC3
LC4
LC5
LC6

Figure 111

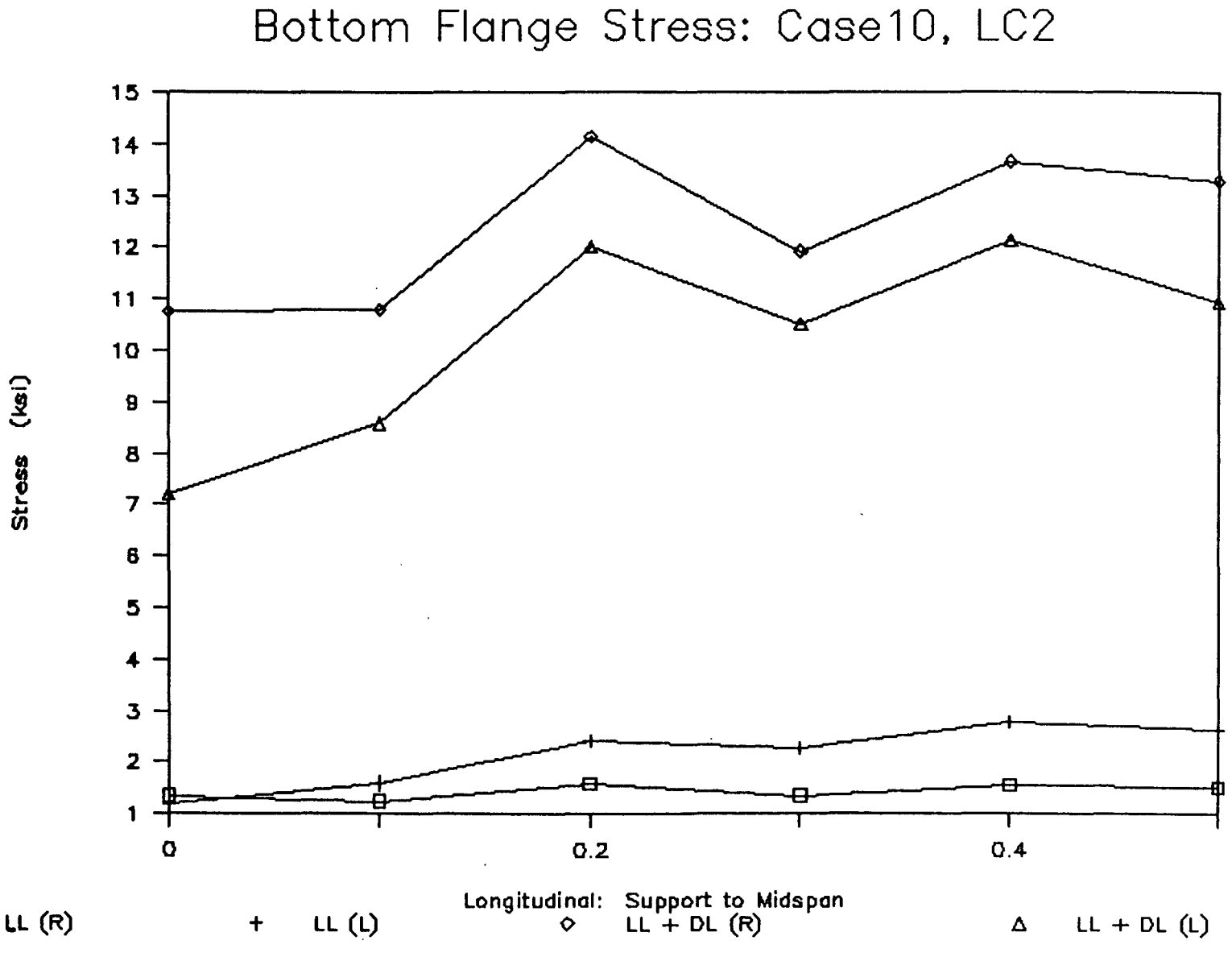
Bottom Flange Stress: Case10, LC2
Stress (ksi)
15
14
13
12
11
10
9
8
7
6
5
4
3
2
1
0
0.2
0.4
Longitudinal: Support to Midspan
LL (R)
+ LL (L)
◇ LL + DL (R)
△ LL + DL (L)

Figure 112

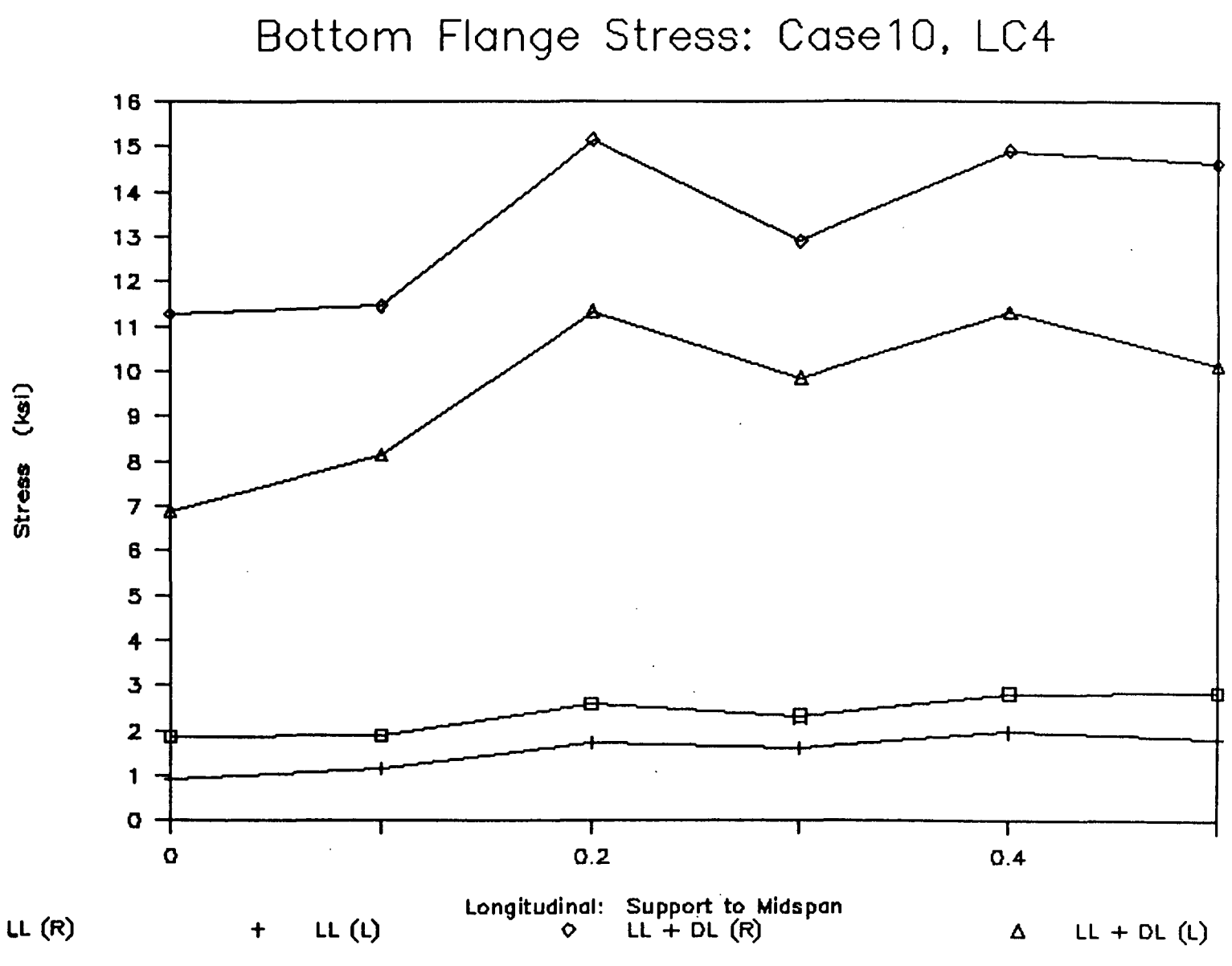
Bottom Flange Stress: Case10, LC4
Stress (ksi)
16
15
14
13
12
11
10
9
8
7
6
5
4
3
2
1
0
0
0.2
0.4
Longitudinal: Support to Midspan
LL (R)
+ LL (L)
◇ LL + DL (R)
Δ LL + DL (L)

Figure 113

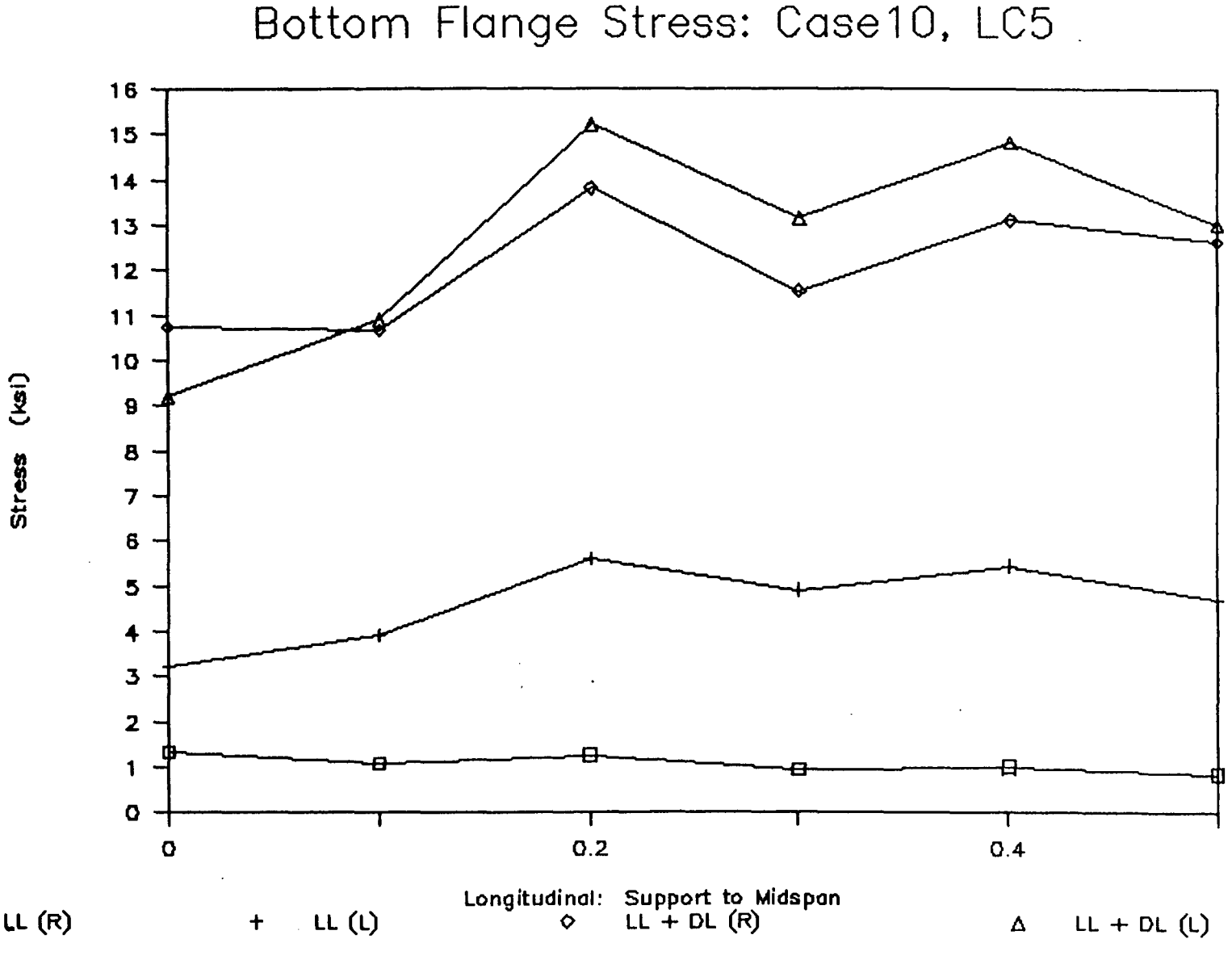
Bottom Flange Stress: Case10, LC5
Stress (ksi)
16
15
14
13
12
11
10
9
8
7
6
5
4
3
2
1
0
0
0.2
0.4
Longitudinal: Support to Midspan
LL (R)
+ LL (L)
◇ LL + DL (R)
△ LL + DL (L)

Figure 114

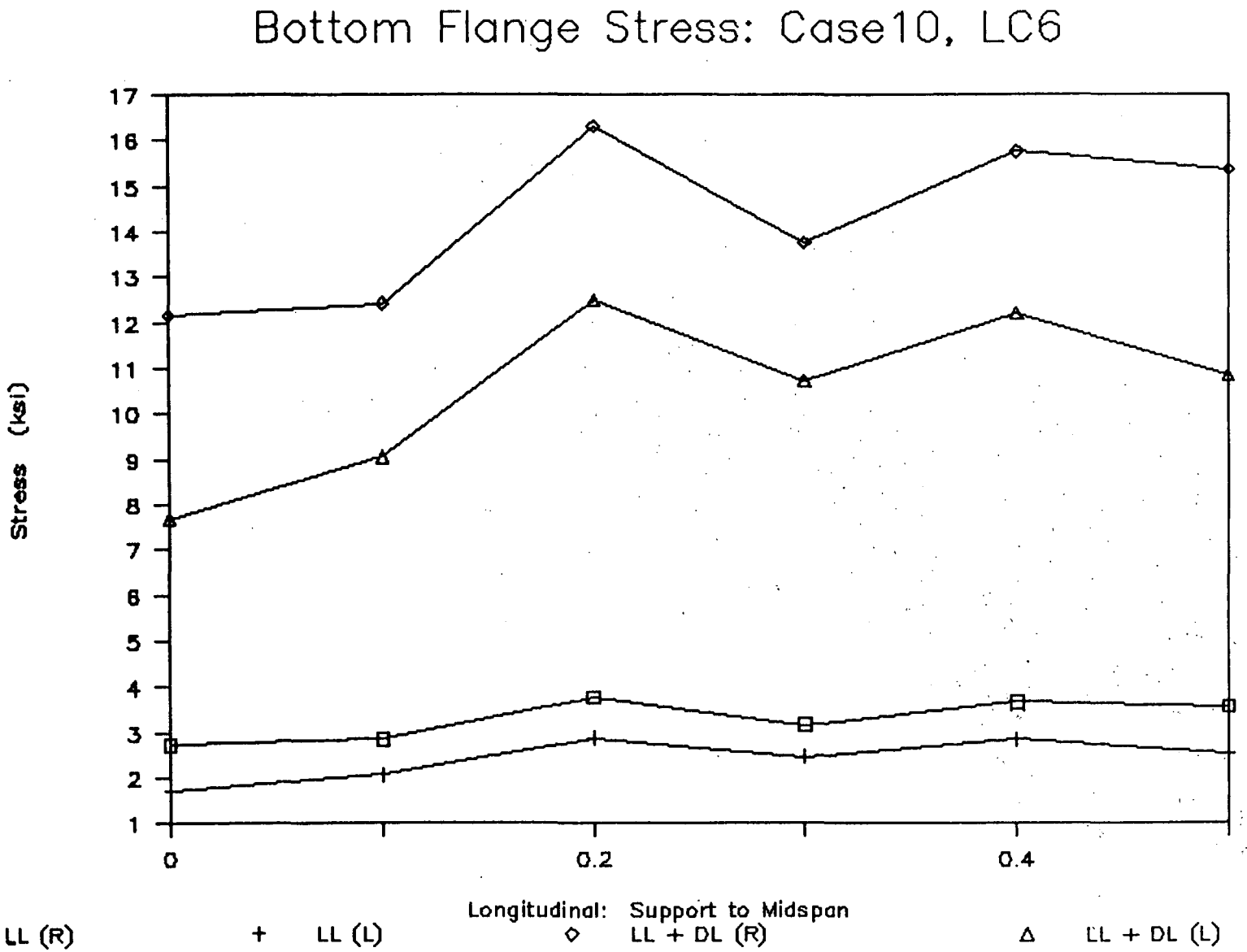
Bottom Flange Stress: Case10, LC6
Stress (ksi)
17
16
15
14
13
12
11
10
9
8
7
6
5
4
3
2
1
0
0.2
0.4
Longitudinal: Support to Midspan
LL (R)
LL (L)
LL + DL (R)
LL + DL (L)

Figure 115

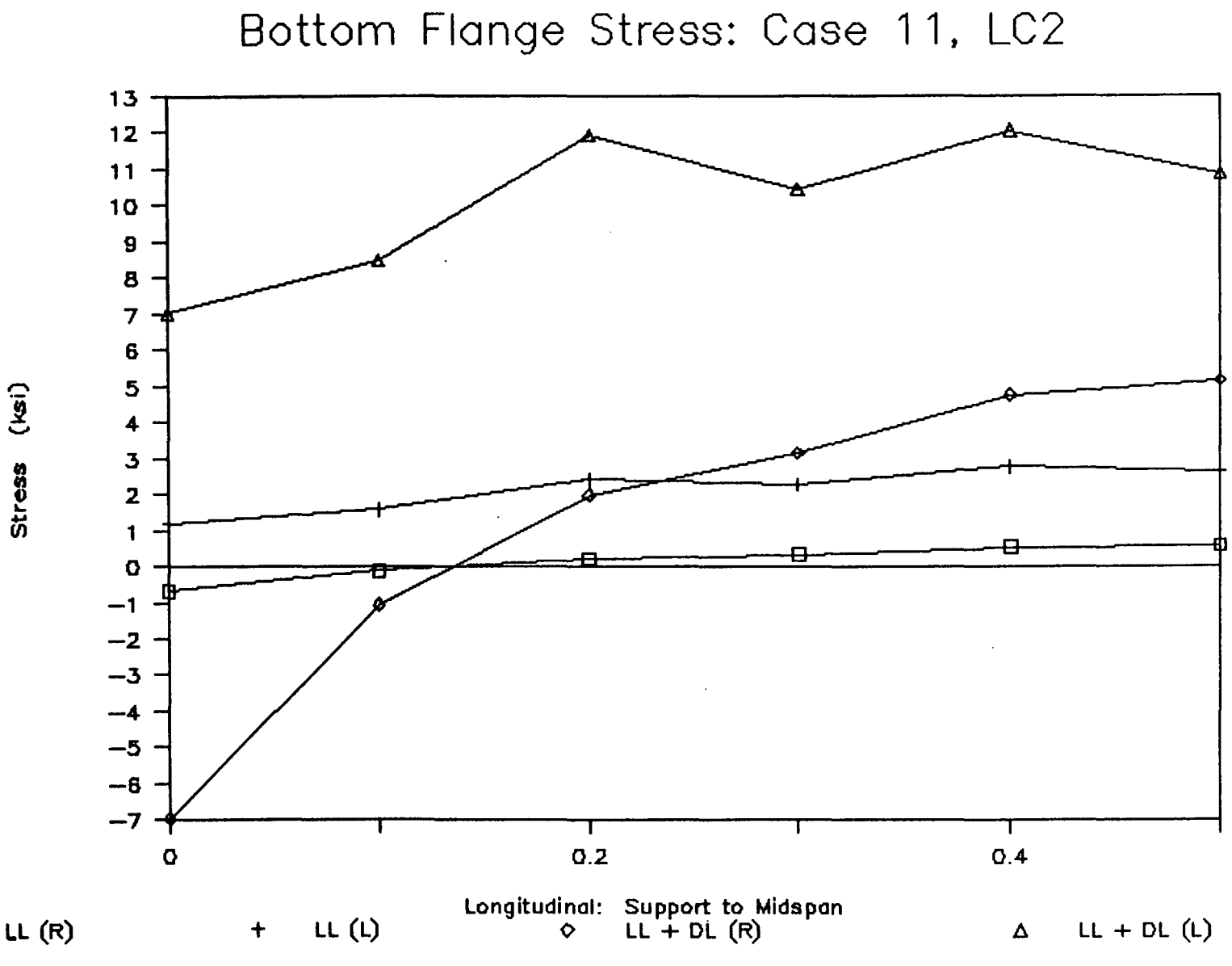
Bottom Flange Stress: Case 11, LC2
Stress (ksi)
13
12
11
10
9
8
7
6
5
4
3
2
1
0
−1
−2
−3
−4
−5
−6
−7
0
0.2
0.4
Longitudinal: Support to Midspan
LL (R)
+ LL (L)
◇ LL + DL (R)
△ LL + DL (L)

Figure 116

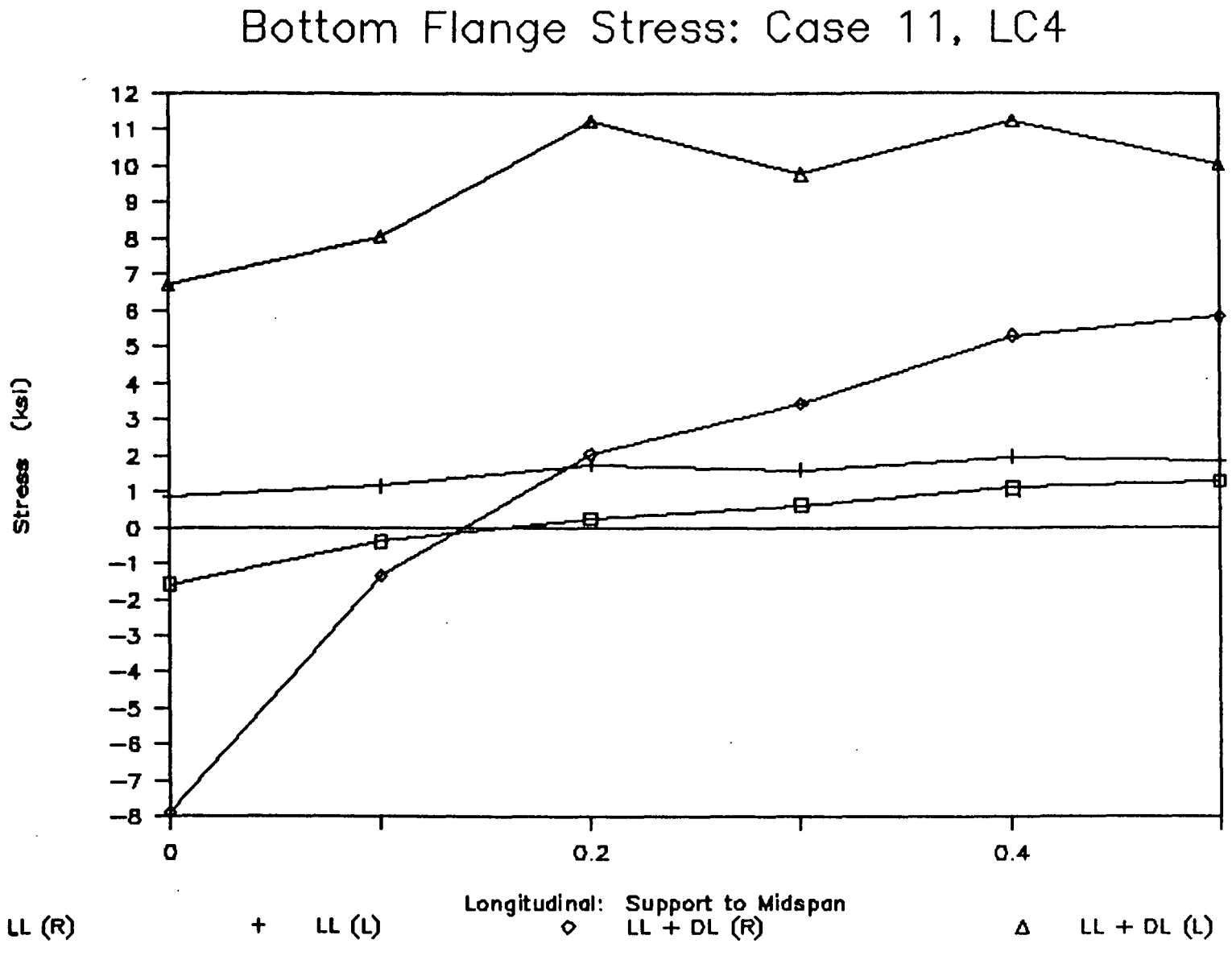
Bottom Flange Stress: Case 11, LC4
Stress (ksi)
12
11
10
9
8
7
6
5
4
3
2
1
0
-1
-2
-3
-4
-5
-6
-7
-8
0
0.2
0.4
Longitudinal: Support to Midspan
LL (R)
LL (L)
LL + DL (R)
LL + DL (L)

Figure 117

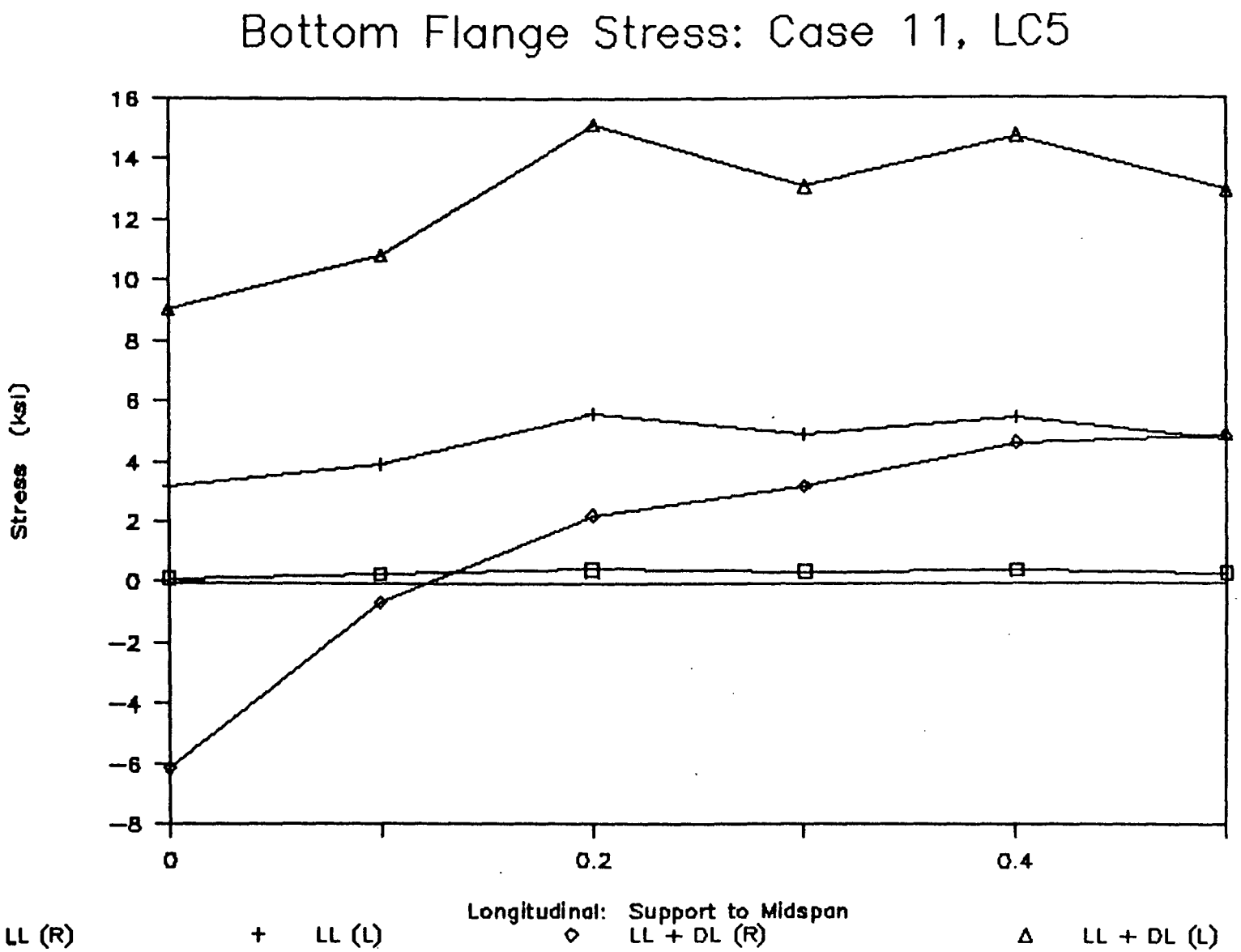
Bottom Flange Stress: Case 11, LC5
Stress (ksi)
16
14
12
10
8
6
4
2
0
−2
−4
−6
−8
0
0.2
0.4
Longitudinal: Support to Midspan
LL (R)
LL (L)
LL + DL (R)
LL + DL (L)

Figure 118

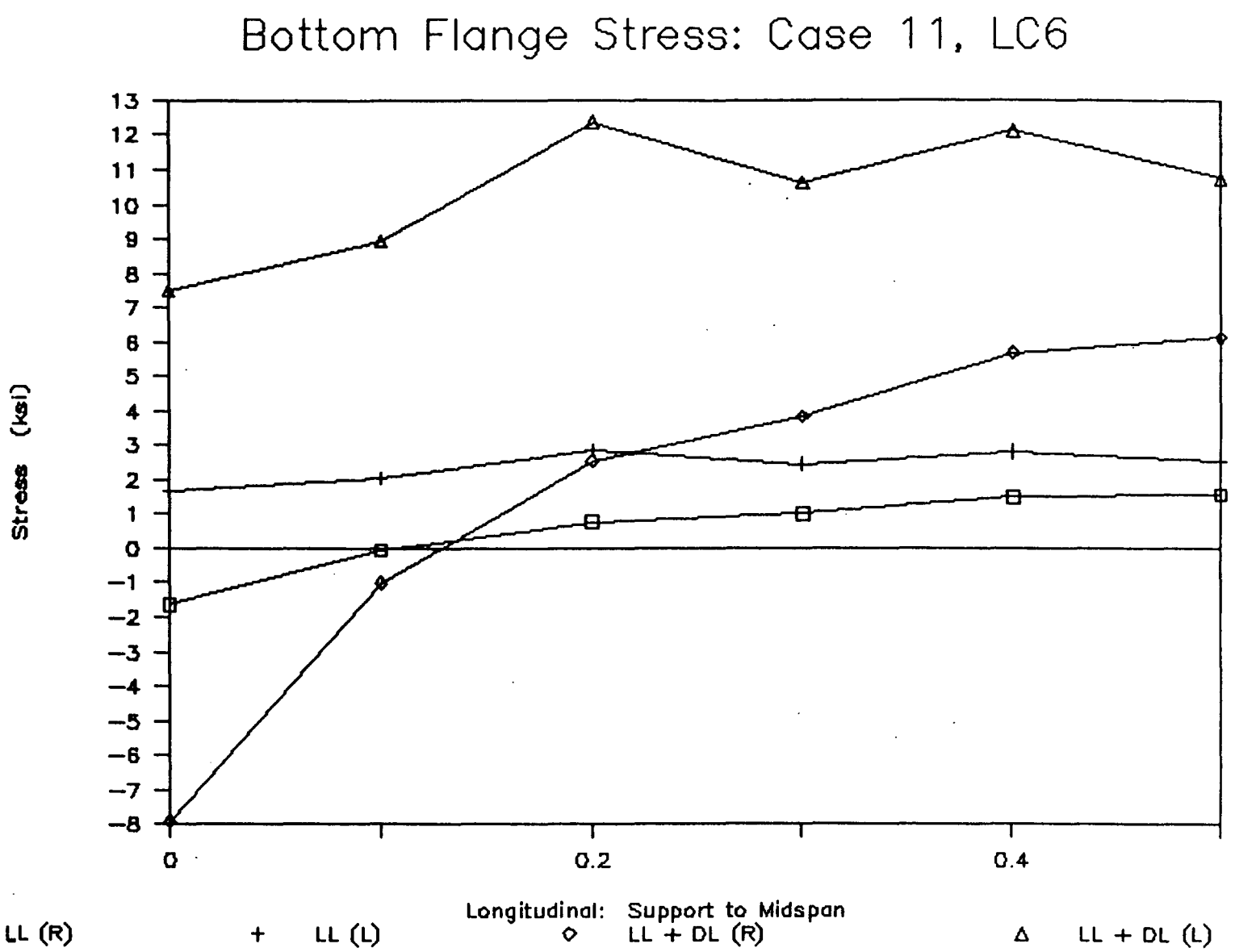
Bottom Flange Stress: Case 11, LC6
Stress (ksi)
13
12
11
10
9
8
7
6
5
4
3
2
1
0
−1
−2
−3
−4
−5
−6
−7
−8
0
0.2
0.4
Longitudinal: Support to Midspan
LL (R)
+ LL (L)
◇ LL + DL (R)
△ LL + DL (L)

Figure 119

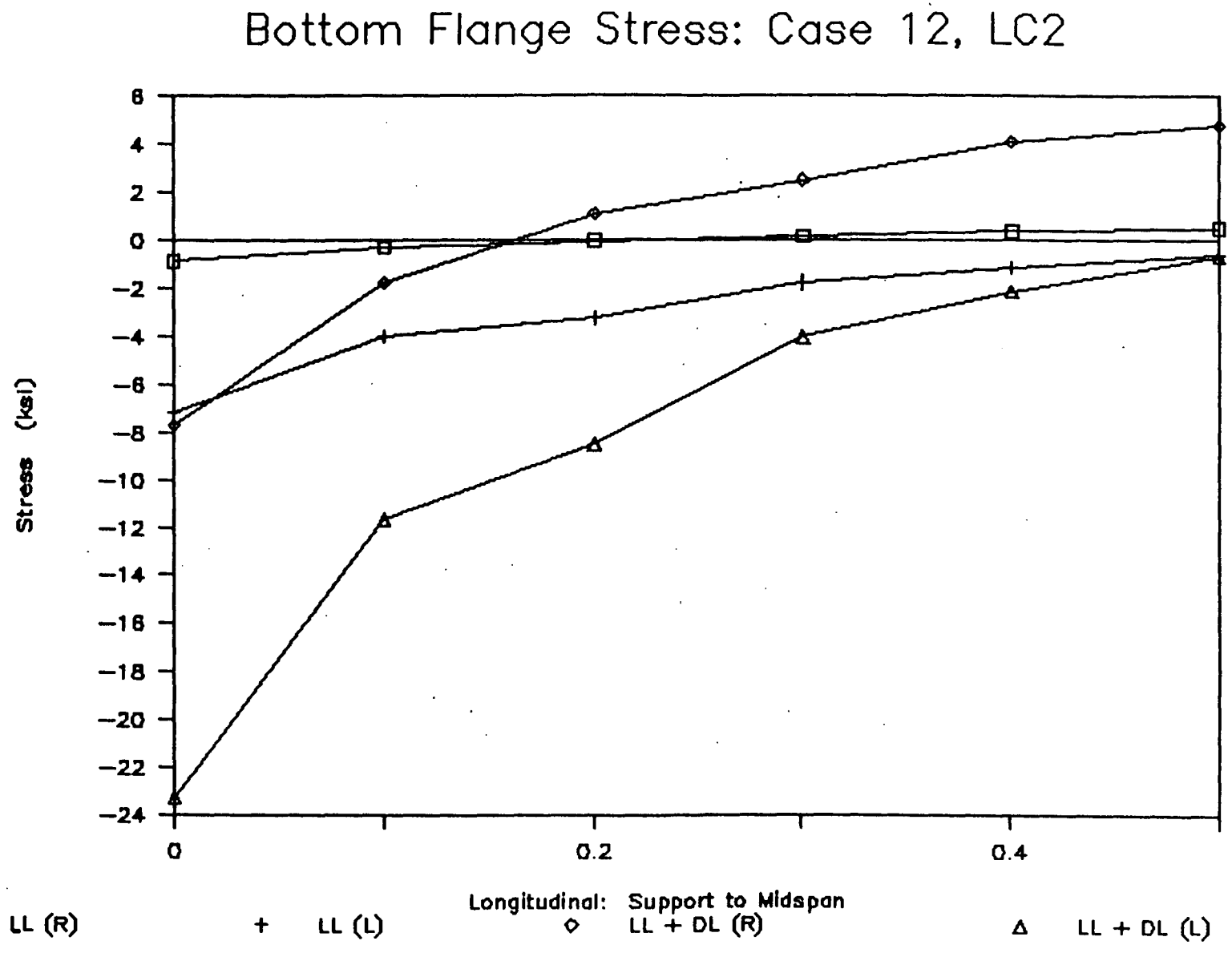
Bottom Flange Stress: Case 12, LC2
Stress (ksi)
6
4
2
0
-2
-4
-6
-8
-10
-12
-14
-16
-18
-20
-22
-24
0
0.2
0.4
Longitudinal: Support to Midspan
LL (R)
LL (L)
LL + DL (R)
LL + DL (L)

Figure 120

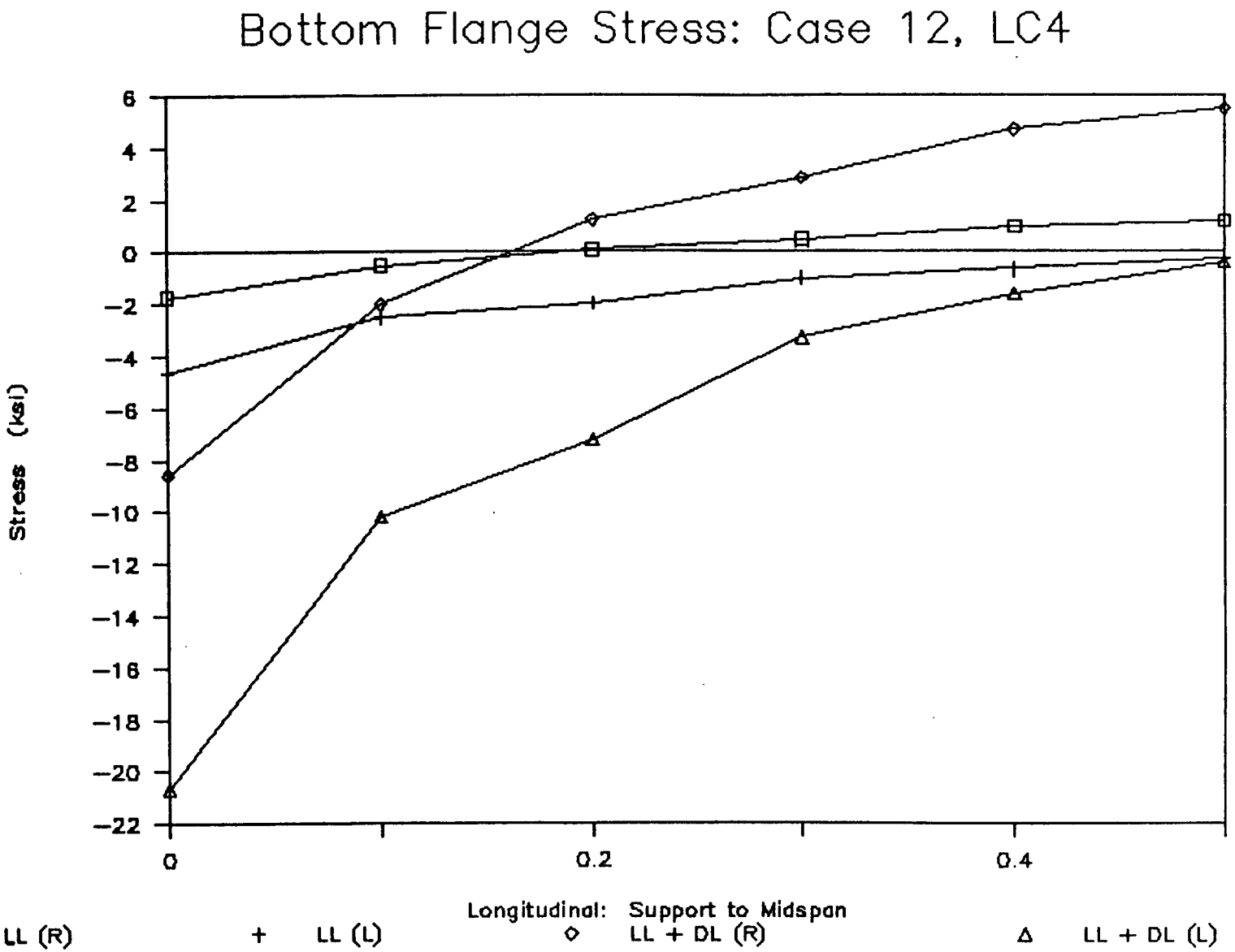
Bottom Flange Stress: Case 12, LC4
Stress (ksi)
6
4
2
0
-2
-4
-6
-8
-10
-12
-14
-16
-18
-20
-22
0
0.2
0.4
Longitudinal: Support to Midspan
LL (R)
+ LL (L)
◇ LL + DL (R)
△ LL + DL (L)

Figure 121

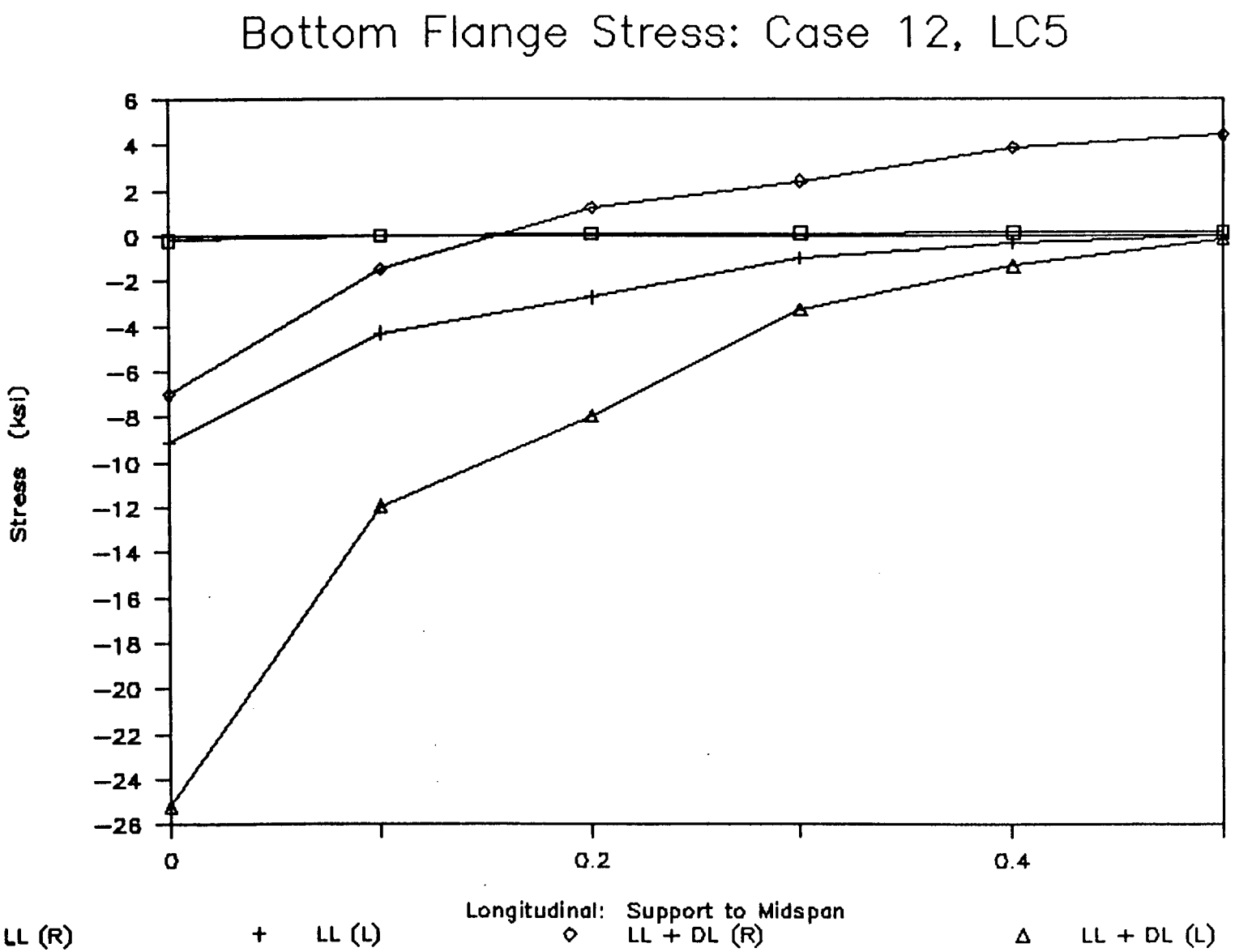
Bottom Flange Stress: Case 12, LC5
Stress (ksi)
6
4
2
0
-2
-4
-6
-8
-10
-12
-14
-16
-18
-20
-22
-24
-26
0
0.2
0.4
Longitudinal: Support to Midspan
LL (R)
LL (L)
LL + DL (R)
LL + DL (L)

Figure 122

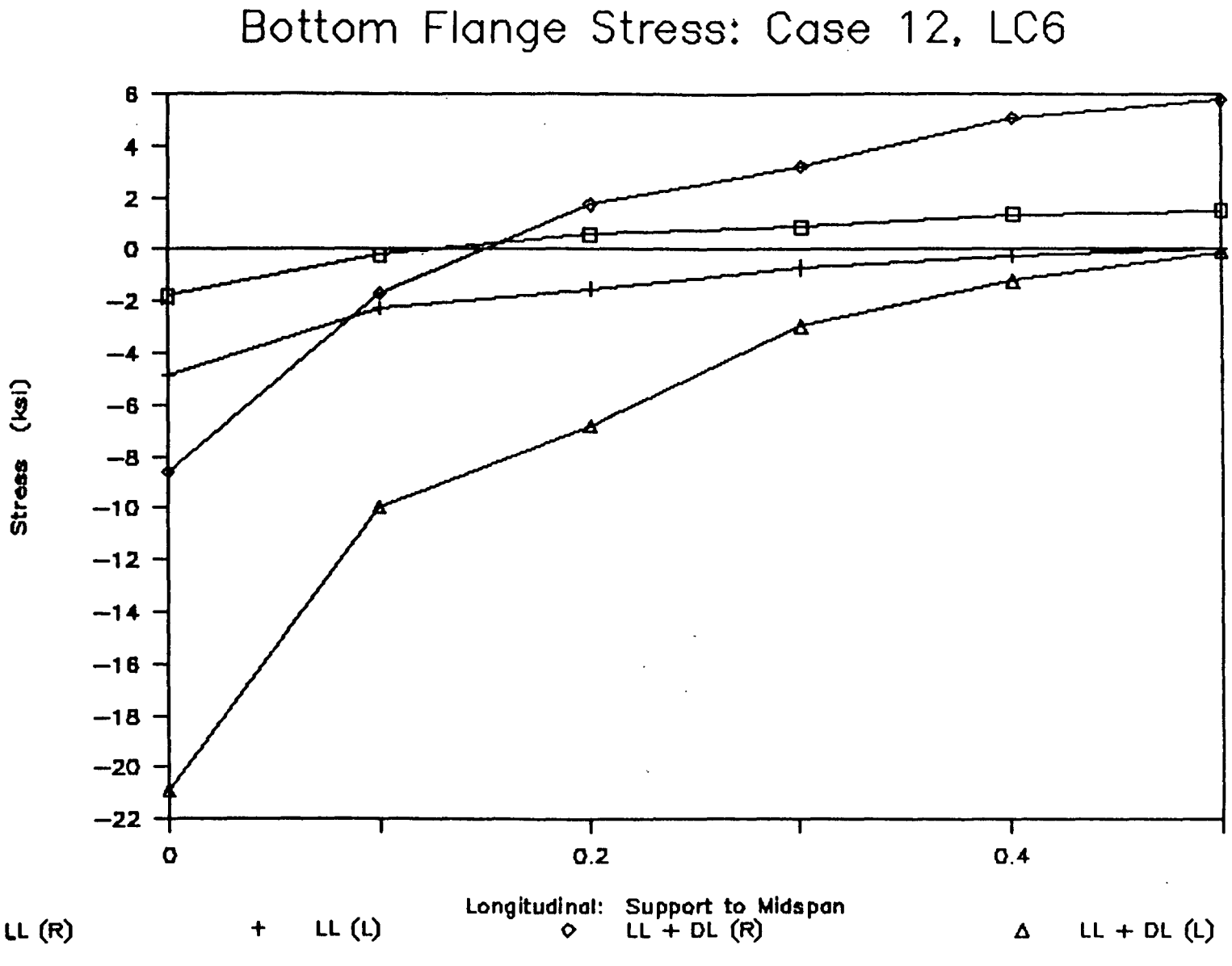
Bottom Flange Stress: Case 12, LC6
Stress (ksi)
6
4
2
0
-2
-4
-6
-8
-10
-12
-14
-16
-18
-20
-22
0
0.2
0.4
Longitudinal: Support to Midspan
LL (R)
LL (L)
LL + DL (R)
LL + DL (L)

Figure 123

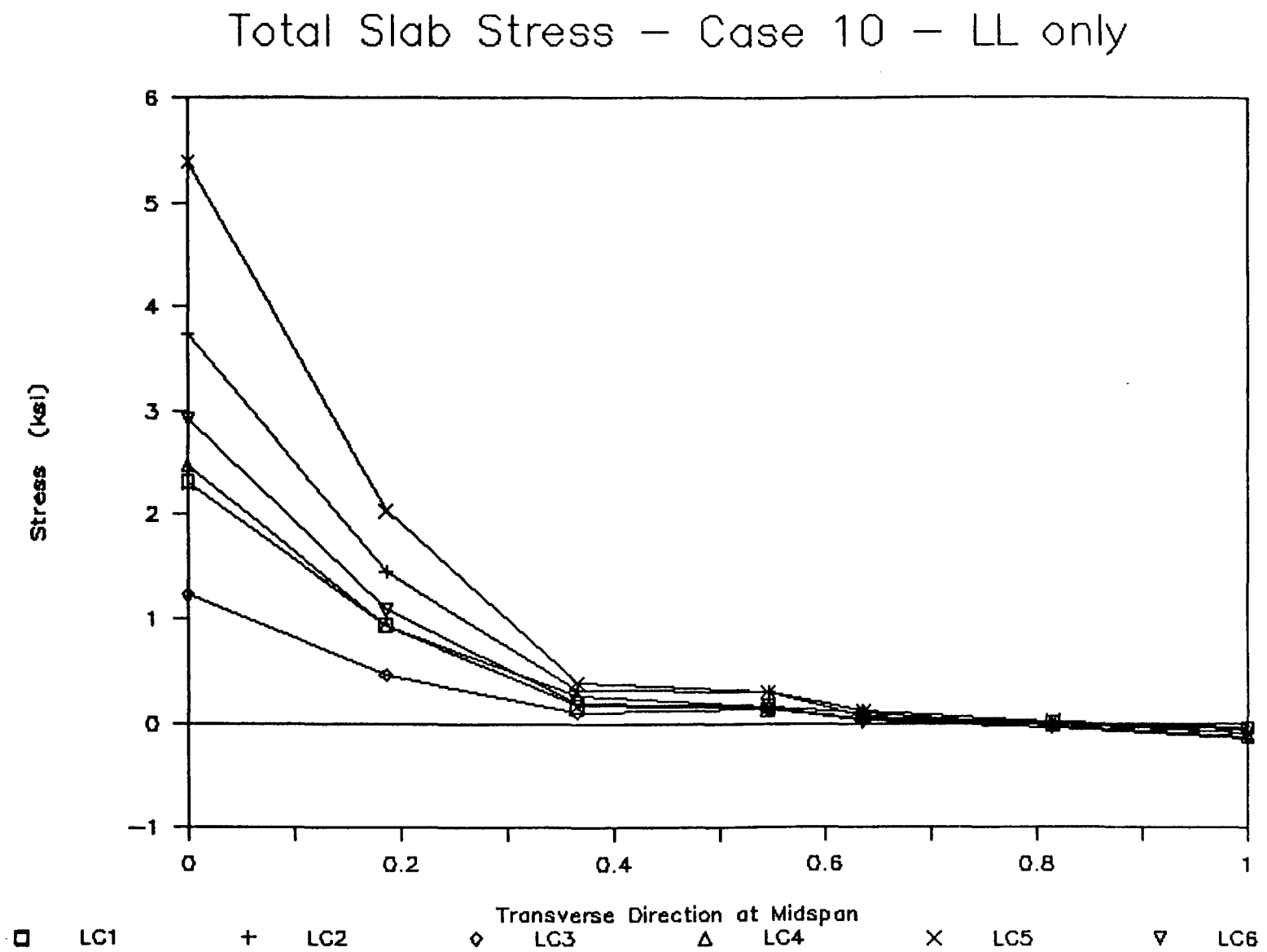
Total Slab Stress – Case 10 – LL only
Stress (ksi)
6
5
4
3
2
1
0
-1
0
0.2
0.4
0.6
0.8
1
Transverse Direction at Midspan
LC1
LC2
LC3
LC4
LC5
LC6

Figure 124

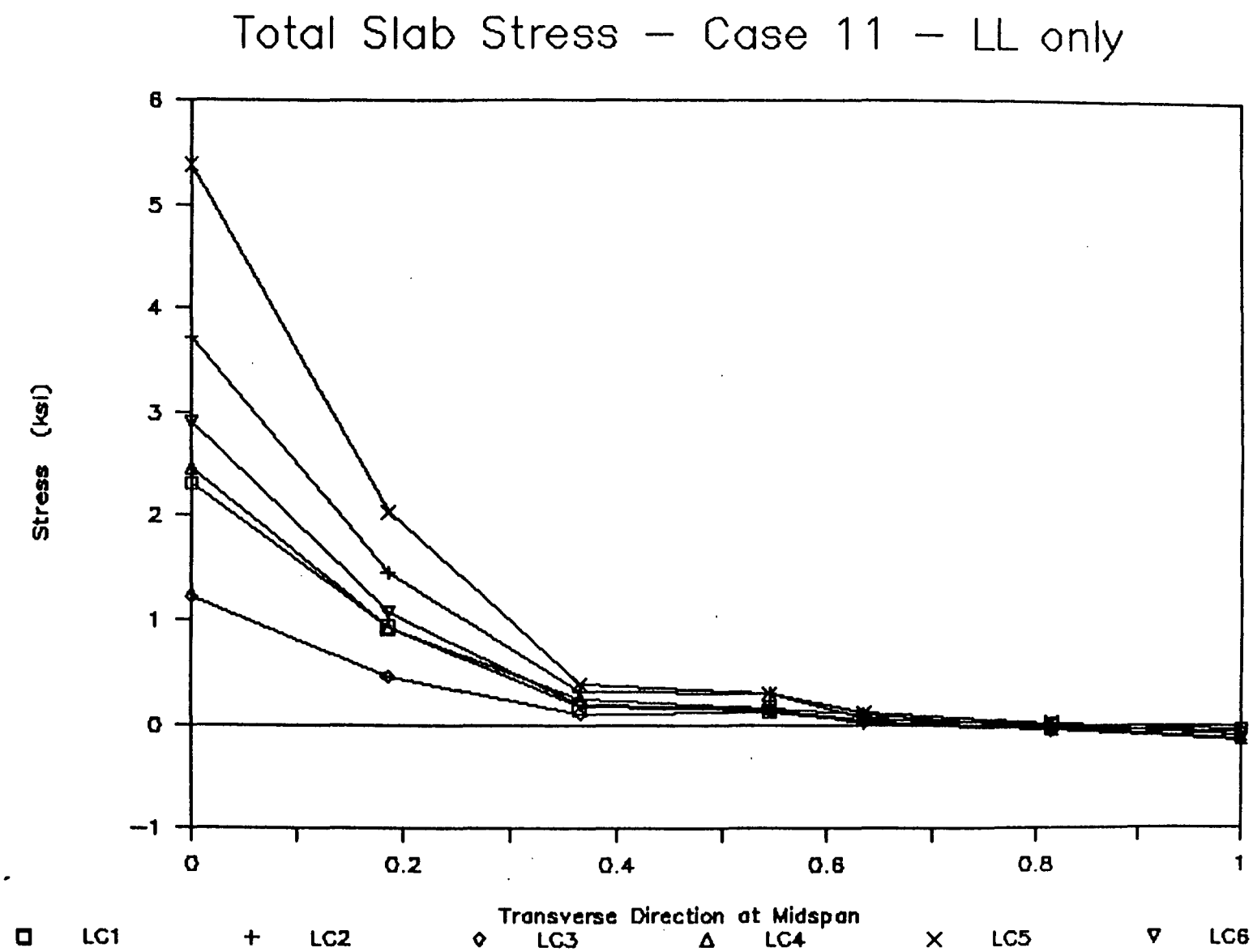
Total Slab Stress – Case 11 – LL only
Stress (ksi)
6
5
4
3
2
1
0
-1
0
0.2
0.4
0.6
0.8
1
Transverse Direction at Midspan
LC1
LC2
LC3
LC4
LC5
LC6

Figure 125

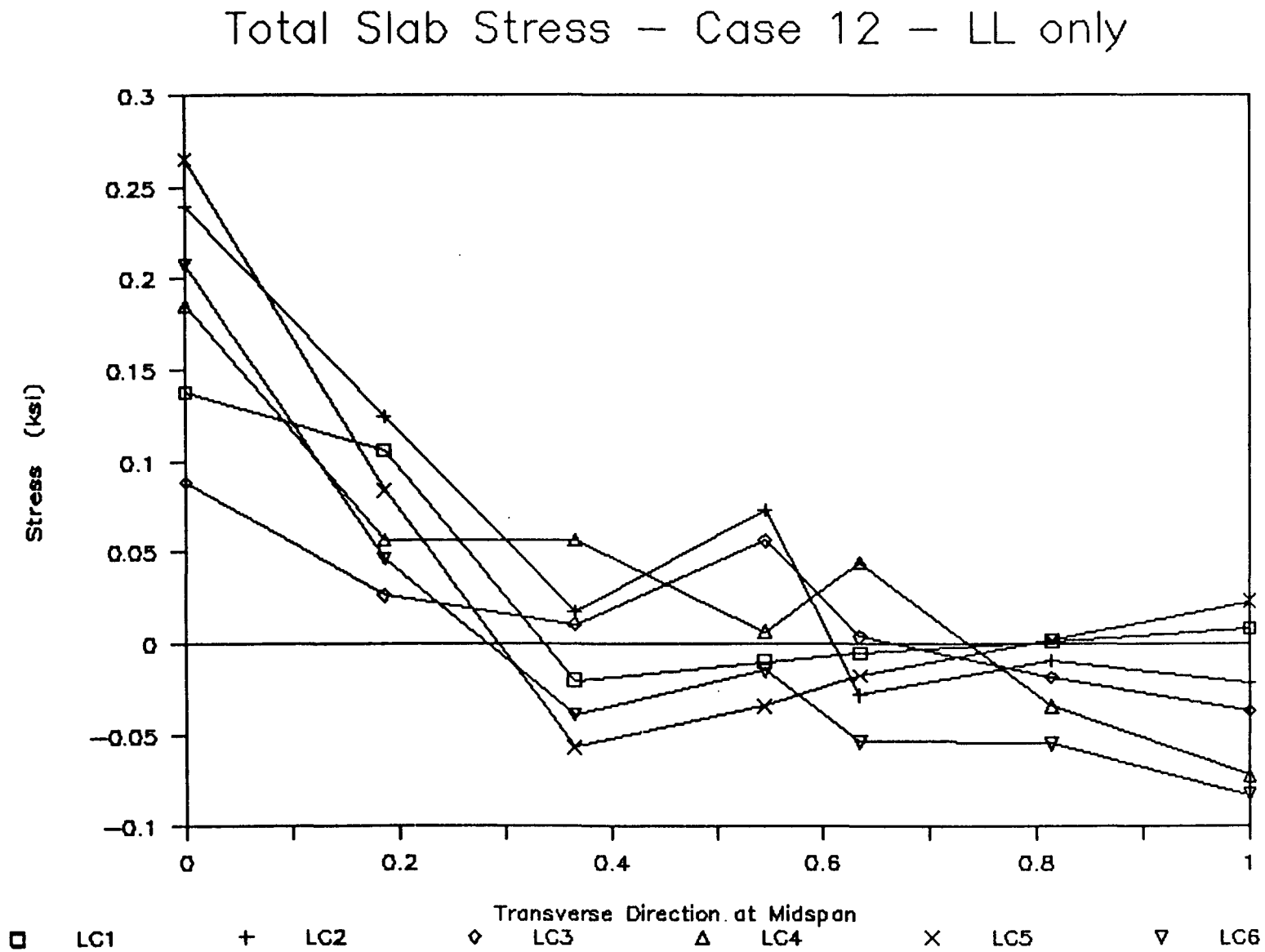
Total Slab Stress – Case 12 – LL only
Stress (ksi)
0.3
0.25
0.2
0.15
0.1
0.05
0
-0.05
-0.1
0
0.2
0.4
0.6
0.8
1
Transverse Direction at Midspan
LC1
LC2
LC3
LC4
LC5
LC6

Figure 126

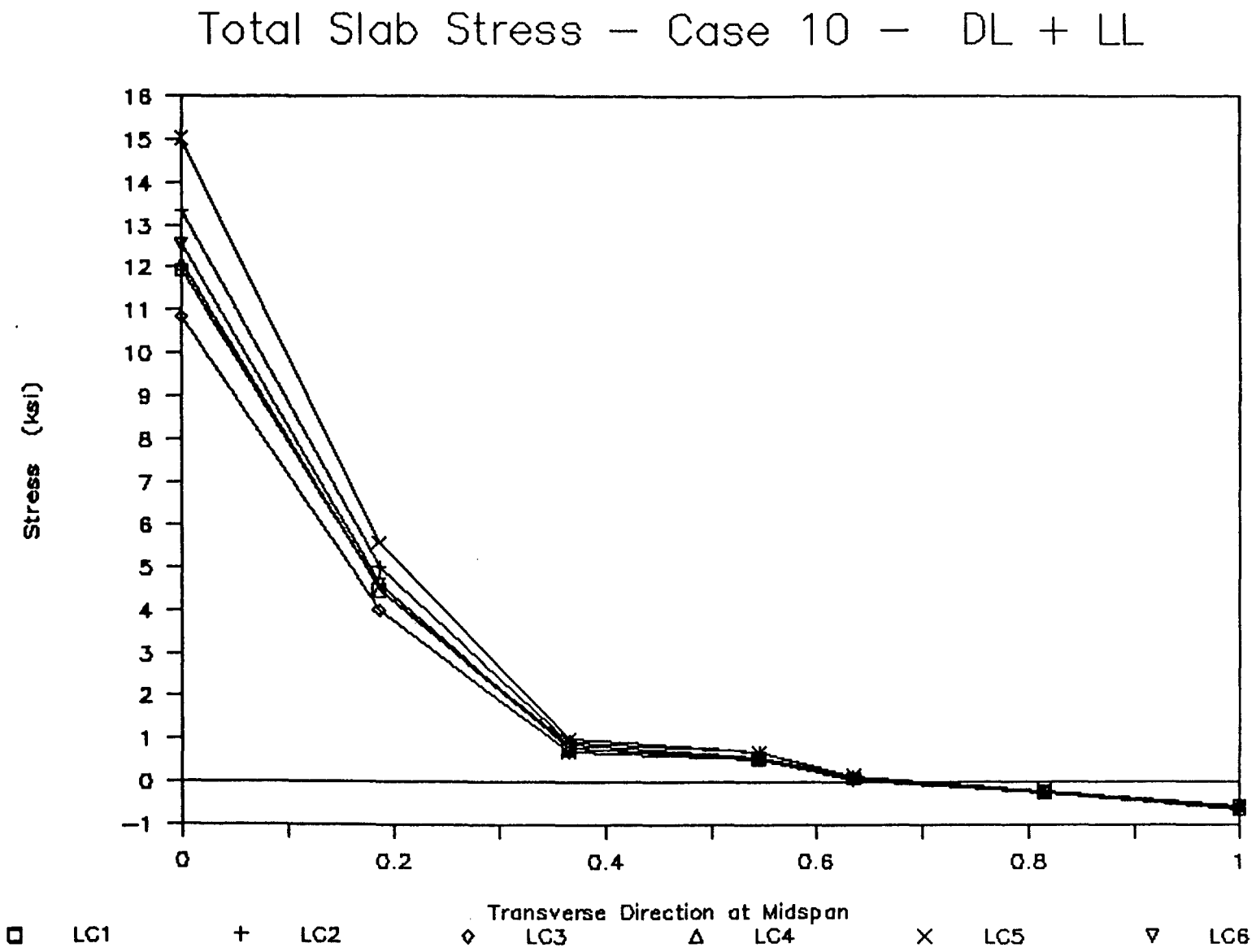
Total Slab Stress – Case 10 – DL + LL
Stress (ksi)
16
15
14
13
12
11
10
9
8
7
6
5
4
3
2
1
0
-1
0
0.2
0.4
0.6
0.8
1
Transverse Direction at Midspan
LC1
LC2
LC3
LC4
LC5
LC6

Figure 127

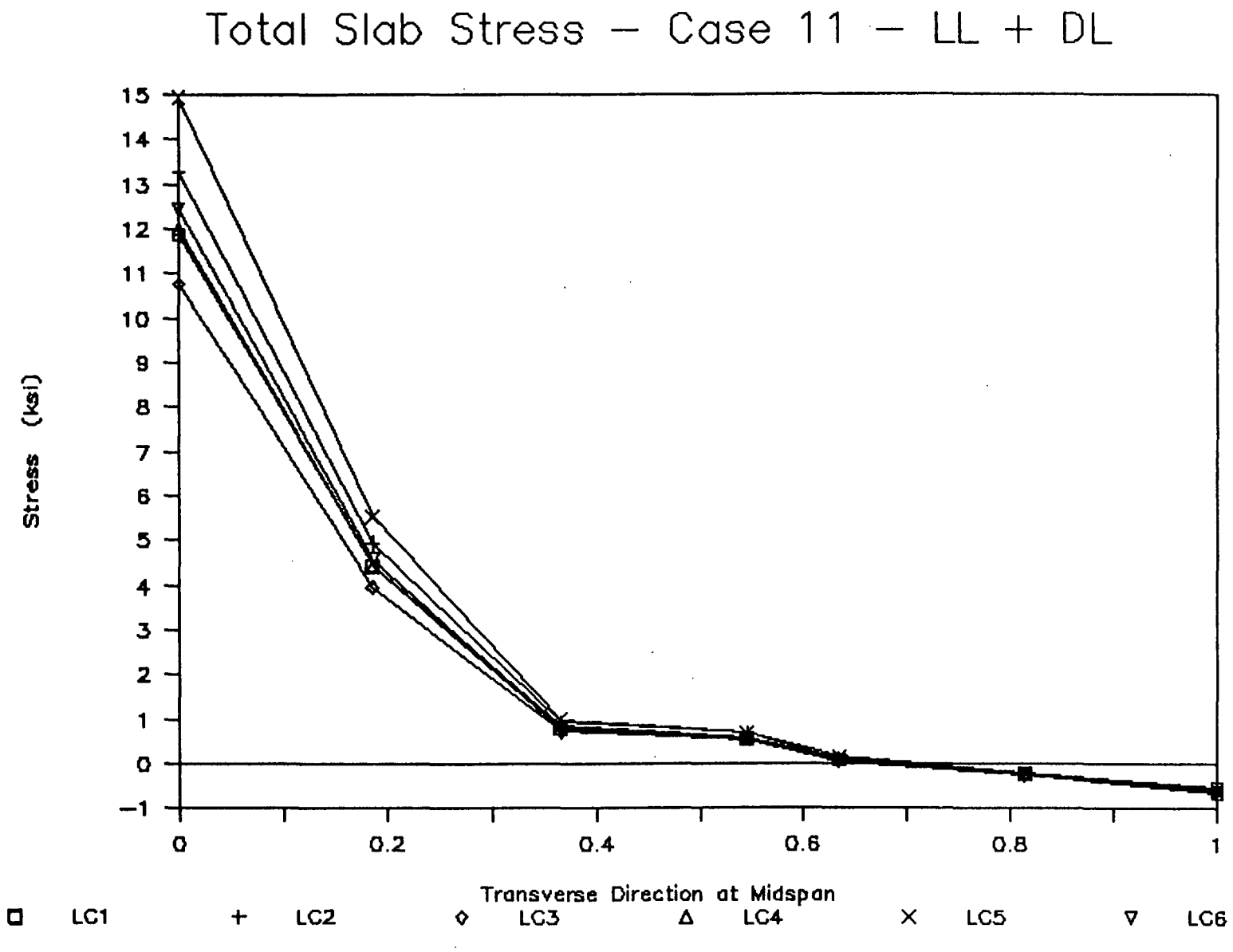
Total Slab Stress – Case 11 – LL + DL
Stress (ksi)
15
14
13
12
11
10
9
8
7
6
5
4
3
2
1
0
−1
0
0.2
0.4
0.6
0.8
1
Transverse Direction at Midspan
LC1
LC2
LC3
LC4
LC5
LC6

Figure 128

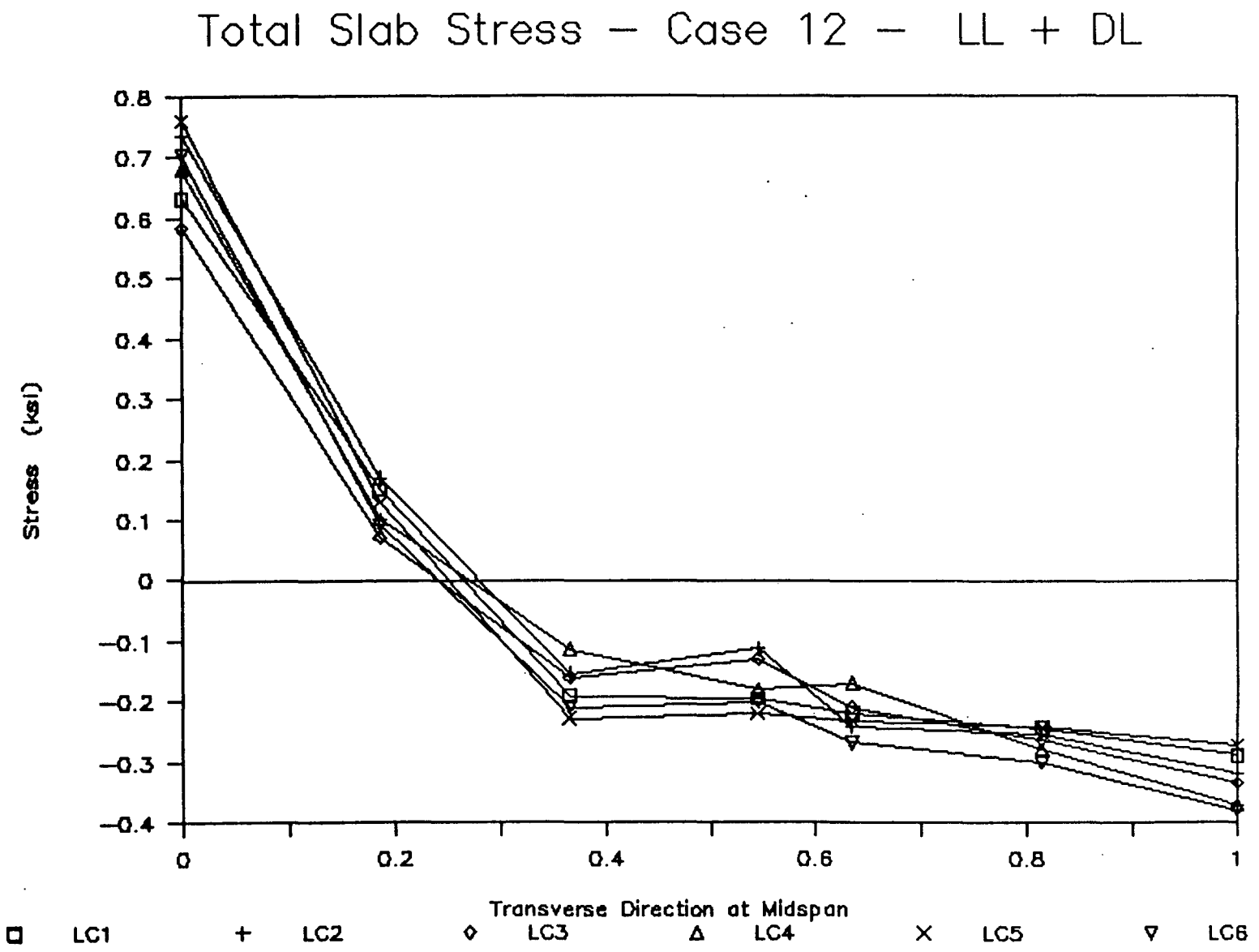
Total Slab Stress – Case 12 – LL + DL
Stress (ksi)
0.8
0.7
0.6
0.5
0.4
0.3
0.2
0.1
0
-0.1
-0.2
-0.3
-0.4
0
0.2
0.4
0.6
0.8
1
Transverse Direction at Midspan
LC1
LC2
LC3
LC4
LC5
LC6

Figure 129

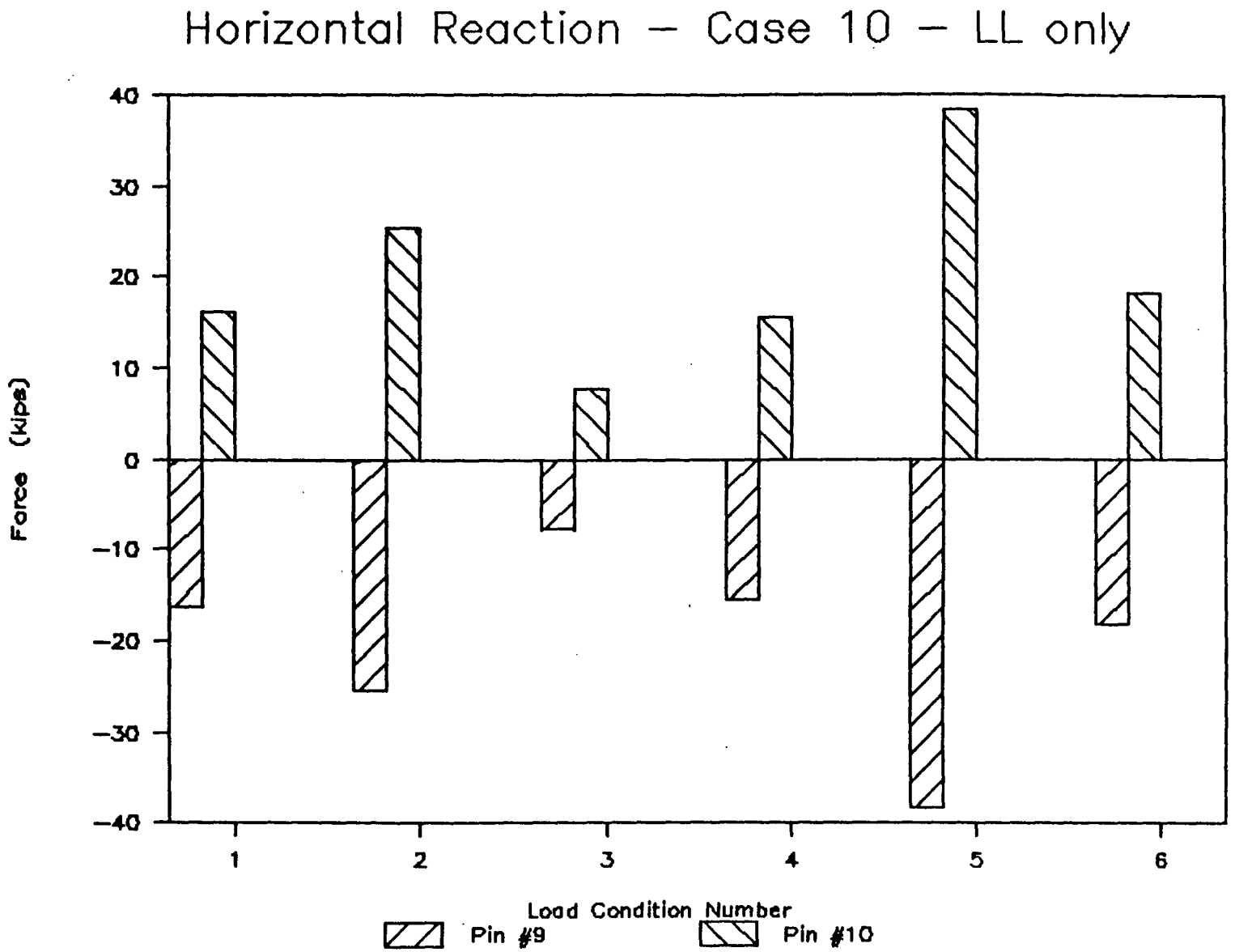
Horizontal Reaction – Case 10 – LL only
Force (kips)
40
30
20
10
0
-10
-20
-30
-40
1
2
3
4
5
6
Load Condition Number
Pin #9
Pin #10

Figure 130

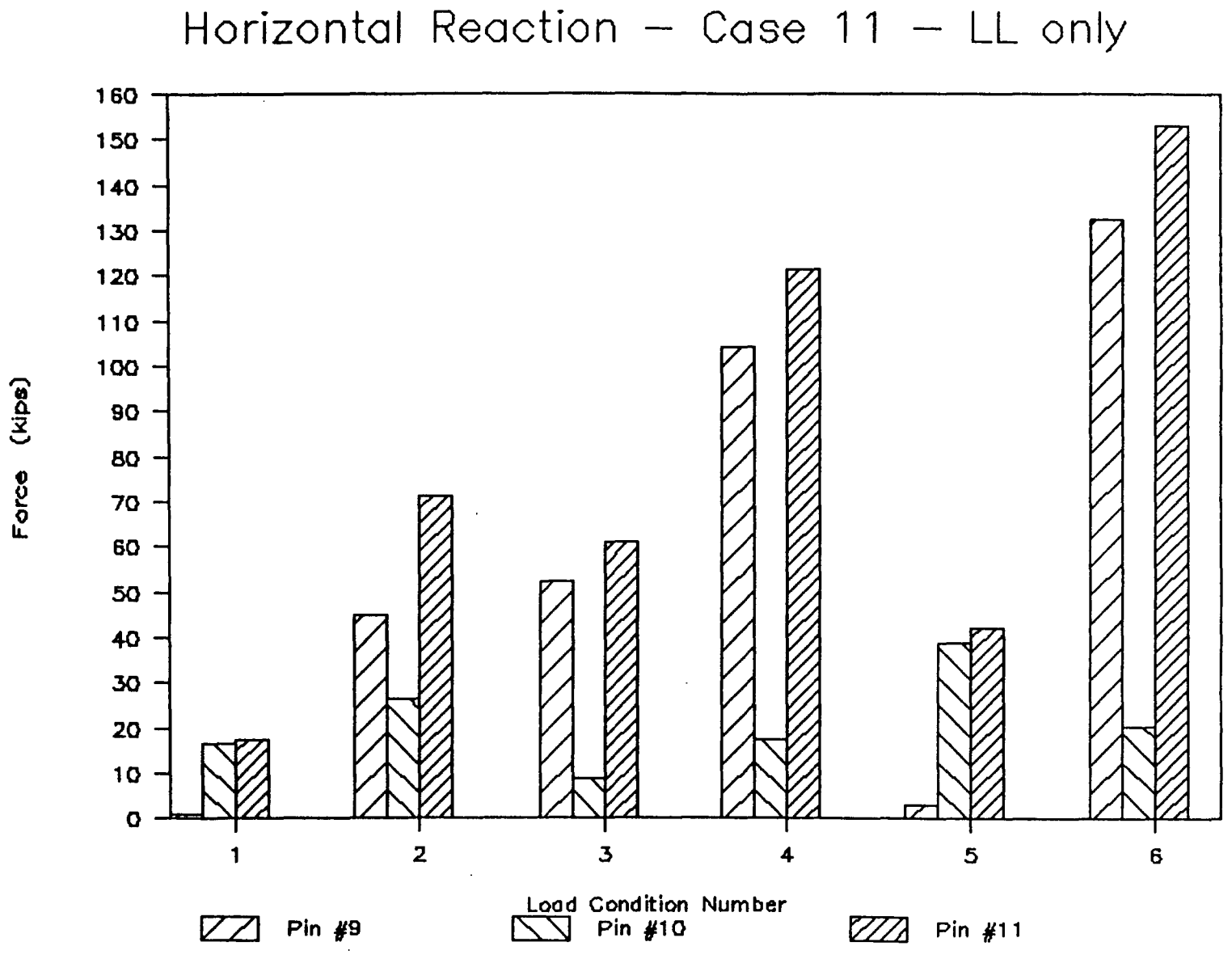
Horizontal Reaction – Case 11 – LL only
Force (kips)
160
150
140
130
120
110
100
90
80
70
60
50
40
30
20
10
0
1
2
3
4
5
6
Load Condition Number
Pin #9
Pin #10
Pin #11

Figure 131

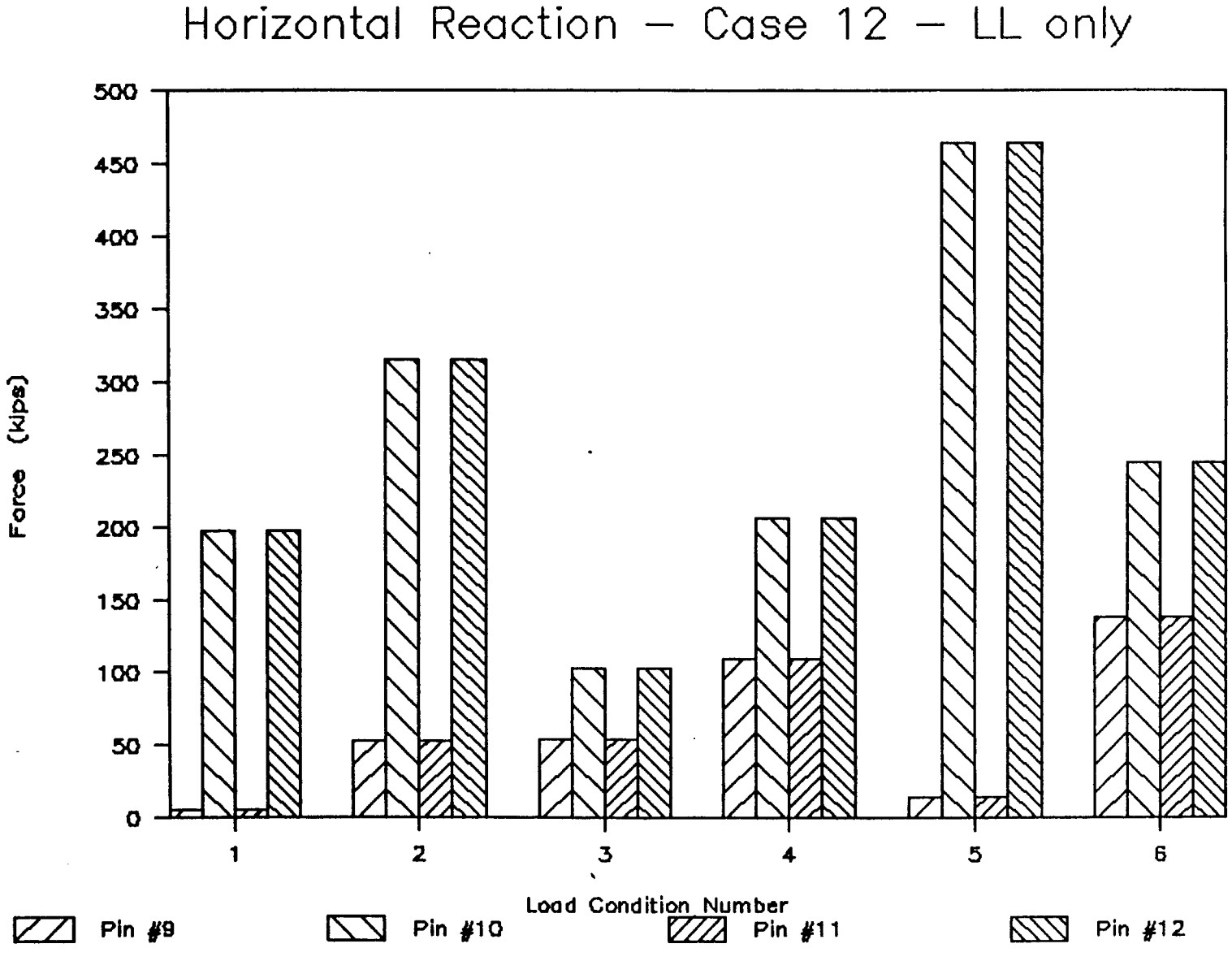
Horizontal Reaction – Case 12 – LL only
Force (kips)
500
450
400
350
300
250
200
150
100
50
0
1
2
3
4
5
6
Load Condition Number
Pin #9
Pin #10
Pin #11
Pin #12

Figure 132

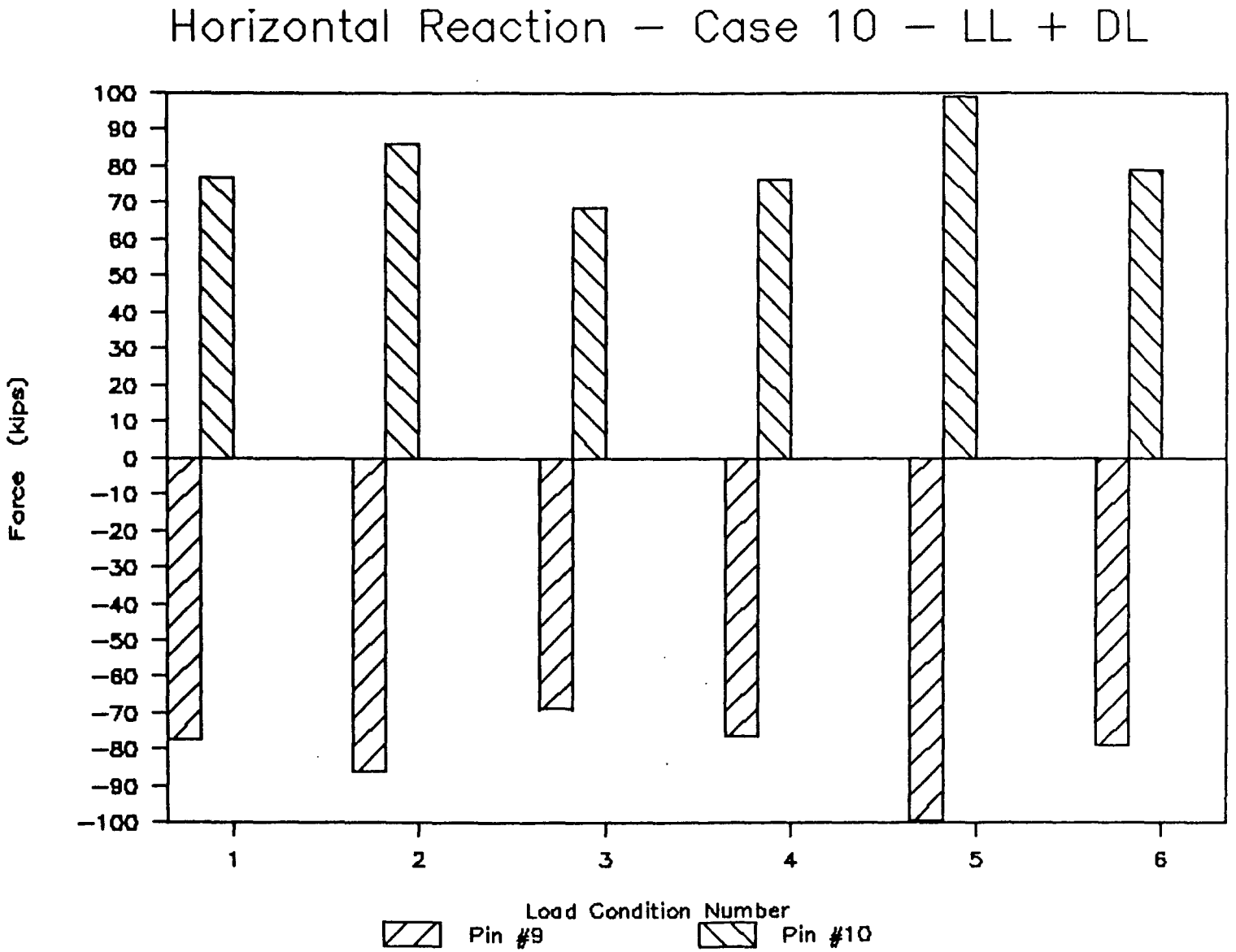
Horizontal Reaction – Case 10 – LL + DL
Force (kips)
100
90
80
70
60
50
40
30
20
10
0
-10
-20
-30
-40
-50
-60
-70
-80
-90
-100
1
2
3
4
5
6
Load Condition Number
Pin #9
Pin #10

Figure 133

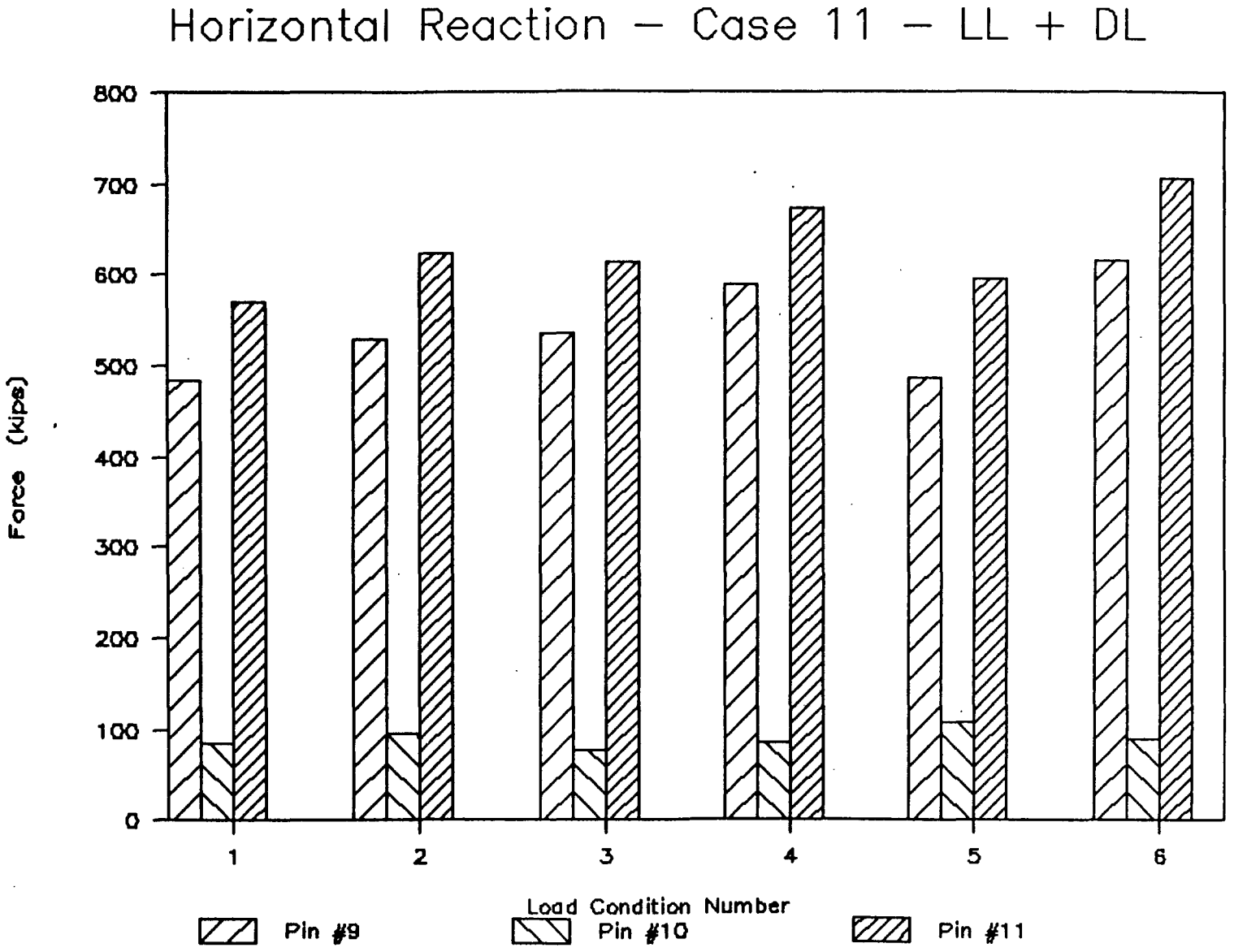
Horizontal Reaction – Case 11 – LL + DL
800
700
600
500
400
300
200
100
0
Force (kips)
1
2
3
4
5
6
Load Condition Number
Pin #9
Pin #10
Pin #11

Figure 134

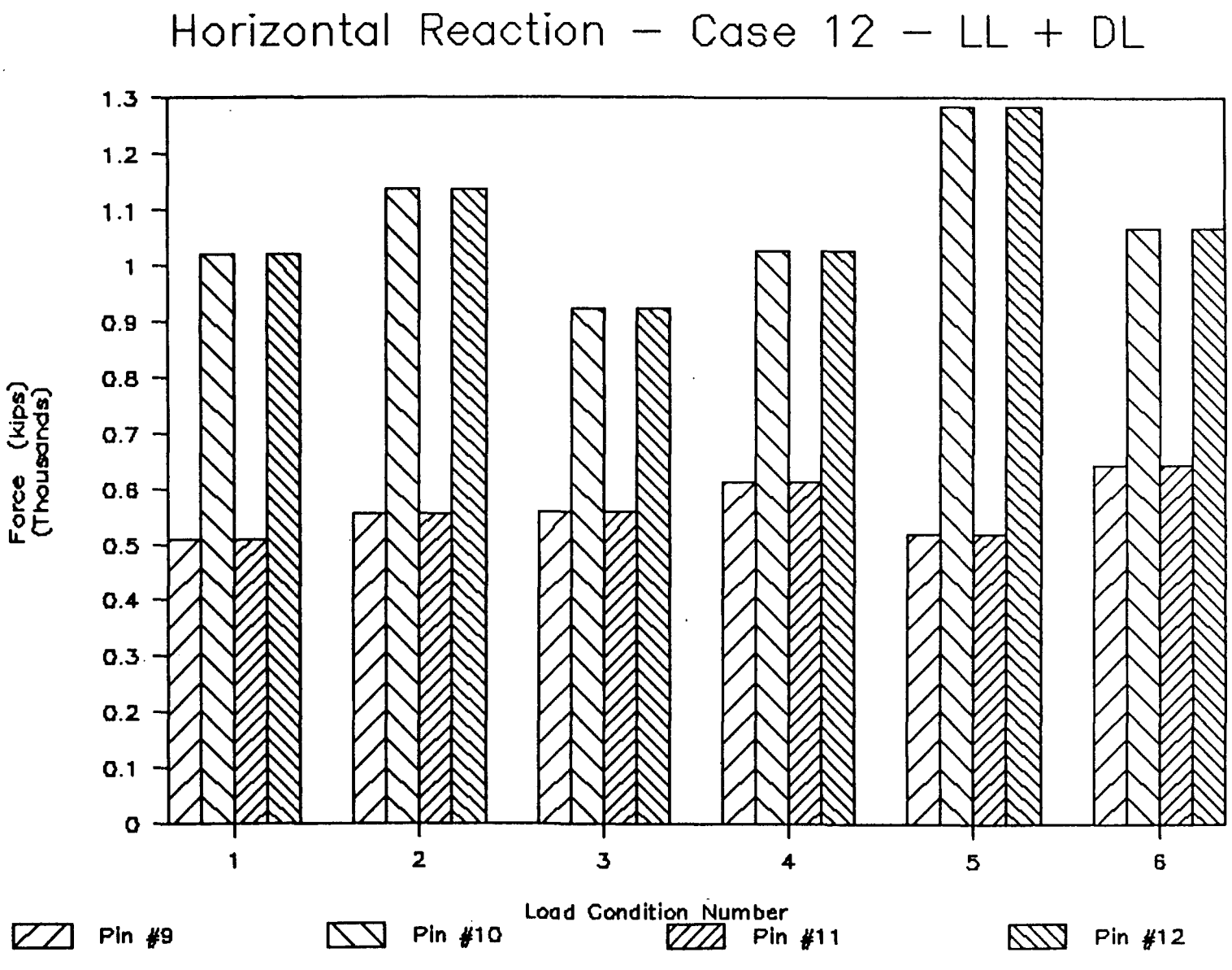
Horizontal Reaction – Case 12 – LL + DL
Force (kips)
(Thousands)
1.3
1.2
1.1
1
0.9
0.8
0.7
0.6
0.5
0.4
0.3
0.2
0.1
0
1
2
3
4
5
6
Load Condition Number
Pin #9
Pin #10
Pin #11
Pin #12

Figure 135